

INFORMATION TO USERS

This manuscript has been reproduced from the microfilm master. UMI films the text directly from the original or copy submitted. Thus, some thesis and dissertation copies are in typewriter face, while others may be from any type of computer printer.

The quality of this reproduction is dependent upon the quality of the copy submitted. Broken or indistinct print, colored or poor quality illustrations and photographs, print bleedthrough, substandard margins, and improper alignment can adversely affect reproduction..

In the unlikely event that the author did not send UMI a complete manuscript and there are missing pages, these will be noted. Also, if unauthorized copyright material had to be removed, a note will indicate the deletion.

Oversize materials (e.g., maps, drawings, charts) are reproduced by sectioning the original, beginning at the upper left-hand corner and continuing from left to right in equal sections with small overlaps.

Photographs included in the original manuscript have been reproduced xerographically in this copy. Higher quality 6" x 9" black and white photographic prints are available for any photographs or illustrations appearing in this copy for an additional charge. Contact UMI directly to order.

ProQuest Information and Learning
300 North Zeeb Road, Ann Arbor, MI 48106-1346 USA
800-521-0600

UMI[®]

UNIVERSITY OF ALBERTA

Rediscovery and characterization of the *aeroplane (ae)* mutant and its identification as a mutation in a tissue-specific enhancer of the *teashirt (tsh)* gene in *Drosophila melanogaster*.

BY

Kelly Howard Soanes



A thesis submitted to the Faculty of Graduate Studies and Research in partial fulfillment of the requirements for the degree of Doctor of Philosophy.

IN

MOLECULAR BIOLOGY AND GENETICS

DEPARTMENT OF BIOLOGICAL SCIENCES

Edmonton, Alberta

Spring, 2000



National Library
of Canada

Acquisitions and
Bibliographic Services

395 Wellington Street
Ottawa ON K1A 0N4
Canada

Bibliothèque nationale
du Canada

Acquisitions et
services bibliographiques

395, rue Wellington
Ottawa ON K1A 0N4
Canada

Your file *Votre référence*

Our file *Notre référence*

The author has granted a non-exclusive licence allowing the National Library of Canada to reproduce, loan, distribute or sell copies of this thesis in microform, paper or electronic formats.

The author retains ownership of the copyright in this thesis. Neither the thesis nor substantial extracts from it may be printed or otherwise reproduced without the author's permission.

L'auteur a accordé une licence non exclusive permettant à la Bibliothèque nationale du Canada de reproduire, prêter, distribuer ou vendre des copies de cette thèse sous la forme de microfiche/film, de reproduction sur papier ou sur format électronique.

L'auteur conserve la propriété du droit d'auteur qui protège cette thèse. Ni la thèse ni des extraits substantiels de celle-ci ne doivent être imprimés ou autrement reproduits sans son autorisation.

0-612-60022-X

Canada

UNIVERSITY OF ALBERTA
LIBRARY RELEASE FORM

NAME OF AUTHOR: Kelly Howard Soanes

TITLE OF THESIS: Rediscovery and characterization of the *aeroplane (ae)* mutant and its identification as a mutation in a tissue-specific enhancer of the *teashirt (tsh)* gene in *Drosophila melanogaster*.

DEGREE: Doctor of Philosophy

YEAR THIS DEGREE GRANTED: 2000

Permission is hereby granted to the University of Alberta Library to reproduce single copies of this thesis and to lend or sell such copies for private, scholarly or scientific research purposes only.

The author reserves all other publication and other rights in association with the copyright of the thesis, and except as herein before provided neither the thesis nor any substantial portion thereof may be printed or otherwise reproduced in any material form whatever without the author's prior written permission.

Jan 27/00

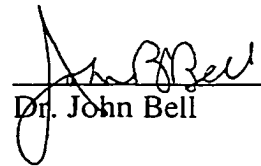


Kelly Howard Soanes
10710-60 Ave.
Edmonton, Alberta, Canada
T6E 2C9

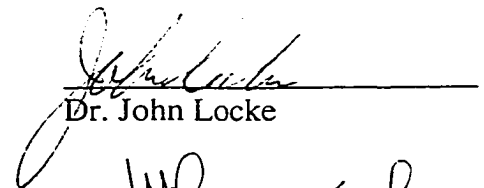
UNIVERSITY OF ALBERTA

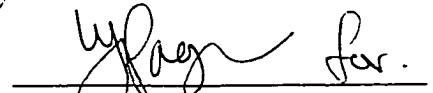
FACULTY OF GRADUATE STUDIES AND RESEARCH

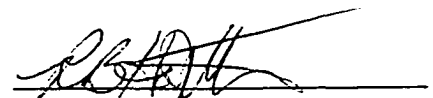
The undersigned certify that they have read, and recommended to the Faculty of Graduate Studies and Research for acceptance, a thesis entitled "Rediscovery and characterization of the *aeroplane (ae)* mutant and its identification as a mutation in a tissue-specific enhancer of the *teashirt (tsh)* gene in *Drosophila melanogaster*" submitted by Kelly Howard Soanes in partial fulfillment of the requirements for the degree of Doctor of Philosophy in Molecular Biology and Genetics.

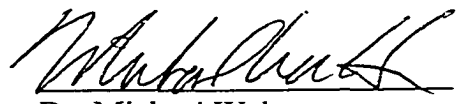

Dr. John Bell


Dr. Michael Russell


Dr. John Locke


Dr. John Phillips


Dr. Ross Hodgetts


Dr. Michael Walter

Jan 26/00

Abstract

In 1931, Theodore Quelprud characterized a novel spontaneous mutation in *Drosophila melanogaster*, which was named *aeroplane* (*ae*) based on its abnormal wing posture (Quelprud, 1931). Although the characterization of the original *ae* allele was minimal, it is very likely that another allele of this extinct mutation has now been identified. The *aeroplane-like* (*ae-l*) allele was isolated as a by-product of a Carnegie 20 (Cy20) transformation experiment. This homozygous viable allele initially was cytologically mapped to 39E2-F1; 40A4-B1 at map position 55.8.

The phenotype is caused by a defect in the hinge region of the wing and the base of the halteres. The proximal ventral radius at the base of the wing is fused to the thorax in the region of the pleural wing process, and in the halteres the base is fused to the thorax just below the pedicellar sensillae. Initial complementation analysis of *ae-l* suggested that this mutation might represent an allele of a novel gene. A molecular examination, however, revealed that it is likely an allele of the homeotic gene *teashirt* (*tsh*). The apparent wing paralysis and the drooping halteres are not caused by muscle or neurological defects. The identification of an I element within the 3' non-coding sequence appears to affect a wing and haltere specific enhancer of *tsh*. The cis-acting regulatory element is required to drive *tsh* in the regions of the developing adult that give rise to proximal wing and haltere tissues. Thus, loss of this expression results in the fusion of the proximal structures of the wing and halteres to the thoracic cuticle.

Resolving the etiology of the abnormal wing and haltere posture in the *ae-l* mutant has led to the identification of a wing hinge-specific enhancer of the *tsh* gene,

providing a better understanding of the regulation of *tsh* and its function during the developing adult.

Acknowledgements

This work was supported by a Natural Sciences and Engineering Research Council (NSERC) of Canada granted to Dr. John Bell. I also wish to acknowledge the generosity of M. Scott in providing *tsh* antibodies, stocks and genomic clones, S. Kerridge for *tsh* stocks, clones, the E4.8 enhancer line and communicating unpublished results with us. We would also like to thank Dr. Carl Thummel for the two pCaSpeR vectors used in this work (pCaSpeR hs 43 and pCaSpeR 4) and to Andrea Brandt for kindly providing the pGATB vector used in generating the *ae*-GAL4 construct. Special thanks to Shelagh Campbell for her technical advise on microinjections. To Rakesh Bhatnagar for his help with the TEM work and confocal microscopy, George Braybrook for his help with the SEM work. Thanks to Brian Staveley for introducing me to John, the lab and for the helpful advice. Thanks to Andrew Simmonds for his constant encouragement and to Sandra O'keefe for the technical advice and lunch time conversations. To a great friend Julie (NB), for the lessons in pool. A special thanks to John for the support, patience and freedom to allow me to try just about anything I wanted to in the lab and of course for the great road trips. Finally to my Mom and Dad, Thank you! (Yes Dad, I 'm almost done).

Table of contents

Chapter I – Introduction	1
Sequence and Functional Conservation	1
Gene Regulation	7
Cis-Acting Regulatory Elements	9
Transvection	15
Pattern Formation	17
Adult Cuticle Formation	21
Wingless Signaling	26
Wing Posture Mutants	29
Chapter II – Phenotype and Mapping	37
Phenotype	37
Mapping	37
Chapter III - P element Mutagenesis and Molecular Mapping	43
Isolation of 3' Flanking Genomic Sequences	55
Phenotypic Severity of the Derivative Lines	56
Molecular Analysis of P1370 Derivative Lines	57
Northern Analysis	65
Molecular Mapping	66
Chapter IV – Etiology	72
Indirect Flight Muscles	72
Direct Flight Muscles	75
Adult Cuticle	76
Wing Posture Mutants	80
Chapter V - <i>aeroplane</i> Enhancer and Genetic Analysis	91
4.8 kb Fragment Analysis	115
<i>Rpw</i> and <i>vg^U</i>	118
C(1)DX	118
UAS/GAL4	121
Mini-Library Sequences	132

Preliminary Sequence Analysis	133
Genetic Analysis	134
Chapter VI – Discussion	142
Muscle Analysis	142
A Tissue Specific Null Allele	142
Northern Analysis and <i>teashirt</i> Protein Detection	143
<i>tsh</i> [04319] Derivative Chromosomes	144
Complementation	149
Genetic Interactions	152
The “Strong” <i>aeroplane</i> Phenotype	154
Enhancer Tested Fragments	156
Larval Midgut Expression	158
Eye Imaginal Disc Expression	159
Antennal Disc Expression	160
Reporter Gene Expression	160
<i>I</i> element	161
Etiology	165
A Role For <i>teashirt</i> In the Adult	166
UAS- <i>tsh</i> ; 30A-GAL4	167
<i>Rpw</i> , <i>vg</i> ^U and E4.8	170
Orientation Dependent <i>lacZ</i> Expression	175
Future Directions	179
Chapter VII - Materials and Methods	183
Stocks and Crosses	183
Transmission Electron Microscopy	183
Scanning Electron Microscopy	186
Histochemical Staining	186
Antibody Staining	187
Gamma Irradiation	187
Genomic Extractions and Southern Blot Analysis	187

Mini-Library	190
Ligations	191
Competent Cells	191
RNA Extractions and Northern Analysis	192
PCR	193
<i>Taq</i> DNA Polymerase	193
Elongase Amplification of the <i>ae</i> Insert	194
PFU DNA Polymerase	194
Plasmid and Lambda Preparations	195
Enhancer Fragment and Enhancer Tester Constructs	196
Microinjections	198
Bibliography	203
Appendix	221

List of Figures

Figure 1. Wing Hinge Diagram.	23
Figure 2. Haltere Diagram.	25
Figure 3. Phenotype.	39
Figure 4. Genetic and Cytological Map	41
Figure 5. <i>P</i> element Mutagenesis Scheme.	45
Figure 6. pP{PZ}Insert Site and Vector.	52
Figure 7. <i>tsh</i> [04319] Expression Pattern.	54
Figure 8. Derivative <i>tsh</i> [04319] Chromosomes Schematic.	62
Figure 9. Northern Blot.	69
Figure 10. Molecular Mapping of <i>aeroplane</i> .	71
Figure 11. Indirect Flight Muscles.	74
Figure 12. Direct Flight Muscles.	78
Figure 13. <i>aeroplane</i> Etiology.	83
Figure 14. <i>tsh</i> [04319] ^{8.1} Wing.	85
Figure 15. <i>tsh</i> [04319] ^{8.1} Thorax.	87
Figure 16. Wing Posture Mutants.	90
Figure 17. <i>tsh</i> Histochemical Staining.	94
Figure 18. <i>tsh</i> Antibody Staining.	96
Figure 19. <i>I</i> Element Insert.	99
Figure 20. <i>aeroplane</i> Enhancer Schematic.	102
Figure 21. Wing and Haltere Imaginal Disc <i>Lac Z</i> Expression	104
Figure 22. E4.8 Second Instar Staining	106
Figure 23. Midgut Expression.	108
Figure 24. Eye-Antennal Expression.	112
Figure 25. Constructs and Their Orientations.	114
Figure 26. 4.8 kb Sequence.	117
Figure 27. <i>Rpw</i> , <i>vg</i> ^U , E4.8.	120
Figure 28. <i>C(1)DX</i> ; <i>ae</i> Phenotype.	123

Figure 29. UAS / GAL4 Hinge Results.	125
Figure 30. UAS / GAL4 Ectopic Bristles	127
Figure 31. UAS / GAL4 Halteres	129
Figure 32. Mini-library Sequence Blast Search Schematic.	137
Figure 33. Mini-library sequences	139
Figure 34. Group II Breakpoints	148
Figure 35. Enhancer Model.	178
Figure 36. <i>ae</i> -GAL Line Construction	202

Tables

Table 1. Complementation Table.	46
Table 2. <i>P</i> element Mutagenesis Results.	47
Table 4. <i>tsh</i> [04319] Derivative Lines.	59
Table 5. Muscle Table.	81
Table 6. Primers.	200
Table 7. AT Rich Motifs of HB1.0	140
Table 8. Mat2.1 Inspector Data Base Results	141
Table 9. Stocks and Origins.	185

Appendix

Table 3. *Rpw* Enhancers.

223

Chapter I

Introduction

Sequence and Functional Conservation

The work presented in this thesis helps one to understand the role that the homeotic gene *teashirt* (*tsh*) plays during embryonic, larval and adult development of *Drosophila melanogaster*, as well as the role that *tsh* homologues may play in other organisms as distantly related as humans. These studies should also help in the understanding of gene regulation in eukaryotes in general by the identification and preliminary examination of cis-acting regulatory elements such as the aeroplane enhancer element presented herein. This is made possible because of the conservation that is observed between different developmental systems. The conservation of genomic sequences as well as the functional conservation between model system invertebrates like *Drosophila* and *C.elegans* with vertebrates like mice and humans has proven to be an invaluable tool in the study of development in both groups. Any information gained from one group can aid in the study and understanding of development within the other. The conservation of various pathways such as the Wg/Wnt pathway (reviewed by Cadigan and Nusse, 1997), the RAS/MAP kinase pathway, (reviewed by Tan and Kim, 1999), the players involved in limb development (reviewed by Brook et al., 1996; Irvine and Fogt, 1997) or the homeobox containing genes (review by Lawrence and Morata, 1994) is intriguing. One of the earlier observations of conservation of sequence and function was identified from the studies examining homeobox genes. Collectively these genes share a conserved DNA binding motif of 61 amino acids, referred to as the homeobox domain (reviewed in Hayashi and Scott, 1990). Initially, the homeobox was identified as a motif conserved between genes of the two homeotic complexes in *Drosophila*, the Bithorax complex (BX-C) and the Antennapedia complex (ANT-C) (Scott and Weiner, 1984 and McGinnis et. al. 1984a). The genes found within the ANT-C (i.e. *labial*, *lab*; *proboscipedia*, *pb*; *Deformed*, *Dfd*; *Sex combs reduced*, *Scr*; *Antennapedia*, *Antp*) and the BX-C (*Ultrabithorax*, *Ubx*; *abdominal-A*, *abd-A* and *Abdominal-B*, *Abd-B*) each encode homeobox domains in the cognate proteins. The results of mutations in homeotic genes are well documented. The loss of function mutations led to the replacement of one body part by another. The BX-C and ANT-C master control genes each play a key role in

setting up the body plan of the developing fly (Lewis, 1978; reviewed by Lawrence and Morata, 1994). Presumably, these types of genes act individually or in concert near the top of a cascade of gene expression, regulating downstream effector genes, which then specify the developmental fates within each metamere. The homeodomain gene-complexes has been identified in a number of organisms as distantly related as invertebrates like *Drosophila hydei* and *D. melanogaster*; the red flour beetle (*Tribolium*); nematodes (*C. elegans*), and the earthworm (*Lumbricus terrestris*) and also within vertebrates like chickens, mice and humans (McGinnis et al., 1984b).

The conservation within these two groups of homeotic selector genes exists at three levels. The first is the structural conservation or the conservation of the gene order within the genome of each of the organisms. The mouse Antp-like homeobox containing genes (Hox) are clustered into four tightly linked complexes on different chromosomes (Duboule and Dollé, 1989). Two of the clusters appear to be complete or close to complete duplications of the HOM-C in *Drosophila*. The HOM-C in *Drosophila* consists of both the BX-C and the ANTP-C, collectively. The order of the genes within these clusters is colinear with the order in which they are required and expressed for patterning and segmental specification along the anterior-posterior axis of the body in the developing fly, or the central and peripheral nervous system and mesodermal derivatives in the mouse (Duboule and Dolle, 1989; Graham et al., 1989). Similar observations were made in studies examining the Hox genes within humans (Bonicinelli et al., 1988).

The second order of conservation between homeotic homologues exists at the protein and nucleic acid sequence level. Homeodomain sequences of two genes in different organisms often are more similar to each other than those within the same organism. For example, a fly homologue may more closely resemble the human or mouse Hox counterpart, than other homeotic genes within the fly (Malicki et al., 1990). This suggests that the body plans of humans, mice, and flies are specified by homeotic gene complexes (HOM-C) derived from an ancestral HOM-C in their last common unsegmented ancestor. The segmentation would therefore presumably be superimposed upon the “front-middle-back” coordinate system provided by the HOM-C (reviewed in Akam, 1989).

Finally, the conservation of amino acid sequence is suggestive of a possible functional conservation of homologues between organisms. Many examples exist for functional conservation among the homeotic gene products. *Dfd* function is required for proper development of the maxillary and mandibular segments in the head of *Drosophila* (Merrill et al., 1987). In each of the four Hox clusters in mice and humans there are also *Dfd*-like genes. The human *Hox 4.2* gene has the highest sequence conservation of the four copies with 36% identity to *Dfd* throughout the protein, and the highest region of conservation is the homeodomain, sharing 55 of 61 amino acids. The results from the misexpression of the *Hox 4.2* cDNA in *Drosophila* embryos and developing adults under the control of a heat shock 70 promoter (*hsp 70*) are the same as observed by the misexpression of *Dfd* protein under the same experimental conditions. These results imply a functional conservation between the *Dfd* protein and the *Hox 4.2* protein and indicate that it represents the human homologue of the *Dfd* gene (McGinnis et al., 1990). Other experiments have shown that *Hox 1.3* in mouse, which closely resembles the *Drosophila* selector gene, *Scr*, is capable of activating similar downstream genes in the fly, based on the homeotic transformations observed upon ectopic expression in flies (Zhao et al., 1993). Misexpression of the *Antp* gene, which is required for the proper specification of the thoracic identity in larvae and adults, can also be mimicked by misexpression of the *Hox 2.2* mouse cognate (Malicki et al., 1990).

It is not surprising that the homologues tested appear to be functionally equivalent. The mouse genes that exhibited the highest conceptual amino acid sequence conservation within the homeodomain, when compared to the *Drosophila* copy, were used in the above experiments. Although these homeodomain containing genes are grouped together based on this conserved motif, several reports have shown that not all of the regulatory specificity identified between the different homeotic selector proteins lies within this conserved domain (Kuziora and McGinnis, 1989; Mann and Hogness, 1990; Ekker et al., 1992). The homeodomain homeobox is not the only region of importance for regulatory specificity. Deletions that lead to the loss of the N-terminal sequence but retain the homeobox of the *Dfd* gene result in the loss of regulatory activity (Ptashne, 1988). Also, *in vitro* comparisons between the *Ubx* and *Antp* proteins show they have

indistinguishable sequence preferences for DNA binding (Ekker et al., 1994), suggesting that the specificity must be imparted by cofactors.

Analysis of the DNA binding recognition sequence of the homeotic proteins *Dfd* and *Ubx* indicates that they both fall into a category of regulatory proteins that share a common TAAT core DNA binding sequence (Ekker et al., 1992; 1994). The importance of this core sequence in DNA recognition is apparent, based on the number of selector proteins that recognize the same core sequence (Ekker et al., 1991; 1994 and Florence et al., 1991). *Ubx*, *engrailed (en)*, *fushi tarazu (ftz)*, *bicoid (bcd)*, *Antp* and *Dfd* are all members of this group of TAAT core recognition proteins. This is not entirely unexpected for the *Antp-like* genes within this group, because they have similar homeodomains. However, the *en* protein has a homeodomain sequence divergent from the *Antp-like* class (Desplan et al., 1985).

Although some of the functional specificity of each of the Hox proteins lies within the homeodomain, other regions within the protein are also known to play a role in the regulatory specificity. Amino acid residues outside the homeobox have been implicated in homeodomain regulatory specificity *in vivo* (Zeng et al., 1993). One cofactor that has been implicated in HOM/Hox DNA binding specificity is the *extradenticle (exd)* protein and its vertebrate homologue, *Polybithorax (Pbx)* (Chang et al., 1995; Neuteboom et al., 1995). The *exd* gene was identified because of its influence on segment identity without affecting the transcription of particular Hom genes. The *exd* gene encodes a homeobox protein that was found to cooperatively bind with Hom-C gene products and contribute to the specificity of DNA recognition (van Dijk and Murre, 1994). The conserved hexapeptide on the N-terminal side of the homeodomain has been shown to play a role in protein-protein interaction between the Hom/Hox proteins and the *exd/Pbx* cofactor. However, this short conserved stretch of amino acids does not appear to be sufficient for the complete *exd* or *Pbx/Hox* interaction. Other regions within the C-terminal end of the homeodomain of the protein also appear to be required for the cofactor-Hox protein-protein interaction. It appears that *exd* may alter the N-terminal arm of the Hom proteins, thereby altering the base pairs with which it interact. Alternatively, *exd* may affect the conformation of the DNA so that the target site-homeodomain contact is altered (for a review of the *Pbx/Hox* interaction see Mann and

Chan, 1996). The body segments in which each of the Hom/HOX proteins affect segmental identity are simply not the result of the expression of each gene within the respective domains. The phenomenon referred to as phenotypic suppression in *Drosophila*, or posterior prevalence in vertebrates occurs when the more posteriorly expressed homeotic genes functionally suppress the more anteriorly expressed genes, and as a result further restrict the functional domains of each Hom/HOX protein (Gonzalez-Reyes and Morata, 1990). The posterior prevalence must function at a level other than transcriptional or translational regulation, because the protein encoded by the gene undergoing suppression is still detected in cells of the more anterior segments. One likely scenario is that suppression may result from competition between the two homeotic proteins for binding sites at the regulatory elements of the effector genes.

It has also been proposed that phosphorylation by kinases may play a role in phenotypic suppression by modifying the effect of selector proteins. The serine / threonine kinase, casein kinase II (CKII) appears to play a role in modifying *Antp* function during development (Jaffe et al., 1997). In general, it appears that the phosphorylated form of the *Antp* protein causes a hypomorphic phenotype and the unphosphorylated form appears to cause a neomorphic phenotype in that it exhibits functions not attributed to ectopic expression of the *Antp* protein. CKII has also been implicated in modifying *engrailed (en)* function by increasing the binding affinity of the phosphorylated form of the protein compared to the unphosphorylated form (Bourbon et al., 1995).

Each of the homeotic selector genes within the HOM-C acts by responding to cells with position-specific cues. This is accomplished by activating downstream genes which then are responsible for providing the segment-specific patterning or characteristic morphology of a particular position along the anteroposterior axis (reviewed in Botas, 1993). The control of these subordinate genes is believed to be at the transcriptional level because of the structural similarities between the homeodomain of the HOM-C genes and the related helix-turn helix motifs of the transcriptional regulators of prokaryotes (Otting et al., 1990).

Genetic examples within *Drosophila melanogaster* show the complex pattern of auto and cross regulation among these genes (Mathog, 1990). Much work has focussed

on the molecular mechanisms of the auto and cross regulation of the selector genes within the HOM-C. In order to initiate and maintain these temporal and spatial patterns of expression within the developing embryo, each gene is equipped with cis-acting regulatory sequences (Lewis et al., 1995; Bender et al., 1983; Celniker et al., 1990).

As has been shown for a number of the homeotic genes, maintenance of their expression requires autoregulation. Again, a good model for the study of genes in terms of autoregulation is the cis-acting regulatory region upstream of the *Dfd* gene. Autoregulation of *Dfd* is required to maintain *Dfd* expression within mandibular and maxillary segments in the head of the developing embryo. Enhancer module E is located 5' to the coding region and is required for proper autoregulation. A single *Dfd* binding site along with a proposed cofactor binding site are both required for proper activation of reporter gene expression *in vivo* (Zeng et al., 1994), making it an excellent system by simplifying the study of regulation at this particular gene. In addition to module E, there are other modules in the 5' flanking genomic region of the *Dfd* gene that are required for proper expression in the developing head structures of the embryo. The sum of the expression from the individual modules fails to represent the expression pattern observed when the elements are linked and tested together, suggesting a cooperative requirement of relevant modules in proper regulation. Several examples of non-homeotic genes that are able to regulate their own expression include *even-skipped (eve)*, *vestigial (vg)* and *tsh* (Jiang et al., 1991; Halder, et al., 1998; de Zulueta et al., 1994). Unlike *eve* and *vg*, the method by which *tsh* regulates its own transcription during embryonic development is still unknown.

Within the last decade, however, the examination of homeotic genes has shifted to molecular analyses of the downstream genes that confer the segmental identity or morphological characteristics within each of the specific segments. The hunt for the target genes of the HOM-C genes goes towards answering how these regulatory proteins can impose positional identity within a developing organism. The homeobox gene *empty spiracles (ems)* has been identified as one of the effector genes for the homeotic gene *Abdominal B (AbdB)*. The *ems* protein is required for the normal development of both the anterior larval head segments and the posterior filzkörper. *AbdB* is required for

proper regulation of the *ems* gene, binding directly to the cis-acting regulatory element identified for proper regulation of *ems* in parasegment 12 (Jones and McGinnis, 1993).

Another example of a downstream gene is the zinc finger, segment-specific homeotic gene, *teashirt* (*tsh*). Two cis-acting regulatory elements have been identified 3' to the coding region. The homeotic response element (HOMRE) requires the binding of *Antp* and *Ubx* proteins for the maintenance of *tsh* expression within the thoracic epidermis of the developing embryo (McCormick et al., 1995). The second regulatory sequence identified downstream of the *tsh* coding region is the *ftz* regulatory element (Core et al., 1997). The activator, *ftz*, is required for proper regulation of *tsh* in the developing embryo. The binding of the HOMRE by the *Ubx abdA* and *AbdB* proteins is required for proper expression of *tsh* within the somatic mesodermal tissues. Activation of *tsh* expression is also observed upon misexpression of *Antp*, suggesting a direct positive regulation of *tsh*. Thus, the *ems* and *tsh* downstream genes and many other identified downstream genes encode regulatory proteins in their own right. The current data thereby present a picture of a cascade of gene expression ending in segment-specific morphology.

Gene Regulation

Proper gene expression is the result of a composite input from all of these cis and trans-acting DNA elements as well as the collection of transacting factors that regulate them. By dissecting a gene into its smallest divisible functional units, represented by cis-acting regulatory elements, gene regulation from the more complex genes can be studied at the simplest possible level. An example of an elaborate collection of cis-acting regulatory elements comes again from the HOM-C and the *engrailed* genes. Herein, we suggest that the *tsh* gene provides another example of such a complex gene. The three genes within the BX-C are responsible for assigning proper segmental identity from parasegment 5 (PS5) to parasegment 14 (PS14), which corresponds to the third thoracic (T3) segment and all the abdominal segments (A1-A9) of the adult (White and Wilcox, 1984; Beachy et al., 1985; Karch et al., 1990; Macias et al., 1990; Celniker et al., 1990; Sanchez-Herrero, 1991). The proper regulation of these genes within these segments is the function of a large array of cis-acting regulatory elements. Proper expression of *Ubx*

in PS5 and PS6 is the result of the *abx/bx* and *pbx/bxd* regulatory modules, respectively. Expression of *abd-A* in PS7 to PS9 requires the regulatory modules *iab2-4*, respectively. The *Abd-B* gene encodes two functions, m and r. *Abd-B* (m function) expression within PS10-13 is achieved by regulatory modules *iab5-8*, respectively. Finally, the *Abd-B r* subfunction is predicted to be expressed within PS14 and PS15. The three genes of the BX-C are found within approximately 300 kb of DNA, of which only a small percentage is coding sequence. The remaining sequence encodes a vast array of cis-acting regulatory modules. The ANT-C mirrors the findings observed within the BX-C. It also presents a large array of regulatory sequences flanking relatively small coding regions, in order to maintain the complex expression pattern. The *en* gene requires 70 kb of 5' flanking genomic sequence for the maintenance of proper expression and regulation during development (Kassis et. al, 1989). The complex expression pattern of the *tsh* gene within the adult and developing embryo overlaps that of the HOM-C genes. It is expressed within the trunk segments of the developing embryo and throughout the adult cuticle, except in distal appendages (Calleja et al., 1996). This suggests that the large non-coding flanking genomic sequence around *tsh* might encode regulatory elements required for its elaborate spatial and temporal expression. As described above, previous analysis has identified two regulatory modules within approximately 25 kb 3' to the coding region. These two elements are responsible for only a fraction of the total expression pattern observed from the enhancer trap allele *tsh*[04319]. The *tsh*[04319] allele is an enhancer trap line resulting from a P{PZ} construct inserted, 5' to the *tsh* coding region. P element-generated *tsh* alleles have already been mapped to both 5' and 3' flanking genomic sequences spanning what is believed to be a distance of approximately 50 kb (pers.comm. Kerridge, S.). To better understand the spatial and temporal regulation of complex genes such as *tsh*, it is essential to dissect the gene into smaller functionally divisible units. One way that this can be achieved is by analyzing each gene in terms of functionally separate tissue-specific enhancers.

The study and identification of these cis-acting regulatory elements has obviously not been restricted to just the HOM-C genes and their target genes. The *vestigial (vg)* gene is an example of a gene consisting of a much less elaborate composite of enhancer elements. The two intron enhancer elements (intron II and intron IV) identified within

the *vg* gene appear to be sufficient for directing the complete expression pattern of *vg* within the presumptive wing and haltere tissues (Williams et al., 1994; Kim et al., 1996). As a result of the characterization of these two enhancer elements, the role of *vg* in terms of the regulation of wing patterning and growth is much clearer.

Cis-Acting Regulatory Elements

Generally, the study of gene regulation has started with the identification of cis-acting regulatory sequences required for the proper spatial and temporal expression of a particular gene and then identification of the transacting factors that are required for the activation of these regulatory elements. The binding of the regulatory proteins to sequence-specific sites acts to regulate gene expression either positively (enhancers) or negatively (silencers or insulator elements). The importance of these elements is obvious in terms of proper regulation and expression of all genes. One of these DNA regulatory elements, the enhancer, was categorized based on its ability to elevate gene expression when present in either orientation with respect to the coding region, upstream or downstream of the RNA start site and independent of distance. In *Drosophila*, enhancer elements have been identified in every possible location with respect to the gene that they regulate. Many examples of tissue specific enhancer elements are currently known. Listed below are only a few examples representing the possible locations of these regulatory elements.

Several examples exist of enhancer elements that are located inside the transcription unit; the *vestigial* gene is one example. *vg* has two wing specific enhancer elements located within the second and fourth introns, the D/V boundary element and the quadrant enhancer, respectively (Williams et al., 1994; Kim et al., 1996). The stripe 2 enhancer of the *even-skipped* (*eve*) gene, which is activated by cooperative binding of the maternal morphogen *bicoid* (*bcd*) and the gap gene *hunchback* (*hb*) protein, is located approximately 2 kb upstream of the transcript start site (Arnosti et al., 1996). The ability to act over large distances is one characteristic of enhancer elements and the *cut* (*ct*) wing margin enhancer, located over 85 kb upstream of its RNA start site, is an example of this type of enhancer (Jack et al., 1991). The *iab5* enhancer element activates gene expression from the *Abd-B* gene within the BX-C. It functions from a position

downstream of the coding region, over 60 kb from the start of transcription (Busturia and Bienz, 1993). The HOMRE and the ftz regulatory elements of *tsh* mentioned earlier represent other examples of downstream enhancers and both are located approximately 20 kb downstream of the *tsh* coding region (McCormick et al., 1995 and Core et al., 1997). A third downstream tissue-specific enhancer element of the *tsh* gene, the *aeroplane* (*ae*) enhancer, is located within 3 kb of the transcription termination site and is the subject of this thesis.

Although several methods have been proposed to suggest how the sequence-specific binding of activators or other regulatory proteins to stretches of DNA can translate into elevated gene expression, the actual mechanisms are still in question. The enhancer directs its regulatory action at the core promoter elements of its cognate gene. The core promoter has been referred to as all those sequence components that are required for a basal level of transcription by RNA polymerase II. The core promoter sequences are located between -40 and +40 relative to the RNA start site. For most protein encoding genes this includes the upstream TA rich TATA box, and the initiator (Inr) element that overlaps the transcription start site approximately 25-35 bp downstream of the TATA box. The position of the Inr with respect to the TATA box is significant because *in vitro* analysis suggests that an increase in the distance between the two elements results in a loss of the synergistic interaction observed between the elements. Both of these core elements are known to act synergistically to increase gene expression upon activation of transcription *in vitro* (Emami et al., 1997). In TATA-less promoters, a conserved Inr is functionally analogous to the TATA box element (Smale, 1997). A third element located between 28 and 34 bp downstream of the Inr is referred to as the “downstream promoter element” (Dpe). The Dpe was shown to cooperate with the Inr element in providing a binding site for the TFIID complex within TATA-less promoters like the downstream promoter of the *Antp* gene (P2) or the internal *jockey* promoter (Burke and Kadonaga, 1996). The Inr and Dpe elements are both required for basal transcription from TATA-less promoters. It has been suggested that the Dpe in conjunction with Inr is a downstream counterpart to the TATA box element in TATA-less promoters (Burke and Kadonaga, 1997) because in the absence of a functional TATA box element the Dpe and the Inr can initiate a basal level of transcription. The distance

between each of the three core promoter elements is also important for the binding of the TFIID complex and transcriptional activation. For a review of all core element components see Orphanides et al. (1996).

Two possible models have been proposed to explain the mechanism by which enhancers, when given a choice, exhibit promoter selection. Because enhancers can act over large distances (like the *ct* wing enhancer), there is an increased probability that the enhancers would overlap or be very near the boundaries of another gene and the enhancer elements of that gene. The AE1 enhancer element is located between the *Scr* and *fushi tarzu* (*ftz*) genes of the ANTP-C and equidistant from each (approximately 7kb). Yet the AE1 enhancer element only activates transcription from the *ftz* promoter (Gorman and Kaufman, 1995). The IAB5 enhancer element is located between the *abd-A* and *Abd-B* genes of the BX-C approximately 60 kb from either locus. The enhancer recognizes the *Abd-B* promoter and not that of *abd-A* (Busturia and Bienz, 1993). Therefore, there must be a way in which enhancer elements can differentiate between equally distant alternative promoters. One suggestion is that differences between the core promoter elements provide a method of promoter selection. Structural and functional differences between the core promoter elements such as TATA or TATA-less promoters, the presence or absence of Dpe elements, Inr elements, and variations on the sequences of all core elements likely play a role in promoter selection (Burke and Kadonaga, 1997). The AE1 enhancer from the ANTP-C and the IAB5 enhancer from the BX-C have been shown to prefer the Type I or TATA box element-containing promoter whereas the NEE enhancer doesn't discriminate between Type I, Type II or TATA-less promoters (Ohtsuki et al., 1998). The binding of the TFIID complex depends on the combination of the three different core elements in the promoter. The combination of the different core elements is known to affect the way in which the TFIID complex contacts the promoter and, as a result, presumably affects the shape of the TFIID complex. A change in the conformation of the complex at different promoters as a result of the promoter could then provide the activator-enhancer complex with a more desirable conformation for the promoter-enhancer interaction at one promoter versus another. The conformation of the TFIID complex could also depend on the presence of different tissue specific TAFs associated with different core promoters, leading to a conformational change in the

complex at the promoter. A combination of the differences at the core promoter and the binding of associated promoter-specific regulatory factors may restrict the enhancer-activator complex choice to one of these groups of regulatory factors, thereby limiting promoter activation to only one of the genes. One interesting observation that came out of the promoter selection studies was the ability of one promoter to block the activation of distal promoters. This occurred when identical promoters (*eve*) were used for the analysis (Ohtsuki et al., 1998). This result would suggest that the enhancer-activator, promoter-regulatory complex is not a transient association. This, however, was not a feature observed for all enhancer studies when two different enhancers were used.

A second method of promoter selection could result from the placement of insulators or boundary elements between the enhancer and undesirable promoters. The insulators prevent enhancer-promoter interaction without affecting the function of either element. The best characterized insulators or boundary elements from *Drosophila* are the gypsy retrotransposons that act as artificial boundary elements within the *Fab 7* region of the BX-C, the boundary element from within the *Mcp* region located between the *iab4* and 5' cis regulatory units, and the *scs* and *scs'* elements from the 87A1 *hsp70* gene (Mihaly et al., 1997; Geyer and Corces, 1992; Kellum and Schedl, 1992). The boundary element identified within the *Fab7* region of the BX-C insulates the parasegmental-specific cis-regulatory regions of the *iab-6* and *iab-7* domains. These regulatory domains are required for the parasegmental-specific initiation and maintenance of the short *Abd-B* transcription unit within PS11 and PS12, respectively (Mihaly et al., 1997). Within each of the cis-regulatory domains of HOM-C genes, two separate positive regulatory functions exist for the initiation and maintenance of the parasegmental-specific expression patterns. Parasegmental identity is initiated by activation of HOM-C expression through the binding of the transcription factors encoded by the gap and pair-rule genes (Irish et al., 1989; Riley et al., 1991; Jack et al., 1988; Martinez-Arias and White, 1988). The transcription factors initiate activation of the HOM-C genes by binding the cis-acting elements. Once expression of the gap and pair-rule genes has been terminated and the proteins have degraded, the imprinting of chromatin conformation and the maintenance of the HOM-C gene expression throughout the rest of development falls under the negative control of the *Polycomb* group genes and the positive control of the

trithorax group genes. The containment of negative regulatory functions is maintained within specific parasegments by the function of the boundary elements. The 340 base pair fragment containing the 12 *Suppressor of Hairy wing* (*Su(Hw)*) binding sites from within the gypsy retrotransposon and the scs boundary elements have similar enhancer-blocking abilities when tested in combination with the *eve* stripe two and three enhancers (Small et al., 1992). When placed between the promoter and a distal enhancer, both boundary elements failed to affect the ability of the enhancer to activate more distal promoter elements. This suggests that the influence of boundary elements on the promoter-enhancer interaction is not affecting the chromatin structure, because the distal enhancers are still capable of activating expression of more distal promoters (Cai and Levine, 1995). Interestingly, the boundary elements tested do not block the negative effects of the *zen* silencer element on the promoter-enhancer interaction. The method of promoter selection, however, is likely a combination of both the negative affects of the boundary elements and the particular promoter profile.

Two promoter models presently used to explain enhancer function on promoter regulation are the probability model and the progressive model (for review see Blackwood and Kadonaga, 1998). The probability model suggests that the level of transcription from a particular promoter be not affected when activated by an enhancer. The activity of the enhancer increases the probability that a particular promoter will be transcriptionally active. The level of transcription from a promoter in this model is therefore a function of the promoter or results from the strength of the promoter. The model states that an increase in the enhancer activity would increase the probability of any one cell within that population to activate transcription at that particular gene. However, the level of transcription in a single cell would not change as a result of an increase in enhancer activation but only the number of cells expressing that gene would change. Therefore, the mode of gene regulation for this model is either on or off. The second possible model used to explain enhancer function is the progressive model. This model suggests that the level of transcription is a function of the enhancer, not the promoter as the first model implies. Therefore, the level of transcription is a consequence of the level of activation from the enhancer. An increase in enhancer activity would lead

to an increase in the level of transcription from that particular gene in all cells within a population.

In order for the activator bound enhancer to direct its function on the promoter, there must be a method by which the enhancer can identify and regulate the promoter sequence. The functioning of the enhancers is the result of forming contacts between the DNA-binding-factor-enhancer complex and the DNA-binding-factor-promoter complex. As a consequence of enhancer activation, it is also likely that modifications to proteins associated with the chromatin structure and the transcriptional machinery take place. For example, the acetylation of histones and basal transcription factors has been observed in activated promoters. The acetylation of histones has been implicated in the relaxation of transcriptional repression associated with the chromatin structure. Although the structure of chromatin provides a substrate for accurate long distance enhancer-dependent promoter activation, the action of enhancers has also been associated with counteracting the effects of chromatin repression by destabilizing chromatin structure. Enhancer activation may also be associated with a remodeling of nucleosomes, which controls the accessibility of binding sites for transcription factors required for activation of core promoter sequences (reviewed by Kingston et al., 1996). The non-random distribution of active and inactive genes within the nucleus of eukaryotes suggests that the nuclear substructure may play a role in localization of promoter-enhancer complexes to areas within the nucleus that are conducive to activation of promoters, because of pools of localized regulatory factors. The active genes are often associated with the periphery of the distinct regions referred to as chromosomal territories. The enhancers may play a role in this non-random distribution within the nucleus (Lamond and Earnshaw, 1998).

To date, the best supported model to account for the method by which enhancers function in the regulation of promoter activation is the facilitated tracking model. The enhancer bound by its DNA binding factors and proposed co-activators moves along the chromatin in small steps until it reaches a suitable promoter. Once a promoter has been found, a stable loop associated with enhancer activation is established (Ptashne and Gann, 1997). The stable loop is thought to form after the enhancer-promoter complex is established, rather than forming this complex as a result of the stable loop.

Transvection

Enhancer sequences have also been used to explain one method by which transvection phenomena can occur (reviewed by Henikoff and Comai, 1998). Transvection, initially identified in *Drosophila* (Lewis, 1954), is an interaction whereby correct somatic pairing of two homologues is required for proper regulation at a particular gene. This pairing-dependent regulation can also be used to explain some examples of intragenic complementation whereby mutations within the same gene are able to complement one another. The method by which transvection occurs has been studied extensively at the *yellow* (*y*) locus (Morris et al., 1998). Mutations within the *y* gene that render tissue specific enhancer sequences unable to regulate the promoter in cis are shown to be able to regulate the paired homologue via transvection. The question of how transvection is regulated was examined, and it appears that an enhancer element has a preference for promoters in cis. This preference for cis promoters excludes transvection from occurring with respect to enhancers in trans. It has been shown that a core promoter element, the TATA box can regulate transvection. The presence of a functional TATA box in cis to the adult cuticular tissue specific enhancers (body, wing and bristle) prevents transvection. Removal of the wild type TATA box sequence, with the use of targeted gene replacement, allowed transvection to take place (Morris et al., 1999). Another promoter core element of the *y* gene was found to regulate transvection in the same way that the TATA box does. The putative initiator (Inr) that includes the transcription start site was mutagenized and also shown to induce transvection. It has been proposed that transvection at the *y* gene could occur in two ways. The first is related to transcriptional strength of a particular promoter and the second is independent of transcriptional activity and is dependent on locus topology. One interesting observation arose from work dealing with transvection at the *Ubx* gene. It appears that somatic pairing leads to elevated expression from both homologues in a wild type fly in addition to the regular cis activation observed from the wild type gene (Goldsborough and Kornberg, 1996). This suggests that transvection is occurring at the same time that cis-acting regulation is occurring.

The method by which tissue specific enhancers regulate expression from a particular gene goes towards explaining how transvection occurs. With respect to the

first possible mode of transvection at the *y* locus, enhancers have a preference for *cis* promoters, but once a promoter is made non-functional by mutations this allows the enhancers to seek out the next available promoter. Differences in promoter strengths are believed to play a role in enhancer preferences. A reduction in transcriptional efficiency from a particular promoter as a result of mutations in the core sequences, attributable to the destabilization or a reduced binding affinity of transcriptional associated proteins, allows the enhancers to seek out stronger promoters. Differences in core promoter strengths have been observed *in vitro* based on the presence of core promoter elements. The presence of the Inr element promotes elevated levels of expression from TATA containing promoters due to a synergistic interaction between the two elements (Emami et al., 1997). The destabilization of a promoter complex would create a weaker promoter. Even though the preference would be to seek out another promoter in *cis*, the promoter in *trans* may have the protein complex that is attractive to the enhancer. At the *y* locus, however, it appears that even when transvection does occur, the enhancers are also capable of acting in *cis*, albeit with a less desirable promoter (Morris et al., 1999).

The second mode of transvection may be unrelated to transcriptional activity but rather due to the topology of a particular locus. Thus, the accessibility of a particular promoter may also play a role in promoter choice. By the displacement of a promoter from its *cis* enhancer, a promoter in *trans* may become more favored due to proximity to the enhancer. Transvection could also be affected by the way in which a particular chromosome is packaged, such as in the scaffold. As a result of a rearrangement, the folding of the chromosome may become more conducive to an intermolecular interaction between an enhancer and promoter.

The “scanning” model of enhancer function predicts that the enhancer-activator complex moves along the chromosome in *cis*, scanning for desirable promoters. The “facilitated tracking” model however can explain transvection phenomena where the scanning model is unable to (Blackwood and Kadonaga, 1998). The major difference between the two models is the small steps or jumps that are made in the “facilitated tracking” model. In the “DNA scanning” model the enhancer-binding-factor complex slides along the DNA seeking a suitable promoter. This model would not permit the movement of the enhancer complex to a closely synapsed homologue for promoter

regulation in trans. The facilitated tracking model, however, allows for the activation of transcription in trans because of the ability to jump along the chromosome.

Pattern Formation

Pattern formation resolves a developmental field into discrete domains. In the study of *Drosophila melanogaster* development, embryogenesis has been used to examine pattern formation. Within the embryo a positional coordinate system is established with the use of maternal gene products. These form a concentration gradients within the syncytial blastoderm, along both the anteroposterior and dorsoventral axes (reviewed by St. Johnston and Nusslein-Volhard, 1992). Subdivision of the embryo along the anteroposterior axis and specification of head, thoracic and abdominal structures requires the formation of monotonic gradients of the proteins translated from maternally deposited *bicoid* and *hunchback* mRNAs (Struhl et al., 1992). These proteins are at the top of a cascade of transcription factors, which leads to an increasingly narrowed spatial expression of gene products required for proper metamer organization and pattern formation of the developing embryo (reviewed by St Johnston and Nusslein-Volhard, 1992).

A problem with studying the process of pattern formation in early embryogenesis is that the subdivisions of these developmental domains occur in the multi-nucleated syncytium. The processes involved in pattern formation of multicellular organisms would likely differ from that of the syncytium because of the obvious constraints on morphogen diffusion. However, for the study of pattern formation in a multicellular field, the imaginal discs provide an excellent model.

Pattern formation of the adult epidermis in *Drosophila melanogaster* has been studied extensively in the wings and legs. Wings have been used to study pattern formation for a number of reasons. The wings are non-essential and subtle alterations to gene expression within this organ can lead to visible structural defects of a number of different pattern elements including the triple row of bristles of the wing margin, the wing veins, sensory bristles and the elements of the wing hinge. In the wing and haltere imaginal disc, progenitor cells of the adult organs can be identified during early embryogenesis by cells that express the *vestigial (vg)* gene (Williams et al., 1991).

The wing primordia are specified early in embryogenesis, arising from an invagination of the embryonic epidermis at the parasegmental boundary. A wing primordium during dorsal closure consists of a group of approximately 30 cells, and by the end of third instar the wing discs are comprised of approximately 52000 cells. In order to achieve the characteristic pattern elements of the adult wing and its homologous structure the haltere, the developmental compartments must first be established. The compartments are defined by the establishment of a cell lineage restriction, whereby the cells of one compartment are restricted from mixing with those of another based on the expression of a selector gene which specifies a particular developmental fate in one of the groups of cells (Garcia-Bellido, 1975). The wing becomes compartmentalized in a binary fashion. The developmental compartments are defined by either the expression or non-expression of a selector gene. The compartments arise within the imaginal wing disc by the creation of the Antero-Posterior (A/P) and Dorso-Ventral (D/V) axis (Garcia Bellido et al., 1976).

The A/P axis of the wing is established during embryogenesis as early as the cellular blastoderm stage. The wing disc primordia arise from two groups of cells that flank the parasegmental boundary, such that each of the cells that will form the wing has already been specified as anterior or posterior in fate prior to invagination and formation of the wing disc. The segment polarity gene *en* encodes a homeodomain protein that is expressed within the posterior parasegments in the developing embryo and has been shown to function as the selector gene for the establishment of the posterior compartment. Cells within the wing disc expressing *en* and *invected* (*inv*) are specified as posterior cells while those that fail to express these genes assume the anterior cell fate (Sanicola et al., 1995). . Thus, these two groups of cells within the wing disc inherit the A/P positional cues (*wg* and *en* expression) from their location within the segment pattern of the embryo (Cohen et al., 1993).

Both the A/P and D/V boundary act as organizing centers for growth and pattern formation of the developing wing (Brook et al., 1996). Both organizing centers act synergistically to promote formation of the proximal-distal axis in the developing wing. This requires communication between the anterior and posterior compartments as well as the dorsal and ventral compartments. The communication between the anterior and

posterior compartments is initiated by posterior, *en*-expressing cells. *en* activates expression of the secreted protein encoded by the segment polarity gene *hedgehog* (*hh*) (Tabata et al., 1992). The *hh* protein acts as a posterior signal for the induction of expression of the secreted Transforming Growth Factor-B family (TGF- β) protein, *decapentaplegic* (*dpp*). The *dpp* morphogen then functions to organize the A/P axis from the anterior side of the A/P border (Nellen et al., 1996). *hh* is unable to induce *Dpp* expression in posterior cells because of the negative affect *invected* (*inv*) and *en* play in making the posterior cells unresponsive to the signal. Just inside the anterior compartment at the A/P boundary, *hh* activates the expression of *dpp* resulting in a gradient of *dpp*. *Ci*, which is expressed throughout the anterior compartment of the wing disc, activates *hh*-specific downstream targets. In the presence of the *hh* signal, *Ci* regulates the *hh* specific target genes such as *patched* (*ptc*) and *dpp* (Aza-Blanc et al., 1997; reviewed in Ruiz i Altaba, 1997). In the absence of the *hh* signal, the *Ci* protein is proteolytically processed forming a repressor (*Ci75*) which inhibits the activation of *Ci*-regulated genes.

The D/V compartment boundary also plays a role in the establishment of an organizing center for the pattern elements of the wing. Unlike the A/P compartments, the D/V compartments are set up *de novo* and arise during early second instar. Prior to the formation of the D/V boundary, *wg* is expressed in cells that correspond to the ventral wing (Couso et al., 1993). The D/V compartments are also the outcome of a binary decision resulting from the differential expression of a selector gene. Expression of the LIM-homeodomain protein *apterous* (*ap*) in early second instar wing discs specifies cells to take on the dorsal fate and the non-*ap* expressing cells assume the ventral fate (Diaz-Benjumea and Cohen, 1993). This juxtaposition of *ap* and non-*ap* expressing cells initiates a complicated and dynamic set of interactions within the imaginal wing discs from second to late third instar (review Irvine and Fogt, 1997).

A simplified, but not complete, view of D/V patterning and growth is as follows. During second instar this juxtaposition of *ap* expressing and non-expressing cells leads to the expression of *Serrate* (*Ser*), the *Notch* (*N*) ligand, and the secreted protein *fringe* (*fng*) in dorsal cells (Kim et al., 1995). The general wing disc expression of *Delta* (*Dl*), another *N* ligand, is slightly higher on the ventral side. *fng* has opposing functions for the

two ligands by modulating the ability of *N* expressing cells to respond to the ligands. In the dorsal cells, *fng* enables *N* expressing cells to respond to *Dl* but not to the *Ser* signal. This activates the *N* signaling pathway in ventral cells by the *Ser* ligand in a dorsal to ventral direction, and activation of *N* signaling in dorsal cells by *Dl* in a ventral to dorsal direction. The *Ser*-dependent activation of the *N* pathway along the D/V boundary in third instar wing discs then activates the expression of *wg* and *vg* along the D/V border (Kim et al., 1995 and 1996). Later, *wg* along the D/V boundary, regulates the expression of *Dl* and *Ser* in flanking cells, and in turn *Dl* and *Ser* down-regulate D/V specific *wg* expression. *Ser* and *Dl* proteins are kept from the D/V border by activating expression of the homeodomain protein *cut* (*ct*) along the D/V boundary (Neumann and Cohen, 1996). *ct* then acts to inhibit expression of *Ser* and *Dl* near the D/V boundary, but also helps to maintain *wg* expression along the border. *vg*, which is required for patterning and growth of the wing, is initially activated along the D/V margin by the transcription factor *Suppressor of Hairless* (*Su(H)*) as the result of the *N* signalling pathway. Shortly thereafter, expression of the *vg* protein is initiated throughout the wing pouch by the activation of the quadrant enhancer via the two morphogens originating from the D/V and A/P margins, *wg* and *dpp* respectively (Kim et al., 1996). However, activation of *vg* via the quadrant enhancer also requires its own expression along the D/V boundary. This convergence of two axes on the regulation of *vg*, a gene known to be required for growth and patterning, appears to focus both axes on the formation of the proximal distal axis of the wing (Kim et al., 1996).

The intersection of two different compartment boundaries leads to an organizing center, which can function as a focal point for patterning and cell growth. As previously discussed, the A/P and D/V boundaries between the two respective compartments lead to the formation of the proximal/distal axis of the developing wing. The identification of this third boundary, established between the wing and notum, is laid down at approximately the same time as the D/V compartment boundary. The establishment of the three separate compartment boundaries resolves the wing into eight different developmental units (Garcio-Bellido et al., 1976). A third organizing center for the proliferation and pattern formation was suggested to exist in the wing hinge (Ng et al., 1995). The *nubbin* (*nub*) or *pdm-1* gene encodes a transcription factor that belongs to the

POU protein family, possibly representing a downstream mediator of an organizing center located within the wing hinge, analogous to the D/V organizing center for wing proliferation and patterning. The wing is divided into three separate domains, the wing margin, blade and the hinge. The wing and halteres each have characteristic reproducible pattern elements (**Figure 1 and 2**). The wing hinge can be further subdivided into three subdomains: the proximal, medial and distal costa (Bryant, 1975). Clonal analysis suggests there is a requirement for *nub* within the wing hinge for growth and pattern formation of the entire wing. Loss of function *nub* alleles led to a loss of pattern elements from the medial and distal costa regions of the hinge. Loss of function *nub* mutant clones originating in the hinge exhibit a dramatic non-autonomous loss of wing tissue not resembling any mutations in genes involved in establishing the organizing centers of the D/V or A/P compartment (Ng, et al., 1995). Loss of function *nub* alleles also lead to a reduction in *wg* expression from the hinge region in third instar wing discs as visualized through the *wg-lacZ* reporter gene expression. This may represent a novel organizing center for growth and pattern formation within the wing. Hinge specific defects have also been observed in the *tsh* regional null mutant, *aeroplane (ae)* (presented herein). However, the location of the defects in the *ae* mutant are in the proximal costa, in a region that is not affected in the *nub* loss of function mutants.

Adult Cuticle Formation

The investigation of thoracic or abdominal cuticular pattern formation in *Drosophila* has been relatively neglected until recently (Calleja et al., 1996). Precursors to the adult structures arise and are determined from embryonic tissue and are selected and separated from the larval precursor cells by the invagination of the epithelial layer. At the onset of pupariation the imaginal discs undergo morphogenesis, and eventually give rise to a continuous layer of adult epithelium. Each disc is a continuous layer of diploid epithelial cells amongst surrounding larval polyploid cells. Each disc appears as a sac of epithelial cells with characteristic morphologies such as size, shape, folding, and position within the larvae. Within the folded disc proper, the cells are columnar in shape while the cells on the peripodial membrane side appear squamous (Fristrom, 1976). Disc

Figure 1. A diagram of the wing hinge taken from Bryant, (1978). **A)** and **B)** Represent the dorsal and ventral view of the wing hinge, respectively. The abbreviations are as follows; PAA; prealar apophysis , ANWP; anterior notal wing processes, UP; unnamed plate, Teg; tegula, HP; humeral; plate, Pco; proximal costa, Mco; medial costa, Dco; distal costa, HCV; humeral cross veins, SS; scuto-scutellar suture, IS; intrascutal suture, PNWP; posterior notal wing processes, ASI, 2, 3, 4; axillary sclerite 1-4, AC; axillary cord, PVR; proximal ventral radius, YC; yellow club, TR; triple row of bristles (anterior margin), AL; alar lobe (alula), PWP; pleural wing process, BS; basalar sclerite and AP; axillary pouch, PR; posterior row, respectively.

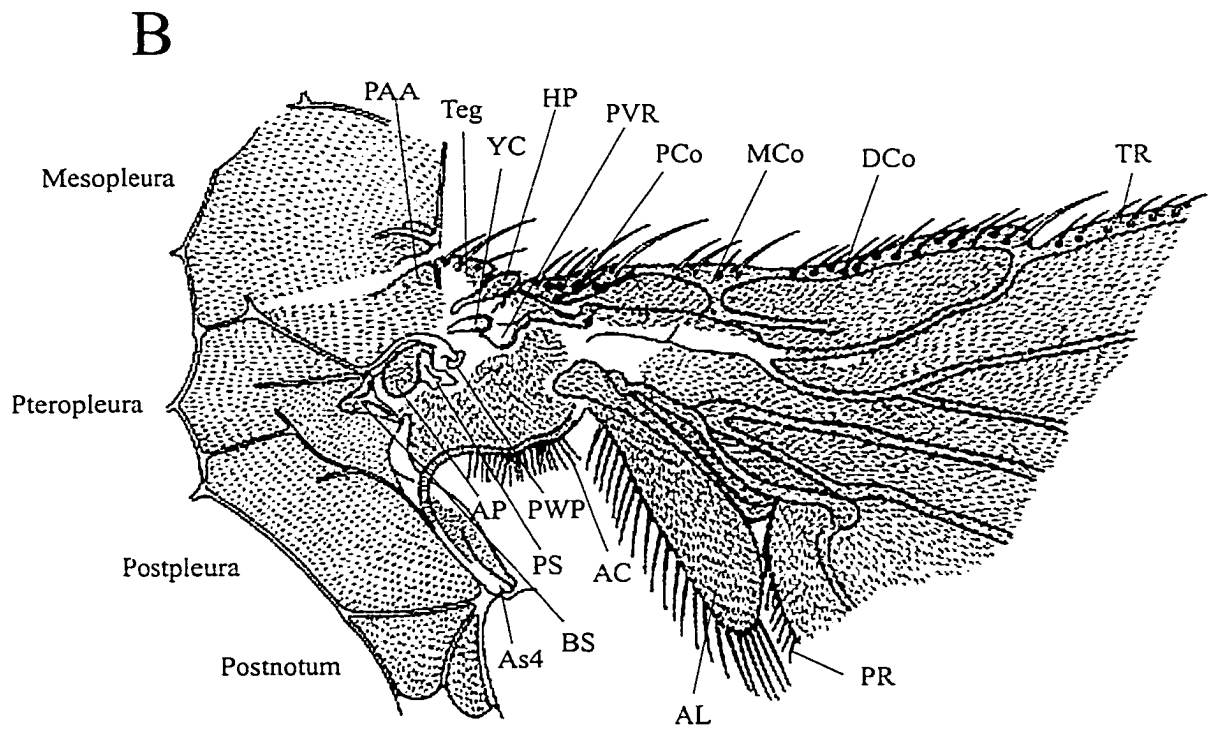
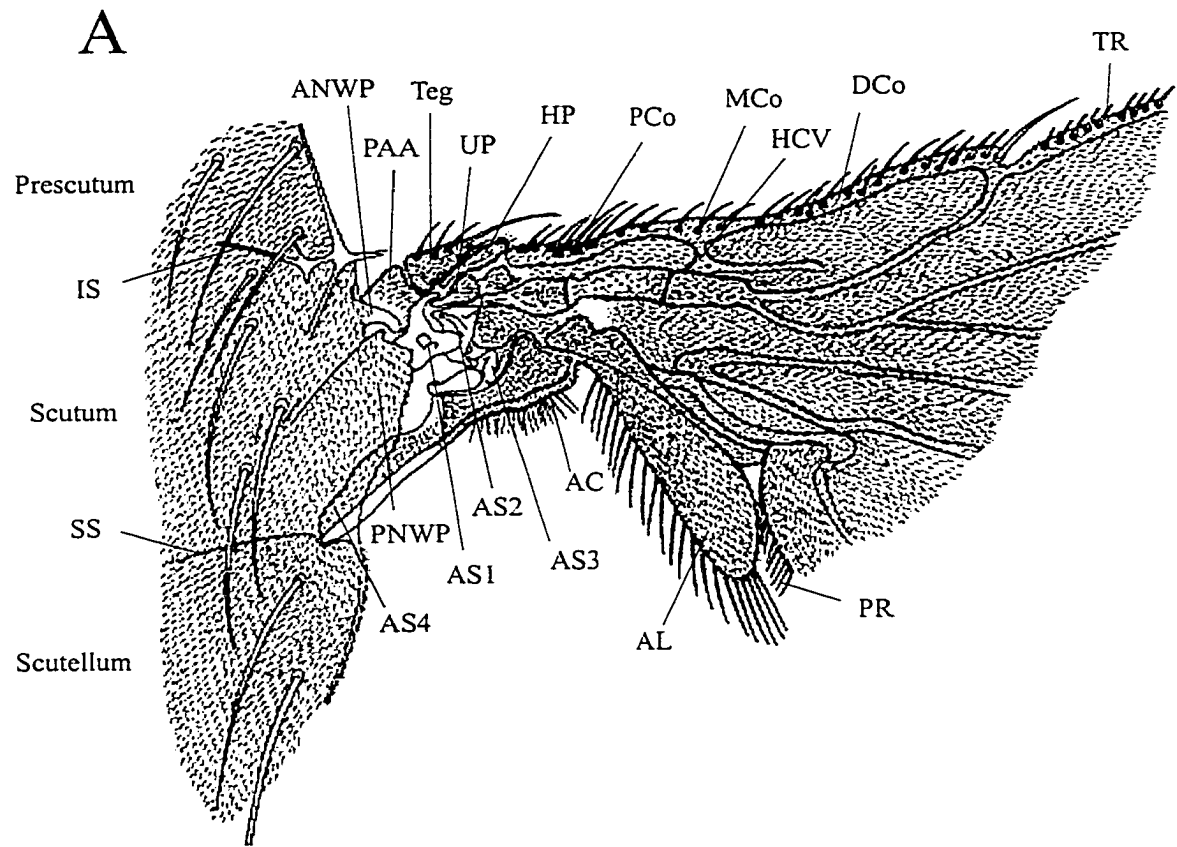
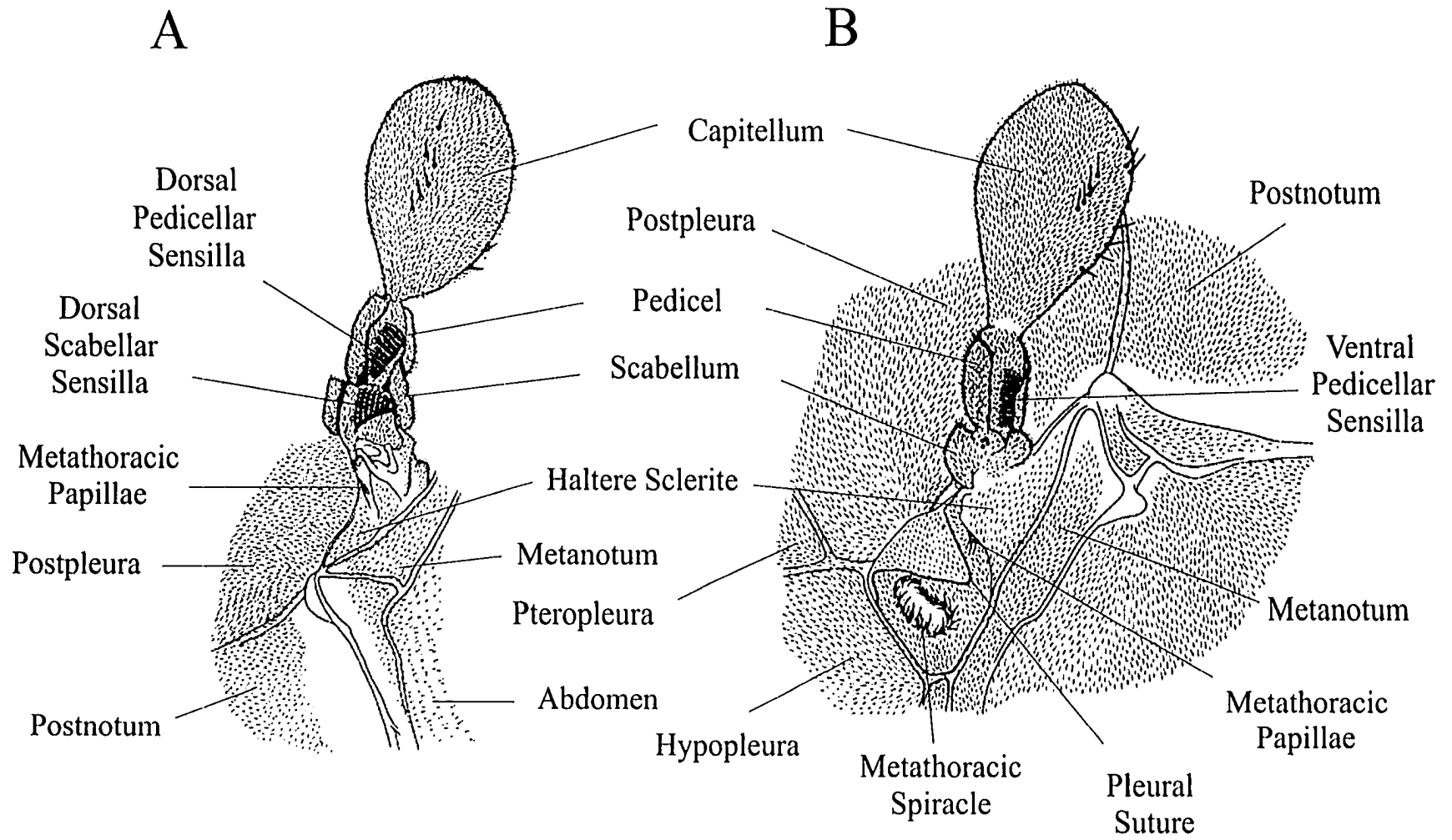


Figure 2. A diagram of the haltere taken from Bryant, 1978. **A)** and **B)** represents dorsal and ventral views of the haltere, respectively. Each of the relevant features is marked on the Figure.



transplantation experiments have produced a detailed map of the imaginal tissues and the corresponding adult tissues that they give rise to (Bryant, 1978). Although the disc proper side of each of the imaginal discs are generally credited with the production of adult tissues, the peripodial membrane side also contributes to the adult epithelium and resulting cuticle by contributing to the tissues that lie between those that arise from the disc proper side of the imaginal discs. The inner or apical surface of each of the discs everts and gives rise to the adult epidermis, which is responsible for the secretion of two layers of cuticle. The first is the pupal cuticle layer, which is deposited during pupariation at around 18 hr APF (after puparium formation). This cuticle layer then undergoes apolysis, creating a separation between the epidermis and the cuticle. The pupal cuticle forms the transparent layer between the pupal case and the developing adult. The separation created between the adult and the cuticle and the epidermis allows for the deposition of the second cuticle layer. This adult cuticle will be the visible exoskeleton seen in the mature adult, including the characteristic bristle patterns observed covering the cuticle. The adult cuticle deposition is complete by 80hrs APF (25°C). The regional specific defects associated with cuticle formation or deposition can therefore be traced back to the epidermis arising from the respective imaginal discs. A complete review of the adult epidermis and cuticle deposition and formation can be seen in Fristrom and Fristrom (1993).

Wingless Signaling

Patterning in the embryo and limbs of both insects and vertebrates requires the wingless (Wg)/Wnt signaling pathway. The reiterated pattern of denticle belts on the ventral side of the *Drosophila* embryo and the wing margin-specific bristle patterning both require the function of the secreted protein encoded by the *wingless (wg)* gene (Phillips and Whittle, 1993; Couso et al., 1994). Members of the Wnt protein family are secreted glycoproteins. The *Drosophila wg* protein acts as a morphogen, a diffusible factor that can affect cell identities in a concentration dependent manner. The *wg* protein has been detected up to 25 cell diameters from its source at the presumptive wing margin. The best example showing *wg* as a morphogen is seen in the third instar wing discs where the *wg* target genes, *Distal-less (Dll)*, *vg*, and *achaete (ac)* are differentially activated in a

wg protein concentration-dependent manner (Neumann and Cohen, 1997). In the embryo, *wg* is expressed in the anterior compartment of every parasegment and is required for establishing and maintaining *en* expression in the posterior compartment of each parasegment (Bejsovec and Martinez-Arias, 1991). The expression of *wg* in the developing wing evolves from the expression pattern seen from first to early third instar where it is confined to the tissues that will give rise to the wing (Williams et al., 1993). The pattern then changes to a pair of concentric circles surrounding the presumptive wing blade, and the inner circle of expression is bisected by the *wg* expression along the presumptive wing margin (Phillips and Whittle, 1993). Many of the players involved in the *wg* signal transduction pathway have been identified through genetic analysis and others through the use of cultured cell studies. The *wg* protein requires the function of the transmembrane protein encoded by the *porcupine* (*porc*) gene which appears to aid in post translational modifications of the *wg* protein (Kadowaki et al., 1996). One of the proposed *wg* receptors is a transmembrane protein that belongs to the *frizzled* family of proteins. The *Drosophila frizzled 2* (*Dfz2*) protein binds the *wg* protein and is able to transduce the *wg* signal in cultured cells (Bhanot et. al 1996). The examination of the *wg-Dfz2* relationship in the wings has shown that *Dfz2* creates a negative feedback loop where its repression is dependent on the *wg* signal. *Dfz2* acts by stabilizing the *wg* protein signal for transduction of the *wg* signal (Cadigan et al., 1998). The receptor presumably transduces the signal through the cytoplasmic *disheveled* (*Dsh*) protein. This is a PDZ (protein interaction domain)-containing protein that undergoes phosphorylation and may act as a modular protein in conjunction with other components of the *wg* pathway (Willert et al., 1997). *Dsh* then presumably either directly or indirectly negatively affects the serine/threonine kinase function of the *Shaggy / zeste white 3* (*zw3*) protein. *zw3* is involved with the repression of the *armadillo* (*arm*) protein, by destabilizing the protein. The action of *zw3* protein kinase to negatively regulate *arm* is unlikely to be a direct one, because *in vitro* analysis has indicated that there is no direct interaction between the two proteins and the kinase activity is unable to phosphorylate the protein *in vitro*. Two forms of the *arm* protein exist, one associated with the cytoskeleton and the other a cytoplasmic form. Both are encoded by the same gene but result from alternatively spliced exons (Orsulic and Peifer, 1996). It is predicted the

protein is sent down the proteasome ubiquitin degradation pathway as the result of phosphorylation of conserved serine/ threonine kinase phosphorylation sites in the N terminal end of the protein (Aberle et al., 1997; Pai et al., 1997). The unphosphorylated, stabilized form of the *arm* protein is then free to associate with the ubiquitous DNA-binding transcription factor *Drosophila T-cell factor (DTcF) / Pangolin* which regulates the *wg* target genes (Brunner et al., 1997). The *arm/DTcF* complex then can bind cis regulatory elements of the *wg* target genes such as *en* and *Ubx* in the embryo or *vg*, *Dll* or *ac* in the wing (Bejsovec and Martinez-Arias, 1991; Neumann and Cohen, 1997).

The hypophosphorylated form of the *arm* protein is also associated with a hypophosphorylated form of the regional specific homeotic gene, *tsh*. Patterning of the ventral ectoderm during embryogenesis requires *tsh* for *wg* signaling (Gallet et al., 1998). *tsh* binds the C-terminal trans-activating domain of the *arm* protein and leads to an increase in the nuclear localization of *tsh* in cells with stabilized *arm* protein. The phosphorylation of the *tsh* protein is in part dependent on the *wg* signal pathway. However, there appear to be other kinases independent of the *zw3* protein kinase that also acts on the *tsh* protein. The hyperphosphorylated form of the *tsh* protein is found to accumulate in the nucleus. The nuclear accumulation of *tsh* protein is dependent on the function of *zw3*, with which the product of the *tsh* protein has been shown to associated *in vivo*. However, it is not known if *zw3* is the kinase directly responsible for *tsh* phosphorylation (Gallet et al., 1999). Both *tsh* and *arm* accumulate in the nuclei of cells that will give rise to naked cuticle.

A positive regulatory feedback loop involving *en* and *wg* ensures that *en* expressing cells maintain *wg* expression across the parasegmental boundary. As in the establishment of the A/P compartment boundary in the wing, *en*-expressing cells secrete the *hh* protein across the parasegmental boundary. The *hh* signal binds to the *patched (ptc)* transmembrane receptor protein on the anterior target cells but requires the formation of the *Smoothened/ Patched* receptor complex for the transduction of the signal into the cell. The *hh* signal is transduced via a large complex consisting of protein products from *Ci*, *fused (fu)* and *Costal2 (Cos2)*, reaching the nucleus and activating the expression of *hh* specific target genes such as *wg* in embryonic segments and *dpp* in the leg and wing imaginal discs (Sisson et al., 1997; Robbins et al., 1997).

The *wingless* expression pattern within third instar larval wing discs resembles a θ . The two rings of *wg* expression correspond to tissues that will give rise to both dorsal and ventral presumptive wing hinge (Bryant, 1975). As described above, *tsh* plays a role in modulating *wg* function in the embryo. Also, *lacZ* reporter constructs of *tsh* and *wg* have shown that in pharate adults the expression of both genes can be detected within the wing hinge (Calleja et al., 1996; Soanes et al., submitted). Interestingly, the domain of expression observed from a *wg lac Z* reporter gene in the distal costa region in pharate adults is close to the most distal domain of expression observed for the *tsh* [04319] enhancer trap line. The requirement for *wg* function in the developing hinge, the expression observed in third instar wing discs in the presumptive wing hinge, the expression detected in the hinge of the pharate adults, along with the proposed role of *tsh* in *wg* signaling in the embryo, all suggest a possible functional relationship between *wg* and *tsh* in the developing adult wing hinge as well. The *ae* enhancer, the subject of this thesis, is also activated by the time in second instar when *wg* is activated in tissues destined to give rise to wing as opposed to notum tissue (Williams et al., 1991; Ng et al., 1996).

Wing Posture Mutants

Mutations that affect wing posture in *Drosophila melanogaster* are quite common possibly due to the sensitivity of the muscle or neuronal balance to subtle changes. A list of only a few of these posture mutants include, *taxi* (*tx*), *bent^D* (*bt^D*), *dv* (*divergent**), *divergent wings* (*dvw**), *erect wing* (*ewg*), *outspread* (*os*), *angle wing* (*ang*), *eagle* (*eg*), *spread* (*spr*), and *IFM(2)-11* (Lindsley and Zimm, 1992). A review of the literature for abnormal wing posture mutants quickly reveals a common etiology for these types of mutants. Most of the mutations that have been studied in any detail point towards defects in either musculature or neuronal abnormalities.

The dominant “wings held up” posture associated with the dominant Indirect Flight Muscle mutant, *IFM(2)-11* is not completely penetrant. This mutation was isolated as a dominant flightless mutant along with many others. Subsequent analysis of the indirect flight muscle proteins using two dimensional gel electrophoresis revealed alterations to the myofibrillar protein profiles (Mogami and Hotta, 1981). Except for

alterations of protein profiles, the actual cause of the abnormal wing posture was not determined.

The *bent Dominant* (*bt^D*) gene was also identified based on an abnormal “bent” wing posture. This recessive lethal mutation is the result of an inversion in the coding region of the projectin gene. One break point lies within the coding region and causes a deletion of the kinase domain found in the COOH end of the protein. The projectin protein has been identified within all the muscles of *Drosophila*, in both synchronous and asynchronous types. In the two different types of muscle, however, different isoforms of the protein are localized to different regions of the sarcomere. Analysis of homozygous *bent^D* embryos suggests that the deletion of the COOH terminal end of the protein likely affects the efficiency of contraction rather than the contraction itself (Ayme-Southgate et al., 1995). These results are not unexpected because of the identification of other wing posture mutants that are associated with other mutations in muscle proteins (Mahaffey et al., 1985; Beall and Fyrberg, 1991; Deek, 1977).

Another wing posture mutation associated with musculature or neuronal defects is the *erect wing* (*ewg*) mutation (Fleming et al., 1983). The *ewg* gene encodes a nuclear protein that most closely resembles a DNA binding protein similar to those identified in mammals and sea urchins. Although most *ewg* alleles are embryonic lethals, certain combinations are viable and exhibit an abnormal wing posture where both wings are held out and away from the body. This phenotype is associated with a drastic reduction or a complete loss of the indirect flight muscles (IFMs). The *ewg* gene appears to play two roles in development. The first is an essential role during embryogenesis where it is required in all embryonic neuronal nuclei. The second is involved in the development of IFMs. During metamorphosis, the *ewg* protein is expressed and required in the imaginal myoblasts, which are the progenitor of the IFMs. The loss of *ewg* protein expression from these myoblasts is associated with the degeneration of the IFMs, with a stronger affect in the dorso-longitudinal muscles (DLM) compared to the dorso-ventral muscles (DVM) (DeSimone et al., 1995).

Specific alleles of the *held out wings* (*how*) gene, at cytological position 93F13, share a similar adult phenotype to *ae-1*. Flies heterozygous for either of the hypomorphic alleles, *how 13* or *15*, with the original enhancer-trap line 1A122 are unable to fly and

their wings are held out at right angles to the body, presumably due to reduced muscular activity (Zaffran et al., 1997). The *how* protein closely resembles the mouse *quaking* protein that is required for myelination of nerve fibers (Ebersole et al., 1996), although *Drosophila* nerve fibers are not myelinated. Based on sequence identity, the *quaking* gene belongs to the signal transduction and activation of RNA (STAR) subfamily of the KH domain-containing proteins. The STAR proteins are believed to provide a link between a signal transduction pathway and RNA metabolism (Ebersole et al., 1996). It has been suggested that the *how* protein may act similarly in RNA processing of downstream genes that are involved in muscle function. Antibody staining has revealed that the protein is localized in the nuclei of tendon cells attached to the indirect flight muscle fibers (Zaffran et al., 1997). The β -galactosidase expression pattern in the 1A122 insertion line also shows that the gene is expressed in the nuclei of the somatic body wall muscles of third instar larvae (Lo and Frasch, 1997). The downstream target genes that *how* may be involved in regulating have not yet been identified. However, considering the similarity in phenotypes and the lack of any gross structural abnormalities when comparing *ae-1* and *how*, as well as the overlapping domains of expression of *tsh* and *how*, *tsh* may represent one of these target genes.

Like the other mutants described, *eagle* (*eg*) was identified based on its abnormal wing posture. Homozygous adults for hypomorphic alleles hold their wings out at right angles to the body axis. However, unlike the previously described posture mutants the etiology of the *eg* mutants appears to be neuronal in nature. The *eg* gene encodes a zinc finger protein that resembles proteins from the steroid receptor family (Higashijima et al., 1996). The *eg* protein is expressed and is required for determining the cell fates of the 7-3 neuroblast (NB) lineage including the serotonin producing neurons (Lundell and Hirsh, 1998). The role of *eg* is in neuronal specification and not in the lineage divisions of the NB 7-3 because the cells are restrained but fail to assume the wild type neuronal fate. Null alleles of the *eg* gene result in a loss of serotonin expressing neurons. The proper expression of *engrailed* (*en*) and *zfh-2* proteins in the developing serotonin producing neurons within the central nervous system is also dependent on *eg* function.

Because of the obvious phenotypes associated with these mutations a number of them were identified early in the study of *Drosophila*. Unfortunately, many of the

original wing posture mutants are no longer extant for further characterization. One of these extinct mutations is *aeroplane* (*ae*), originally isolated by Mohr as a spontaneous event in a *Notch* 8 laboratory stock, and characterized by Quelprud (1931). Animals homozygous for the *ae* mutation showed a variable abnormal wing posture. The phenotype ranged in severity from both wings outstretched to a normal resting wing position. Genetic mapping by Quelprud placed *ae* at 54.3 between *purple* (*pr*) and *cinnabar* (*cn*) on the second chromosome. In addition to the wing posture, *ae* flies exhibited abnormal drooping halteres. Like the other wing posture mutants already discussed, longitudinal and transverse sections through *ae* flies revealed some abnormalities associated with the anterior-most dorso-ventral indirect flight muscles (IFM). However, this etiology failed to be consistent with the phenotype.

We have recently isolated another abnormal wing posture mutant. From the literature, it most closely resembles *ae* in phenotype and was therefore given the name *aeroplane-like* (*ae-l*). *ae-l* possessed the same variable phenotype with no additional detectable visible abnormalities. This homozygous viable mutation arose as a by-product of a transformation experiment involving the Carnegie 20 vector (Cy20). Although a single copy of the Cy20 transposon was present in the original *ae-l* stock, the *ae-l* phenotype often segregated from the *rosy* transformation marker of the Cy20 construct.

The *ae-l* mutant phenotype was mapped genetically and cytologically to the proximal region of 2L, very near the location of the original *ae* mutation at position 2-54.3 (Quelprud, 1931). Initial complementation analysis involving alleles of previously identified genes within the region suggested that *ae-l* may represent a novel gene. Complementation analysis utilized various *P* element enhancer trap alleles from the Spradling and Rubin collection in addition to stocks from private collections. One of these mutants that complemented the *ae-l* phenotype was the homeotic gene *teashirt* (*tsh*). As in the primary homeodomain containing genes, loss of function mutations of the *tsh* gene lead to transformation of the trunk segments to head tissue and ectopic expression of the *tsh* protein in more anterior segments leads to a transformation of these regions to more anterior fates (Fasano et al., 1991).

Unlike the HOM-C genes, *tsh* is a putative transcription factor with unique widely spaced zinc fingers motifs (Fasano et al., 1991). Northern analysis, in situ hybridization

and indirect reporter gene analysis, however, reveals that it is expressed throughout development and within a number of different tissues. Acting in conjunction with *Ultrabithorax (Ubx)* and *Antennapedia (Antp)*, *tsh* is required for proper specification of the trunk segments in the embryo by establishing the basal developmental fate which the homeotic complex genes can then build upon (Roder et al., 1992). In addition, within the embryo *Antp*, *Ubx* and *abd-A* are required to activate *tsh* indirectly within the endoderm of the midgut where it specifies the location of two of the three constrictions within the developing gut (Mathies et al., 1994). *tsh* is also required for proper specification of a subset of ventro-lateral peripheral nerves in the embryo (Roder et al., 1992).

Contrary to its functions within the embryo, *tsh* also plays a role in the developing head structures of the adult by presumably repressing *Antp* expression within the eye-antennal discs. Loss of *tsh* along with ectopic expression of the *Antp* gene within the eye results in an eye to head cuticle transformation (Bhojwani et al., 1997). Further, misexpression of *tsh* under the control of the *decapentaplegic (dpp)* wing enhancer leads to the activation of the eye specification pathway in tissues not regularly fated for eye identity, indicating that *tsh* also plays a role in the activation of this pathway (Pan and Rubin, 1998). Except for the role of *tsh* during eye specification and head development, knowledge of its function in the adult is limited. Histochemical and antibody staining show that the *tsh* expression pattern in third instar imaginal discs is localized to within tissues fated to give rise to the proximal structures of the developing appendages in the adult (Bryant 1975; Cohen 1993), including within the presumptive notum (Ng et al., 1996). In a UAS-y, GAL4 screen used to identify genes involved in adult pattern formation, *tsh* was shown indirectly to be expressed throughout the cuticle of the thorax, abdomen and proximal appendages (Calleja et al., 1996).

To better understand the spatial and temporal regulation of complex genes such as *tsh*, it is essential to dissect the gene into smaller functionally divisible units. One way this can be achieved is by analyzing each gene in terms of functionally separate tissue-specific enhancers. As discussed above, the dissection of cis-acting regulatory sequences for *tsh* have thus far identified two such embryonic regulatory elements, the *ftz* enhancer (Core et al., 1997) and the *UBX/Antp* Homeotic Response Element (McCormick et al.,

1995) thus far. Each of these elements is localized to genomic sequences 3' to the coding region.

Previously, it was proposed that the cause of a rediscovered wing posture mutant, *aeroplane-like (ae-l)*, results from the disruption of another 3' cis-acting regulatory sequence (Soanes and Bell, 1999). Unlike the two previously identified elements, however, this third region is proposed to be required for proper expression and function of *tsh* in the developing adult. *ae-l* is a recessive null mutation which affects both wing and haltere posture (Quelprud, 1931 and Soanes and Bell, 1999). Flies homozygous for this null allele hold the wings out and away from their body and also exhibit drooping halteres, (Soanes and Bell, 1999). This, and other evidence, led to the conclusion that *ae-l* is *ae*, and henceforth will be called *ae*. Herein, an examination of the adult structures reveals that the ventral hinge and ventral proximal haltere structures in the *ae* mutant are fused to the thorax resulting in the apparent wing paralysis and drooping halteres. No other defects have been observed in the flies, including the direct (DFM) and indirect flight muscles (IFM) or neuronal innervation of the DFM. The notum and most pleural structures of the thorax also show no obvious abnormalities (Soanes and Bell, 1999).

Data reported herein show that *tsh* is expressed in the appropriate regions of the third instar larval wing and haltere discs that give rise to the proximal hinge region in the adult fly. Tissue-specific enhancer elements have been identified that are required for proper spatial and temporal expression of the *tsh* gene within the presumptive hinge regions of the wing and halteres. The wing hinge-specific enhancer is also located 3' to the *tsh* coding region but 5' to the previously identified cis-regulatory elements downstream of *tsh*. This regulatory sequence is independent of the HOMRE and *ftz* enhancer elements because the deficiency *Df(2L)R6* removes both the HOMRE and *ftz* enhancer sequences but is still capable of complementing the *ae* phenotype (Soanes and Bell, 1999). This wing hinge specific enhancer is localized within a 4.8 kb *EcoRI* sequence, previously identified as containing an insertion within the *ae* allele, and is capable of driving expression in the presumptive dorsal and ventral hinge region. Using the enhancer tester pCaSpeR hs 43 (Thummel and Pirrotta, 1992), the 4.8 kb *EcoRI* fragment was subdivided, identifying a smaller fragment still capable of ventral haltere

and ventral wing hinge-specific expression. The reporter gene expression from this ~915 bp *P* element coincides with tissues fated to give rise to the structures identified as abnormal in the *ae* mutant.

It is often seen when making comparisons between vertebrates and invertebrates, that the coding and regulatory non-coding regions of the genome are very often evolutionarily conserved. Conservation is also observed in certain classes of transposable elements. Two general classes of transposons can be categorized based on the method of transposition, either by reverse transcription via a RNA intermediate or by the mobilization of a DNA element (Finnegan, 1989). The insert within the ventral wing and haltere specific enhancer (*ae* enhancer) sequence has been identified as a 5.4 kb I element, a retrotransposon similar to the long interspersed nuclear elements (LINEs) identified in humans (Fawcett et al., 1986). These elements transpose via a RNA intermediate, which may be synthesized by a putative reverse transcriptase, encoded by the element. The long interspersed nuclear elements (LINEs), non-viral or non-LTR (long terminal repeat) retrotransposons in humans have been linked to formation of tumors and hemophilia (Kazazian et al., 1988; Morse et al., 1988). In *Drosophila*, I elements have also been associated with mutations of the pericentric loci of the second chromosome (Dimitri et al., 1997). The mobilization of these elements occurs in the germline of dysgenic SF females that are the progeny of an inducer (I) males and reactive (R) females (Pelisson, 1981). The main effect of the hybrid dysgenesis in the SF females is a dramatic reduction in the viability of the embryos, caused by lethal mutations associated with rearrangements and insertions induced by mobilization of the I elements. A SF female that arises from a cross using a strong I strain can lead to 100% embryonic lethality. The difference between I and R strains is the presence of ~15 active I elements in the euchromatin of the I strain, although both I and R strains have numerous defective I elements associated with the pericentric heterochromatin. The I element in the *ae* mutant is inserted within a 34 bp *Dra*I sequence in the *ae* enhancer element. This I element has presumably led to the loss of *tsh* expression from the ventral hinge specific enhancer in the *ae* mutant, resulting in the defects associated with the *ae* phenotype.

By identifying the etiology of the wing and haltere posture in the *ae* mutant, it is possible to propose a function for the *tsh* gene within the developing adult cuticle. It is

likely that *tsh* plays a role in the specification of the proximal wing hinge region and homologous structures in the halteres. The null *ae* allele leads to the fusion of the wing and halteres to the cuticle. This suggests that *tsh* could either play a role in helping define the division between the proximal appendages and the thorax or that it is required for the proper specification of the proximal structures in the developing appendages. Ectopic expression of the *tsh* gene, however, suggests possible differences in function for *tsh* in both the ventral and dorsal hinges.

Chapter II - Phenotype and Mapping

Phenotype

Flies homozygous for the *aeroplane-like* (*ae-l*) mutation have an abnormal wing posture and initially this phenotype was also variable, like that reported for the original *ae* mutation (Quelprud, 1931). The *ae-l* flies held their wings out at varying angles with respect to the horizontal and the body axis. Possibly through recombination and selection, the wing posture of the present stock is now phenotypically stable (**Figure 3A** versus **B**). *ae-l* mutants also exhibit drooping halteres (**Figure 3C** versus **D**), again in concordance with the original *ae* mutation. Mutants are unable to fly or fold their wings back into the resting position. However, some flies are capable of limited vertical wing movement. In our original *ae* stock, flies with apparently normal wing posture were also incapable of flight. Although *ae-l* flies have an abnormal wing posture, the wing blade and thorax show no readily detectable abnormalities. When flies from the same isogenic stock were grown at 29°C, 24°C or 18°C, the expressivity of the phenotype in adults was not effected. Except for a slight delay in development associated with the *cinnabar* (*cn*), *black* (*b*) *ae-l* stock, no other gross developmental defects were identified.

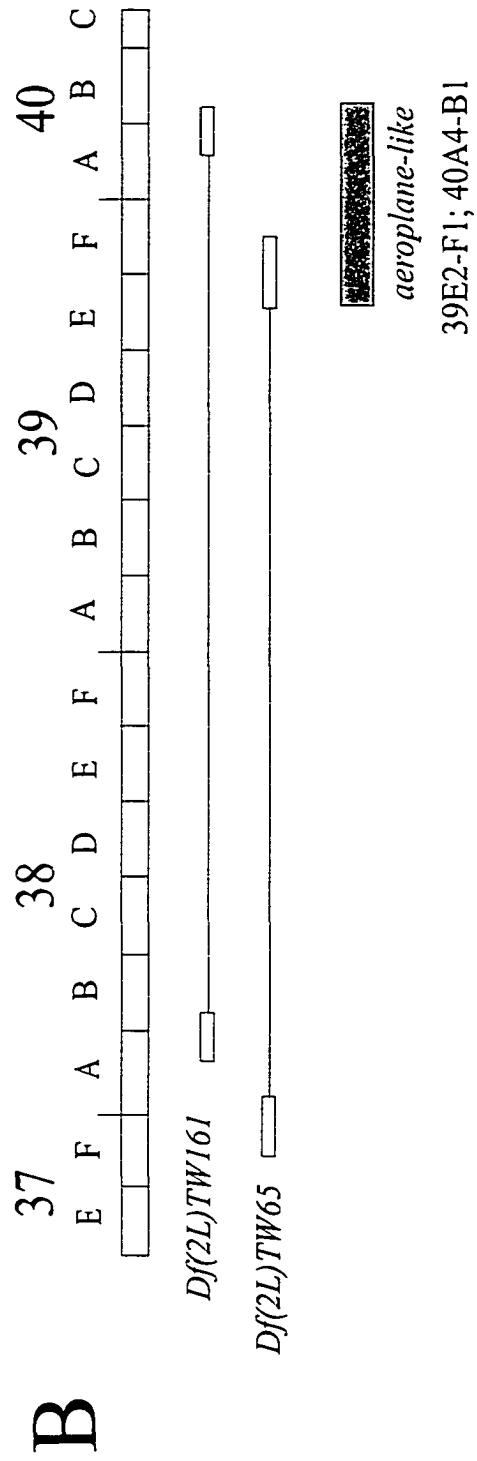
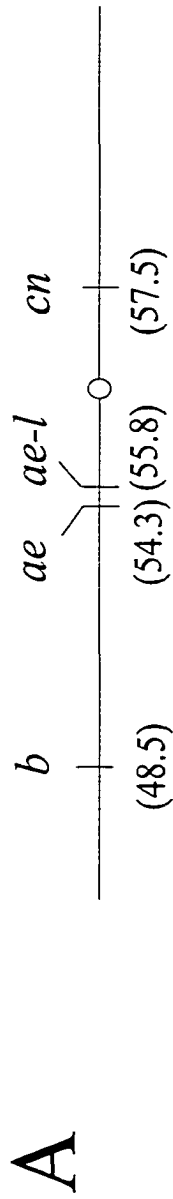
Mapping

The *ae-l* mutation maps to the second chromosome at position 55.8 between the *cn* and *b* loci (**Figure 4A**) near the location of the original *ae* mutation. The calculated interval distances for *b; ae-l* and *ae-l; cn*, show an approximate fifty percent reduction of recombination frequencies compared to the theoretical published distances (Lindsley and Zimm, 1992). Despite this discrepancy, no obvious polytene chromosomal abnormalities are observed in *ae-l* heterozygotes. The genetic map position for *ae-l* (**Figure 4A**) was derived from the recombinant classes in the smallest interval containing the *ae-l* mutation, and was calculated by using the theoretical *b-cn* distance multiplied by the fraction of recombinants in the *ae-l-b* and *ae-l-cn* intervals. Recombination in the *ae-l* background was tested to determine if the reduction in recombination frequency was a feature of the mutation or the region in which *ae-l* was situated. Recombination on the X chromosome was tested using the multiple marked chromosome, *y, cv, ras v, f*. However,

Figure 3. Phenotypic comparisons between *ae-l* and wild type wings and halteres. **A)** Normal wing posture of a wild type Oregon R female. **B)** Abnormal wing posture in an *ae* female (*b cn ae-l, ry*). **C)** A scanning electron microscopy image (SEM) of a normal female Oregon R haltere. **D)** A SEM of a mutant haltere in a *b ae-l cn* female fly exhibiting the drooping phenotype. Taken from Soanes and Bell, 1999.



Figure 4. Cytological and genetic mapping of the *aeroplane-like* mutation. **A)** A genetic map showing the location of *ae* with respect to second chromosome markers. Values below each gene (except for *ae-l*) represent the genetic map distances according to Lindsley and Zimm (1992). *b*, *black*; *cn*, *cinnabar*; *ae*, *aeroplane*; *ae-l*, *aeroplane-like*. **B)** Cytogenetic localization of the *ae-l* mutation to the proximal region of 2L. Open boxes represent the position of the deficiency break points. Break points corresponding to *Df(2L)TW161* and *Df(2L)TW65* are 38A6-B1; 40A4-B1 and 37F5-38A1; 39E2-F1 respectively, as reported by Lindsley and Zimm, (1992). The grey box indicates the minimal *ae-l* region defined by complementation results between *ae-l* and the deficiencies. Taken from Soanes and Bell, 1999.



all these recombination frequencies were considered normal, suggesting the reduction of the recombination frequency was a result of the region of the genome in which the mutation responsible for the *ae-l* phenotype mapped. The reduction in recombination frequencies within the proximal regions of chromosome 2L compared to published distances has also been observed in other unrelated research (Hilliker pers. comm.).

By definition, *ae-l* is a null mutation since flies homozygous for *ae-l* or hemizygous over a deletion exhibit the same mutant phenotype. Failure of the deficiency *Df(2L)TW161* to complement the *ae-l* phenotype positions the mutation cytologically to the centromere-proximal region of 2L (**Figure 4B**). The ability of deficiency *Df(2L)TW65* to complement *ae* narrows the region to 39E2-F1; 40A4-B1 (**Figure 4B**). A stock, *Dp(2:Y)H2*, with a duplication of the proximal region of 2L (36B5-38B2 and 39E3-40F) transposed to the Y chromosome (Hodgetts, 1980) confirms the cytological localization of *ae-l* by its ability to rescue the phenotype. All males homozygous for the *ae-l* mutation and carrying the transposed genomic fragment on the Y are wild type while the female siblings still express the *ae-l* phenotype. These mapping results for *ae-l* agree with the previously mapped location of the original and now extinct *ae* (**Figure 4A**) allele by Quelprud (1931). Based on the phenotypic and mapping similarities, we are confident that *ae-l* is allelic to the original *ae* mutant and therefore we will refer to *ae-l* as *ae* for the remainder of the thesis.

Chapter III – P element Mutagenesis

Once the *ae* phenotype was mapped to the proximal region of 2L, alleles of known genes in this region were used in complementation tests for a functional analysis. Each of the *P* element insertion lines that mapped within the *ae* region complemented the *ae* phenotype (**Table 1**). These enhancer-trap *P* element insertion lines, along with a number of other ammunition chromosomes, were used in *P* element mutagenesis experiments in an attempt to tag the *ae* gene. The example presented in **Figure 5A** uses the P1370 enhancer trap line, however the method by which the *P* element mutagenesis was carried out is the same for all ammunition chromosomes. See **Table 9**, Materials and Methods, Stocks and Crosses, for a summary of the all the stock genotypes.

The ammunition chromosomes used for the *P* element mutagenesis included: the *Birmingham* chromosome, the C-92 enhancer trap, the YASH-9 chromosome and two enhancer trap alleles from the Bloomington stock center, P1370 and P897. A summary of the results from the *P* element mutagenesis screens can be seen in **Table 2**.

The *P* element mutagenesis involving the *Birmingham* second chromosome (*Birm2*) was carried out as presented in **Figure 5A** except for the differences in the *Birm2* third chromosome genotype, which is *Sb/TM6Ubx*. The *ebony* (*e*) allele found on the *Sb* $\Delta 2-3$ and the *TM6* balancer chromosomes was used to select the *w*; *Birm2/CyO*; *Sb* $\Delta 2-3/TM6Ubx$ F1 males from the *Sb/TM6Ubx* flies. The *Birm2* chromosome is a stock that contains a second chromosome with 17 defective *P* elements (Bingham et al., 1982). This particular mutagenesis experiment did not produce any chromosomes that failed to complement the *ae* phenotype. The progeny arising from the dysgenic males were often associated with black patches (resembling the *Black Cell* (*BC*) phenotype) of what appeared to be cell necrosis. This phenomenon did not occur frequently in any of the other *P* element mutagenesis experiments.

A second ammunition chromosome used in *P* element mutagenesis was the line nick-named the YASH 9 chromosome. The YASH-9 line contains a rescueable P{PZ}enhancer trap construct on the X chromosome. The rescueable enhancer constructs are of the P{PZ} type with a *ry*⁺ transformation marker and a *lacZ* reporter gene for enhancer detection. The reason for using this line was the ease with which the parental enhancer

Figure 5. *P* element mutagenesis experiments with *ae*. **A)** An example of a *P* element mutagenesis screen used to generate *ae* alleles. *P897* was also used (data not shown). **B)** A screen designed to select for a proximal jump from *tsh* and insertion into *ae* using *P1370*. **C)** Screen to determine the excision frequency of *P1370* from the *tsh* gene. **D)** Screen to measure reversion of the lethality associated with the derivative lines generated in **A)** with the concomitant separation of *ae* from the lethality associated with the *P* element construct. Lines 23.7 and 23.2 are representative of the weak derivative class. The *P* element *P1370* used in each cross was the strong *tsh* allele *P {PZ}_{tsh}[04319]*. *P1370** refers to *P1370* chromosomes that have been modified and fail to complement *ae*. *P1370R* refers to chromosomes that have been modified so they no longer exhibit the homozygous lethality associated with the *P1370* insertion line. Taken from Soanes and Bell, 1999.

Generating *ae-l* with *P1370*.

A

♀ *P1370/CyO; ry* X ♂ *Sp/CyO; SbΔ2-3/TM6*
↓
♂ *P1370/CyO; SbΔ2-3/ry* X ♀ *b cn ae-l/b cn ae-l; ry*
↓
P1370/b cn ae-l; ry/ry*
Select for *ae* phenotype
Frequency = 102 *ae*/24000 = 0.43%

***P1370* reversion with *ae-l* insertion.**

B

♀ *P1370/CyO; ry* X ♂ *Sp/CyO; SbΔ2-3/TM6*
↓
♂ *P1370/CyO; SbΔ2-3/ry* X ♀ *Df(2L)TW161/CyO; ry*
↓
P1370/Df(2L)TW161; ry*
Select for *ae-l* phenotype
Frequency = 0 *ae* / 15000 = 0%

***P1370* reversion frequency.**

C

♀ *P1370/CyO; ry* X ♂ *Sp/CyO; SbΔ2-3/TM6*
↓
♂ *P1370/CyO; SbΔ2-3/ry* X ♀ *P1370/CyO; ry*
↓
P1370R/P1370
Select for *P1370* revertants of lethality
Reversion Frequency = (530 Revertants/4694) X 2 = 22.3%

Reversion of lines 23.7 and 23.2.

D

♀ *P1370(ae)/CyO; ry* X ♂ *Sp/CyO; SbΔ2-3/TM6*
↓
♂ *P1370(ae)/CyO; SbΔ2-3/ry* X ♀ *Df(2L)TW161/CyO; ry*
↓
P1370(ae)/Df(2L)TW161
Select for *ae-l* phenotype and *P1370* lethality reversion
Revert *tsh* lethality and *ae-l* phenotype in lines 23.7 and 23.2

Table 1. Complementation Analysis Involving <i>ae</i> and <i>tsh</i> Alleles.					
Stock #	Allele	F1 results			
		<i>Df(2L)tsh8</i>	<i>Df(2L)305</i>	<i>Df(2L)R6</i>	<i>ae</i>
P1370	<i>tsh</i> (04319)	<i>l</i>	<i>l</i>	+	+
P832	<i>tsh</i> (4-3)	v (+)	v (+)	+	+
P805	<i>tsh</i> (51)	+*	<i>l</i>	+	+
P897	<i>tsh</i> (B4-2-12)	<i>l</i>	<i>l</i>	+	+
P842	(A3-2-66)	+	+	+	+
P1352	<i>l</i> (2)03832	+	<i>l</i>	+	+
P1176	<i>l</i> (2)02074	+	<i>l</i>	+	+
	<i>ae</i>	<i>ae</i>	<i>ae</i>	+	<i>ae</i>

The complementation results are as follows with respect to the *ae* phenotype: *ae*, *aeroplane*; +, wild type; *l*, lethal. Allele designations for *tsh* alleles are provided by Kerridge (Flybase, 1996 FBrf0091269). Stock # refers to Bloomington Stock Center number. The alleles tested within the region near the cytological location of *ae* were isolated in the following laboratories: 4-3 and 51 from Rubin; A3-2-66 and B4-2-12 from Y.N. Jan; 02074, 03832 and 04319 from A. Spradling. The *tsh* alleles are indicated as such. An asterisk indicates results described by S. Kerridge (Flybase, 1996 *ibid.*). Kerridge reports that homozygous P805 has a phenotype similar to *ae*, however our *ae* mutation complements P805. *Df(2L)R6* is an approximately 20 kb deletion, which lies 3' to the *tsh* coding region. *Df(2L)tsh8* is a deficiency that includes all of the *tsh* coding region (Fasano et al., 1991). *Df(2L)305* deletes *tsh* and four additional complementation groups centromere-distal to *tsh* (S Kerridge in Flybase, 1996 *ibid.*). v indicates viable F1 progeny.

Table 2. Summary of <i>P</i> element Mutagenesis F1 Screens.		
Line	Number of F1's screened	Independent mutants
YASH	~74000	2
<i>b cn C-92; ry</i>	~75000	1*
<i>tsh</i> [04319]	~24000	15
<i>tsh</i> [B4-2-12]	~9000	3
<i>Birm; Sb/TM6Ubx</i>	~45000	0

The * indicates the *Serrate* allele, *Rpw*, recovered from the screen. *Rpw* was not identified based on abnormal wing posture, but on scalloping of the wings. Independent mutants refer to the number of “wings held out” alleles generated from each ammunition chromosome and known to be of independent origin.

traps could be separated from any induced mutant chromosomes. Once the dysgenic F1 males are crossed to homozygous *b cn ae; ry* flies, all phenotypically *ae* males would no longer carry the parental ammunition chromosome. This line was also known to be successful in previous *P* element mutagenesis experiments (S. Tiong, pers. comm.). However, this screen was also unsuccessful in generating any chromosomes that fail to complement the *ae* phenotype. Two wings held out flies were recovered from this experiment, but each was dominant and did not resemble the *ae* phenotype.

These new mutants mapped to the third chromosome and the abnormal wing posture was apparently caused by the visible slight thoracic defects. Both of the mutants were independent in origin (each arising from separate bottles), however they were later determined to be allelic. These mutants, nick named *YASH 31A* and *YASH 27*, were determined by complementation analysis to be members of the *Polycomb group (PC-G)* genes. Both *31A* and *27* were crossed with several *PC-G* alleles available through the Bloomington stock center and each exhibited interactions characteristic of *PC-G* genes (Cheng et al., 1994). Thus, they were not considered further in this thesis.

The enhancer trap line *C-92*, localized to the proximal region of 2R at cytological position 42A, was first used in our *P* element screen to attempt a local hop into the *ae* gene from its location in the proximal region of 2R (Brook, 1994). The F1 screen was carried out as shown in **Figure 5A**, but it did not produce any chromosomes that failed to complement the *ae* phenotype. However, from this screen a mutation with a scalloped wing phenotype was generated. The mutant was nicknamed “*Ripped wing*” (*Rpw*) and later determined to be an allele of the *Serrate (Ser)* gene. Genetically, *Rpw* resembled the “*Beaded of Goldschmidt*” (*Bd^G*) allele (Lindsley and Zimm, 1992), in that it was lethal in trans to *Bd^G* while complementing the *Ser^l* allele. The initial penetrance of the *Bd^G* and *Rpw* alleles was very low, and the *Rpw/TM6b* stock now fails to exhibit any wing phenotype. The *Rpw* phenotype is also temperature dependent, in that the higher the temperature the less severe the phenotype.

Southern analysis of the *Rpw* stock in comparison to its parental *C-92 cn; ry* line failed to detect any *P* element sequences in the *Rpw* line, indicating, that the phenotype was not caused by a *P* element insertion. The *Rpw* allele was used to screen the P{PZ}, *P* element lethal collection (available through the Bloomington stock center) looking for

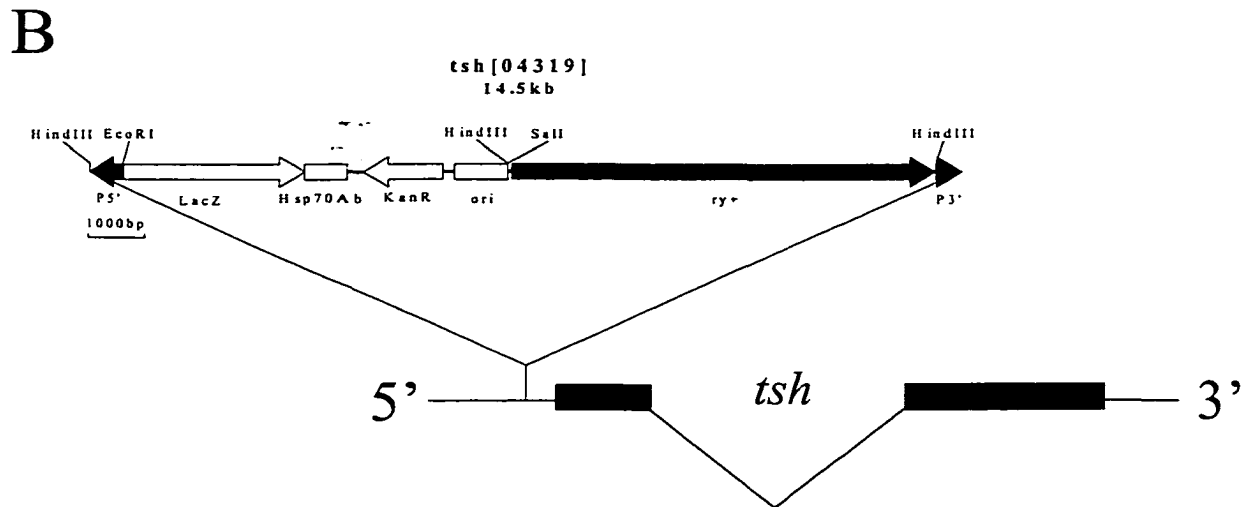
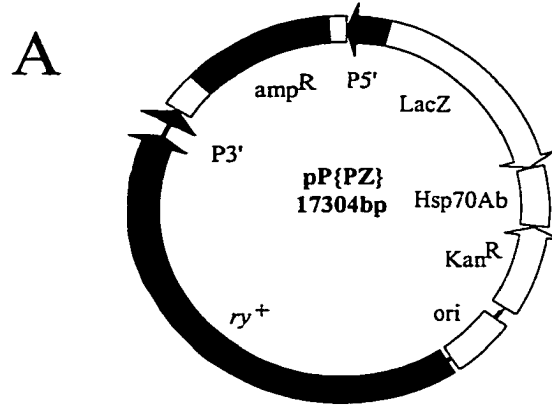
phenotypic interactions. A number of *P* element alleles showed a phenotypic enhancement of the *Rpw* phenotype (**Table 3, Appendix**). The trans heterozygotes showed a dramatic loss of wing and haltere tissue. In addition, a number of F1 progeny with a “wings held out” phenotype were recovered from the screen. However, these failed to breed true. This appeared to be a common artifact of the *P* element mutagenesis experiment.

Originally, the *ae* phenotype was thought to be localized to the proximal region of either the 2R or 2L based on the results from deficiency mapping using a *Df(2R)bw^{vDe2L}Cy^R / In(2LR)Gla* stock. Cytologically, the breaks of the deficiency were localized to 41A; 42A7-8. Approximately 25% of deficiency / *ae* transheterozygotes exhibited a wings held out phenotype. Deficiency heterozygotes (+/Df) presented a slightly lower penetrance of about 10%. The low penetrance was similar to that seen in the original *ae* stock so it was assumed that this deficiency uncovered the *ae* locus. In an attempt to localize, if possible, the arm in which the *ae* phenotype was situated, deletions from both side of the chromosome 2 centromere were crossed into the *b ae cn ; ry* stock. A much stronger non-complementing interaction was observed with the *Df(2L)TW161* with breaks occurring in the proximal region of 2L (**Figure 4B**) compared to the apparent interaction with deficiencies on the proximal region of 2R. Enhancer traps, available through the Bloomington stock center, that were localized to the minimal *ae* cytological region of 39E2-F1 to 40A4-B1 were used in the same F1 screen described for the other ammunition chromosomes above (**Figure 5A**). Enhancer traps were used within this region in order to ‘tag’ the *ae* gene by local hopping (Tower et al., 1993). Two of the complementing enhancer trap alleles, P1370 and P897, were capable of generating chromosomes that fail to complement the *ae* phenotype at a relatively high frequency of ~0.5% (**Figure 5A**). From a small scale screen using P1370 to generate new *ae* alleles, 102 of 24000 second chromosomes tested failed to complement the *ae* phenotype (**Figure 5A**) and these 102 derivative second chromosomes represent at least 24 independent events. The P1370 line is a P[PZ] construct with a *rosy* (*ry*⁺) transformation marker at the 3’ end and a *lacZ* reporter gene enhancer detector at the 5’ end (**Figure 6A**). Initial analyses revealed that most of the derivative chromosomes generated (26/33, or ~79%) lost the *ry*⁺ marker, suggesting either an excision of the construct or a break in the *ry*⁺

coding region. Further analysis revealed that about half of the derivative lines (15/33, or ~45%) still express the β -galactosidase marker in a pattern similar to the parental P1370 enhancer-trap line (**Figure 7**). This indicates that at least the 5' end of the P[PZ] construct containing the *lacZ* reporter gene remains intact or maintains its position in the genome with respect to the P1370 insert site. Like the *ry*⁺ marker results, this suggests that ~55% of the lines may result from complete excision of the entire P[PZ] construct. Alternatively, the loss of expression is the result of mutations or breaks within the *lacZ* reporter gene. Loss of the P1370 *lacZ* expression pattern and the *ry*⁺ marker from the derivative lines reveals a polarity or directionality of alterations to the P[PZ] construct with more breaks or alterations occurring at the 3' end in comparison to the 5' end. Each of the derivative lines also failed to complement the lethality associated with the P1370 insert, implying an imprecise excision of the *P* element construct within the lines that lost the *ry*⁺ and/or *lacZ* markers. An imprecise excision could lead to a deletion by either the loss of the P{PZ} construct and flanking genomic sequences from the insert site or a deleted P{PZ} construct in combination with a deletion of the flanking genomic sequence.

During further characterization of the derivative chromosomes, it was determined that the P1370 and P897 enhancer traps were alleles of the homeotic gene *teashirt* (*tsh*) (S. Kerridge, pers. comm.). Because the two enhancer-traps used to generate new *ae* alleles were capable of complementing the *ae* phenotype (**Table 1**) and were also considered to be strong *tsh* alleles by virtue of their lethality as homozygotes (S. Kerridge, pers. comm.), it was assumed that *tsh* and *ae* were independent genes. Initially, it was expected that the generation of *ae* alleles by *P* element excision could take place via a clean excision from the *tsh* gene and reintegration within the *ae* gene. The reversion frequency of the *tsh* [04319] insert, as measured by loss of the homozygous lethality, was about 23% (**Figure 5C**). If *tsh* [04319] and *ae* were two independent genes, then of the 102 derivative *ae* chromosomes about 23 might be *tsh*⁺ by chance. However, as reported above all of the derivative chromosomes remained homozygous lethal for the *tsh* gene. Thus, it seems that the derived *ae* lines did not become mutant within the *ae* gene by a proximal hop of the enhancer trap from *tsh*.

Figure 6. Enhancer trap pP{PZ} map and its insertion site in *tsh* [04319]. **A)** Schematic representation of the enhancer trap vector pP{PZ} (Spradling and Rubin, 1983; Rubin and Spradling, 1983; Mlodzik and Hiromi, 1992). **B)** Schematic representation of the P{PZ} transposon insertion, *tsh* [04319] relative to the *tsh* gene. **C)** The untranslated leader sequence of *tsh* with the P1370 insert site indicated. The lowercase, bold, underlined bases at position 281 and 282 indicate where the P1370 insert site is located. The bold uppercase lettering denote *tsh* translated sequences. The arrows in the vectors indicate the direction of transcription for each of the coding regions. *LacZ* indicates the β -galactosidase coding region. *ry*⁺ indicates the *rosy*⁺ transformation marker. *Kan*^R indicates the selectable marker used when performing plasmid rescue of flanking genomic sequence. The *amp*^R indicates the antibiotic selection for amplification in *E. coli*. The two flanking arrows on either end of the construct marked as P5' and P3' show the 5' and 3' P element sequences. Hsp70Ab indicates the poly-adenylation signal fused to the end of the *lacZ* coding region. Restriction enzyme sites; *Eco*RI, *Hind*III and *Sal*I are indicated in panel **B**. The total size of each of the constructs is indicated in bp.



C

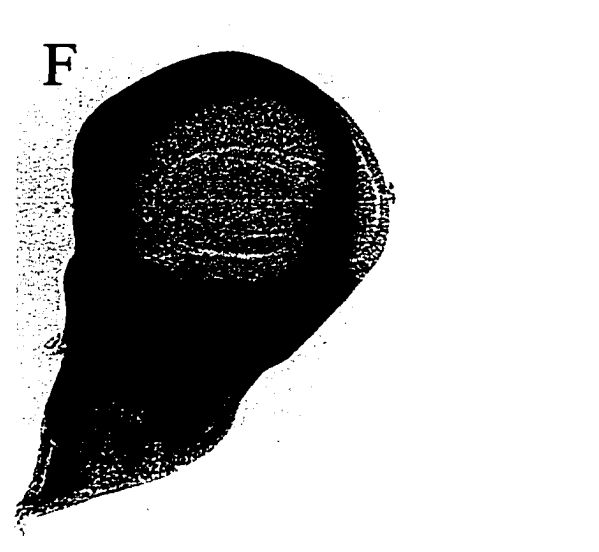
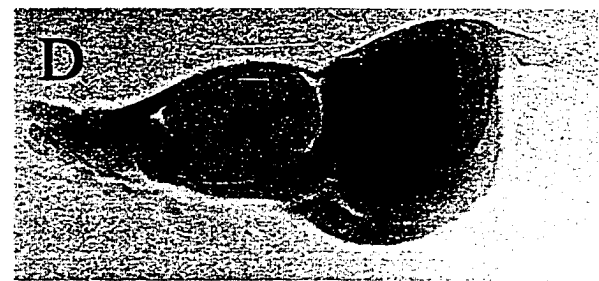
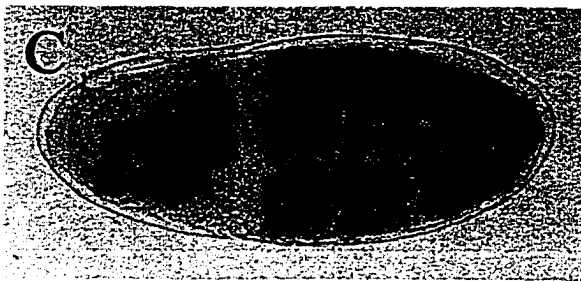
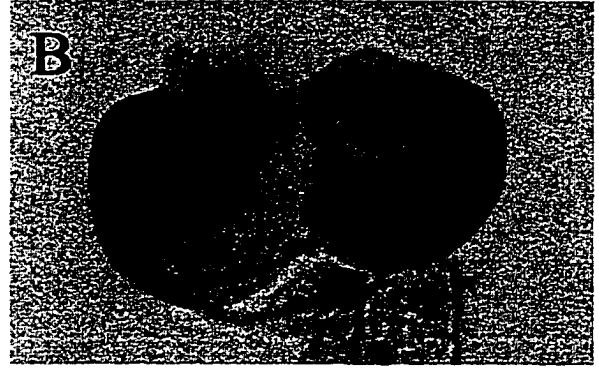
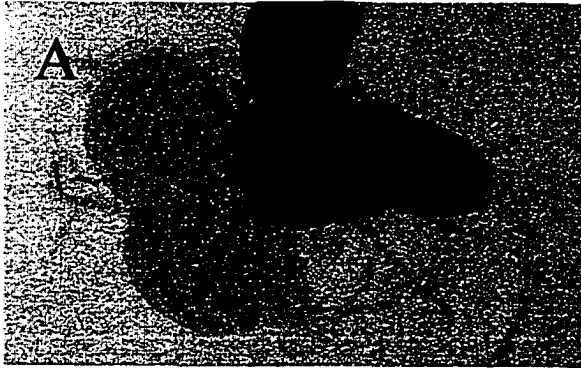
```

1       ttttttttttttttttttttttggattttatgcttgttttggttgagttccctccaacacagcgtgttttccatgaaatcaacattacatataatcaat
101    caattttcatcaattcacgggtacaatatctctcagctccaacacattggagacaaacatactatatatttgcacacctctcaataaacattgcatgaga
201    cgatggcgcgaaatagcccaatttagtgaggaacgtggccaacccttgatatactgtgaggcaactcccgaaatcgggactttcggttcggtagtgacgacgaa
301    tccggatgagaagacgcacgcatacgcaccggcttccgccagaacagtgaaattctcagctttaaacgcgcttttggggggaggatagaacgagtggtttcc
401    aggcgcatcatatcttagtcaaagaagcagaggtttgatctctcgaacgcaaaatgctcgatcaagactgaaacatacgcgaaaacatcacaactcaaat
501    ggttcaacaaagtatacgtaaaactaccacaagctaaacaaaataaccacaaaataatatttattaccacaaactaaagataaaactattgcaaatattta
601    cattaacgggtatttaattcaccacaaattacactacatacataatgtaaaggcaqtacttaaatcaacaaacctaacgaagtatacgttcaatgcaa
701    ttaataaattaaatttaatacacaacaaattaggaattaaaatacacaacgcctcgaacgctcattttttgtctgacatacgcgaaagttaaataattaca
801    aatccccaaaaataaaatcaatcagttatcgcgtgcaacaacaagaagttatacacaacgtaccgaagtcaaaaacaatagattatatacgtatcgtgctc
901    aaactaaagttaagtcccaaatcccaactaaaaatcctcggtgttctccaaaaagagcaaacccatccaagtccagcaaacggtcaaaaatcagcaaaa
1001   tttaaaaATGTTACACGAGGCTCTGATGCTCGAGATCTACAGACAGGCGCTAAATGCCGG...

```

Reproduced with permission of the copyright owner. Further reproduction prohibited without permission.

Figure 7. P1370 (*tsh*[04319]) enhancer trap expression pattern. Blue color indicates the β -galactosidase expression pattern in **A)** a third instar larval brain; **B)** third instar genital discs; **C)** early embryonic expression during germband extension; **D)** eye-antennal disc from a third instar larva; **E)** third instar larval haltere discs and **F)** wing discs. Anterior is to left for **A)**, **C)**, **E)** and **F)**. Dorsal is down for **E)** and **F)**. The arrow in **F)** indicates the presumptive dorsal notum specific repression of *tsh* expression.



Under the assumption that *tsh* and *ae* were two separate genes these results could also imply that the lethality associated with each of the derivative lines arose from deletions that break within both *ae* and *tsh*. A deletion breaking in both *ae* and *tsh* would permit “jumping” into the *ae* gene by walking across the break from *tsh* into *ae*.

A second possibility that could account for the parental P1370 *lacZ* expression pattern and the P1370 lethality in some of the derivative lines could be the mobilization and integration of a copy of the parental P1370 enhancer trap into a second location, presumably *ae*. This would account for the lethality and maintenance of the parental *lacZ* expression pattern. This possibility would still permit the cloning of the *ae* gene by retrieving the flanking genomic sequence from the second P{PZ} copy. A molecular examination of the lines was necessary to determine which category each of the derivative lines could be grouped into.

Isolation of 3' Flanking Genomic Sequences

In order to characterize the derivative lines at the molecular level and detect any alterations to the P{PZ} construct that would have led to the generation of the *ae* phenotype, mini libraries were utilized for cloning genomic sequences from the derivative lines. Initially, when probed with the 3'-most 233 bp of *P* element sequence, a Southern analysis revealed that the derivative line P1370^{6.1} contained two or at least part of two P{PZ} transposons within the genome. A *Hind*III genomic Southern blot indicated that one of the 3' *P* element ends and flanking genomic sequence had a similar mobility to the parental *tsh*04319 transposon, implying that the 3' *P* element and flanking genomic sequence remained unaltered. The second 3' *P* element ran significantly slower. The *Lac Z* staining of the derivative line P1370^{6.1} remained unchanged from the parental expression pattern, and the line also remained *ry*⁺. These results taken together suggest that in P1370^{6.1}, one copy of the 3' *P* element corresponds to the original P1370 insert (P1370') with the additional 3' *P* element sequence introduced elsewhere in the genome, possibly within or near the *ae* locus.

The genomic sequence flanking the 3' *P* element end of the P1370' transposon was recovered from a *Hind*III mini library of the derivative line P1370^{6.1} (see materials and methods for mini library) by probing with the 3' *P* element sequence. A *Hind*III

library was used because *HindIII* cuts in the 3' end of the P{PZ} construct and again in the flanking genomic sequence. This allows the removal of the 3' *P* element fragment along with some 3' flanking genomic sequence (3'FGS) (**Figure 6B**). Using the 3'FGS as a probe for Southern analysis, it was revealed that the sequence was the same as that of the parental P1370 insert. Using the 3' *P* element sequence as a probe for the same Southern blot, it was also determined that both sequences comigrated in the P1370 and P1370^{6.1} lines. This indicated that the 3' *P* element sequence in the P1370 and P1370^{6.1} lines is linked to the same genomic fragment, and therefore the 3' FGS could be used to analyze the remaining derivative chromosomes for alterations to flanking genomic sequence. Sequencing of the flanking genomic fragment revealed that the P1370' transposon is localized to the untranslated leader (UTL) sequence between base positions 281 and 282 (**Figure 6C**) of the *tsh* gene. In order to determine if any of the derivative chromosomes are the result of 3' deletions of flanking genomic sequences, the 3'FGS was used to characterize the remaining derivative lines to identify such an event.

Prior to the identification of the P1370 enhancer trap as an allele of the *tsh* gene, a walk was started from the 3'FGS rescued from the P1370^{6.1} line, still under the assumption that P1370 and *ae* were independent genes. P1 genomic clones available through the Berkley Genome Drosophila Project (BGDP) were analyzed using Southern blots probed with the 3'FGS. Four overlapping clones were identified from this screen; DS00218, DS02775, DS03846 and DS05959. Each of these P1 clones was going to be used on the chromosome walk from the P1370 insert to the *ae* gene. Personal communications with Stephen Kerridge indicated that approximately 150 kb of ordered overlapping lambda genomic clones had been recovered when the *tsh* gene was cloned (Fasano et al., 1991). These lambda clones were then used to identify any polymorphisms associated with the *ae* allele.

Phenotypic Severity of the Derivative Lines.

Each of the derivative lines was also tested for the strength of genetic interactions with the *ae* allele. The phenotypes of the derivative chromosome / *ae* transheterozygotes range in severity, and were therefore considered weak (W), moderate (M) or strong (S) (**Table 4**). The "weak" class of derivative alleles exhibit a weak phenotypic interaction,

such that the derivative/*ae* transheterozygotes are not fully penetrant for the wing phenotype. Less than 100% express the “full” *ae* phenotype. The “full” *ae* phenotype refers to alleles that show complete 100% penetrance and full expressivity. Flies expressing the full *ae* phenotype hold both wings out and away from the body and also have drooping halteres. The “moderate” derivative class is when all of the F1 transheterozygotes exhibit the “full” *ae* phenotype without any other obvious defects. The “strong” derivative class are those lines that not only show a full *ae* phenotype but also exhibit other defects not usually seen in the *ae* mutant, such as thoracic and / or wing defects in addition to the abnormal wing and haltere posture. All derivative lines were also crossed to Oregon R to determine if they exhibit any dominant phenotypes not obvious in the progeny of the other crosses. None of the lines exhibited any dominant effects associated with the derivative chromosomes.

Molecular Analysis of P1370 Derivative Lines

In addition to the *ry* and *lacZ* staining results presented above, the derivative lines were also characterized based on genomic Southern analysis comparisons with the parental P1370 line. The 3' and 5' *P* element sequences and 3' flanking genomic sequences were used as probes in the analysis of each of the derivative lines. Each derivative was categorized based on three possible observations with respect to the 3'FGS. The first possibility was that the 3'FGS had a similar mobility to that of the parental line. The second possibility is that the mobility of the 3'FGS is altered with respect to the parental fragment. The third possibility would be a reversion of the 3' FGS to a mobility similar to that of the fragment on the balancer chromosome. This can be caused by either a deletion removing the entire 3' flanking fragment or a clean excision of the enhancer trap from its location in the 5' UTL. Similar possibilities existed for the derivative lines probed with the 3' and 5' *P* element sequences, in addition to the duplication and noncontiguous reintegration of the 5' and / or 3' *P* element sequences.

Twenty-one derivative chromosomes were chosen at random for molecular characterization. Each of the lines was grouped into one of six general categories based on Southern analysis results, the expression of the *lacZ* reporter gene and the severity of

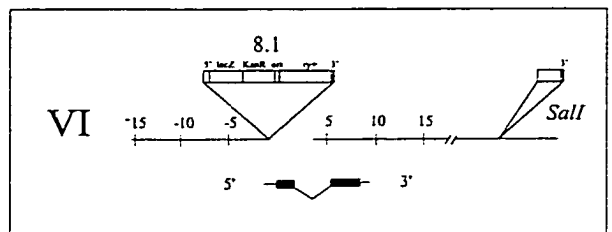
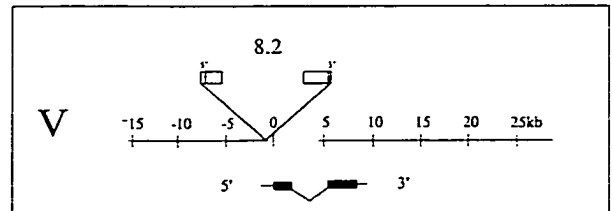
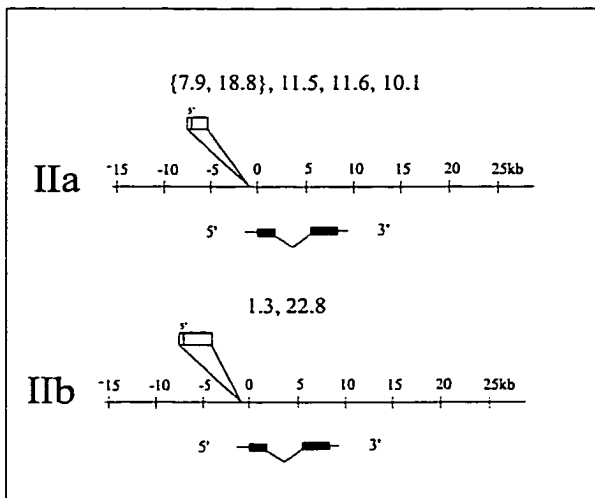
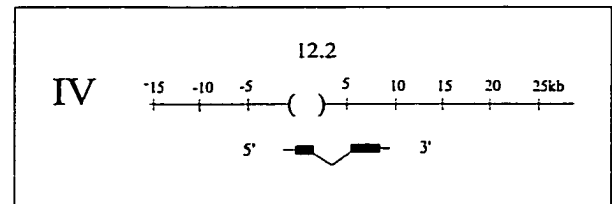
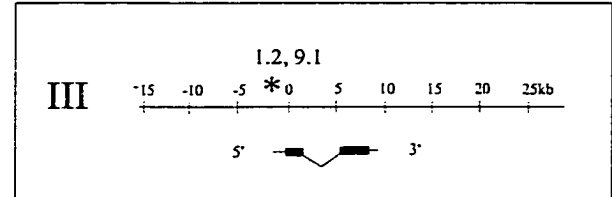
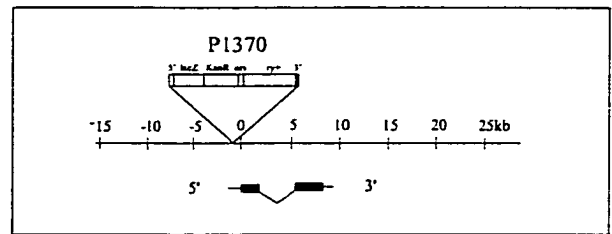
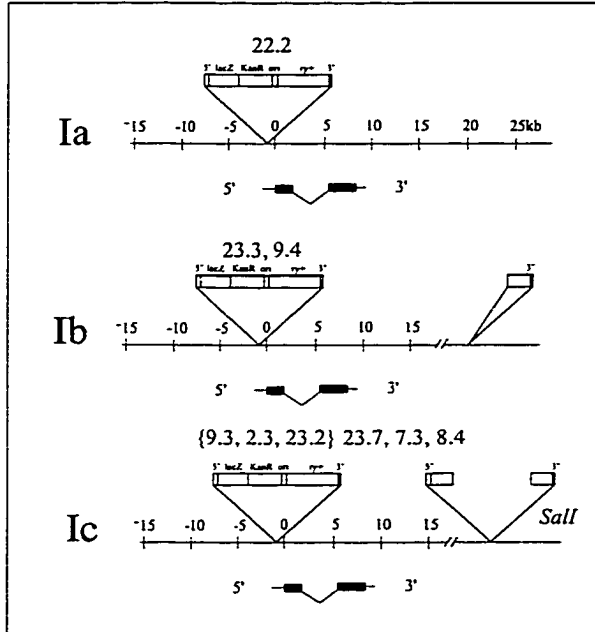
Table 4. The bracketed values refer to the percentage of flies exhibiting the full *ae* phenotype. Full *ae* phenotype refers to both wings held out and away from the body. The categorization of the derivative lines into strong moderate and weak are based on two criteria of the Derivative / *b cn ae* transheterozygotes. The first is the expressivity of the phenotype. Transheterozygotes with a full *ae* phenotype have both wings held out and drooping halteres. Flies with less than both wings held out are not considered to have a full *ae* phenotype. The results under the heading F1 compare the viability of the transheterozygotes to the *CyO/b cn ae* sibling class from the F1 generation of the cross indicated. The numbers in the column under P1 indicate the identifying number for each derivative line. The first number of each derivative line indicates the bottle that the particular line arose from. The second number of each derivative line indicates a specific *ae* F1 fly from that bottle. The phenotype of crosses between the various derivatives and *b cn ae; ry* or P1370 are presented under their respective headings. The “NC” and “C” under the P1370 heading indicates that a derivative line fails to complement or complement the lethality associated with the P1370 enhancer trap line, respectively. In cases where complementation occurs the wing phenotype is normal. The *ae* phenotypes presented under the Der. / *b cn ae* heading indicate the wing phenotype of each transheterozygote between a derivative line and the *b cn ae* chromosome. The results from the *lacZ* staining are presented under the *lacZ* heading. A “+” indicates that the derivative line *lacZ* expression pattern resembles the parental P1370 line and a “-“ indicates that the line fails to show any *lacZ* reporter gene expression. Each of the derivative lines was homozygous lethal and is balanced over *CyO*. The Group column refers to the categorization of the derivative lines with respect to Southern analysis and *lacZ* expression as seen in **Figure 8**. Those lines without a group designation were not tested using Southern analysis. The a or b in the group column represents subgroups within a particular category. The W, M or S indicate weak, moderate and strong *ae* alleles, respectively. Der. refers to derivative chromosomes. The asterisk indicates the derivative with the modified parental *lacZ* expression.

Table 4. <i>tsh</i> [04319] Derivative Chromosome Summary.					
Group	P1 gen.	F1 generation from <i>B. cn ae</i> X		<i>Lac Z</i>	Compl.
		Derivative / <i>CyO</i>			
	Derivative	<i>CyO/b cn ae</i>	<i>Deer./b cn ae</i>		<i>Der / P1370</i>
Ia	22.2/ <i>CyO</i>	119	800 (100) M	+	NC
Ib	9.4/ <i>CyO</i>	43	1007 (0) W	+	NC
Ib	23.3/ <i>CyO</i>	75	1006 (20) W	+	NC
Ic	2.3/ <i>CyO</i>	82	11.9 (63) W	+	NC
Ic	7.3/ <i>CyO</i>	58	661 (0) W	+	NC
Ic	8.4/ <i>CyO</i>	44	723 (33) W	+	NC
Ic	9.3/ <i>CyO</i>	83	11.3 (21) W	+	NC
Ic	23.2/ <i>CyO</i>	130	1009 (20) W	+	NC
Ic	23.7/ <i>CyO</i>	114	1220 (0) W	+	NC
Iia	7.9/ <i>CyO</i>	37	529 (100) M	-	NC
Iia	10.1/ <i>CyO</i>	80	1077 (100) M	-	NC
Iia	11.5/ <i>CyO</i>	110	1000 (100) M	-	NC
Iia	11.6/ <i>CyO</i>	100	1023 (100) M	-	NC
Iia	18.8/ <i>CyO</i>	54	879 (100) M	-	NC
Iib	1.3/ <i>CyO</i>	118	132 (100) S	-	NC
Iib	22.8/ <i>CyO</i>	62	1005 (100) S	-	NC
III	1.2/ <i>CyO</i>	96	76 (100) ¹ M	-	C
III	9.1/ <i>CyO</i>	100	62 (100) ¹ M	-	C
IV	12.2/ <i>CyO</i>	93	890 (100) M	-	NC
V	8.1/ <i>CyO</i>	87	422 (100) S	+	NC
VI	8.2/ <i>CyO</i>	104	655 (100) M	-	NC
	2.2/ <i>CyO</i>	111	1305 (27) W	+	NC
	5.1/ <i>CyO</i>	83	1004 (15) W	+	NC
	6.1/ <i>CyO</i>	110	906 (20) W	+	NC
	11.2/ <i>CyO</i>	87	788 (40) W	+	NC
	11.4/ <i>CyO</i>	94	1009 (100) M	-	NC
	14.1/ <i>CyO</i>	97	11.4 (50) W	-	NC
	14.3/ <i>CyO</i>	70	79 (70) W	-	NC
	18.1/ <i>CyO</i>	84	900 (100) M	-	NC
	19.2/ <i>CyO</i>	85	1006 (100) S	+	NC

the phenotypic interaction with the *b ae cn; ry* chromosome (**Figure 8**). Seven out of the twenty-one lines tested (33%) fell into the first category (**Figure 8, I**). Each of these lines contains a P{PZ} construct that is indistinguishable from the parental insert and expresses the *lacZ* reporter gene in a pattern resembling the *tsh*[04319] expression pattern (**Figure 7**). This group was further divided into three subgroups. **Ia**, comprises 3 lines which each contained only a construct indistinguishable from the parental *tsh*[04319]. The other two subgroups contained the parental P{PZ} construct, but also additional 5' and/or 3' *P* element sequences elsewhere in the genome. Two of the lines in subgroup **Ib** have the parental insert common to all the other lines within this group and also what appear to be a 3' *P* element sequence located elsewhere in the genome. Four of the lines were placed into the third subgroup **Ic**, with each member containing an additional 3' and 5' *P* element sequence in the genome. Each of the additional 3' and 5' *P* element sequences appear to be molecularly linked, indicating they are part of an internally deleted *P* element. If the *ae* mutation generated on each of the derivative chromosomes in group **I** arose as a result of a *P* element insertion event, then the lines most likely to have resulted from such an event would be those in subgroups **Ic** and **b**. Interestingly however, each of the lines in these two subgroups were “weak” alleles whereas the lines in subgroup **Ia** which most closely resemble the parental line and lack any additional detectable P{PZ} construct sequences have a “moderate” phenotype according to the criteria presented above (**Table 4**).

The second group also contains seven members. Each of these lines contains a deleted P{PZ} construct with only the 5' *P* element end remaining at the original parental insertion site. The 5' *P* element sequence was shown to be linked to the 3' FGS, implying the original insert site is retained. Loss of the *ry*⁺ marker and the parental *lacZ* staining pattern implies that the deletion within the P{PZ} construct deleted as far in from the 3' end as the *lacZ* reporter gene (**Figure 8, II**) but likely left the 3' FGS intact. This group can further be subdivided into two subgroups based on the strength of each allele. The first subgroup, **IIa**, contains five of the seven lines, which are considered moderate alleles with an expressivity of 100%. The second subgroup, **IIb**, is represented by two members each exhibiting a strong *ae* phenotype with additional defects not associated with the original *ae* allele. This second group was the most interesting and informative because

Figure 8. Diagrammatic representation of the different classes of derivative lines generated by mobilization of the P1370 enhancer trap line. Each of the derivative lines was categorized based on the presence, absence or altered mobility of fragments corresponding to the 5', and 3' *P* element ends, 3' flanking genomic sequence and the *lacZ* staining all relative to the parental line P1370. All members of group **I**) contain a copy of the parental construct in its original location. This group is further divided into three subgroups. **a)** Derivative lines containing only what resembles the parental insert. **b)** Lines containing the parental insert as well as additional noncontiguous 3' *P* element sequences. **c)** Lines containing a parental copy and additional 3' and 5' *P* element sequences. The second group of derivative lines, **II**), all contain the 5' *P* element sequence from the construct at the original insert site. This group may also be further subdivided into two. Group **IIa** consists of all moderate alleles while group **IIb** contains strong alleles retaining more of the 5' construct sequence. Group **III** contains no detectable P1370 construct sequence in the genome in either of the lines and also appears to delete the insert site. The asterisk indicates the suspected polymorphism associated with the derivative lines in Group III. Group **IV** consists of a single member that appears to be the result of a clean excision of the enhancer trap. Group **V** has a single member that has an internally deleted P{PZ} construct and likely a 3' flanking deletion with an undetermined breakpoint. Group **VI** also consists of a single derivative with has an additional 3' *P* element sequence elsewhere in the genome and also retains more of the 5' P{PZ} construct than member **V** as indicated by the *lacZ* staining **VI**. The derivatives that fall into each group are indicated above each of the schematic representations. A P{PZ} parental construct is indicated in a separate box labeled P1370. The P{PZ} construct is represented by open boxes and all relevant sequences retained in the respective derivative lines are listed above the box (see **Figure 6** for abbreviations). The distance in kb relative to the transcription start site is indicated above the *tsh* coding region represented by the black boxes. The breaks in the kb scale lines indicate that the exact location of the additional construct sequences is undetermined. In each case these extra sequences are arbitrarily placed downstream of the coding region. The brackets indicate derivative lines that are similar according to Southern analysis.



each line represents an *ae* mutation but appears to contain only the *tsh* specific insertion. This molecular evidence along with the complementation data suggests that *ae* and *tsh*[04319] may represent complementing alleles.

The third group of derivative lines includes those with no detectable 5' or 3' *P* element sequences present in the genome, suggesting an excision of the entire enhancer trap (**Figure 8, III**). Two of the derivative lines tested fit this category, *tsh*[04319]^{1,2}, and *tsh*[04319]^{9,1}. These two lines complement the *tsh*[04319] lethality and also contain the *b cn* and *ae* mutations. This indicates the lethality associated with these lines is independent of the parental *tsh*[04139] lethality and would have arisen on the *b cn ae* chromosome. It is not likely that the lethality was introduced onto the parental *tsh*[04319] chromosome and then recombined onto the *b cn ae* chromosome, because in order to avoid this problem only males from the screen that exhibited the *ae* phenotype were selected for characterization. In fact, the derivative lines *tsh*[04319]^{9,1} and *tsh*[04319]^{1,2} were each recovered from the screen as males and therefore could not have arisen by a simple recombination event. Although both of these lines complement the lethality associated with the *tsh*[04319] insert they still retain the *tsh*[04319] allele designation because of their origin. Each of the two lines has an introduced lethal on the second chromosome. However, each of the lethals belongs to a separate complementation group since *tsh*[04319]^{9,1} / *tsh*[04319]^{1,2} heterozygotes are viable and exhibit the *b cn ae* phenotype. Both of these lines are also considered moderate *ae* alleles resembling that conferred by the *b ae cn* chromosome. According to Southern analysis, the insert site sequence has also been modified such that it resembles a deletion of the genomic sequence surrounding the insertion. This is unlikely because each of the lines is *tsh*⁺. Any deletion of this size within this region would likely lead to a null *tsh* allele and therefore lethality. This suggests that the band shifts are likely due to a polymorphism associated with the *Hind*III site upstream of the *tsh* gene.

The fourth group consists of a single line, *tsh*[04319]^{12,2}. This group resembles group **III**, but it fails to complement the lethality associated with the parental enhancer trap line. According to Southern analysis, the loss of the 5' and 3' *P* element sequences, the loss of parental *lacZ* expression pattern, and the presence of a parental sized *Hind*III band detected on Southern analysis, suggests an excision of the P{PZ} construct and a

deletion of at least part of the coding region corresponding to the probed region, the 3'FGS. The chromosome is most likely a deletion rather than a clean excision, because a clean excision would revert the lethality associated with the *tsh*[04319] line. The *tsh*[04319]^{12.2} allele is likely caused by a deletion large enough to remove the sequence that corresponds to the 3'FGS which would include the first *tsh* exon, leading to a true null of the *tsh* gene. A small deletion undetectable under the conditions used for our Southern analysis would likely not lead to the lethality within the *tsh* gene because the deletion would only remove a small portion of the 5' UTL sequence (**Figure 6C**).

The fifth group (**V**) of derivative lines are those which have what appear to be an internally deleted P{PZ} construct. *tsh*[04319]^{8.2} is the only member that appears to fall into this category. The moderate allele, *tsh*[04319]^{8.2} fails to exhibit any *lacZ* reporter gene expression and appears to also have a deletion of the 3'FGS. The internal deletion appears to break in the *lacZ* reporter gene and within the *ry*⁺ gene in the 3' end of the construct, such that digests with *SaII* show a link between the 3' and 5' *P* element sequences (**Figure 8, V and Figure 6B**).

The last group (**VI**) also consists of one derivative line, *tsh*[04319]^{8.1}. The construct within this line appears to be intact because of the presence of *lacZ* expression and the presence of both 5' and 3' *P* element sequences (**Figure 8, VI and Figure 6B**). *tsh*[04319]^{8.1} is similar to the group **V** member because it appears to contain a deletion of the 3' FGS. *tsh*[04319]^{8.1} is unique among the lines analyzed, because the reporter gene expression pattern within the wings, halteres and legs appears to be a modified parental *tsh*[04319] pattern, showing an incomplete expression pattern in each of the imaginal discs (**Figure 17 B versus C and E versus F**). The *tsh*[04319]^{8.1} allele is considered the strongest allele of all the derivative lines. Not only does the *tsh*[04319]^{8.1}/*ae* transheterozygote exhibit a full *ae* phenotype but they also show thoracic and wing defects (**Figures 15 and 14**). The wings often show blistering and a pinching at the distal part without loss of wing tissue. There are also problems with cell adhesion in the wings in some of the transheterozygotes, as indicated by an apparent failure of the dorsal and ventral wing surfaces to form proper contacts. A full description of the thoracic and wing defects is given below.

A mini library of derivative line *tsh*[04319]^{8.1} was also created to clone the genomic sequence now flanking the 3' *P* element. From Southern analysis it appeared that this derivative line resulted in a 5' deletion of the *tsh* coding sequence 3' to the insert site (**Figure 8, VI**). Based on the strong phenotypic interaction of the *tsh*[04319]^{8.1} derivative lines with the *ae* allele, (see discussion below) it was predicted that *tsh*[04319]^{8.1} might contain a deletion of the sequence flanking the *P* element in the *tsh* gene.

As indicated above, each of the derivative lines was also tested for *lacZ* reporter gene activity. Each was compared to the parental expression pattern and recorded in **Table 4**. All the derivative lines that produced an expression pattern resembling the parental pattern were closely re-examined for any subtle differences.

In general, Southern analysis of the derivative lines revealed that most of the chromosomes still contain enhancer-trap sequences inserted into the untranslated leader sequence of *tsh*. Three (out of seven) of the derivative lines that showed no detectable alterations to the enhancer trap or surrounding sequence were used for further characterization. If a second event, independent of the *tsh P* element, generated the *ae* phenotype in these three lines, excision of the *P* element at *tsh* should separate the *tsh* lethality from the *ae* phenotype. When lethality in two of the lines (*tsh*[04319]^{23.7} and *tsh*[04319]^{23.2}) was successfully reverted (**Figure 5D**) the *ae* phenotype was also lost. Interestingly, there appears to be a progressive loss of expressivity from the weak derivative lines. At the time each of these lines were used for the reversion experiment they were considered weak alleles with less than 50% of the transheterozygotes expressing the *ae* phenotype. Now, however, 20% and 0% of the transheterozygotes (*tsh*[04319]^{23.7}/*ae* and *tsh*[04319]^{23.2}/*ae*) express the *ae* phenotype, respectively. An additional screen was designed to select for clean excisions from the *tsh* gene with a concomitant insertion into the *ae* gene (**Figure 5B**). However, no derivative chromosomes failing to complement the *ae* phenotype were produced from this screen.

Northern Analysis

By definition the *ae* mutation is a null allele since flies hemizygous or homozygous for *ae* are phenotypically the same. Because *ae* is a homozygous viable null

allele and molecular and genetic evidence suggest it is an allele of the homeotic gene *tsh* which is homozygous lethal, it was relevant to determine if *ae* causes alterations in the *tsh* transcript. These results are presented in **Figure 9**. Generally, the amount of RNA loaded in each lane is comparable with slightly more loaded in the last three lanes of Oregon R and the last lane of *ae* (**Figure 9 C**). The bands on the Northern blot correspond to the 5.0 and 5.4 kb *tsh* RNA species (**Figure 9 A**). Two larger previously reported species (Fasano et al., 1991) were not detected on the Northern. However, the two smaller fragments are known to encode the *tsh* protein. Because there is a slight developmental delay in the *ae b cn; ry* line this could account for the slight reduction in mid first instar levels of the *tsh* transcript in the *ae b cn; ry* mutants. Although *ae* is considered a null allele, the two protein coding transcripts can be identified at levels comparable to the Oregon R stock. This suggests the *ae* mutation may represent a regional or a domain specific null allele of the *tsh* gene.

Molecular Mapping.

Since the genetic data in **Figure 5** and the molecular characterization presented above suggest that *ae* may be a novel allele of the *tsh* gene, an attempt was made to map the *ae* phenotype with respect to the *tsh* coding region. The failure of the deficiency *Df(2L)tsh8* to complement *ae*, in combination with the ability of *Df(2L)R6* to complement *ae*, locates the lesion within an approximately 18 kb region that includes the *tsh* coding region (**Figure 10**). Southern analysis comparisons between the DNA from *b ae cn; ry* flies with that from Oregon R, and the *b cn* (*ae* parental stock) revealed two polymorphisms that fall within or near the critical region defined by the deficiencies seen in **Figure 10**. One polymorphism, 5' of the *tsh* coding region, was present in both *ae* and the *b cn* parental stock, and was therefore not considered significant (data not shown). A second polymorphism that is unique to *ae* was detected 3' to the coding region (**Figure 10B**). Within a 4.8 kb *EcoR1* fragment found in Oregon R and *b cn*, an approximately 5.5 kb insert was identified (**Figure 10A**) in DNA from *ae*. This site is located between the previously described *Ubx/Antp* HOMRE motif (McCormick, 1995) and the 3' end of the *tsh* coding region. The insertion was subsequently mapped to a 34 bp *DraI* fragment

found within a larger 915 bp *Bam*HI / *Hind*III sequence, which in turn is included within the 4.8 kb *Eco*RI fragment (**Figure 19**).

Figure 9. Northern hybridization analysis of total RNA from *ae* and Oregon R embryos, larvae and adults. **A)** Northern blot with 10 µg of total RNA loaded in each lane. Lane 1 removed in panel **A)** however present in panel **C)** has 9.5-0.24 kb RNA ladder (Gibco), lanes 3-7 correspond to *b ae cn; ry* total RNA and lanes 2, 8 and 15 were left blank. Lanes 9-14 correspond to Oregon R total RNA. Lanes 3 and 9; 4 and 10; 5 and 11; 6 and 12,13; 7 and 14 correspond to 0-24hr embryos; midstage first instar; midstage second instar; wandering third instar larvae and; adults, respectively. The Northern blot was probed with the 3.0, 2.9 and 2.8 kb *EcoRI* genomic fragments from the *tsh* gene and surrounding genomic sequences. The asterisks in panel **B)** indicate the fragment used as probes. Arrows indicate the 5.4 and 5.0 kb *tsh* transcripts. **B)** A schematic diagram of the *tsh* coding region from a $\theta 6$ genomic lambda clone, with the 3.0 kb, 2.9 and 2.8 kb genomic fragments marked with asterisks. **C)** a negative image of a photograph of the gel in panel **A)** stained with EtBr. The dark bands indicate the ribosomal species, which were used as a loading control. The arrowhead indicates the bands that are clustered together corresponding to the 28s and 18s rRNA species of sizes (1.64 kb and 1.93 kb) and 1.85 kb, respectively. The RNA standard is indicated along side the negative of the photograph.

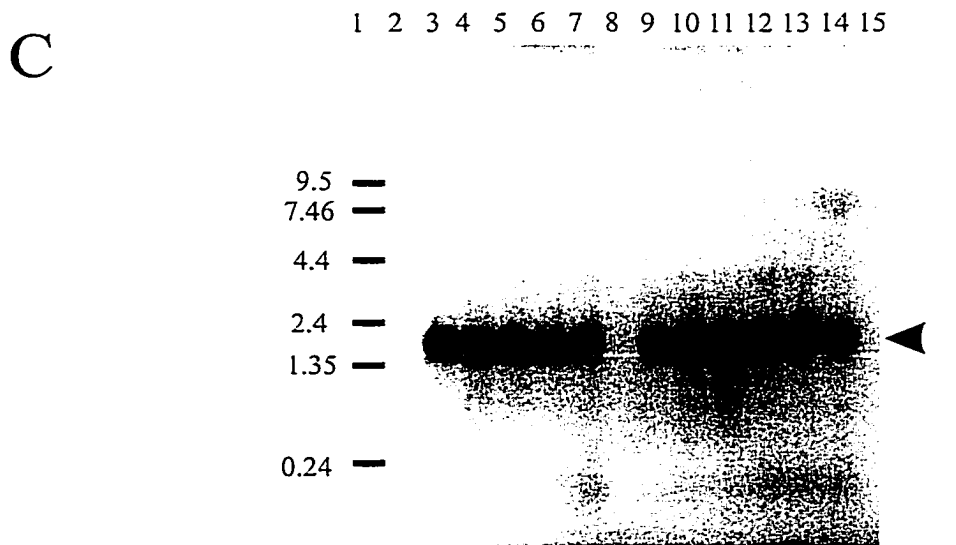
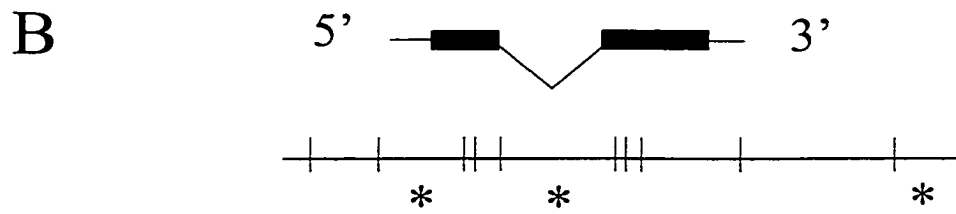
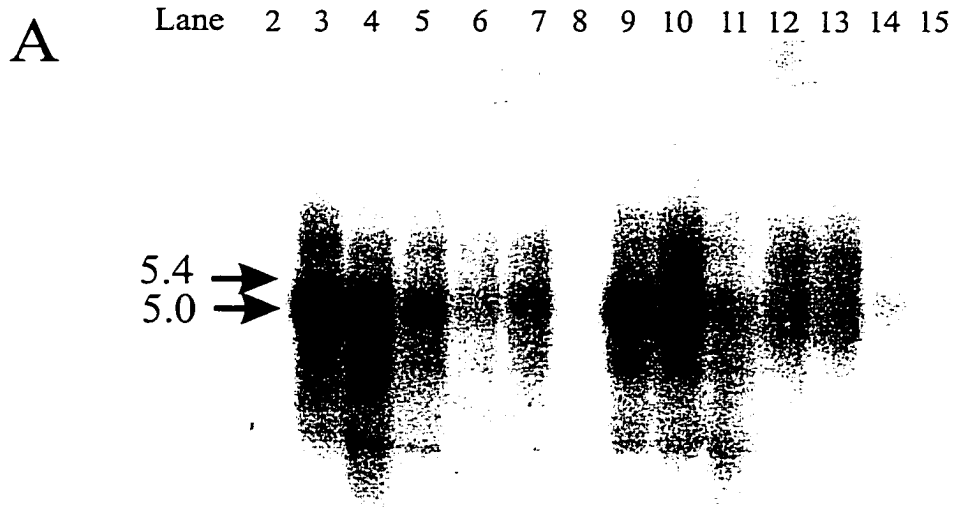
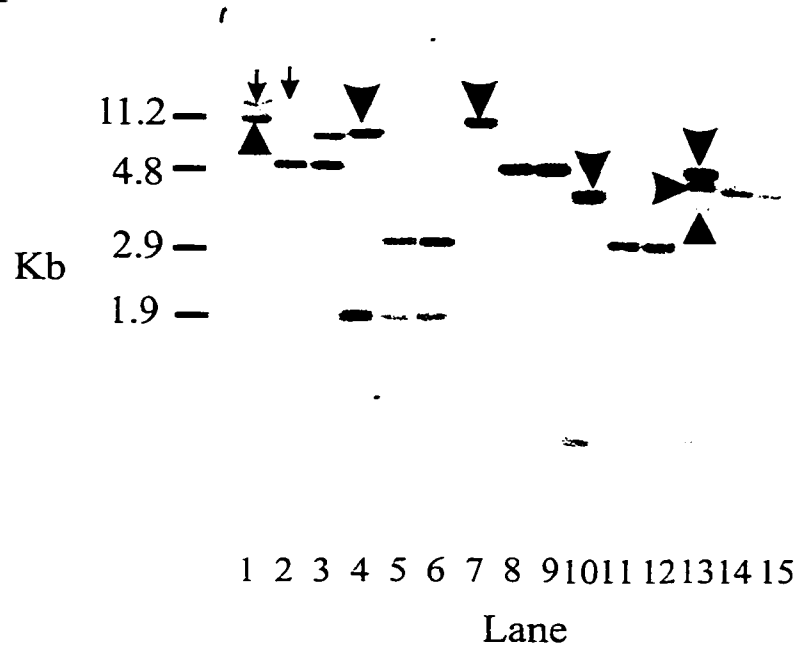
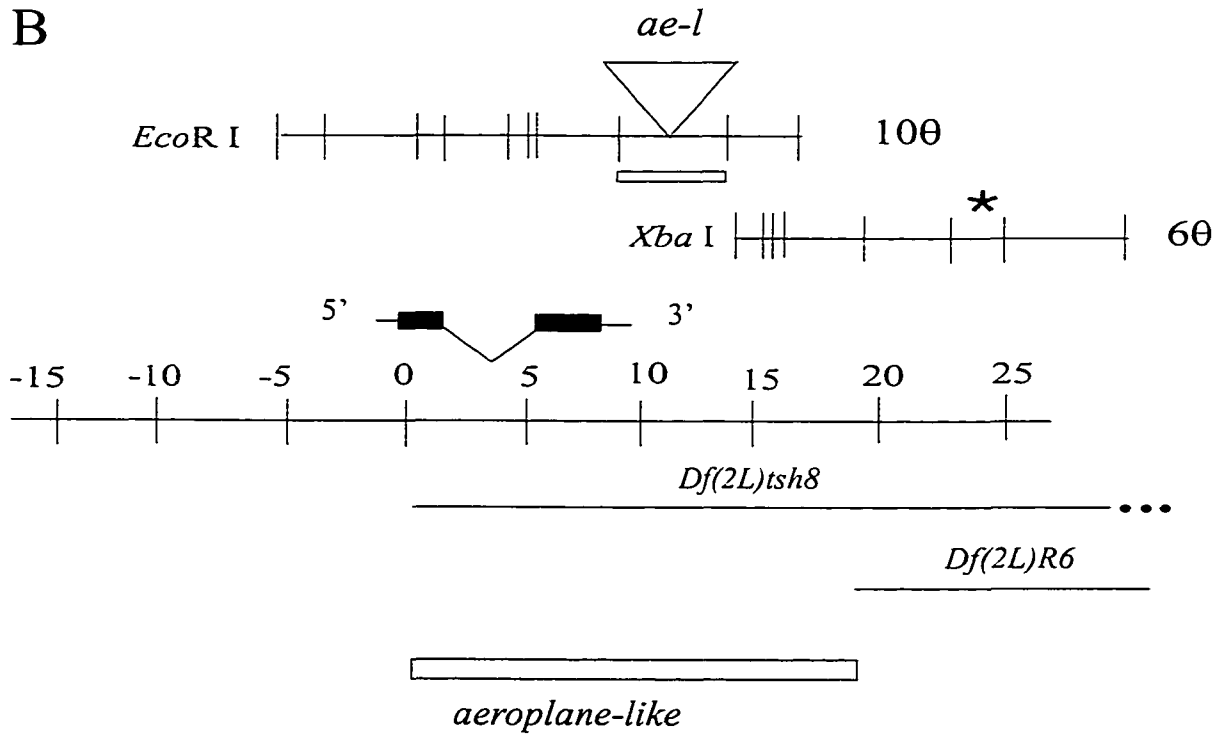


Figure 10. Molecular analysis of the *tsh* gene in an *ae* genetic background. **A)** Southern blot analysis comparing *ae*, Oregon R and the *ae* parental stock (*b cn*). Lanes 1, 4, 7, 10 and 13 contain *b cn ae* DNA digests. Lanes 2, 5, 8, 11 and 14 contain *b cn* DNA digests from the *b cn* parental chromosome. Lanes 3, 6, 9, 12 and, 15 contain Oregon R DNA digests. Lanes 1-3 are *Bam*HI digests, 4-6 are *Eco*RI/*Bam*HI digests, 7-9 are *Eco*RI digests, 10-12 are *Eco*RI/*Hind*III digests and 13-15 are *Hind*III digests. The arrowheads in each of the *ae* lanes indicate the polymorphisms associated with the *ae* phenotype compared to the parental and wild type chromosomes. The arrows in lanes 1 and 2 indicate faint bands of the same mobility. **B)** Restriction map of the *tsh* gene as published by Fasano et al. (1991). The HOMRE location is indicated with an asterisk. Clone 10 θ is shown as an *Eco*RI restriction map and clone 6 θ is shown as a *Xba*I restriction map. The triangle labeled *ae* on the map refers to location of the polymorphism associated with the 3' insert identified in the *ae* mutant. The Southern blot in **A)** was probed with the 4.8 kb *Eco*RI genomic fragment just 3' to the coding region, marked by an open box under the 10 θ clone. Finescale physical mapping located the *ae* mutation to an approximately 18 kb region including the coding region of *tsh* (summarized below the *tsh* schematic). The location of break points for *Df*(2L)*tsh*8 and *Df*(2L)*R6* as well as the *Eco*RI/ *Hind*III restriction map of the *tsh* gene as reported by McCormick et al. (1995). The *tsh* coding region reads from left to right, 5' to 3'. The 5.5 kb insertion in DNA from *ae* is the only change detected within the 18 kb region defining the *ae* locus. Taken from Soanes and Bell, 1999.

A



B



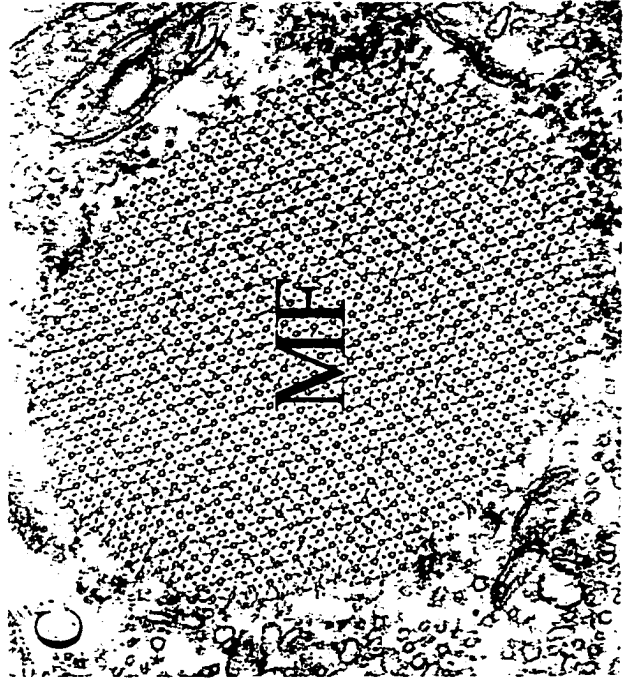
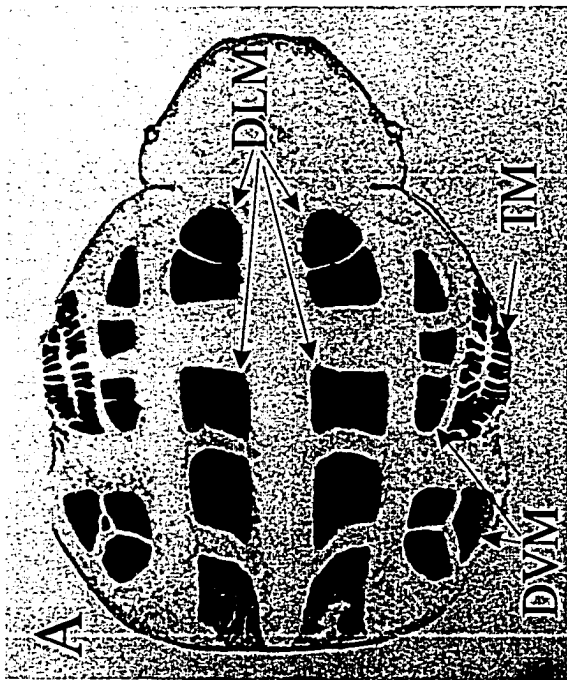
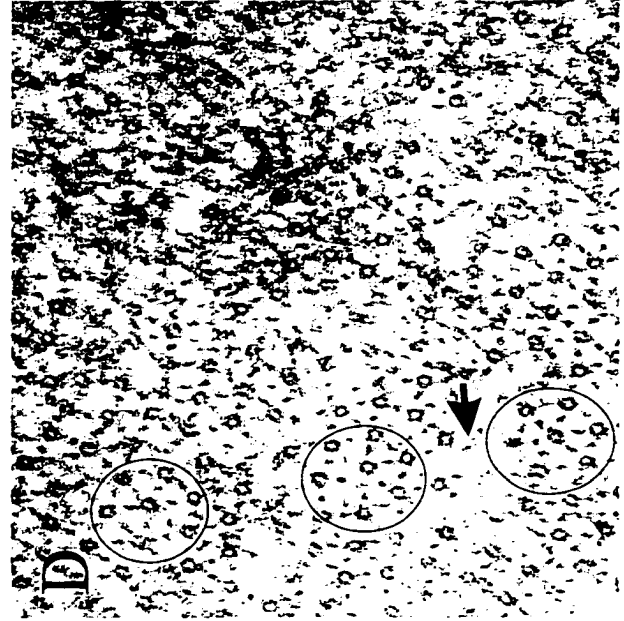
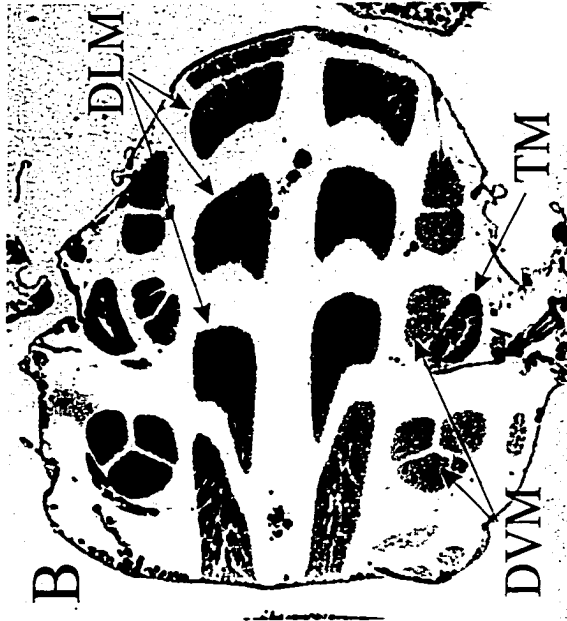
Chapter IV - Etiology

Indirect Flight Muscles

The initial analysis of the original *ae* mutation (Quelprud, 1931) revealed some abnormalities associated with the anterior-most dorsoventral (DVM) indirect flight muscles (IFMs). The IFMs are two antagonistic groups of fibrillar muscles that provide the power for flight by distorting the thorax. The dorsal longitudinal muscles (DLMs) depress the wings by arching the scutum whereas the DVMs elevate the wings by drawing the scutum downward. The abnormalities observed in the original *ae* mutant, however, failed to be consistent with the phenotype. Defects in the anterior DVMs were not always associated with the abnormal wing posture. Thoracic sections from *ae* flies failed to show any gross abnormalities like those reported in the original mutant. Comparisons between Oregon R and *ae* flies failed to reveal any gross abnormalities in the IFM in either the DVMs or DLMs (**Figure 11** and **12**). The difference in the shape of the exoskeleton observed in the *b cn ae; ry* transverse section compared to the Oregon R control is due to the difference in depth from which the section was taken. Analysis of the exoskeleton from *b cn ae; ry* flies shows no gross abnormalities and is indistinguishable from the wild type control.

Lack of any gross abnormalities led to the examination of the IFM at the ultra structural level. Transmission electron microscopy was utilized for ultra structural analysis of the DLM groups in both Oregon R and the *ae* mutant. Both Oregon R and *ae* DLMs contain myofibrils of wild type morphology as well as myofibrils exhibiting a fragmented appearance. In what appear to be fragmented myofibrils there is a mixture of apparently normal hexagonal arrays among unordered or absent arrays (compare **Figure 11 C** and **D** circles and arrows). In *ae*, however, many of the myofibrils examined appear fragmented and in the Oregon R sections the opposite was true. Because wild type myofibrils were observed in both Oregon and *ae* flies exhibiting the full *ae* phenotype (both wings held out and drooping halteres), it was concluded that defects in the ultra structure of the IFMs are not the cause of the *ae* phenotype and that the myofibrils with a fragmented appearance were artifacts. However, the fact the fragmented appearance in myofibrils of the *ae* mutant were observed much more often than in wild type indicate

Figure 11. Indirect flight muscle analysis. **A)** and **B)** are 1 μm transverse thoracic sections through Oregon R and *b cn ae; ry* adult flies, respectively, observed using light microscopy. The abbreviations are as follows; DVM indicates the dorso-ventral muscles, DLM indicate the dorsal lateral muscle group, and TM indicates the tergal depressor of the trochanter jump muscle. **C)** and **D)** are transmission electron micrographs of 60-90nm ultrathin cross sections of a single myofibril from a thoracic section of the DLM group of an Oregon R and *aeroplane* fly, respectively. **D)** is a higher magnification than **C)**. The *ae* section in **B)** was taken more dorsally from within the animal compared to the Oregon R section. This explains the difference in the shape of the adult cuticle as well as the size of the TM, which is larger in the dorsal thorax. MF indicates a single myofibril. Circles in panel **D)** indicate the hexagonal array of an apparently normal arrangement of thick and thin filaments among unordered or absent arrays (arrow).



that they could be related to the abnormal wing posture, but not directly to the etiology of the abnormal wing posture. It is not the primary cause of the wing phenotype because in that case one might expect all myofibrils in the *ae* mutant to be affected in the same way.

Direct Flight Muscles

The lack of any gross abnormalities associated with the IFMs is not completely unexpected because these muscles are required in generating the power for flight and not for wing posturing. If abnormalities associated with the *ae* mutant are the result of musculature defects, then the more likely muscle groups to be affected are the direct flight muscles (DFM). The DFM and axillary muscles are a set of tubular muscles, which are attached directly to wing base sclerites in the thorax (**Figure 12A**). These muscles are believed to control wing movement by articulating the wing base sclerites. Most of the 17 pairs of DFMs are believed to play a role in flight control, courtship (Ewing, 1979) and initial wing posturing during escape (Nachtigall and Wilson, 1967). The functions of each of the specific DFMs are poorly understood for *Drosophila melanogaster*. Much of what is known about the DFMs and axillary muscle functions is based on information from homologous structures in larger dipterans such as *Calliphora vomitoria* (Ritter, 1911), *C. erythrocephala* (Heide, 1971), and *Musca domestica* (Nachtigall and Wilson, 1967).

The best-characterized DFMs in *Drosophila melanogaster* are 49 through 54 (**Figure 12A**). See **Table 5** for DFM numbering and corresponding terms and synonyms. From the studies of *Muscoïd* species, DFM 51 and 49 appear to be required for initial wing “opening” or “extension” during the escape response (Nachtigall and Wilson, 1967). Experiments with *D. melanogaster* designed to identify functions for specific DFMs, controlled by the giant fiber pathway during escape response, showed that continuous stimulation of DFMs 51 and 49 produced an outstretched wing posture paralysis. However, electrical stimulation failed to produce permanent paralysis or the fully extended wing phenotype (Tanouye and King, 1983) as observed in the *ae* mutant. In *ae* flies each of these muscle groups is present and appears normal in comparison to Oregon R controls (**Figure 12A** versus **B**). In similar experiments, DFMs 53 and 54 were shown to be required for wing elevation during the escape response (Tanouye and

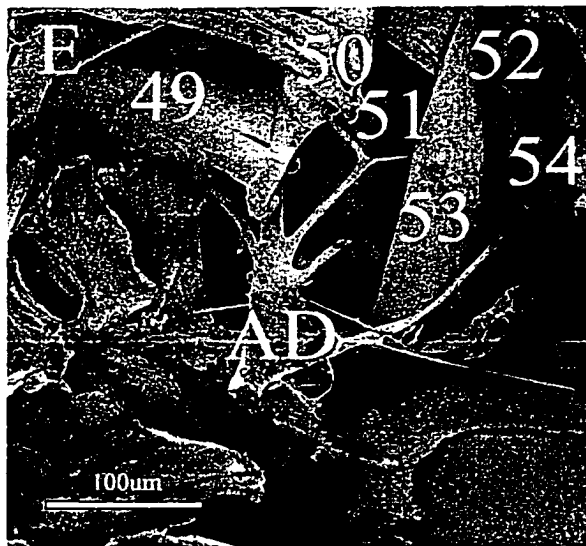
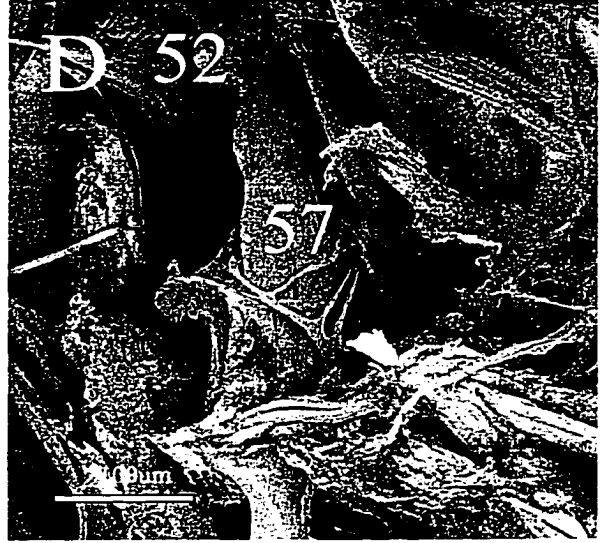
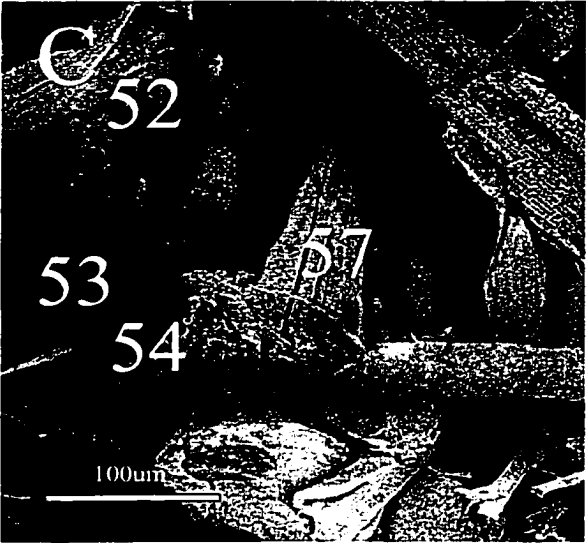
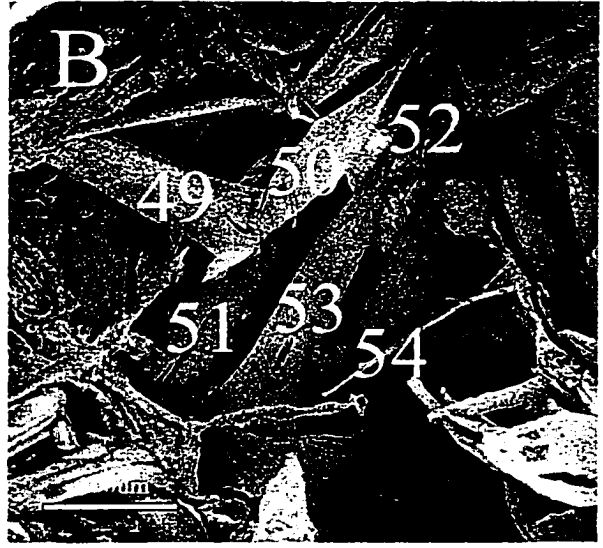
King, 1983). These groups of muscles are also present and appear normal in *ae* flies (**Figure 12A versus B**). Functionally more relevant to the phenotype of *ae*, experiments designed to assign functions to the various DFMs in *C. vomitoria* showed that muscle 57 is required to draw the wings back into the resting position (Ritter, 1911). Because of its homologous function in *C. vomitoria*, DFM 57 would be an excellent candidate for the abnormal wing posture in *ae* flies. However, DFM 57 is present and apparently normal in *ae* animals (**Figure 12C versus D**).

Since no obvious muscle abnormalities were observed in *ae* flies, an analysis of neuronal innervation to the relevant DFMs was undertaken. DFMs 49-53 are innervated by the anterior dorsal mesothoracic nerve (AD) and DFM54 is innervated by the mesothoracic accessory nerve (MACN) (King and Tanouye, 1983). From a number of SEM preparations of *ae* flies, it was observed that DFMs 49-53 are each innervated by an apparently normal AD (**Figure 12E**).

Adult Cuticle

The lack of any gross visible defects associated with the abnormal wing posture is not unexpected, considering that the majority of “wings held out” mutants are the result of neuronal or musculature defects. However, initial analysis of the *ae* mutant with regards to neuronal and muscle function indicated that the abnormal posture is not the result of defects in these functions, suggesting that it may result from a structural defect. Since no gross thoracic defects can be identified in the mutant (**Figure 13 A versus B**) a more detailed examination of the wing hinge was undertaken. The cause of the abnormal wing posture was found to result from a fusion of the proximal wing hinge to thoracic pleural structures found near the base of the wing. The fusion occurs between the proximal ventral radius (PVR) in the wing hinge and the pleural wing process (PWP) region of the thorax (**Figure 13C versus D**). The thoracic PWP and the PVR act to anchor the wing into a held out position during flight or for wing posturing during courtship. The PVR slips over the PWP so that the wing is locked into flight position. The PVR corresponds to the proximal-most region of vein three and, because the wing veins provide structural support to the wing blade, the fusion of the wing blade to the

Figure 12. Comparisons of direct and axillary flight muscles (DFMs) in wild type and the *ae* mutant from Scanning Electron Micrographs (SEM). **A)** SEM of Oregon R DFMs 49-54 and 57. **B)** SEM of *ae* DFMs 49-54. DFM 57 was removed during preparation. **C)** SEM of the abductor muscle 57 in Oregon R flies. **D)** SEM of abductor muscle 57 in *ae* mutants. **E)** Neuronal innervation of DFMs 49-54 by the anterior dorsal mesothoracic nerve in the *ae* mutant. This is visually identical to a similar SEM from Oregon R (not shown). In all panels left is anterior and dorsal is up. AD; anterior dorsal mesothoracic Nerve. The numbering system follows the *Drosophila melanogaster* studies of Miller (1950). See **Table 5** for corresponding muscle terminology and synonymous terminology from other references. Taken from Soanes and Bell, 1999.



thorax led to the posture defect. In addition, within the same general area the yellow club (YC) structure is missing from the mutant. (**Figure 13C** versus **D**). No other defects are observed for the rest of the pleural structures or the notum (**Figure 13A** versus **B**). Furthermore, all of the underlying direct (DFM) and indirect flight muscles (IFM) are unaffected as detailed in **Figure 11** and **12** (and Soanes and Bell, 1999). This subtle structural defect of the cuticle prevents the mutants from folding their wings back into resting position. A similar explanation can be applied for the mutant etiology of the homologous halteres. In wild type flies on the ventral side at the base of the halteres, there is a characteristic “hinge” like folding just below the ventral pedicellar sensilla (VPS) (**Figure 13E**). In the mutant the ventral surface of the halteres do not have the “hinge” like folding, but appear to have a continuous layer of cuticle from just below the ventral pedicellar sensilla to the thorax within the area of the haltere sclerite (**Figure 13E** versus **F**). The crack in the cuticle at the base of the haltere observed in **Figure 13 F** is presumably a processing artifact, since the ventral surface of the halteres in the *ae* mutant had to be pried upwards before viewing.

In the initial characterization and cytological mapping of the *ae* phenotype it was observed that the *ae/tsh8* transheterozygote had a more severe phenotype than the *ae* mutant alone. The transheterozygotes for *ae* and either the null allele, *tsh8*, or derivative line *tsh(04319)^{8.1}*, both show characteristic abnormal wing and haltere posture. However, they are also associated with wing blade and thoracic defects (compare **Figure 14A** versus **B** and **15E** versus **F**). A comparison between Oregon R and the *tsh [04319]^{8.1}/ae* *b cn* wings shows an abnormal longitudinal folding of the wing blade and often a pinching of the wing in distal regions and less frequently a alteration to the posterior wing margin (**Figure 14 A** versus **B** and **C**). The wing defect observed with *tsh [04319]^{8.1}/ae b cn* transheterozygotes is likely caused by a complete loss of function from the *tsh* gene in the derivative chromosome. We believe that the *tsh[04319]^{8.1}* allele is a transcriptional null allele due to a deletion of a part or the whole *tsh* coding region (**Figure 8**). This is also the phenotype observed in the *b cn ae / tsh8* flies. *tsh8* is a large deletion that includes the entire *tsh* coding region.

Another aspect of the strong *ae* phenotypic interaction observed between the derivative allele, *tsh[04319]^{8.1}* and *ae*, is the thoracic phenotype. In the

transheterozygotes it appears that the mesopleural plate (MP) the pre-alar apophysis (asterisk **Figure 15 C and D**) is pushed anteriorly towards the vertical cleft (VC). The cuticle of the MP on the posterior side of the VC appears to be forced either into the VC or under the MP, based on the reduced distance between the VP' and the AP' (double headed arrows in **Figure 15C and D**). This causes a buckling of the cuticle at the base of the wing (compare **Figure 15C and D**, area denoted by asterisk). There is also buckling of the cuticle in the suture between the notopleurite (NP) and the MP. Presumably this also causes the MP to be forced outwards in the region where the plate abuts the NP (arrowhead **Figure 15D**). These defects, associated with the sutures and thoracic plates on the lateral surface of the thorax with respect to the base of the wing, coincide with previous work that suggests *tsh* may be required for proper specification of patterning of thoracic structures in the adult (Calleja et al., 1996). These studies used a GAL4/UAS-*y* system to identify genes, which are expressed in the adult cuticle. From this screen they determined that *tsh* is expressed throughout the adult cuticle. A comparison between the *tsh*-GAL4; UAS-*y* and their *y w* siblings reveals that *tsh* is expressed in the proximal wing and haltere tissues and lateral thoracic pleural plates (**Figure 15 E versus F**)

Wing Posture Mutants

The hinge regions of two abnormal wing posture mutants *taxi* (*tx*¹) and *outstretched* (*os*^o) were also analyzed using SEM along with *ae*. The variable pressure SEMs of the mutants reveal that both *os* and *tx* contain all relevant features in the wing hinge, but no fusion of the cuticle as in *ae* (**Figure 16A and B**). However, both *os* and *tx* possess subtle differences in the wing hinge. In the hinge of the *tx* mutant there is a very small cuticular outgrowth protruding just below the tegula (arrowhead in **Figure 16 C**). It is unlikely that the wing posture in *tx* is attributable to this subtle cuticular outgrowth, but one cannot be certain. The *tx* mutation also has subtle effects on the wing blade.

Although all structures identified in the wild type hinge can also be identified in the *os* mutant, the tegula (T) is considerably closer to the pleural wing process (PWP), such that the yellow club is almost concealed by the T (**Figure 16D**). The SEM of the *os* wing hinge is taken more anteriorly than those for the other panels in **Figure 16** because the wing posture made it difficult to view at the same angle. When preparing the *ae* flies,

Table 5. Direct Flight Muscle Synonymous Nomenclature. Modified from King and Tanouye, 1983.

Reference	Organism	Muscles					
Miller (1950)	<i>Drosophila melanogaster</i>	49 Muscle of prealar apophysis	50 Muscle of prealar apophysis	51 Basalar muscle	52 Basalar muscle	53 Musclee of the first axillary sclerite	54 Muscle of the third axillary sclerite
Nachtigall Wilson (1967)	<i>Muscoid sp.</i>	m.ab.1	m.gr.	m.ab.2	m.an.	m.le.1	m.le.2
Williams Williams (1943)	<i>Drosophila repleta</i>	2nd basalar	1st basalar	sternobasalar	3rd and 4th basalar	anterior muscle of 1st axillary sclerite	Anterior muscle of 3rd axillary sclerite
Zalokar (1947)	<i>Drosophila melanogaster</i>	anterior pleural 4	anterior pleural 5	anterior pleural 3	anterior pleural 6	anterior pleural 1	anterior pleural 2
Heide (1971)	<i>Calliphora erythrocephala</i>	1st basalar	presumably 3rd basalar	2nd basalar	tergopleural	1st pterale I	1st pterale III
Ritter (1911)	<i>Calliphora vomitoria</i>	muscle abductor alae primus (mb1)	Musculus gracilis (mg)	Musculus abductor alae secundus (mbII) and Musculus pronator alae (mp)	Musculus anonymus (ma)	Musculus levator alae primus (mc1)	Musculus levator alae secundus (mcII)

Figure 13. A scanning electron micrograph comparison between *aeroplane* and wild type Oregon R flies. **A)** lateral view of an Oregon R thorax. **B)** lateral view of an *ae* thorax. **C)** and **D)** magnification of the hinge region in Oregon R and *ae* flies, respectively. The abbreviations in **A)** and **B)** are as follows: mp, mesopleurum; pt, postpleura; vc, vertical cleft; np, notopleurite; and is, intrascutal suture. The abbreviations in **C)** and **D)** are as follows: PVR, YC, PWP, PS and AP indicate the proximal ventral radius, the yellow club, the pleural wing process, the pleural sclerite, and axillary pouch, respectively. The bracket in **D)** indicates the location where the wing hinge is fused to the thorax in the *ae* mutant. **E)** and **F)** are Oregon R and *ae* halteres respectively. The abbreviations in **E)** and **F)** are as follows: P, S, VPS, HS, and MB indicate the pedicel, scabellum, ventral pedicellar sensilla, haltere sclerite and metathoracic bristle group, respectively. The apostrophe after an abbreviation indicates the relative location of each of the respective structures in the *ae* mutant. The double headed arrow in **F)** indicates the approximate region at the base of the halteres where the cuticle is fused in the mutant. The tear in **F)** is a processing artifact. The squares in **E)** and **F)** surround the metathoracic bristle groups (MB). See Bryant (1975) for nomenclature.

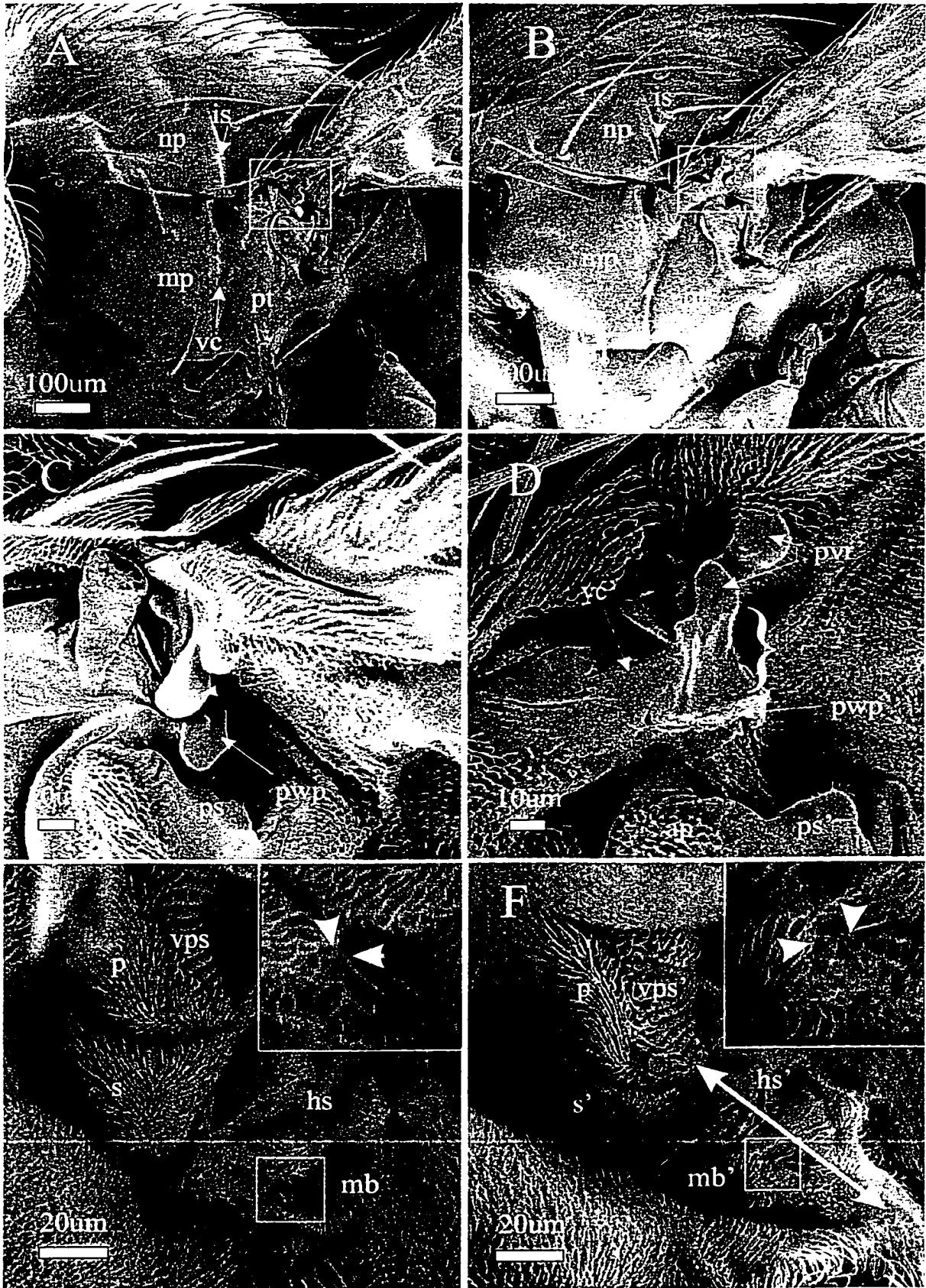


Figure 14. The “extreme” wing phenotypic interaction of the *tsh* [04319]^{8.1} derivative allele with the *ae* chromosome. **A)** Oregon R wing. **B)** and **C)** *tsh* [04319]^{8.1}/*ae b cn* wings. **B)** and **C)** are presented to show the different wing blade defects. The black arrowhead indicates the “pinching” of the distal wing blade often associated with the transheterozygotes. The white arrowheads indicate longitudinal creases in the wing blade. The black arrow indicates a posterior wing margin defect also associated with some transheterozygotes.

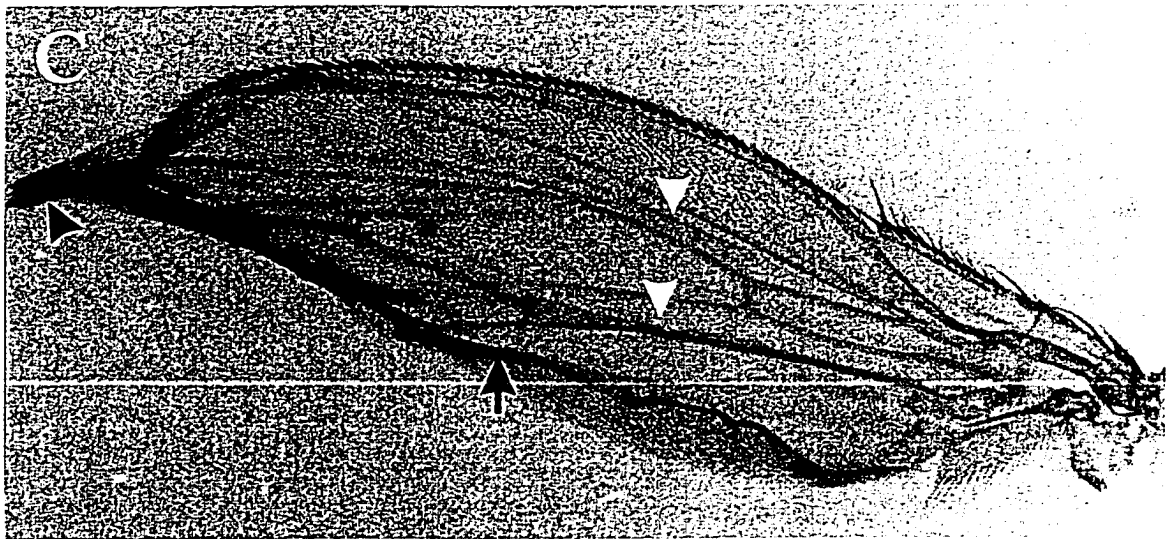
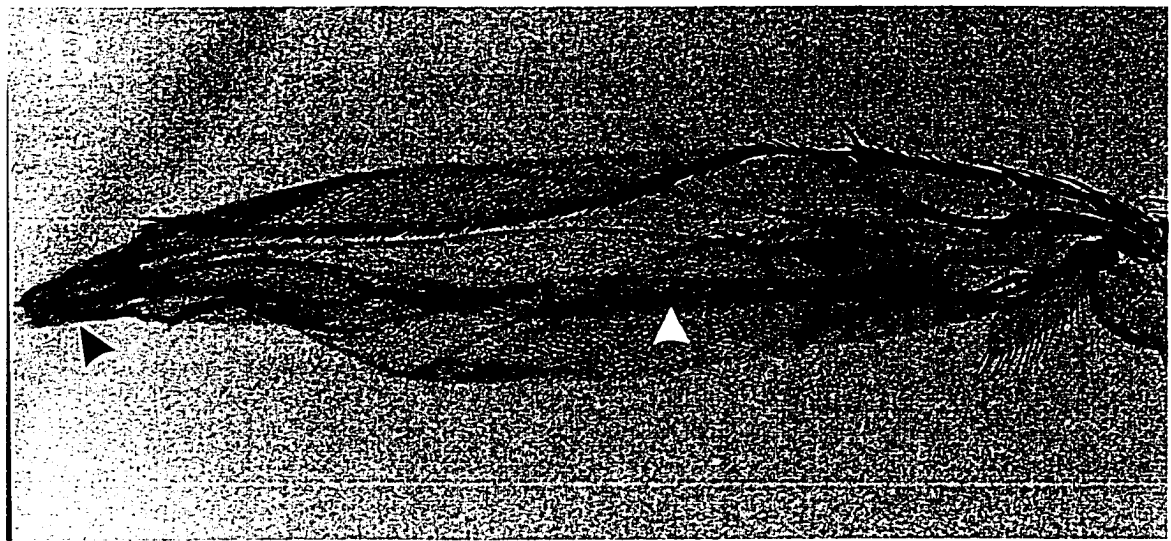
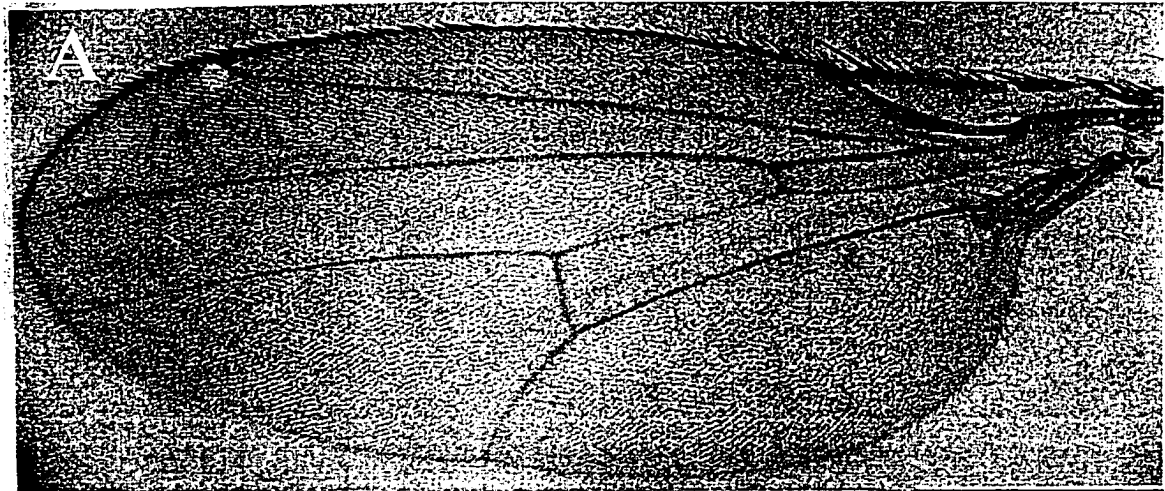
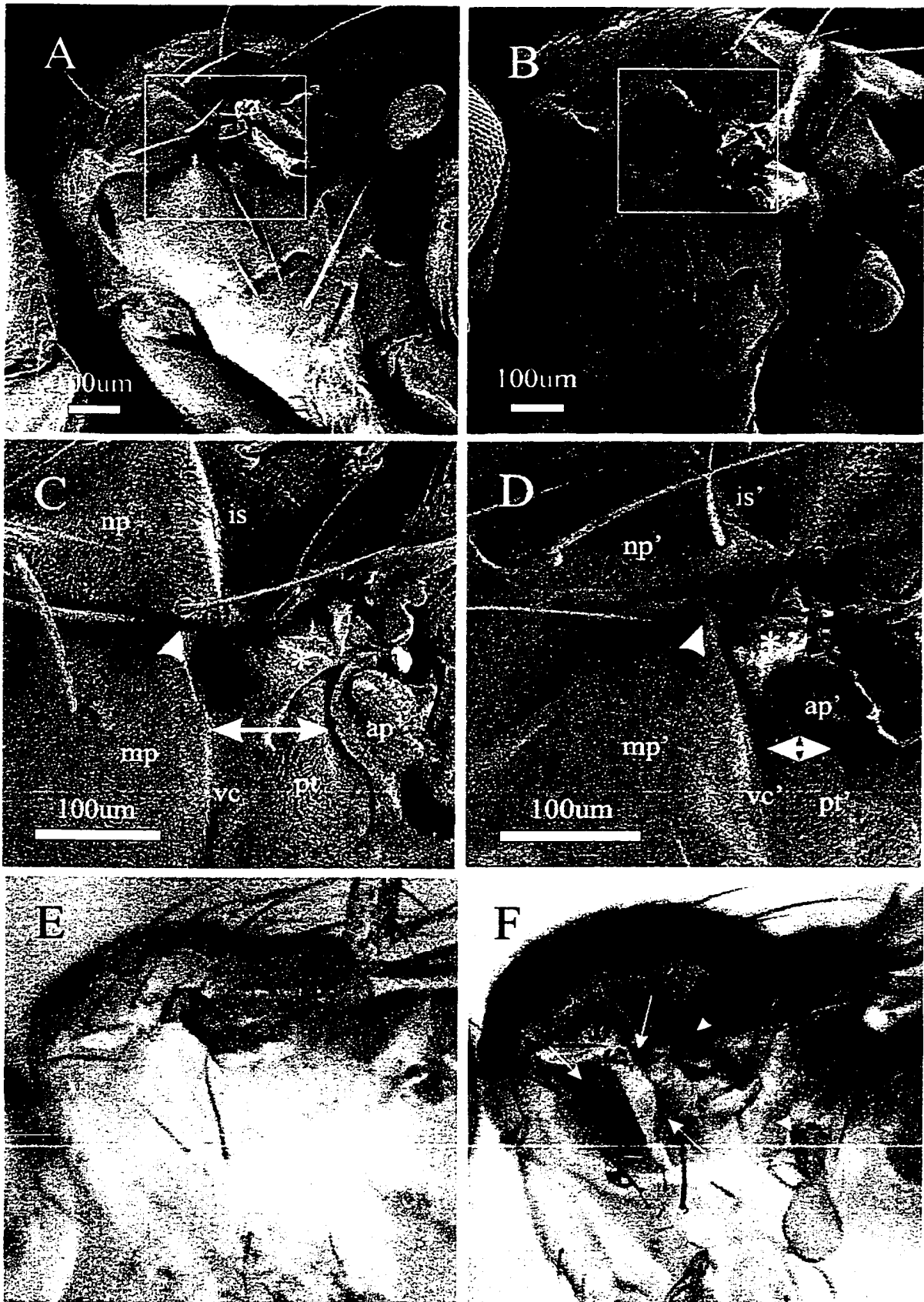


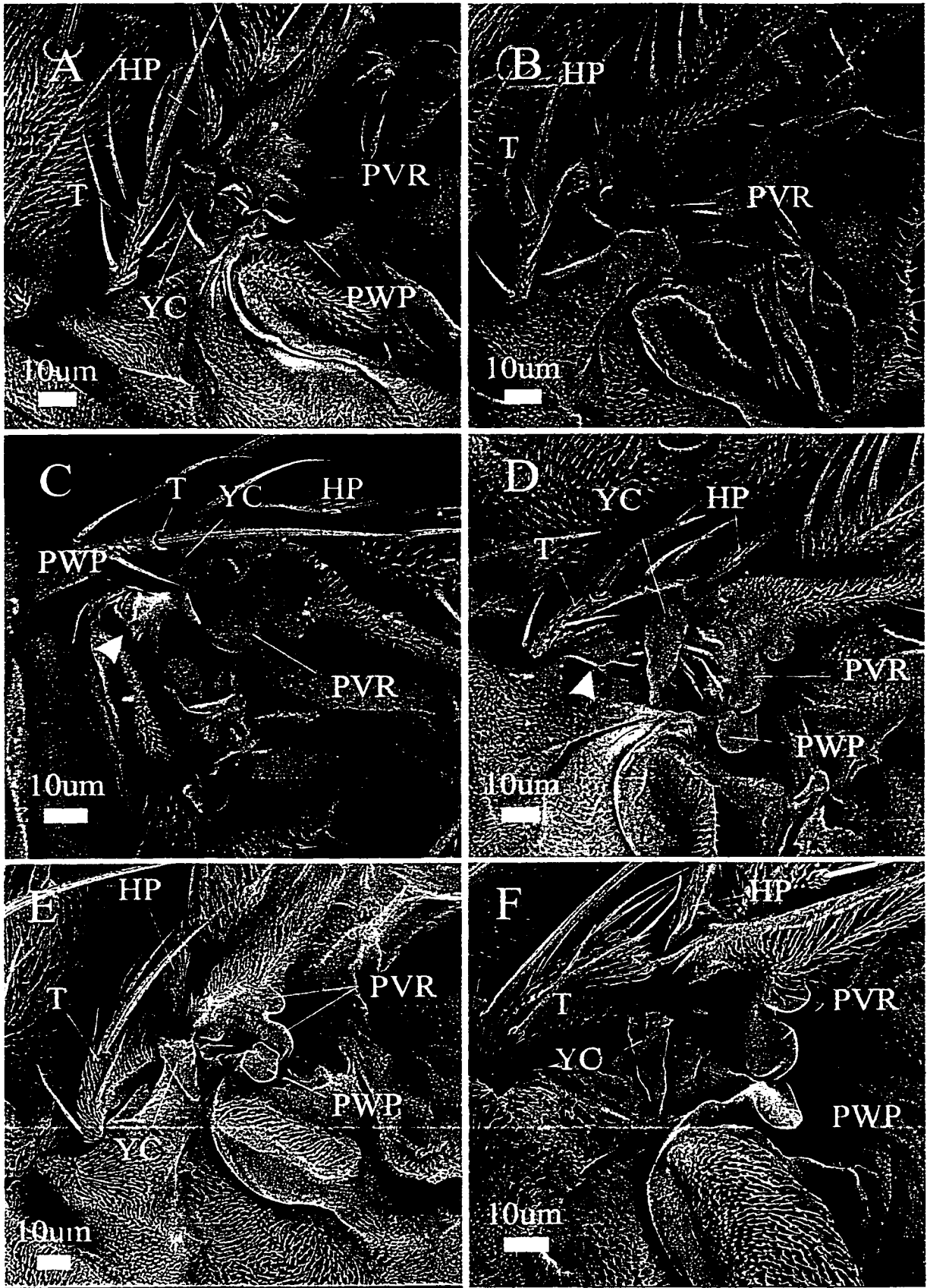
Figure 15. Thoracic structural defects associated with *ae* and *tsh(04319)^{8.1}* transheterozygotes. **A)** and **B)** are scanning electron micrographs showing a lateral view of a thorax from an Oregon R and a transheterozygote *ae/tsh(004319)^{8.1}* fly, respectively (with wings removed). **C)** and **D)** are magnifications of the wing base and surrounding thoracic structures of an Oregon R fly and *ae/tsh(04319)^{8.1}* heterozygote, respectively. The abbreviations in **C)** and **D)** are as in **Figure 13 A)** and **B)**. Double arrowheads indicate the distance between the same landmarks in the Oregon R and the heterozygote. The arrowheads indicate the buckling of the cuticle between the np' and mp'. Boxes in **A)** and **B)** show areas magnified in panels **C)** and **D)**. **E)** and **F)** show a lateral view of a *yw* fly and a *y^{l w1118}; P(w^{+m}W.hs=GawB)md621/CyO; P(w^{+m} C=UAS-yC)MCI/TM2* fly, respectively. In **F)** arrows indicate *y⁺* expression within adult thoracic cuticle and arrowheads indicate the *y⁺* expression within the proximal wing and haltere. The UAS-*y* is driven by *tsh* specific GAL4 insertion. The asterisk in **C)** and **D)** indicates the pre-alar apophysis. See Bryant (1975) for nomenclature. Anterior is left and dorsal is up.



the wings could not be raised (dorsally) for viewing. This may account for some of the reduction in the distance between the PWP and the T. A third mutant analyzed by SEM methods was a dominant *outspread* mutant of *D. simulans* (Green per. comm.). This mutant also failed to exhibit any differences from the *D. melanogaster* control. The fact that the structures within the hinge are present and appear normal suggests that the cuticle structure at the base of the wing is not the cause of the abnormal wing posture. One cannot rule out defects associated with cuticular structures on the dorsal hinge or structures that are not visible in the SEM preparations used. The inability of these flies to fold their wings dorsally also suggests another difference compared to the *ae* mutant. These results imply that both the *tx* and *os* mutants have a different etiology than *ae* and it also explains why neither was able to modify the *ae* phenotype.

The misexpression of the *vg* protein (*UAS-vg*) under the control of the *vg-GAL4* line also causes a “wings held out” phenotype. This abnormal wing posture in these flies was analyzed to determine if they could provide a possible cause for the *ae* phenotype. All flies of this genotype failed to exhibit any defects in the wing hinge resembling those in the *ae* mutant and, in fact, the hinge region appears normal (**Figure 16 F**).

Figure 16. Comparison between three different wing posture mutants using the variable pressure SEM. Variable pressure SEM analysis of the wing hinge from flies of genotype; **A)** Oregon R; **B)** *aeroplane* (*ae*); **C)** *outstretched* (*os^o*) and **D)** *taxi* (*tx^l*). **E)** Standard SEM of dominant wings held out mutant in *Drosophila simulans* and **F)** *vg-GAL4; UAS-vg*. Arrowhead in **C)** and **D)** indicates subtle cuticular difference between *tx*, *os* and Oregon R. The hinge in panel C) is taken from a different angle than the rest because of the posture of the wings. The abbreviations are as follows; T, HP, PWP, PVR and YC indicate the tegula, humeral plate, pleural wing process, proximal ventral radius and yellow comb. Anterior is left and dorsal is up.



Chapter V – aeroplane Enhancer

The *teashirt* (*tsh*) enhancer trap allele, *tsh* [04319], exhibits an accurate representation of the actual expression pattern from the *tsh* gene as observed by *tsh* antibody staining (compare **Figure 17B, E** with **18A, B**) and originally described for the wings by Ng et al. (1996). In the halteres and wings discs the expression is found within tissues that will give rise to proximal structures of the respective appendages (**Figure 17B and E**). Comparing the fate map of the wing discs and halteres as determined by Bryant (1975) to the *tsh-lacZ* reporter gene expression (compare **Figure 17A** versus **B and D** versus **E**), it is apparent that the *tsh* gene is expressed in tissues fated to give rise to the proximal wing hinge in addition to other thoracic structures. Further, *tsh* expression can be observed indirectly in proximal adult wing structures and adjoining thoracic tissues by examining X-gal staining in pharate adult wings from the *tsh* [04319] reporter line (**Figure 17G**). The double arrows indicate the distal most expression of X-gal in the wing.

Genetic data suggest that *ae* and *tsh* are allelic (Chapter III; Soanes and Bell, 1999), although all *tsh* *P* element alleles tested show complementation when heterozygous with *ae*. As discussed above, attempts at generating a null *ae* *P* element allele by mobilizing the complementing enhancer trap *P* element, *tsh* (04319), generated a number of derivative lines. Each line was selected based on the failure to complement the *ae* phenotype. One derivative line, 8.1, shows a modified X-gal reporter gene expression pattern in imaginal discs compared to the parental enhancer trap allele *tsh* 04319 (compare **Figure 17B** versus **C** and **E** versus **F**). The modified pattern indicates that the hinge-specific expression of *tsh* is spatially divisible, resolving the *tsh* hinge expression into presumptive dorsal and ventral domains. This is significant, considering that the defects within the *ae* mutant are confined to the ventral hinge. Within *tsh* [04319]^{8.1} wing imaginal discs, the presumptive ventral hinge and most of the notum expression is lost, leaving only incomplete dorsal-specific expression (**Figure 17C**).

When pharate adult wings are stained, strong expression of the reporter gene is observed in the hinge region of the wing (**Figure 17G**) and the most distal X-gal expression from the enhancer trap allele *tsh* [04319] corresponds to the proximal ventral radius (PVR) (**Figure 17D**). Spatially, this expression within the third instar wing and

halter discs coincide with one of the structures affected in the *ae* mutant (**Figure 17 B and E**). As indicated above, only the ventral hinge is affected in the mutant but the reporter gene expression is present in both the dorsal and ventral hinge. This suggests that in the null *ae* allele only a sub-domain of the wing disc-specific expression from *tsh* should be affected, if *ae* does represent a regulatory region of the *tsh* gene.

The imaginal wing disc is formed as an invagination of a single continuous layer of epithelial cells. Within the area of the ventral hinge, the epithelial sheet folds around from the wing pouch side to the peripodial membrane side of the disc as a continuous layer of cells (**Figure 17H**). Histochemical and antibody staining of third instar wing discs, show that *tsh* is spatially expressed in this continuous layer of epithelial cells (**Figure 17H**, arrow). Direct analysis of *tsh* expression within third instar imaginal wing discs from the *ae* mutant reveals a subtle altered protein expression pattern. Optical sections of wing discs at relatively the same depths from both *ae* and Oregon R larvae, and stained with *tsh* antibodies, reveal a loss of expression within the presumptive ventral hinge in the mutant. The loss of expression in the *ae* discs is restricted to the ventral hinge side of the disc bordering the wing pouch (**Figure 18C versus E**). The *tsh* staining on the peripodial membrane side of the disc remains unaffected (**Figure 18B versus D**). The limited loss of *tsh* expression within the presumptive ventral wing hinge suggests *ae* may represent a regulatory mutant of the *tsh* gene.

Earlier experiments revealed the presence of an insertion within the 4.8 kb *EcoRI* 3' genomic sequence flanking the *tsh* coding region in the *ae* background (also see Soanes and Bell, 1999). Further characterization, through Southern analysis, comparing *ae*, Oregon R and the parental stock of *ae* indicated that the approximate 5.5 kb insertion is localized within a 34 bp *DraI* fragment (**Figure 19**). Sequence analysis of the insert has revealed that the insert is an I element, a retrotransposon similar to the LINEs or L1 elements identified in mammals (Fawcett et al., 1986). The I element is inserted downstream of the *tsh* coding region within the 4.8 kb *EcoRI* fragment (**Figure 19**). It is possible that the insert is disrupting a 3' cis-acting regulatory sequence required for proper regulation of *tsh* within tissues required for normal wing posture. Two such cis-acting regulatory

Figure 17. Histochemical staining of *teashirt* expression in haltere and third instar imaginal wing discs and their corresponding presumptive fates. **A)** and **D)** Diagrammatic representation of the fate maps of third instar wing discs and halteres modified from Cohen (1993) and Bryant (1975). X-gal staining of the *tsh* (04319) reporter gene expression in **B)** and **C)** third instar wing discs, **E)** and **F)** haltere discs and **G)** pharate adult wing from the *tsh* [04319] line, indicating the distal-most X-gal expression within the wing hinge (arrows). **B)** and **E)** are discs from *tsh* [04319]. **C)** and **F)** are discs from derivative line *tsh* [04319]^{8.1}. The arrowheads in **C)** indicate the loss or reduction of β -gal expression within presumptive ventral hinge compared to progenitor line *tsh* [04319], without a noticeable reduction in the presumptive dorsal hinge expression. **H)** 3D drawing of a third instar imaginal disc. The curved arrow indicates the continuous single layer of epithelial cells in the area of the presumptive ventral wing hinge. Abbreviations are as in **Figure 1**.

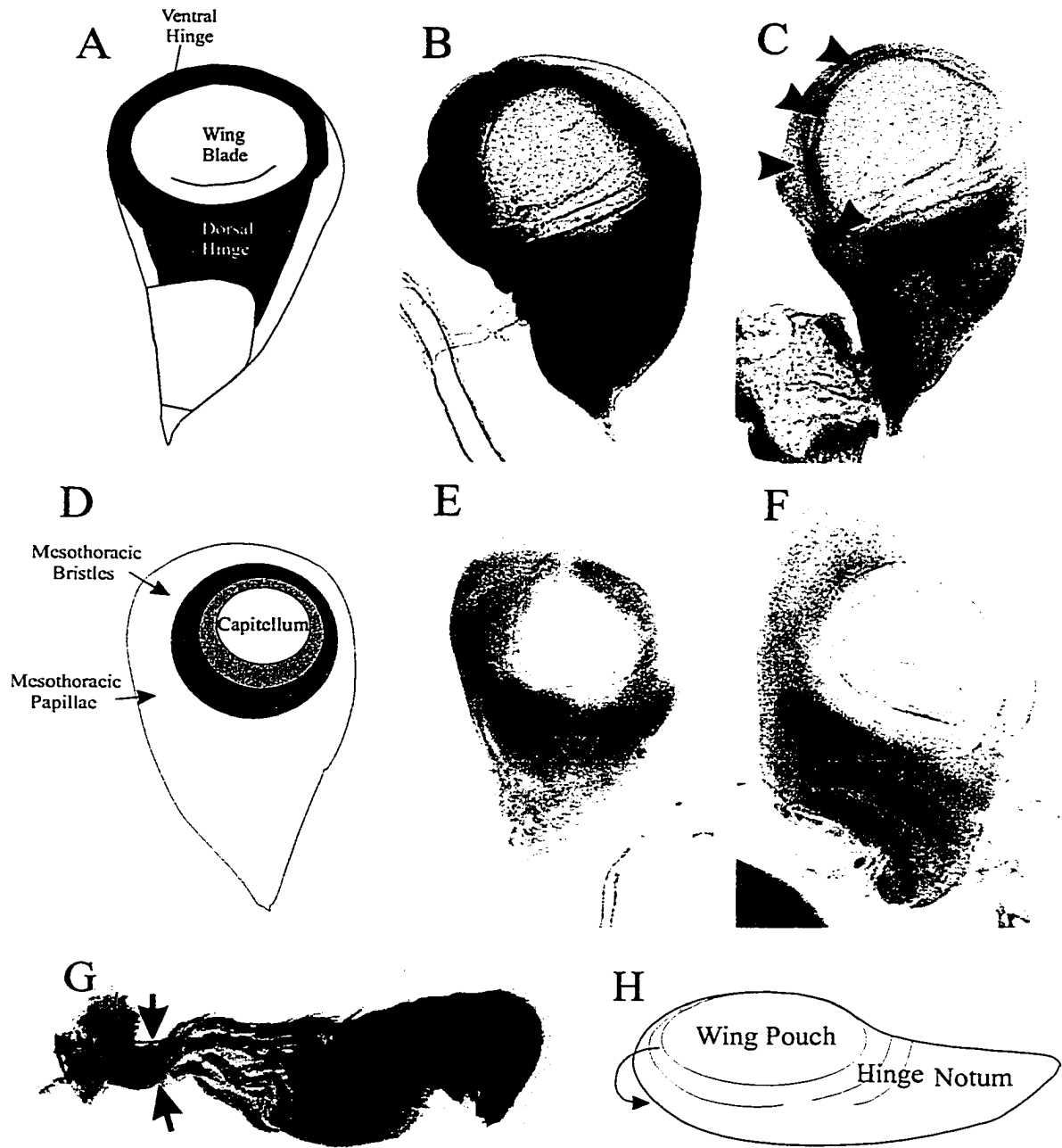
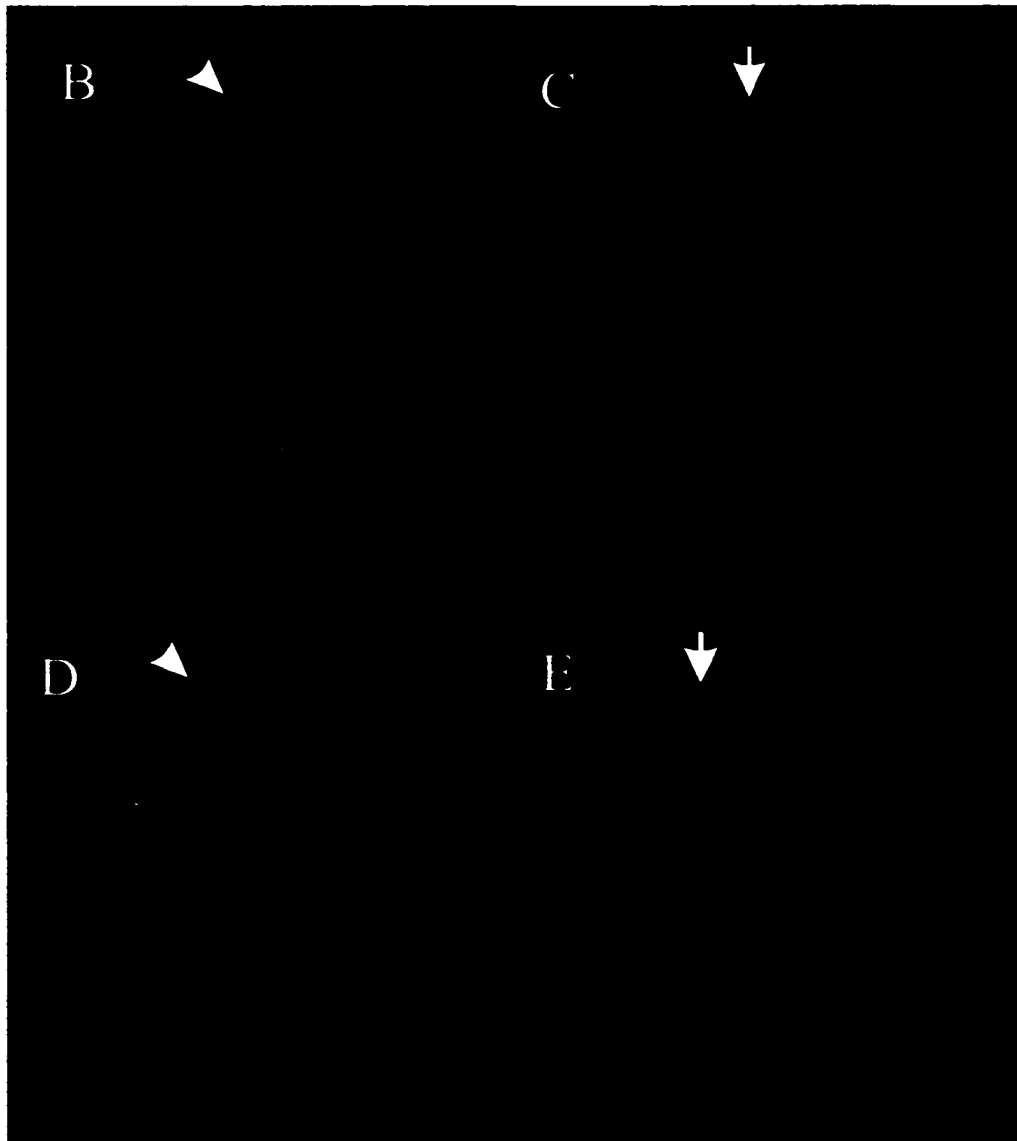
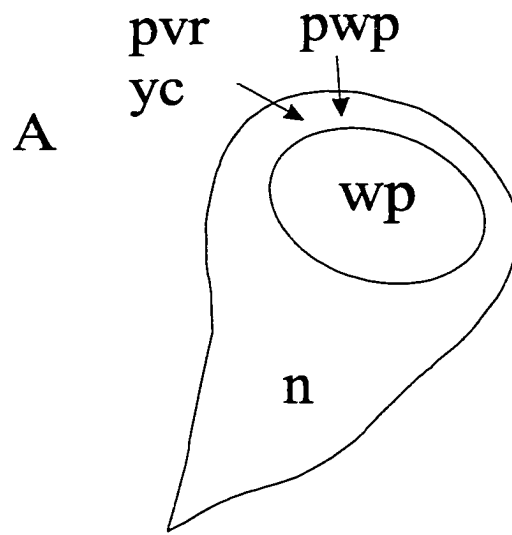


Figure 18. *Teashirt* protein expression in third instar imaginal wing discs as visualized using *tsh*-specific antibodies. **A)** Simplified fate map of the third instar imaginal wing disc with presumptive fates relevant to the *ae* phenotype. Abbreviations are as in **Figure 1** and WP, wing pouch; N, notum. **B), C) and D), E)** are optical sections through the same Oregon R or *ae* third instar wing discs, respectively. **B)** and **D)** are sections through the peripodial membrane side of the discs. **C)** and **E)** are sections through the wing pouch side of the wing discs. The arrowheads point to the presence of *tsh* protein expression within the presumptive ventral hinge on the peripodial membrane side of the wing disc. The arrows points to differences in *tsh* protein expression within the presumptive ventral hinge on the wing pouch side of the wing disc. Anterior is left and ventral is up.

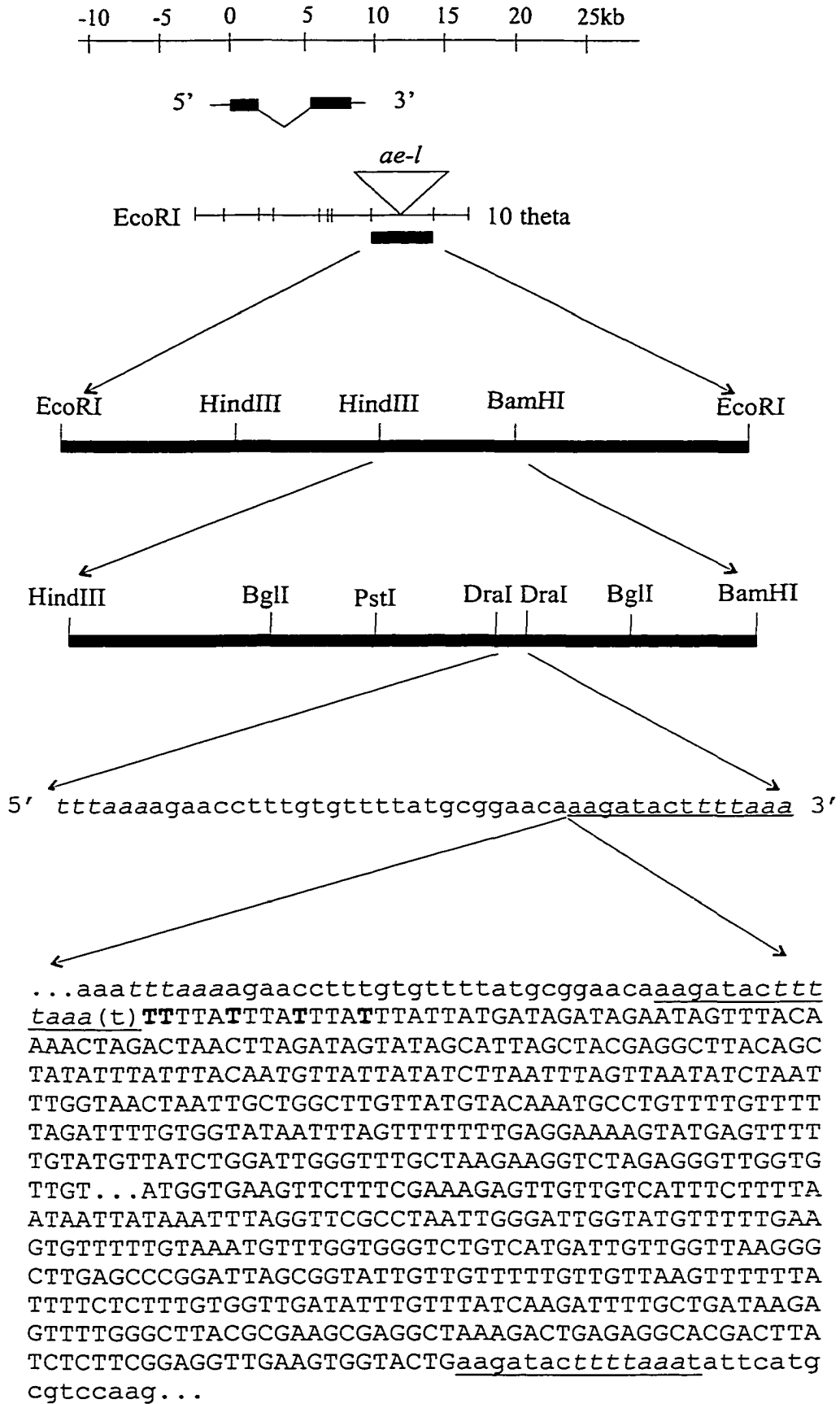


sequences have previously been identified within the 3' genomic sequence flanking the *tsh* gene (McCormick et al., 1995; Core et al., 1997). However, both regulatory sequences are required for proper expression of *tsh* within the developing embryo. As mentioned above, the *ae* mutant is believed to be due to an insertion within or near another 3' regulatory element, causing the loss of *tsh* expression within a small functional sub-domain of its regular expression pattern.

Using the enhancer tester pCaSpeR hs 43, experiments were conducted to look for the presence of any cis-acting regulatory sequences within the region known to contain the *ae* insert. The entire wild type 4.8 kb *EcoRI* (E4.8) sequence was tested, and found to be capable of driving reporter *lacZ* expression within the presumptive wing hinge in addition to limited expression within the presumptive notum (**Figure 20** and **21B**). The arrows indicate the limited X-gal staining within the presumptive notal tissue (**Figure 21B**). Spatially, the E4.8 expression pattern only represents a subset of the total wing and haltere disc expression seen using the *tsh*[04319] reporter line (**Figure 17B** vs. **21B** and **17E** vs. **21F**). The enhancer elements are also activated within the brain as early as second instar and within the midgut in third instar larvae.

The only structures affected in the *ae* mutant, however, are found in the ventral hinge. As previously indicated, the *tsh04319^{8.1}* derivative line reveals that the wing hinge expression is divisible into dorsal and ventral specific components. An attempt was made to define the minimal sequence(s) required for the enhancer function. A summary of the fragments tested and their corresponding spatial expression patterns are presented in **Figure 20**. Expression from the entire E4.8 construct is activated prior to second instar in the wing hinge, ventral ganglion, optic lobes and in the mouth parts (**Figure 22**). The 2.9 kb *EcoRI/BamHI* fragment (EB2.9) is capable of driving expression within the presumptive dorsal and ventral hinge region in addition to the mid gut staining (**Figure 21C** and **G** and **23**). The EB2.9 expression pattern is similar to E4.8 except for the absence of the presumptive notum expression. Further dissection of the enhancer element(s) revealed that the 915 bp *HindIII/BamHI* genomic fragment (HB1.0) is also fully capable of ventral hinge specific expression (**Figure 20** and **21D** and **H**) in addition to brain and mid gut staining. However, this fragment loses its ability to express the

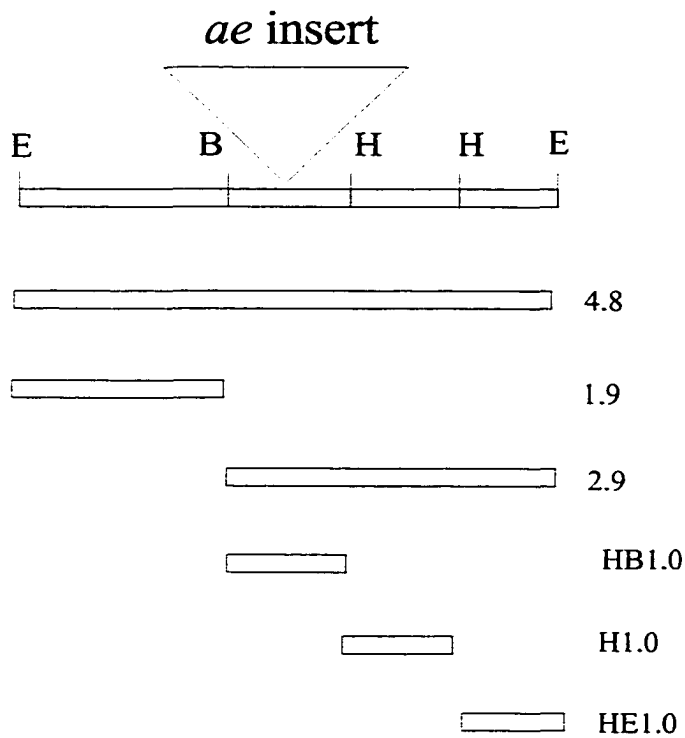
Figure 19. Localization and characterization of the insertion within the 3' genomic sequence flanking the *tsh* coding region in the *ae* mutant. At the top is a schematic representation of the insert site within the *ae* mutant, with respect to the *tsh* coding region. The two exons of the *tsh* coding region and the orientation of the gene are indicated below the kb scale. The 4.8 kb *EcoRI* fragment that contains an insert in the *ae* genome is indicated below and 3' to the *tsh* exons. The insert is denoted by the labeled triangle, indicating its location within the 4.8 kb *EcoRI* sequence, and with respect to the *tsh* coding region. The location of the 915 bp *HindIII/BamHI* fragment within the 4.8 kb *EcoRI* fragment is also indicated. The sequence at the bottom of the figure indicates the position of the I element insertion within the 34 bp *DraI* sequence in the *ae* genome. The lower case type defines the genomic sequence within the *DraI* fragment and the lower case italicized sequence indicates the actual *DraI* sites. The underlined sequence indicates the tandemly duplicated genomic insert site. The upper case letters indicate the sequenced ends of the I element (285nt at the 5' end and 307nt at the 3' end, with ... indicating the boundary of the unsequenced portion). The I element negative strand sequence is presented in the figure, and therefore the AT rich 3' end appears first in the sequence. The bold face type indicates differences between the sequence presented herein compared to the published I sequence (Fawcett et al., 1986). The (t) in the sequence indicates an ambiguous base, which could be classified as either duplicated genomic or I element sequence. Restriction enzymes: *BamHI*, *EcoRI*, *DraI*, *HindIII* and *PstI* were used for mapping the location of the insert site. The *EcoRI* map of the 100 clone of the *tsh* coding region is as published by McCormick et al. (1995).



reporter gene in the presumptive dorsal haltere and wing hinge (compare **Figure 21C** versus **D** and **G** versus **H**). There is an over representation of ATTA sequences within a region of the HB1.0 fragment. Further assays were aimed at determining if the sequence is biologically relevant, since ATTA rich regions are known to be characteristic of some cis-regulatory elements (discussed further below). High fidelity PCR was utilized to analyze the relevant regions with primers designed to amplify two overlapping fragments that contained the ATTA rich regions. Each of the PCR products, a 481 and a 209 bp fragment were cloned into the enhancer tester construct (**Figure 20**). Neither sequence was able to activate the reporter gene expression within the hinge region of wing and haltere discs. However, the 481 bp and 209 bp sequences were still capable of activating expression within regions of the gut also expressed by the HB1.0 fragment.

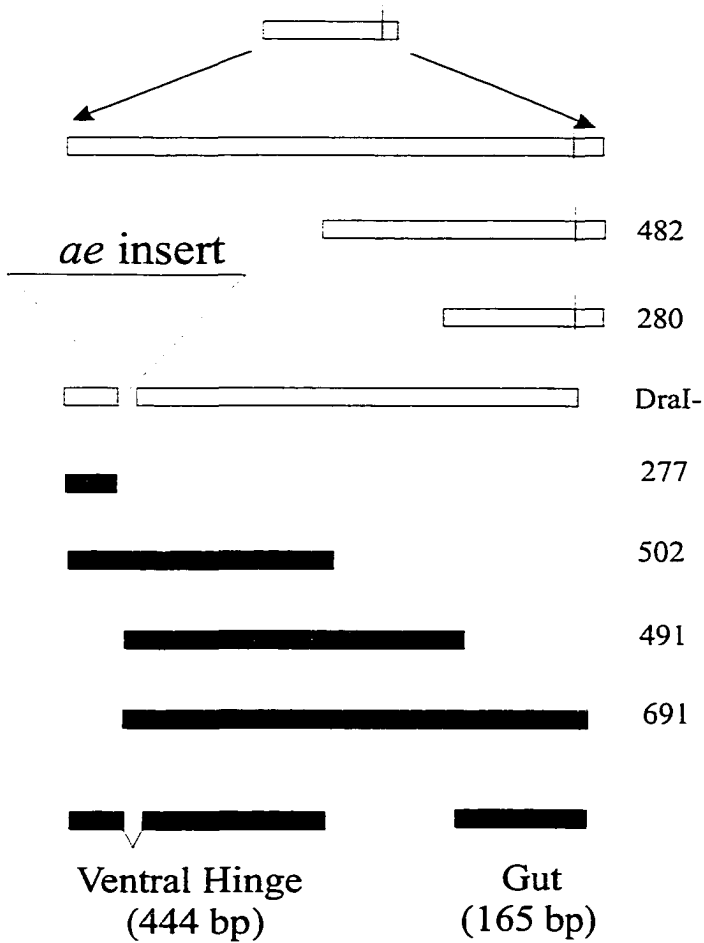
Although the I element in the *ae* mutant was localized to within the 34 bp *DraI* sequence of the HB1.0 fragment, the effect the insert had on the enhancer element's expression pattern was still undetermined (**Figure 19**). The insert could disrupt normal *tsh* expression by inserting directly into an enhancer sequence or it could act over a distance to negatively regulate the enhancer element. To determine if the sequence disrupted by the I element insert was capable of the ventral hinge specific expression, the 34 bp *DraI* fragment was removed from the HB1.0 sequence and the remainder was reintroduced into the enhancer tester. The 34 bp *DraI* deleted sequence (**Figure 19**) exhibited the same ventral hinge specific expression pattern as the HB1.0 genomic fragment (**Figure 20**). A comparison of the simplified fate map of the third instar wing disc with the expression pattern observed from the HB1.0 enhancer reveals that the aberrant structures in the *ae* mutant are derived from the same tissues that express the β -galactosidase in response to the HB1.0 enhancer (**Figure 21A** versus **D** and **E** versus **H**). The pleural wing process, yellow club and the proximal ventral radius all arise from the tissues corresponding to the presumptive ventral hinge (**Figure 21A** versus **D**).

Figure 20. Dissection of the *aeroplane-like* enhancer region. Schematic diagram of the 4.8 kb *EcoRI* 3' enhancer region and the extent of each of the fragments tested for enhancer activity. See **Figure 19** for the location and relative orientation of the 4.8 kb *EcoRI* fragment with respect to the *trh* coding region. Enzyme abbreviations: E, *EcoRI*; B, *BamHI*; and H, *HindIII*. Each bar under the restriction map indicates the position and relative size of the sequence tested for its ability to drive the *lacZ* reporter gene in the enhancer tester pCaSpeR hs 43 (Thummel and Pirrotta 1991). The identifying letters and numbers to the right of each bar indicate the identity of the respective restriction fragment and its approximate size. The *DraI*- fragment is the HB1.0 sequence with the 34 bp *DraI* sequence removed (**Figure 19**). A summary of the expression patterns observed from each genomic fragment is indicated on the right. A plus indicates the presence of X-gal staining in the respective tissues whereas a minus indicates the failure of that fragment to drive reporter gene expression. Tissue abbreviations: D, presumptive dorsal wing hinge; V, presumptive ventral wing hinge; E, eye disc; O, optic lobe; V, ventral ganglion; N/A, unable to test the construct further because the stock was lost. The triangle indicates the position of the 5.4 kb *ae* insert within the 4.8 kb *EcoRI* fragment. The purple bars indicate enhancer constructs created but not yet tested. The “?” indicates results are not yet known. The black bars at the bottom indicate the smallest sequences so far defined that are sufficient for the ventral hinge and gut enhancer elements. The E2.9 construct was lost after initial the staining. The “+” under the brain column indicates specific staining pattern associated with the brain (optic lobe or ventral ganglion) was not determined at the time.



Expression Pattern

Hinge	Gut	Brain	Eye
D,V	+	V/O	E
-	-	-	N/A
D,V	+	+	N/A
V	+	-	E
-	-	-	E
-	-	-	N/A



-	+	-	E
-	+	-	N/A
indistinguishable from HB1.0			
?	?	?	?
?	?	?	?
?	?	?	?
?	?	?	?

Figure 21. X-gal staining of third instar imaginal wing and haltere discs from enhancer-tested fragments (summarized in **Figure 20**) in the pCaSpeR hs 43 vector. **A)** and **E)** a simplified fate map modified from Bryant (1975) of third instar wing and haltere discs, respectively. The map indicates the location of tissues fated to give rise to the structures found to be aberrant in the *ae* mutant wing hinge. **B-D)** third instar wing discs and **F-H)** haltere discs. **B)** and **F)** corresponds to the enhancer expression pattern under the control of the 4.8 kb *EcoRI* fragment (E4.8). **C)** and **G)** correspond to the 2.9 kb *EcoRI/BamHI* fragment (EB2.9). **D)** and **H)** correspond to the 915 bp *HindIII/BamHI* fragment (HB1.0). The abbreviations are as follows: WP; wing pouch, DH; dorsal hinge, VH; ventral hinge, N; notum, PWP; pleural wing process, YC; yellow club, PVR; proximal ventral radius, CS; capitellum, MB; metathoracic bristle group, MS; metathoracic spiracle, MP; metathoracic papillae. Arrowheads in **B)** point to notum specific expression. Arrow in **B)** indicates position of reporter gene derepression compared to *tsh* specific expression pattern in the dorsal hinge as indicated in **Figure 7 F** (arrow). Anterior is left and ventral is up. The lac Z staining pattern in each of the panels is representative of at least two independent lines.

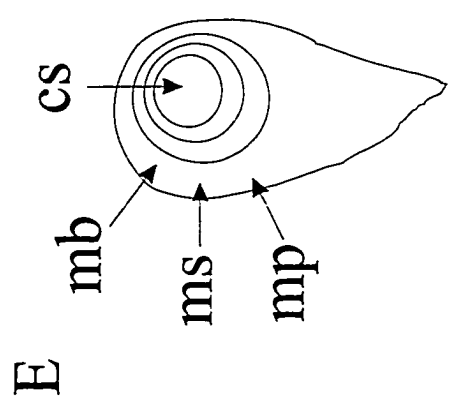
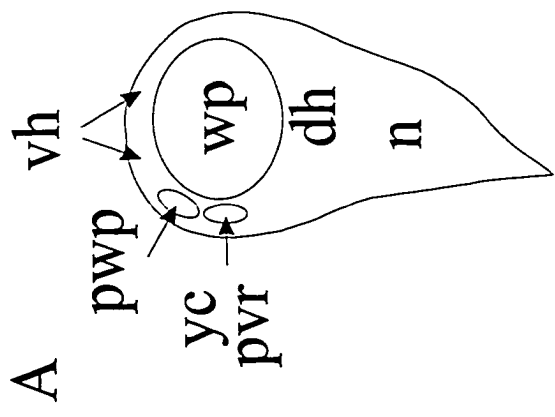
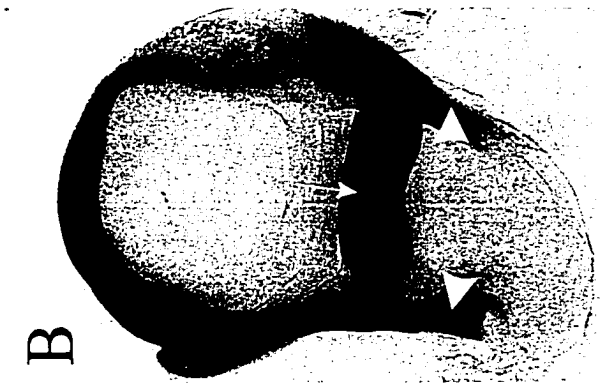
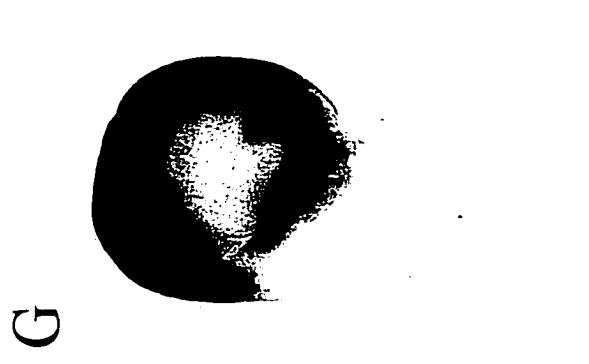
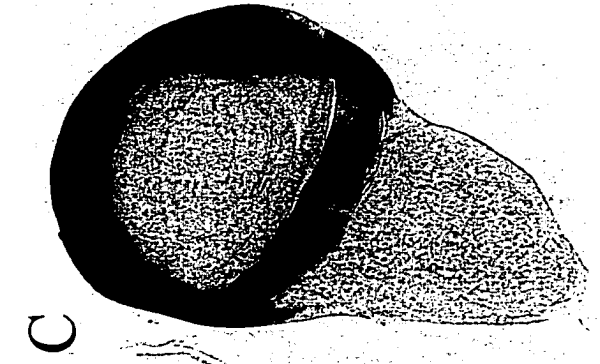
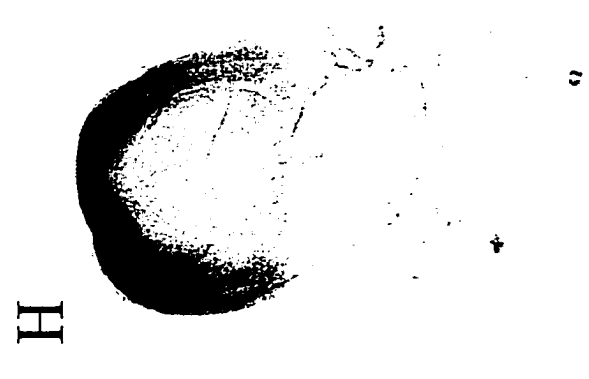
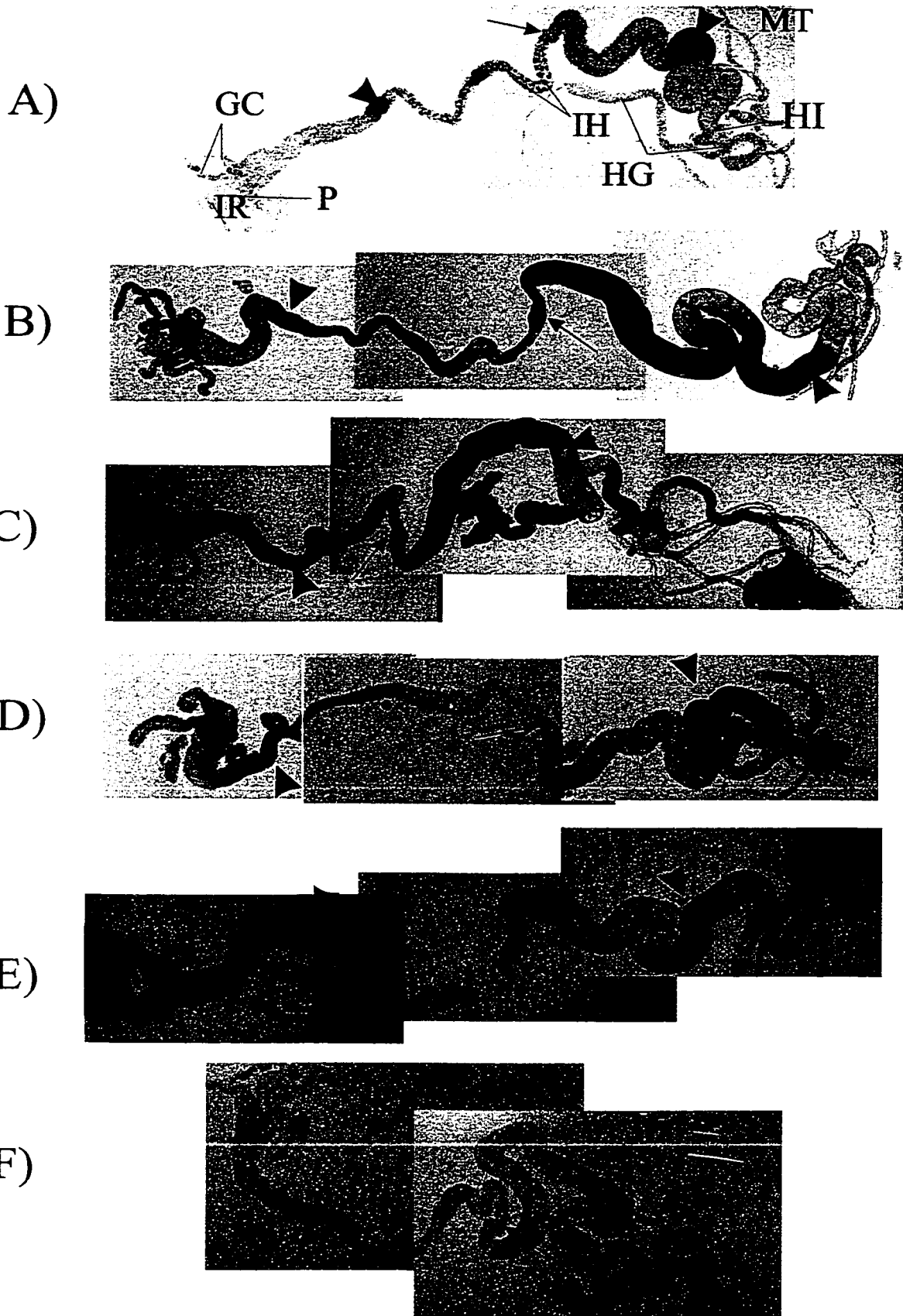


Figure 22. *Lac Z* expression within second instar larvae of reporter E4.8 reporter construct. **A)** second instar wing and haltere discs, **B)** Brain and **C)** mouthparts. W and H indicate the wing and haltere, respectively. The *lac Z* staining pattern in each of the panels is representative of at least two independent lines.



Figure 23. Reporter β -galactosidase expression in midgut tissues of transgenic lines. The blue staining indicates the spatial pattern of reporter gene expression within the midgut of wandering third instar larvae as driven by various enhancer fragments. Larval midgut dissected and *lacZ* detection from **A)** *tsh*[04319], **B)** pCaSpeR hs E4.8, **C)** pCaSpeR hs HB1.0 (or *DraI*), **D)** pCaSpeR hs H1.0, **E)** *yw*. **F)** Dissection and fixation without *lacZ* detection of an *ae* third instar larval midgut. MT, GC, IH, HG, IR, HI and P refer to malpighian tubules, gastric caecum, midgut imaginal histoblasts, hindgut, foregut imaginal ring, hind gut imaginal ring and proventriculus, respectively. The arrowheads indicate the position of *lacZ* expression detected in non-transgenic lines and therefore is considered non-specific. The arrows indicate the morphological marker in the midgut for orientation purposes. The midgut staining between the pCaSpeR hs HB1.0, pCaSpeR hs *DraI*, pCaSpeR hs 209 bp, and pCaSpeR hs 481 is indistinguishable. Therefore, only one midgut representing all four constructs is shown in the **Figure C**. The *lac Z* staining pattern in each of the panels is representative of at least two independent lines. Anterior is left.



The detection of *lacZ* reporter gene expression from the enhancer tester E4.8 transgenic line indicates that the regulatory elements activate expression within the presumptive hinge in the wing and haltere discs prior to mid second instar. Interestingly, the expression within the brain exhibits a dynamic pattern. In second instar the expression is observed within the optic lobes and in the ventral ganglion. By wandering third instar the expression within the ventral ganglion is almost completely lost and only a few *lacZ* expressing cells are detected within the optic lobe.

The gut specific expression observed from the *tsh*[04319] enhancer trap line is considerably less extensive than observed for the other pCaSpeR constructs. The expression from the *tsh*[04319] is localized to what appears to be the imaginal histoblasts (IH) of the midgut. Development of the adult gut results from a complete reassembly of the larval gut after histolysis occurs and these IH are some of the founder cells that will give rise to the adult gut. These imaginal cells arise from spindle cells specified during embryogenesis (reviewed by Skaer, 1993). In *tsh* [04319] gut tissue, the staining of the IH extends from approximately 10% to 50% of the distance from the anterior end of the midgut (**Figure 23 A**). The non-specific *lacZ* expression in all lines including non transgenic controls, at around 10% and 80% the midgut length is indicated by the arrowheads (**Figure 23 A**) and is likely due to bacteria within the gut. The transgenic lines HB1.0, 0.9, *DraI*, 481 bp and 209 bp, all exhibit a similar *lacZ* reporter gene expression pattern in the third instar larval midgut (**Figure 23 C**). The most anterior expression in the midgut begins at the posterior end of the proventriculus (P) and extends, intermittently, the entire distance to the posterior hind gut imaginal ring (HI). This expression also includes the cells that appear to be the IH which also express *lacZ* in the enhancer trap allele. The E4.8 transgenic line differs from the other lines in that it exhibits nuclear staining throughout the midgut whereas the other five lines discussed above shows what appears to be strong cytoplasmic and nuclear staining throughout most of the midgut (**Figure 23 B** versus **C, D** and **E**). E4.8 expression is less extensive than that of the other transgenic lines, however there is a common “strong” domain of expression observed in all of the reporter constructs and absent from the controls. The arrowheads in **Figure 23 C** define this “strong” region. E4.8 differs from the *tsh*[04319] enhancer trap allele in that the nuclear expression observed in the enhancer trap is only

detected in the middle portion of the midgut starting just downstream of the anterior non-specific β -galactosidase expression. In the H1.0 transgenic line the expression of the reporter gene is localized to within regions associated with non-specific β -galactosidase detection. Even though there is a spread of β -galactosidase expression anterior and posterior from these regions, it fails to overlap with the common “strong” expression pattern defined in the E4.8 line. Despite the apparent midgut specific regulatory function of the *ae* enhancer, the *ae* gut appears morphologically normal at the third instar larvae stage (**Figure 23 F**).

The *lacZ* staining observed in the *tsh*[04319] reporter line is present in the third instar eye-antennal imaginal discs. The *lacZ* expression within the antennal disc corresponds to the presumptive third antennal segment in addition to a small patch of tissue near but not including the presumptive maxillary palp (**Figure 24 A**) (reported by Haynie, 1975; Bhojwani et al., 1997). The *tsh*[04319] line also drives reporter gene expression in the presumptive eye tissue. The E4.8 construct drives expression in the same tissues in the imaginal eye disc. However, E4.8 lacks the expression in the imaginal antennal disc that is present in the *tsh*[04319] reporter gene (**Figure 24 A** versus **B**). Each of the transgenic lines 481 bp, HB0.9, E4.8 and H1.0 are capable of activating reporter gene expression in the presumptive eye tissues in a pattern similar to the enhancer trap allele *tsh*[04319]. The H1.0 transgenic line, however, also expresses the reporter gene in the presumptive third antennal segment. Because each of these lines exhibits expression within the presumptive eye tissue, the expression may be an artifact of the enhancer tester construct. If these expression patterns within the eye-antennal discs are the result of an artifact, it is not surprising that there are no eye defects associated with the *ae* mutation.

The pCaSpeR hs 43 transformation vector was designed to test tissue specific regulatory sequences and enhancers elements. It was used for testing the *ae* insert bearing 4.8 kb *EcoRI* fragment (**Figure 25**) for the presence of any cis-acting regulatory elements or enhancers. The vector is equipped with 5' and 3' *P* element ends for stable integration of the construct into the *Drosophila* genome. Transformants of the following constructs drove *lacZ* reporter gene expression in patterns differing from the *yw* transformation line; pCaSpeR hs E4.8, EB2.9, HB1.0, 209 bp and 481 bp. The pCaSpeR

Figure 24. *Lac Z* staining of eye-antennal from reporter lines. **A)** modified fate map from Haynie, 1975. Third instar imaginal eye-antennal discs from; **B)** *tsh*[04319]; **C)** pCaSpeR hs 43 E4.8; **D)** pCaSpeR hs 43 0.9; **E)** pCaSpeR hs 43 481 **F)** pCaSpeR hs H1.0. The arrows indicate similar tissues in each of the antennal discs. The white and black arrowheads indicate similar tissues in each of the eye and antennal discs, respectively. Abbreviations are as follows; Ar: arista, Eye; eye imaginal disc, Ant; antennal disc, A1, 2, 3;: antennal segments 1, 2, 3, respectively, Drst; , Prst; , Post; postoccipital sensilla and Pal; maxillary palps. O.L. indicates the optic lobe in **C)**. The eye disc in both **A)** and **C)** is folded over so the staining in the cells is in different focal plains. The *lac Z* staining pattern in each of the panels is representative of at least two independent lines.

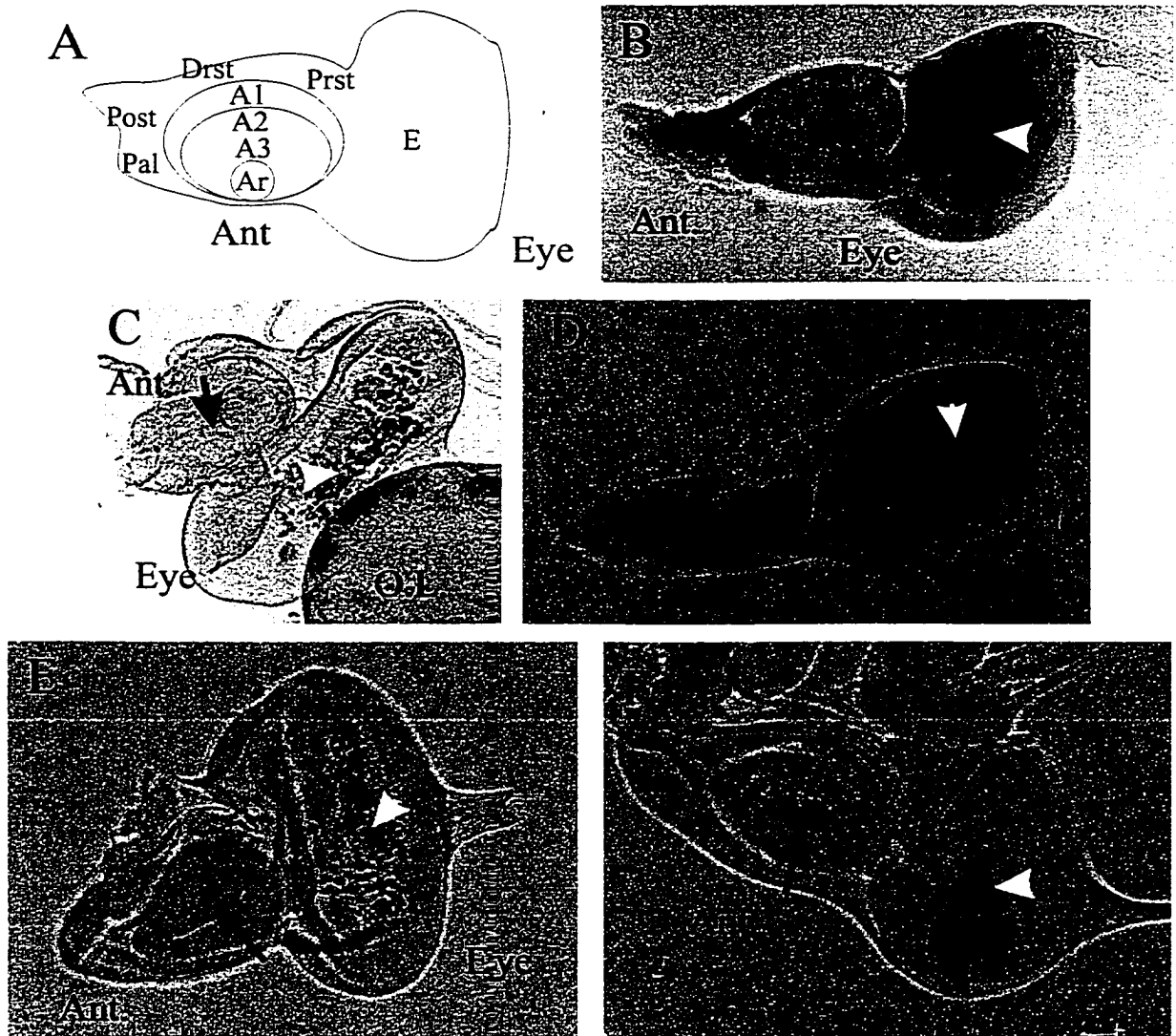
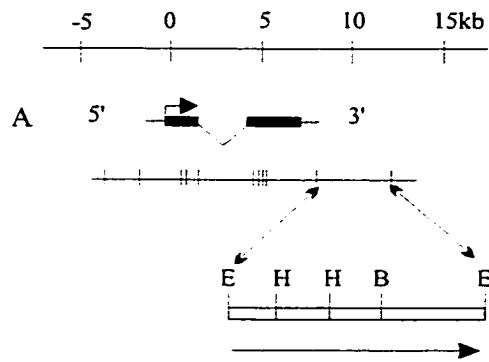
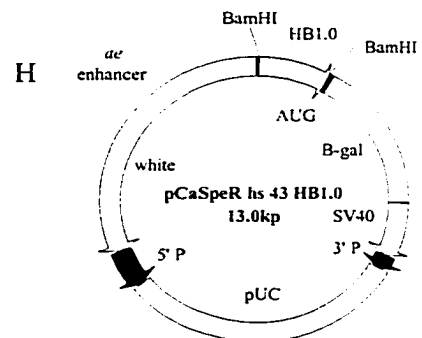
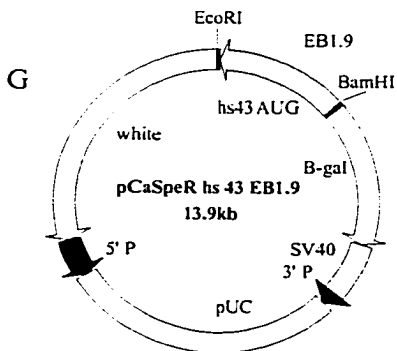
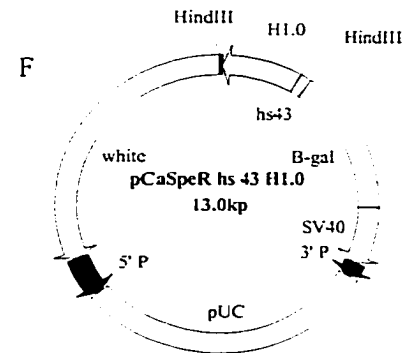
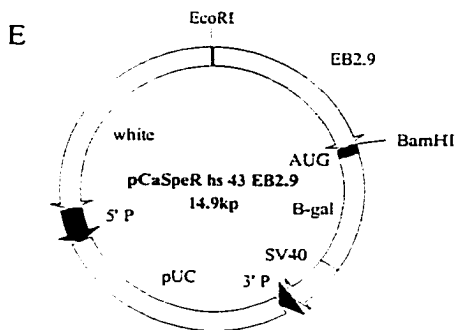
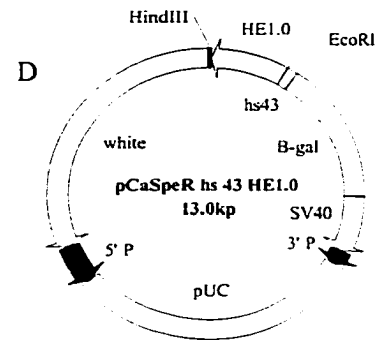
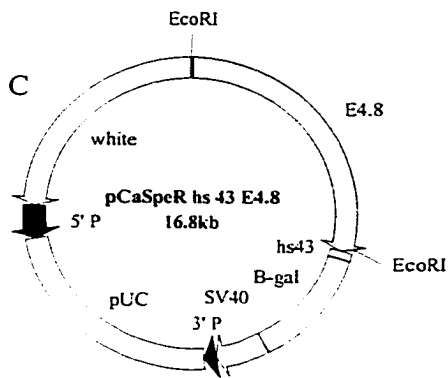
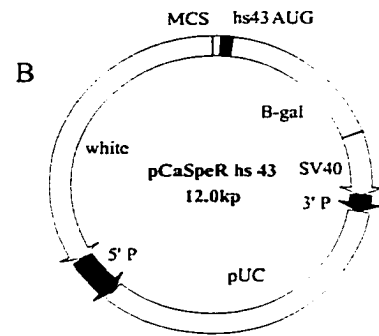


Figure 25. Diagrammatic representation of all the enhancer tester constructs and their orientation with respect to the direction of transcription of the *tsh* gene. **A)** Indicates the orientation of the 4.8 kb sequence with respect to the *tsh* coding region. The arrow below the enhancer 4.8 kb sequence indicates its orientation at its endogenous position with respect to the direction of transcription of the *tsh* gene. The line above the coding region indicates the distance in kb. The arrowhead above the *tsh* gene indicates the direction of transcription. **B)** pCaSpeR hs 43 vector with a simplified version of the multiple cloning site indicating all the unique sites. **C)** pCaSpeR hs 43 E4.8. **D)** pCaSpeR hs 43 HE1.0. **E)** pCaSpeR hs 43 EB2.9. **F)** pCaSpeR hs 43 H1.0. **G)** pCaSpeR hs 43 EB1.9. **H)** pCaSpeR hs 43 HB1.0. Both pCaSpeR hs 43 209 bp and pCaSpeR hs 43 481 bp are in the forward orientation as HB1.0, but not represented in this Figure. The yellow fragment in each of the constructs represents the enhancer sequence derived from the 4.8 kb region as well as their orientation with respect to the minimal heat shock promoter (hs 43) *lacZ* gene fusion. The hs 43 is a minimal promoter derived from the hs70 gene, consisting of sequences of only the 43 bp upstream of the RNA start site (-43) excluding any leader sequences (Thummel and Pirrota, 1992). The black arrows in all the constructs indicate the 5' and 3' *P* element ends. The open arrows correspond to the direction of transcription in each of the coding regions. SV40 corresponds to the polyadenylation signal derived from the simian viral 40 early gene product. White indicates the mini *white* gene transformation marker.



Multiple Cloning Site
EcoRI Sst2 NotI SfiI Spe BamHI XhoI



hs EB1.9, H1.0 and HE1.0 constructs failed to exhibit any difference in staining from the *yw* injection line. Each of the lines that presented some staining were all in the same orientation with respect to the *hs43-lacZ* fusion reporter gene, which was the same orientation as in the endogenous location with respect to the *tsh* promoter. The constructs that failed to give any staining were coincidentally in the opposite orientation to those lines that exhibited differences, and therefore are also in the opposite orientation to their endogenous position with respect to the *tsh* coding region. The staining patterns of each of the reporter constructs can be seen in **Figures 21, 23 and 24**.

4.8 kb Fragment Analysis

The sequence presented in **Figure 26** was obtained from a subclone of the $\theta 6$ lambda clone presented by Fasano et al. (1991). The sequence is presented in the opposite orientation to the direction of transcription of the *tsh* gene. The restriction sites used to arbitrarily dissect the 4.8 kb sequence into three, approximately 1.0 kb fragments and one 1.9 kb fragment are presented in the **Figure 26**. Relative to the entire 4.8 kb of sequence, the I element insertion (**Figure 19**) is localized between base pairs 2246 and 2247 of the HB1.0 fragment and caused either a 13 or 14 bp duplication of the genomic sequence. The uncertainty of the exact duplication size is due to an ambiguous A/T base pair which could have been the result of the duplication or present in the I element 3' sequence. Most I elements cause similar duplications upon insertion, ranging between 10 and 14 bp (Fawcett et al., 1986). All primers created for sequencing and PCR analysis of the region listed in **Table 6** are presented on the sequence. Comparisons between the now available BGDP sequence and the sequence presented in **Figure 26** reveal a few differences. According to the BGDP, part of the sequence of this 4.8 kb sequence is an EST (expressed sequence tagged site). Although according to previous publications (Fasano et al 1991), the *tsh* transcript terminates prior to the beginning of the 4.8 kb sequence (position 4901 according to the **Figure 26**). This suggests that the termination site for the *tsh* gene lies further downstream than initially suggested. The expression pattern of this EST overlaps the *tsh* expression pattern in the embryos, indicating that the published transcribed sequence is likely not the complete mRNA sequence for the *tsh*

Figure 26. The complete sequence of the 4.8 kb *EcoRI* *aeroplane* enhancer element. Restriction enzyme sites, *EcoRI*, *Bam*HI and *Hind*III are shown. Only the two *Dra*I restriction enzyme sites that flank the insert site are shown. The location of the primers listed in **Table 6** are underlined. The (f) and (r) indicate the forward and reverse primers respectively, relative to the sequence as written. KSO22 and KSO7 are overlapping forward primers. The KSO22 primer is italicized and the KSO7 is underlined. The I element insert site between base 2246 and 2247 is underlined. The 14 bp of duplicated genomic sequence found in the *ae* allele caused by the I element insert is denoted in bold type between base 2233 to 2246. The restriction sites relevant to the discussion are underlined and identified by the appropriate abbreviations (*Bam*HI, *Eco*RI, *Hind*III and *Dra*I). The *Dra*I sites flanking the I element insert are italicized and underlined. Bold type between base 4737 and 4901 shows the Expressed Sequence Tag (EST) identified by the Berkley Drosophila Genome Sequencing Project (BGDP). The 4.8 kb of sequence as written is in the opposite orientation to the direction of transcription of the *tsh* gene (see **Figure 25** for comparison).

1 GAATTCATATTCGATTACGACGATCAGTAAGTCTGCCGCTGAATGTCAGTGGTGTACGAGCAGTCGGGGCCCGGATTGGCCCTTTGCCGGTTAAATAAA
EcoRI
101 CATGGCCCAAGATCTGTCGCTGCTCTCTGTGCTGCCAGTTCAGCTGTAGCTGCTCTGTGTGCAAAATGTTCCCTATCGTCACACACTCTTGTAGCTGAGT
201 TTCGTTTTTGATCACCGGACCCGGGTGACGAGGAATTTCCGCTTATCTCGTAGTCTCGTCGTCGACGGGCCAAATGGCCCTGATCCCGGACTCCCG
301 ACTATCGACTCCCAGCTCCCACCTTCGCCCTGGCCGTTCCTGCCCGCCAGGGACTGATTTACGAGCCGAATGGCAACTACTGTGCAATGCCAGTACC
401 GATGCCTTGTGTCATGATCGCGGGGAGGTGAGTACCATTACTTCTGGCCAAATTCGCCATTGTTACAAATGCTAAATTTTGATATTTTGTATTTAAATGC
501 ACGGGAAGCAGGCGCTGAGACCAACTCGGCTTCAGCATCAGCAGCTGTTCTGCCAGAAGAACCTGGATAAACTCTATCTTTATCATAAACCTGTACGC
KS017 (f)
601 CGGAGTTCAAGTGTGTGTAGAAATATCCATTTGAATACAACCTCCGCTAGGTTTTATTTTTGTGTCATGATATTTCTGTTTGTACTTTCCCTG
701 AGAATGTTTCGTGAAATCTGTGTACTTATAATGTGATCTATCTATCTATTGATACCTTTTAAATGCTAAAACTTAAATACATTTCCGGAATCAAACG
801 CTTTTCTTAAATATCACCCAGGAAGATATCCAGTTCATCGATGTAACGAACACCTTGCCAAACGCTTCAGTATTTCTAGTTCATGGGGCAAAT
901 GGGGCATGAAATTCATATCCGAGCTCCAGCCAAATGCTTGGACCTGGCAGGAGCGATCTCAAATGCAATTCACAATCGTATGCGCTCCTCGCTCGTGG
1001 TCCGCTTCTGCACTGATGCTGTGTAATGGATGTTATGTTCTTGGCGGGCAATCGCATGACAGGCGCATGTTTGCAGCCGCTGGCATCCGCGCCATTAT
1101 GGSCAAGAGTCGGAGCTGGGAGTAGCCACCGTGGCCCAATGCAATGCAATTCGCCAAAAGCGTGAATCAATAAACAACGAGAGCCATCGCCATCGG
1201 AGCTTCTCTCTGTGTCGACTATCTGGCGTCTGGCTTCTTCGGGATCTTTGGACAGGATAGGATGGCTGGACCTATGGCATCTCCCATGTGGCGGTGT
1301 AACCTATGGGAATCCGCTGGGATGCGCTCGATGTTATCTGCTTCCGCTTTGTTTTATTTTAGTATTCGTGCGGGATAATGATCCATGTTTTCATC
1401 CTGAATGTTTTAAATGCACCCAGTCCGCGGAACCGCGGAGTATTCACCTCCGCTCACTTTGTTTTGGCTGCCTCATCATCGTCAACGGGTGCAACA
1501 TATCTGGAGCTCTAGTGGCGAAATGAGATCGGAAATGCTTGGCTTTACCTCAGATCGGTTAATGAAAAGTTTTTCTGTGCGAAATACATTACCTGC
KS016 (r)
1601 GCCCGATCAGATGATGCTGCAATGCTGCTATGGAATACTATACAATTTACGAATAATTCAGAAATCCGATCTTGGTGAAGTATGATGTCAT
1701 CGTCCCACTTAAATTTGCCAGTCAAAATCAGCAATAAAGCCTTTGCCCTTGGCGTTGAACCTTCTGTGAAATGATCTTTCAGGAAGACCGAAATGTG
1801 TTAGGACATGTAGGATAAGTCAATCAGACCCAGGCTAAAACAAATTTGCCAGTGGGGCCAAATAATTCAGGAATGGATACAACTAAATAAATCACTC
1901 AGAAGGACAACACCCAGTGGCAGAGGGATCCACCCGCTATTCGGAATCCGATTCGGATTCGCATTCGCATGTGGGGATCGTCAATACTGTGTGGC
2001 TGTCATGATGGCAACGTTTTCCGTTTGGCCAGCAAAAAAGCAGGAGCAAGAATGAGTCCCGCTAAATGACCCATTGTTGGAGCTGCCTCGCTGGCC
BamHI
2101 CCTGAACAATGTTCTGCCTGACTGACATGGGGTGGGATGCTGCTGTTGTTCTGATTTGGGAAGAAACAATCCATCTTTGGGCTGAAAGCGAT
2201 CTCTCTCTGCGCAAAATACACGCTGAATAATTAAGTATCTCTTGTTCGCGATAAAACACAAAGTTCTTTTAAATTTATGGCGCTCAGTAGGACCC
KS07 (f) DraI
2301 GATTTTGTGGAAATGAATTTGTGGTCAGCAGGGCAGTAAACAATCTCAGCAATCAGTTATGAAGGCTCTTCAGGGAAGCGTGCACCCGAGGTCATTTG
DraI
2401 CTTGAATAATTCGGCAGCTTCGCTGTGATTTACTGTCAGATAGAAATCCCGCTCTATGATTAAGGTGCAAGTAAATTCGATGCTCTATCGGCGAGCAAGTC
KS023 (r)
2501 GTTAATCGATTATCTTGCATTCGATAAAATGTTTACTGTCCAAAGCTCTCCAGTCAATACGTAGGCCCAATTTGGCGATACGGATAAAGGATTAGCCAG
KS011 (f)
2601 TTTATGTCATTCACAAATCTTCTCTGTTAGCGACAATAATGATGTTGATAATAATGGCGATGCGGATTTACGGCACAGACATGAGTCTTACATCG
KS010 (r) KS09 (f)
2701 TAAATCACTATTAGCTATCAATTCCTATGATTGATTTACACATGTTTTTIGATCGTTATGATCACATGTTGTTCTTTTTCATATAGATTAGA
2801 TTAATATTATTTAGAACTTAGAAGAAATATTGATAAAGCAATTTATATTAGATCTGGTTAGTTTCACTTCCGTCAGCAATCAGTAAATTTAGTATGAAT
HindIII BlnI (r)
2901 TCATAATCGGAACATTAGGCTGCGAAGAGGCTTGGCGAAGGTCGCTTTGAATAAAGAATAAGATGAAACTCTTACTTGAACCGCACATCGGATTTTTT
3001 GTTTTTTTTTTTTTTTGGGATCTGAGAGTTTTAGGCTTCTTTTAAAGCACTTGGACTTAATAATATATAAAAAATTAATTTTTTGAAGCTCGATAG
3101 CAAGCAATCCACGTCACACCCAGTGTAGATCTTCTCCCATCAGGGGAGCGCTATGTTCTCCGATACACTTTGATTTGAAAGTAAATATAGCGTCTT
KS015 (f)
3201 AATCAGAATCAACCGAGCTTCTGGAAGCTCCAGTCCGATCGCGTATAATACACATGTTAAAGTCTAGCAAACTATAATTTAAATGTTTC
3301 ATCGCATGCGCTGTCAATTCAGCGAGTCAAGGAGCAGCAACATCAAGATCACAACAGCAACAAGTCTTTTTAATGGCAACCAAAAGATCCAAGTCCAG
3401 GGAAGAAGATCGGGCGTACGAAATTTAAATACAAACAATGCGACGGGGCATACGAAAGCGATGCAATGGCGCTCAATCAACCGATGAACAGCAAAA
3501 TTGCCAATAAGACGACACAGCGGCTTGTGTCGGGATCTGATTTGGGAGTCTATGGCCGACTCAAAATATAATGTTGTAATTTGGTGGCGCAGGCTC
3601 CAAGCCGATGAACATTTGTTGAGGACTCGCGGCTACTTGCAAAATACCTTCTAAAATATTGCACATGCTTGGCGTATGGAGCGGCACAGAAGCCG
3701 AAAACGTTCAATCAAGTCAAAATTTGGGAGCACTTGGCAAGTGGCTTGGCTTGCAGTAAAGGATACGACCAAGCTGAGAATCGATGTGTCAC
3801 ATATCGGCAACTGATGGCCGAACAAAGTCTTAAGGTCAAGTATGAAAGCTTTCATTCAGAAAAGAACCAATGAATGAAAGTTTCTTTTCTCAAGA
HindIII
3901 CCTAGATTATAGAACTAGATTATTAGAGACTGAGTTCGACTTCTGTGTCATTATAACGTTCAATTTGCCCGGCGCATTTCCAAATATGCGCTTCAATC
4001 GGCATTTAAGTACTGGAGAATTTTCAACACATGGAATACCCCTGCAATTAATGATTTACCAATTAATAATGTTGGTGTTTTATGATCCGATGATAAA
4101 CGCGTTTCAATTAACATACTACATTTAAATAGAAAAATCATAATATTTAACTTTAATATTTCCAGGCCGAAATATGTAATAATATTATGTTATCTGTG
4201 AAAATGTTGTTGATTGAGGACATAGGTACACAGAAACTAGTAAAGTTGGAACACGCTCTGATTTGCAATATTAAGAGAAGAAATCTGGTACGGGATATAA
4301 AACTGAACCTAAAAGGGCGATATATAACACTGTAGATCAACAACGTAAGTATCAAGAGATTTGTGCGTTTTTGTATATCTGGGATGCCAACGGGAGGC
4401 ACATATGGCACCCGATATTTATTTTCAGCCAGTGAATGTGGAATAGCACATGAGGAAATGGACCGGGCCAGCAATGTAGACTACATTCAGCCATCACT
4501 GATCAATCAAGCACCCCTTTCCACTGCTGCTTCAACCGCTCAACCGTCAAGGTAATTCAGAAAGCGCAATTAATGTTGATGTTCTTCTATCCCTGCTT
KS014 (r)
4601 GTGATTTGCTGAGTTCGCTTTAGCTTATGCTGTTAAATCCAAAAATGCCAAAGCACCAGGAGGAGGAGCACTGTTCCATTTATCTAATCTACTGTC
KS020 (r)
4701 CCGTTTTGCCCCACCAATACATAATCTCTAATAGTTGCAATAAAACTTTTATCTTGTATTTGATCAAAATGTTTTCTTATCCAAATTTTATATCTTTCCG
4801 CCTGGCATGTGACATCCCAACAGGACTCGTGTTCGGGTGAGGGTTCGCTCAGTTCCGTTCAATCTCCGATCAGCAGATAGAACAATCTTTCAA
4901 GGAAATC
EcoRI

gene. The additional sequence could correspond to an extension of the untranslated 3' sequence or an alternatively spliced product corresponding to one of the alternative transcripts identified by Northern blot analysis (Fasano et al., 1991). Four distinct transcript sizes were identified on Northern analysis, 5.0, 5.4, 8.1 and 8.5 kb in length (Roder et al., 1992). The 8.1 and 8.5 kb species are low level transcripts expressed mostly throughout embryogenesis and are believed to be the result of alternatively spliced transcripts. The 5.0 and 5.4 kb sequences correspond to mRNAs that are expressed throughout development and encode the *tsh* protein.

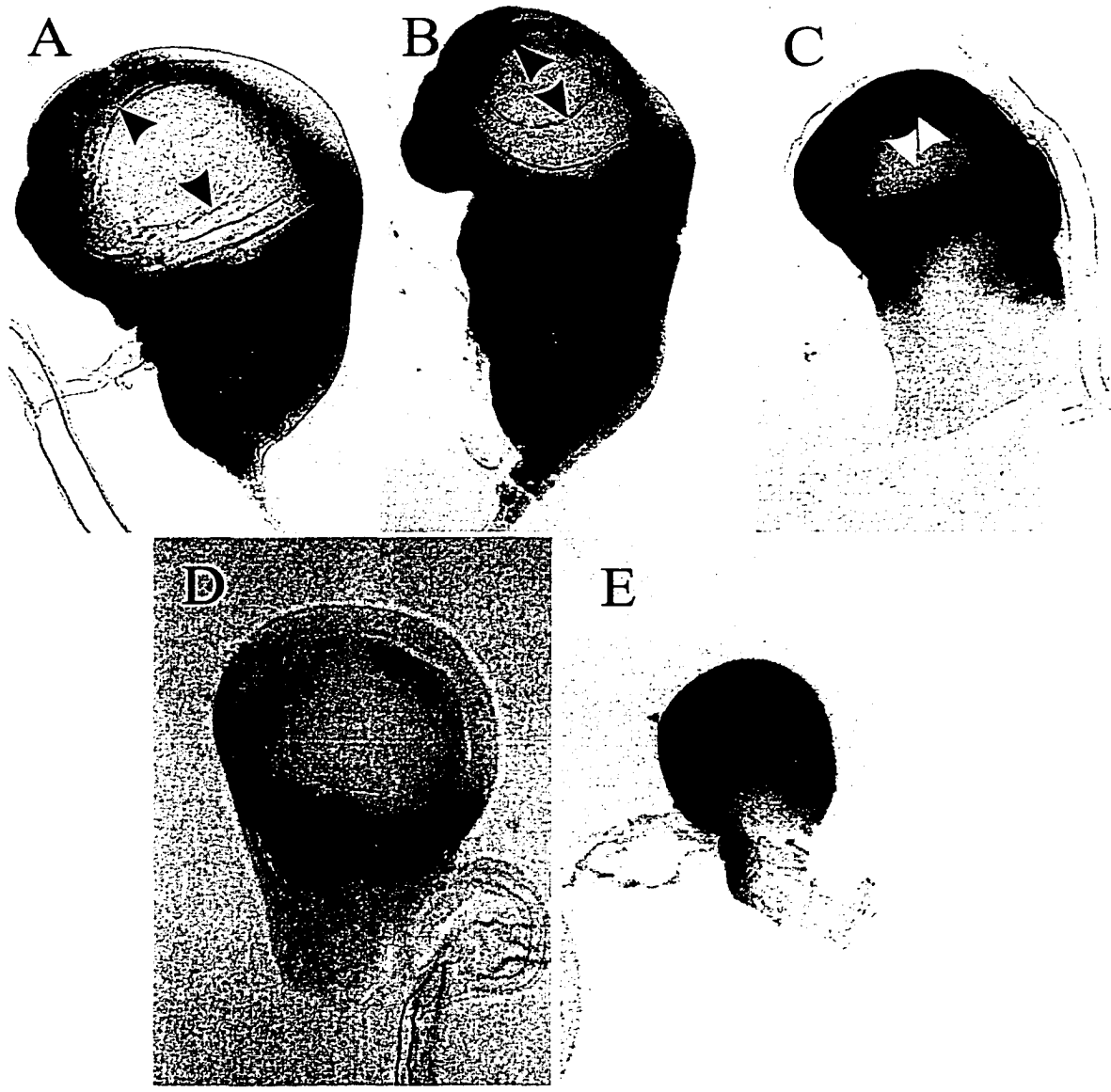
Rpw* and *vg^U

The expression of the *tsh* reporter gene is unaffected by mutations involved in wing patterning and growth. Two dominant mutations *Rpw*, (an allele of the *Serrate* gene) and *vg^U* both show defects in wing patterning and growth, with *Rpw* acting further upstream in the pathway. *Rpw*, discussed earlier, shows a moderate scalloping of wing whereas *vg^U* causes a complete loss of wing tissue. In an enhancer trap screen designed to detect modifiers of the *Rpw* phenotype, an allele of the *tsh* gene (as well as a number of other *P* element enhancer trap lines) were identified as enhancers of the scalloping wing phenotype. Examination of the X-gal staining pattern of the double heterozygote revealed that the *lacZ* expression was unaffected by the dominant mutation (**Figure 27**). The combination of the wing mutants and the reporter construct (E4.8) and the *tsh*[04319] enhancer trap fail to show any reduction in the expression from the reporter gene. The dominant mutations affect the D/V organizing center in the wing pouch of the imaginal wing discs (Speicher et al., 1994). The lack of any interaction is not surprising because the proximal tissues of the wing hinge don't require the D/V organizer for formation of the hinge (Ng et al., 1995). These results are also consistent with observations made with the *b ae cn; Bd^G* double mutant. The *b cn ae; Bd^G* flies show no difference in the wing posture or wing scalloping.

C(1)DX

One interesting interaction was observed between the *ae b cn* chromosome and the compound chromosome C(1)DX (**Figure 28 A versus B and C**). Often

Figure 27. Third instar imaginal disc staining of *tsh* [04319] in combination with wing mutants required for patterning and growth. **A)** *tsh* [04319] third instar imaginal wing disc. **B)** *Rpw/+; tsh* [04319]/+ third instar imaginal wing disc. **C)** *E4.8/+; vg^U/+* third instar imaginal wing disc. **D)** and **E)** third instar imaginal haltere discs from flies of genotype, *tsh* [04319] and *E4.8/+; vg^U/+*, respectively. Arrowheads in panels **A)** – **C)** indicate the dorsal and ventral folds that demarcate the pouch.



females heterozygous for the *b cn ae* chromosome in conjunction with the compound X chromosomes, *C(1)DX*, exhibit defects in cuticle deposition on the abdomen resulting in bare epidermis. However, the defect in deposition only appears to affect the adult cuticle layer and not the first pupal layer of cuticle, which is still visible as the transparent sack that envelops the pharate adult forming a layer separating it from the hard pupal case (Fristrom and Fristrom, 1993). Crosses between *C(1)DX* and Oregon R failed to produce similar cuticular defects in the abdomen. The interaction could not be duplicated with any of the markers on the compound chromosome (*forked (f)* or *scute (sc8)*). This suggests that the phenotype observed may be the result of a combination of the two or of an induced mutation on the compound chromosome. Further analysis of these defects was not carried out because the abdominal cuticle defects were unrelated to the thoracic defects associated with the *ae* mutant. Although the defect does affect the adult cuticle it appears to be a problem associated with deposition and not patterning. In contrast, the *ae* mutant seems to affect the role of *tsh* in patterning in the ventral wing hinge.

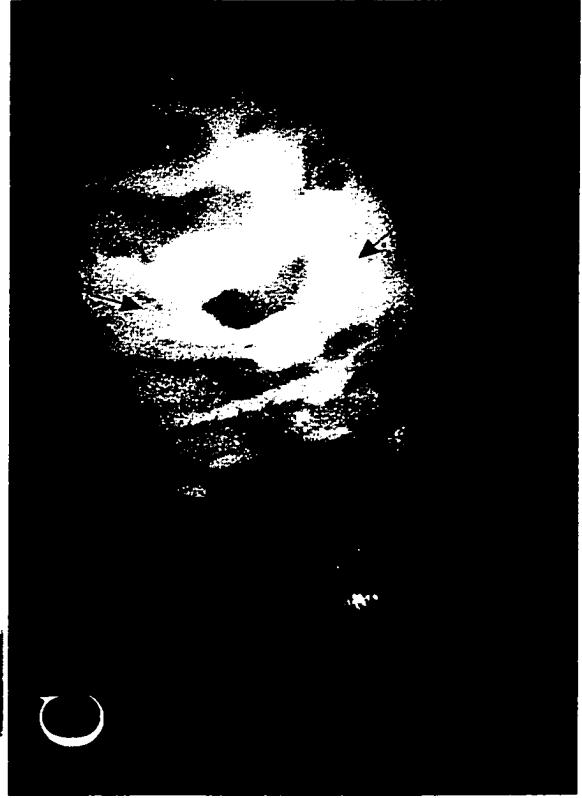
UAS/GAL4

In addition to the conservation observed between *Drosophila* and distantly related organisms like vertebrates, *Drosophila* researchers have a very well established set of tools for the study of development. One tool kit that had been developed in recent years utilizes the yeast encoded DNA binding regulatory proteins (GAL4) and regulatory upstream activating sequences to which they bind (UAS) (Brandt and Perrimon, 1993). This modified UAS/GAL4 system enables the misexpression of any cloned coding region in nearly any pattern at nearly any stage of development. A third chromosome UAS-*tsh* line was utilized to test whether the *ae* phenotype could be rescued by expression of the *tsh* protein in the presumptive hinge. The 30A-GAL4 line generated by Brandt and Perrimon (1993) specifically drives the GAL4 protein expression in the presumptive dorsal and ventral hinge region encircling the wing pouch. The expression from the enhancer trap line *tsh*[04319] and the EB2.9 construct overlap the expression pattern of the 30A line only in the ventral hinge region. The 30A-GAL4 driver is expressed more distally in the presumptive dorsal wing hinge compared to where *tsh* expression is

Figure 28. Phenotypic interaction between the *ae b cn; ry* stock and the compound double X, *C(1)DX*. **A)** Oregon R female. **B)** and **C)** lateral and dorsal view of female *b cn ae/+; C(1)DX* flies. An Oregon R female is used for a control fly so the abdominal tergites are more visible for comparison. The arrows in panels **B)** and **C)** indicate examples of missing tergite cuticle. The arrow in panel **A)** shows an example of a normal abdominal tergite.



A



C



B

Figure 29. SEM analysis of proximal wing structures from flies subjected to directed expression of *tsh* under the control of the UAS/GAL4 system. **A), B)** and **C)** are dorsal views of wing hinges from an adult Oregon R, a fly of genotype UAS-*tsh*; *30A-GAL4*, and a fly of genotype UAS-*tsh*; *vg-GAL4*, respectively. **D), E)** and **F)** are ventral views of wing hinges from adult flies of genotypes; Oregon R, UAS-*tsh*; *30A-GAL4* and UAS-*tsh*; *vg-GAL4*, respectively. **G)** ventral wing hinge from an adult fly of genotype *b cn ae 30A GAL4*; UAS-*tsh*. **H)** A third instar imaginal wing disc from the *tsh*[04319] enhancer trap line, stained for *lacZ* expression. **I)** *Lac Z* staining of a third instar imaginal wing disc from a larvae of genotype *30A-GAL4*; UAS-*lacZ*. The arrowheads indicate the distal most expression of the *30A-GAL4* line with respect to the *tsh*[04319] reporter. *LacZ* expression is in black. Abbreviations are as in **Figure 1A)** and **B)** except for the following: PH, proximal haltere; R, radius; H, haltere; PO, Posterior outgrowth; AO, anterior outgrowth. Anterior is left and dorsal is up. All flies were raised at 23°C.

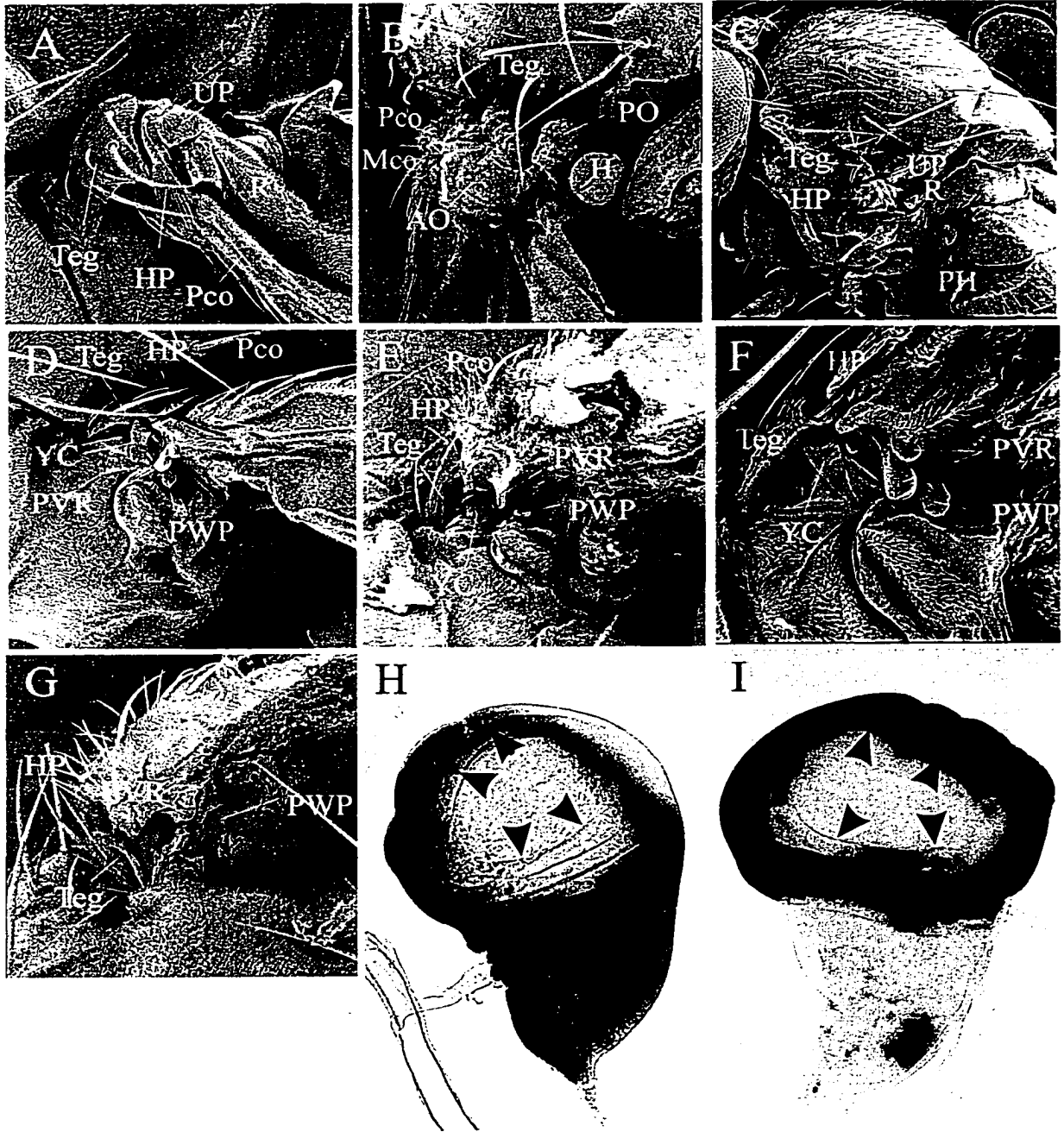


Figure 30. **A)** and **B)** are ectopic bristles from the dorsal and ventral outgrowths of flies of genotype *UAS-tsh; 30A-GAL4*. **C)**, **D)** and **E)** are bristles from the lateral thorax, wing blade and the anterior outgrowth seen in **Figure 29 B)**. The circles in **A)** and **B)** indicate the ectopic bristles associated with dorsal and ventral cuticle deformation, respectively. See **Figure 1A)** and **B)** for abbreviations except for the following; MC; macrochaetes and WH; wing hairs. Panels **C)** - **E)** are all the same magnification. **A)** and **B)** anterior is to the left. All flies were raised at 23°C.

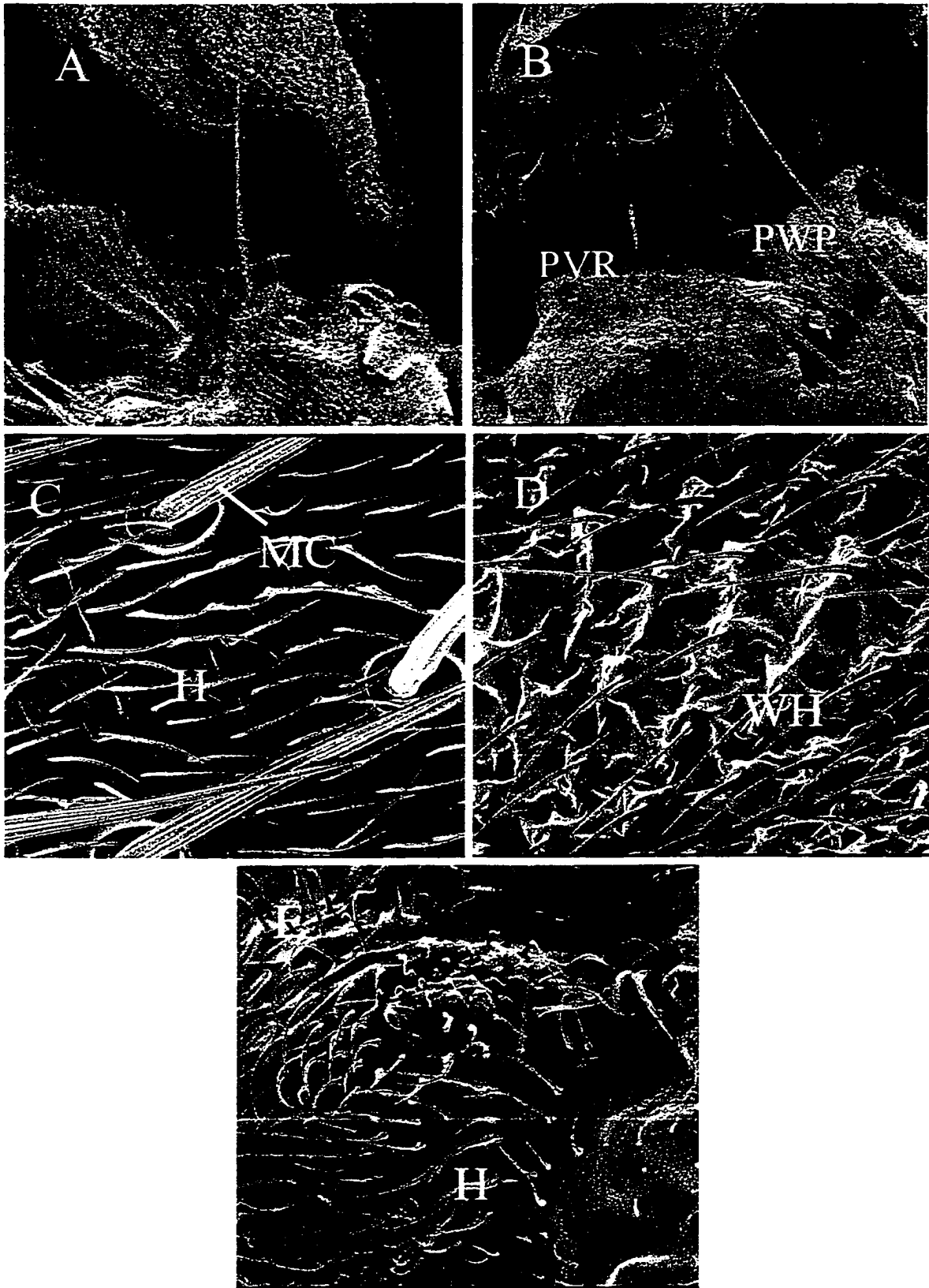
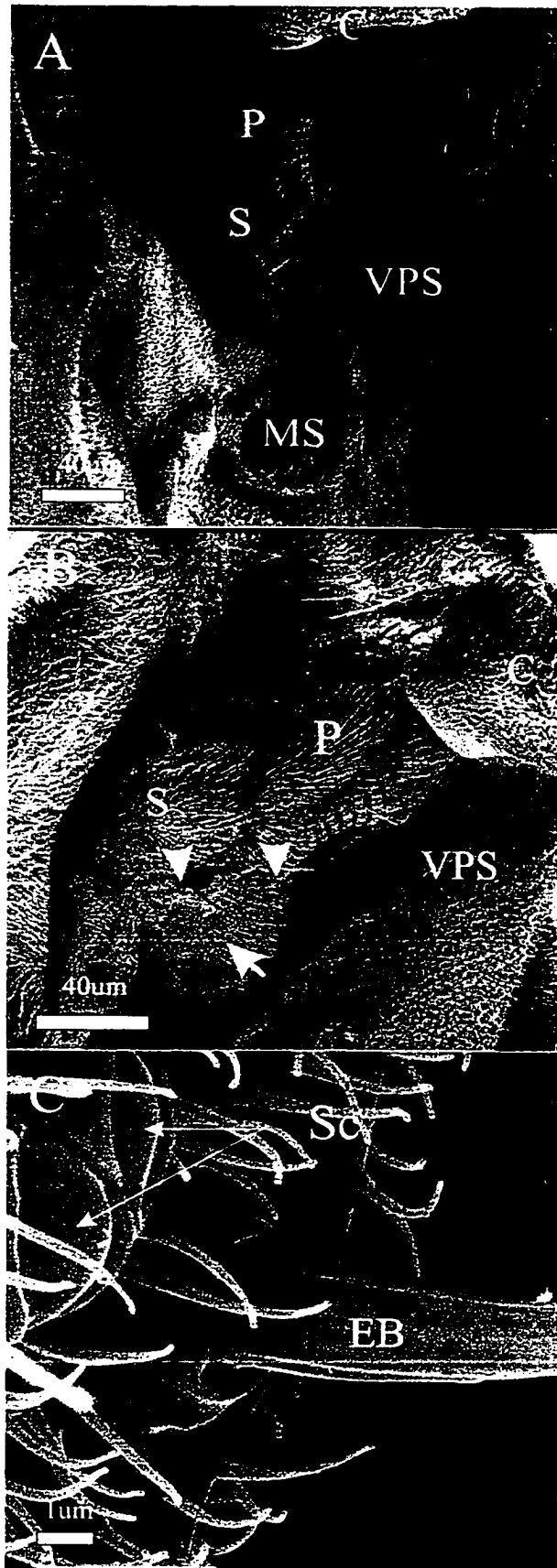


Figure 31. SEM analysis of halteres from flies subjected to directed expression of *tsh* under the control of the UAS/GAL4 system. **A)** is a haltere from an Oregon R fly. **B)** is a haltere from a fly of genotype *30A-GAL4; UAS-tsh* and **C)** is a high magnification of the ectopic bristle at the base of the haltere in **B)**. White arrowheads in **B)** indicate the location of ectopic bristles at the base of the halteres. White arrow indicates the ectopic cuticular outgrowths at the base of the halteres proximal to the ventral pedicellar sensilla. Abbreviations are as follows; VPS, P, S, C, EB, Sc and MS indicate the ventral pedicellar sensilla, pedicel, scabellum, capitellum, ectopic bristle, sensilla campaniformae and the metathoracic spiracle.



normally detected (**Figure 29 H** versus **D**). The expression pattern observed from the *tsh*-specific reporter genes (*tsh* [04319], E4_8 and EB2.9) show that *tsh* doesn't exhibit a symmetrical expression pattern in both the dorsal and ventral hinge (**Figure 29 H, 19 B** and **C**). Spatially the expression in the presumptive ventral hinge is similar for each of the constructs. In the *tsh*-specific transgenic lines and the enhancer trap, the distal limits of the expression fail to reach the wing pouch as in the ventral hinge (black arrowheads in **Figure 29 H**). Ectopic expression of the UAS-*tsh* using the 30A-GAL4 driver leads to outgrowths of the wing cuticle from the dorsal surface of the hinge in addition to defects on the ventral surface of the hinge (**Figure 29 B, E** and **G**). The dorsal hinge defects in the *yw; UAS-tsh; 30A-GAL4* flies always consist of two separate outgrowths (**Figure 29 B**). The colors associated with each of the outgrowths cannot be seen in the SEMs, but the more anterior outgrowth always resembles the yellow cuticle of the thorax. The smaller posterior outgrowth often exhibited the grey color similar to the wing blade but sometimes resembled the yellow color of the thorax. The bristles on the anterior outgrowth do not resemble either the lateral thorax or wing blade bristles (compare **Figure 29 C, D** and **E**). The short, often curled hairs, resemble the hairs of the proximal tegula or the hairs found on pleural plates of the mesonotum in regions close to naked cuticle, for example in the area of the mesopleural plate close to the base of the wing (see **Figure 1A** and **B** for regions of the adult cuticle). The posterior outgrowth is also associated with proximal patches of naked cuticle and socketed bristles often identified at the distal most boundary of the dorsal outgrowth (circle in **Figure 30 A**). However, in one adult of genotype *Xa; UAS-tsh; 30A-GAL4* ectopic bristles were observed through out the ventral surface of the wing hinge (circles in **Figure 30 B**). The size and appearance of the ectopic bristles in both dorsal and ventral hinge are similar to those found on the tegula and costa regions of the anterior/proximal wing margin. The posterior outgrowth appears to originate proximal to the alula (AL) in the region of the axillary cord (AC) (**Figure 29 B**). Some of the bristles of the proximal costa from UAS-*tsh; 30A-GAL4* flies exhibit a polarity defect, often pointing perpendicular to the longitudinal axis of the wing rather than distal (**Figure 29 D** versus **E** and **G**). In the region of the Pco there are often additional bristles present.

Within the ventral hinge of *30A-GAL4; UAS-tsh* flies, the cuticle exhibits defects in the wing hinge distal to the proximal ventral radius (PVR). The yellow club (YC), humeral plate (HP), tegula (Teg), pleural wing process (PWP), pleural sclerite (PS), axillary pouch (AP) and the proximal knuckle of the PVR are present and appear structurally normal (**Figure 29 E**). In tissues more distal to the first knuckle of the PVR, there is an alteration in the cuticle of the wing hinge (compare **Figure 29 D** and **E**). The first and second knuckles of the PVR are fused forming one large PVR projection, which appears to be larger than the two knuckles combined. Structures more proximal to this region are unaffected. Defects associated with the ventral hinge were observed as distal as the medial costa (Mco). However, along the wing margin the effect of ectopic *tsh* only appears to be obvious as distal as the proximal costa (Pco) (**Figure 29 E**). For a map of the features reported here see **Figure 1A and B**.

The dorsal defects, in particular the outgrowths, are much more prominent than defects associated with the ventral hinge surface. The defects observed in the ventral hinge of the *yw; UAS-tsh; 30AGAL4* flies suggest that the proximal domain of ectopic expression of *tsh* roughly coincides with the area where some of the abnormalities associated with the *ae* mutant are expressed; the PVR and PWP (**Figure 29 D** versus **E**). Although the ventral wing hinge is distorted in flies of genotype *UAS-tsh; b cn ae 30A-GAL4*, it appears that there is a rescue of the fusion between the PWP and the PVR that is observed in the *ae* mutant (**Figure 29 G**). However, the YC structure is not rescued in these flies. The distortion makes the identification of any other structures difficult but one can detect what appears to be a naked cuticle in the shape of a knuckle resembling the PVR in roughly the correct area (**Figure 29G**).

On the halteres below the ventral pedicellar sensilla (VPS) and at the base, socketed bristles are observed in the *30A-GAL4; UAS-tsh* flies. In the region of the metathoracic bristle group, there is an ectopic socketed bristle approximately 5X the size of the MTB (white arrowheads **Figure 31 B** and **C**). There is also a blebbing out of the cuticle between the MTB and the base of the VPS in a position referred to as the haltere sclerite according to Bryant (1978) (**Figure 31 A** versus **B**). The drooping haltere phenotype of *ae* is rescued in the *b cn ae; UAS-tsh; 30A-GAL4* line but, it is more likely

due to the outgrowth or blebbing at the base of the haltere pushing the haltere dorsally, as opposed to the rescue of the fusion observed in the *ae* mutant.

To determine if *tsh* could induce thoracic or wing hinge fate in other tissues not fated to do so, *tsh* was misexpressed in the wing pouch under the control of the *vg-GAL4* driver. This ectopic expression led to the loss of wing tissue. To understand if the wing tissue was lost at the expense of new thoracic or hinge tissue, the *UAS-tsh; vg-GAL4* flies were raised at slightly different temperatures to change the level of GAL4 expression. At 25°C there was a complete loss of wing blade tissue with no detectable ectopic formation of thoracic or hinge structures (**Figure 29 C**). The most distal structures remaining in these flies were the humeral plates of the proximal wing hinge. At 22°C the wings were reduced in size, to approximately 10% the normal size. The wings were slightly crumpled, however they still possessed some morphological characteristics of the wing blade. No normal triple row of bristles could be detected in these wings. The anterior wing margin only exhibits the long slender mechanosensory sensilla. The short stout mechanosensory sensilla and the slender chemosensory sensilla were not recognized. The anterior wing margin resembles the double row of bristles found at the distal tip of the wing margin. In some of the wings the remnants of a single wing vein is detected. The grey coloration of a wing blade is also visible.

Mini-Library Sequences

Using the BGDp blast search (Altschul et al., 1990), each of the sequences pulled out using the mini-library protocol (see Materials and Methods) has been positioned along the Bacterial Artificial Chromosomes, BAC D532 and BAC D533. The Berkley Drosophila genome sequencing project has localized these two clones to the left arm of the second chromosome. BAC 532 has nine unordered pieces with several breaks of unknown size in the sequence, however BAC 533 is considered a complete contiguous sequence corresponding to cytological position 40B-40C. Using the DNAMAN sequence alignment program the two BACs were found to overlap (**Figure 32**).

Both *tsh* exons, the *tsh*[04319]^{6.1} and *tsh*[04319]^{8.1} derivatives, the 3' *P* element flanking genomic clone sequence from the forward and reverse universal primers, and the *aeroplane* 5' *P* element flanking genomic clone sequence from the reverse universal

primer were localized to the BAC D532 using the BGDp BLAST search (**Figure 32**). Although the BAC D532 clone has nine unordered pieces, the order of each of the sequences in **Figure 32** is consistent with the expected order of the fragments along the chromosome.

The *tsh*[04319]^{8.1} 3' *P* element flanking genomic sequence from the forward and reverse universal primers was localized to BAC D533. This identification of the *tsh*[04319]^{8.1} sequence identifies the distal break point in the derivative line. The overlap of the two BACs lends support to the hypothesis that the derivative line *tsh*[04319]^{8.1} is the result of a deletion of the *tsh* gene with one break point in the 5' UTL sequences and a second break approximately 214 kb downstream of the coding region (centromere proximal).

Preliminary Sequence Analysis

Within the *Hind*III/*Bam*HI 915 bp fragment, a region noticeably rich in the common core sequence, "ATTA" was observed in the 3' 465 bp of sequence (**Table 7**). Other significant repetitive motifs in the HB1.0 fragment are also listed in **Table 7**. Because the core binding sequence of the HOM-C genes is ATTA and because *tsh* is also regulated by *Ubx*, *Antp* and *ftz*, it made this sequence appealing as a regulatory element. In particular the 3' end of the sequence contains ~64% A/T base pairs. Because of the overrepresentation of the common ATTA core sequence, it was not surprising that a number of putative transcription factor binding sites were identified using the MatInspector V2.1 data base search engine (**Table 8**).

Even without the results from the database search it is clear there is an overrepresentation of ATTA (TAAT) motifs in the 3' end of the HB1.0 fragment. An extension of this motif to GATTA, makes it even more statistically significant. By chance, GATTA would occur approximately 0.6 times in this sequence, however, we see this motif five times. A second motif, GATTTAC, resembling the consensus *exd*-UBX or labial cooperative binding site (CCATAAATCA), is only expected by chance, 0.02 times in ~200 bp, however we observe the site four times (reviewed in Mann and Chan, 1996). Finally, within the last ~200 bps of the HB1.0 fragment an interesting

arrangement of motifs exists, ATCA--ATTA-ATCA. This resembles the consensus binding sequence for the *PBC* gene family-Hox protein complex (C/TC/AATNNATCA).

Genetic Analysis

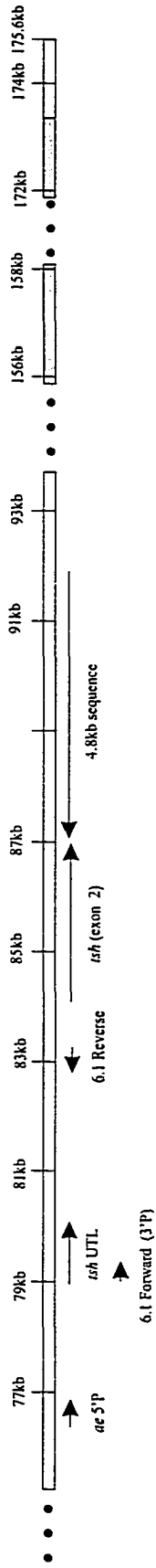
Double heterozygotes were used in an attempt to identify dominant enhancers of the abnormal wing posture. Mutations that affected the wing posture in *Drosophila melanogaster* were crossed into *ae*. Initially, *ae* variable wing phenotype and lack of complete penetrance led us to identify possible dominant enhancers of the *ae* phenotype, as opposed to suppressors of the *ae* phenotype. The wing posture mutants available through the Bloomington stock center, *flapwing* (*flw*[1]), *os*(0), *tx*(1), *ang*(1), *osp*(1), *how* and *eag*(1) were initially crossed with *ae*. Because the cause of each of the characterized genes has been linked to musculature or neuronal function, it is perhaps not surprising that none of the double heterozygotes exhibited any wing posture abnormalities. Double homozygous flies for *ae* and other wing posture mutants had wings held out phenotypes, but it is difficult to interpret these results due to the similarities in wing posture caused by the respective single mutations. One exception to this was the *tx; ae* double heterozygote which exhibited the dusky wing appearance typical of the *tx* mutant. However, the SEM analysis of the *tx* hinge, as reported above, showed that the wing posture in the *tx* mutant is not the result of a defect at the base of the wing.

The results of the MatInspector database search, presented in **Table 8**, reveal a number of putative binding sites for some of the homeotic genes. This is not unexpected based on the overrepresentation of the AT rich motifs in the 915 bp HB1.0 fragment (**Table 7**). As noted above, an attempt was made to identify genes that dominantly interacted with the *ae* phenotype. Presumably, a loss of function mutation in the same pathway as the *ae* mutation would lead to an enhancement of the *ae* phenotype. Alleles from the *bicoid* (*bcd*), *Dfd*, *tramtrak69* (*ttk69*), *ftz* and *Scr* genes all complemented the *ae* phenotype in the double heterozygotes. Two possible genetic interactions were identified in an *ae* homozygous background. In the double homozygote *ae; Dfd*^l, the eye phenotype appears to be suppressed. However, this *Dfd* allele is known to overlap wild type. In our *Dfd*^l, it was observed that about 95% of the flies had the reduced eye phenotype. The *ae; Dfd*^f double homozygotes were very weak and could not be

maintained as a stock. The *ae; Scr²/TM3* flies exhibited a sex specific suppression of the *ae* phenotype. All females in this category appeared *ae⁺* while all the males appear *ae*.

Figure 32. A schematic diagram of the results from mini library cloning of flanking genomic sequences relative to the Bacterial Artificial Chromosomes BAC D532 (accession number: AC006467) and BAC D533 (accession number: AC006415). Sequences derived from mini library sequences were used to search against Drosophila genome sequences available through the BDGP data base. The open boxes indicate the BAC sequences and the arrows indicate the direction of the mini library sequence relative to the BAC sequence. Numbering above each box indicates the relative location along the BAC in kb. The grey boxes in each of the BACs refer to overlapping sequences. The ... indicate sequences not represented in this Figure. The abbreviations are as follows, 3' P; genomic sequence flanking the 3' P element sequence, 5' P; genomic sequence flanking the 5' P element sequence, *tsh* UTL; *tsh* untranslated leader sequence (first exon), 4.8 sequence; sequence in **Figure 26**. The sequences used for the BLAST search are those in **Figure 33**.

BAC D532
(Ac006467)
176kb



BAC D533
(Ac006415)
Chromosome 2L
40B-40C
162kb

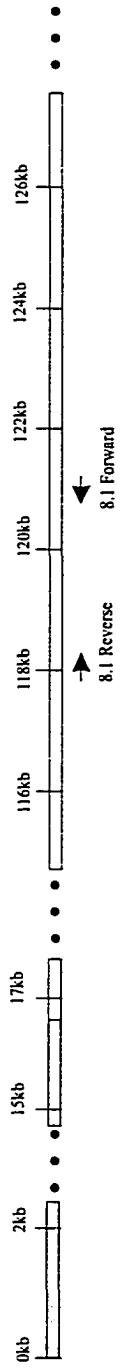


Figure 33. Sequences derived from mini-library cloning. **A)** Sequence of the *tsh*[04319]^{6.1} *Hind*III clone from the forward universal primer. **B)** Sequence of the *tsh*[04319]^{6.1} *Hind*III clone from the reverse universal primer. **C)** Sequence of the *tsh*[04319]^{8.1} *Hind*III clone from the forward universal primer. **D)** Sequence of the *tsh*[04319]^{8.1} *Hind*III clone from the reverse universal primer. **E)** Sequence of the *ae* 5' *P* element clone from the reverse universal primer. An N refers to ambiguous bases. The numbering along the left hand side of the sequences indicates the base position in base pairs.

A)
1 CCTCAGAANCAGCTCGGTACCGGGGATCCTCTAGAGTCGACCTGCAGGCATGCAAGCTTTGCGTACTCGCAAAT
TATTAAAAATAAACTTTAAAAATAATTCGCTCTAATTAATATTATGAGTTAATTCAAACCCACGGACATGCTA
151 AGGGTTAATCAACAATCATATCGCTGTCTCAGACTCAATACGACACTCAGAATACTATTCCCTTCACTCGC
ACTTATTGCAAGCATACTGTTAAGTGGATGTCTCTGCGCAGCGGACCCTTATGTTATTTTCATCATGGTTCGAG
301 TAGTGACGACGAATCCGGATGANAAGACGACGCATCGCGACCCGGATTCGCCGAGAACAGTGAATTCAGTT
TAAAACGCGTTTNTGGGGGAGGATAGAACGAGTGGTTTNCAGGCCGGCATCATATCTAGTCAAGAAGCAGAGGTT
451 GATACTCTCGAACGCAATGNTCCATCAAGANTGGAACATACGAGAACNTACATACNAATGGGTCAACAANGTATA
CGTAAACTACCCAAGCTAACAAANTNTCCNANATNTNTTATTACCAACAGANAANATNGCNATAN

B)
1 CCNCACAGCTTACGCCAAGCTTAAGACTATAGTACGGATCTAAGTCCGCGCACCCAGGATGATTATGCCAACAT
AAGAACTCCTAAGAACAATAGATGCTTATTATGTCAGTAAGTGGCATGATATTTGTTGCACTATAGGAAGTATG
151 ATAAATATGGAATTCAAAATGAAATGACTGATGGGGGAAATAATACCAAACAGAAGAAATAGCCATAAACGAAAA
AAAAACGAACGTGTAAACGCATCAATAGGGGGTTTACTTTTCATTTTATTTATTCGCATTCCGCCGATTCAGACAA
301 TTAAGCTGATCGTTTACAGCTAATCAGCAATCTATCACCTCTGAATATCTGAATTAGAAAACANTTTAAACGACA
GAGCTATCTCGCCCCTTTTCGCCAACCGCCTTTGACTTTTCGCAGGCCAAACATTTCTCCGGTTNANACCGGTACAT
451 AAGCNATCAAAGCCNTGGAAATCGTTATAGTGGGNTTACTATTTATTTGGGCCTCCCCTGTGCTAAATCATT
CGGCCNNGGAACTACAATGGCATCAATGGNAANATATGTTTACATTTTCNATTTGNATCAATTTTCGGACGCCTAA
601 GGCAACCCC

C)
1 CCTCAGAATTCGAGCTCGGTACCGGGGATCCTCTAGAGTCGACCTGCAGGCATGCAAGCTTGAAAAATGGAGAGG
ATCGCAATAGTCGAGGGCCGCAAGTATCAGATAGCCATTTGAAGGATGTGTGCTCAAACAGCAAGTTGACTTCA
151 TTGGAGATTGTATTCAAGTTCGCGGTAACATCACAACAGTATATGTATGTAGTATTTTATTCAAAAAGTTGTTG
CCCTTATTGCTTTATTGCGCTTTATGCATATGAATAATTCAGTGGTGCATTGTTCATCAATAAACCCCTATAGA
301 TTAACATAGTAAACATAAAAACATTTAATCACTTATTTATGCATATGGTTAGCACATCATATAATTTTAAAGGCTA
ACCATTAATAATAAAGCAACCCCTAAGTGCCTCTATCTCGATAAGACTTAATTTTAAACTACAGTAAAGTGGT
451 ATCTAACTAGTCACCTATTTTATATCTATCTATCTATCTATCTATCTATCTATCTATCTATCTATCTATCTATCT
CACGGGGGTCNAAATTGGGGACATAAATTNGNCCTAANTAATCAATGGCNCNTAGNNTTNGGATTTNNNT

D)
1 CCTNACAGGATTACGCCAAGCTTTGCGTACTCGCAAATTTAAAAATAAACTTTAAAAATAAATTCGCTCTAAT
TAATATTATGAGTTAATTCAAACCCACGGACATGCTAAGGGTTAATCAACAATCATATCGCTGTCTCACTCAGA
151 CTCAATACGACACTCAGAATACTATTCCTTCACTCGCACTTATTGCAAGCATAACGTTAAGTGGATGTCTCTTG
CGACGGGACCACCTTATGTTATTTTCATCATGGCACAGTGGGTGTGTAGAGAGCAAGAGAGTGTAGTACTCCTACTG
301 AGTGGGAAAAATGTGGTTCGTTTTCGAGTGCATTTGAATTCAGATTTGAGTGCCTCAGGGAACAAGCCAGCCAT
TACTTATTTATTTATCCGCAACTCCTGGTCACATGAATGAAAAGGAAAAGAGTGGCAAAAATCAAAATGGGTTAA
451 ATCTAGAAAAGAAACCTAACAGCTAAATGGGTATCTAAGCAATACAAACACCAACGAGTATACGTAATCTCT
ACCTAACATANCTAATGGTAAACATTATGGGTCNGTGAACCTANCGANCNATGTNCCAAGNTNATNTTGT

E)
1 CCTCACAGNTTACGCCAAGCTTGCATGCCCTGCAGGTCGACTCTAGAGGATCCCCGGGTACCGAGCTCGAATTC
CATAATAATTTATCAAACGAATTTAATGATCGAAAGCATAAAAATTAATGGGGCGCAGAAAATCAATAGATG
151 ACCCATCGCGAAGAGATCTCTCTCAGAGTGAAGGCAGGAAAAAGAAATTTAATAAAAAATTCCTCAATCAAATTA
TAGAATCGTAAAAGTATTTATTACCACGGAGACCAAGAGGACTCAGATGGGGATGATACTGGAGCCCCAAAAGCA
301 ATGCTCCCGCCCCAGCACCTCTTCTTTAGGGTTGAGTGGATCCACGTGATTTGATTATTTATCGGTTAATGGGT
GGATCGTTAAATCTTTACGATTCGTTTCTCAGCCTTTAACGGAGCCGTTCTGGGAGCAACAAGTGCAGCGAG
451 GATCCCATTTGGGATGAAGACTCAGAAAAACAATAAAAAACNGCGGCAAGCNGAAAAAACGAGCGAGTTNTCGCAT
TTTCGAGTTTATGGCTCCNCAGGATTCGTCAATATGGTANATTTAANTCCGCTTTGATAATGGNGNCCTTNC
601 NNCCA

Table 7. <i>aeroplane</i> Enhancer Repetitive Sequence Motifs.				
Sequence	915 bp		3' 465 bp	
	# expected	# observed	# expected	# observed
ATTA	3.6	7	1.8	7
TAAT	3.6	5	1.8	4
GATTA	0.9	5	0.5	5
ATTTA	0.9	4	0.5	3
TAAAT	0.9	4	0.5	2
CTAAATG	0.06	1	0.03	0
GTAAATC	0.06	3	0.03	2
GATTTAC	0.06	2	0.03	2

A sequence analysis of the *aeroplane* enhancer region for repetitive motifs rich in AT sequence. The table compares the entire 915 bp *aeroplane* enhancer and the 3' AT rich 465 bp of sequence. The expected numbers are based on simple probabilities.

Table 8. MatInspector 2.1 Database Search Results of the <i>aeroplane</i> Enhancer Sequence.			
DNA Binding Factor	Number of Matches	Expected Number (/1kb)	Consensus Sequence
<i>Bicoid</i>	6	0.51	sgGATTan
<i>Tramtrack 69K</i>	3	0.08	ggTCCTgc
<i>Hunchback</i>	10	2.57	smanaAAAAa
<i>Fushi tarazu</i>	1	0.04	anwgyaATTAag
<i>dorsal</i>	1	0.53	ngrGAAAancn
<i>Crocodile</i>	2	0.22	wanarTAAAtatnnn n
<i>Deformed</i>	12	2.86	nnnnnnATTAmynnnn
<i>Snail</i>	2	1.45	ascaccTGTTnnca
<i>Broad-Complex Z4</i>	2	0.4	wwwrKAAAsawaw
<i>Broad-Complex Z2</i>	1	4.83	nnntntnCTATtntt
<i>CF2-II</i>	1	2.73	rtATATrta

The 915 bp corresponding to the *aeroplane* enhancer was analyzed using the MatInspector V2.1 putative transcription factor binding database search (Quandt et al., 1995). The parameters for the search included any putative site with a perfect core similarity (1.0) and a matrix similarity of at least 0.85. The latest search was performed on Wed Oct 6 13:24:23 1999. Under the consensus sequence column, the core sequence is indicated with upper case and the matrix is indicated with lower case letters. The probability refers to the number of respective sites expected in 1 kb of sequence.

Chapter VI – Discussion

Muscle Analysis

Originally, classical complementation data involving alleles from genes located within the proximal regions of chromosome 2L suggested that *ae* was an allele of a novel gene. Although characterization of the original *ae* allele was limited to genetic mapping, phenotypic analysis and gross indirect flight muscle examination, we are confident that the similarities between the original *ae* mutant and the present stock indicate that they are allelic. This is in spite of the fact that no gross defects were observed with the DVMs, in contrast to the original mutant. However, an increase in the frequency of fragmented myofibrils in the mutant compared to Oregon R was observed. This is unlikely a fixation artifact, because of the presence of well preserved hexagonal arrays of thick and thin filaments throughout the myofibril separated by the absence of such arrays. Possibly the fragmented appearance may be a natural deterioration of the muscles and the higher frequency in the *ae* mutant may be somehow caused by the abnormal wing posture as a result of increased stress on the IFMs. The *ae* and Oregon R flies used in the muscle analysis were of the same age (24-36hr old adults), therefore any differences are likely the result of differences between the stocks and not an age dependent artifact. The lack of any defects in the IFMs is also not unexpected because *ae* flies have often been observed exhibiting limited vertical wing movement, which requires the function of the IFMs. A little more surprising is the fact that the DFMs are also unaffected, since these muscles are required for wing posturing during courtship and flight. However, both the structure and innervation of the DFMs was determined to be normal. The negative results observed for both muscle and neuronal innervation in the mutant is also surprising because of the precedent set by the other characterized wing posture mutants. Most of these mutations lead to defects in patterning, specification or function of the neurons and/or muscles of the IFMs.

A Tissue Specific Null Allele

Although all the available *P* element *tsh* alleles complemented the *ae* phenotype, molecular mapping indicated that *ae* is likely a novel allele of the homeotic gene *tsh*. Molecular mapping places the lesion responsible for the phenotype within an

approximately 18 kb region that includes the 10 kb *tsh* coding region and about 8 kb of 3' flanking genomic sequence. Although a homozygous abnormal wing posture *P* element allele of *tsh* had been identified by Kerridge (pers. comm.), it also complements the *ae* wing posture phenotype. The only type of lesion that fails to complement the *ae* phenotype is a deficiency of *tsh*, which is by definition a null mutation for *tsh*. By classical genetic definition, *ae* is also a null mutation since flies homozygous or hemizygous express the same mutant phenotype. In contrast, *tsh* null mutations are homozygous lethal. Flies homozygous for the *tsh8* null allele exhibit the lethal trunk to head transformation (Fasano et al., 1991), whereas no such transformation is seen in the homozygous *ae* mutant. The *ae* allele can therefore be explained as a tissue-specific null allele of the *tsh* gene. A complete null allele such as the *tsh* 8 deficiency would result in a loss of *tsh* function from all *tsh* domains of expression. In the *ae* mutant, however, the complete loss of *tsh* function is only within a non-essential domain of *tsh* function. Thus, the loss of *tsh* expression from only the hinge region of the wing, a non-essential domain, leaves the essential domains of *tsh* function intact. This model of *ae* function also anticipates that it has a regulatory role in *tsh* function rather than a direct affect on *tsh* protein structure.

Northern Analysis and *teashirt* Protein Detection

Northern analysis also supports the region specific null model for the *ae* mutation. Detection of *tsh* transcripts in both Oregon R and *aeroplane* reveals, as expected, that the null *ae* allele is not a complete null mutation of the *tsh* gene. Although the previously reported 8.0+ kb RNA species was not detected in either of the strains, the two protein encoding transcripts (5.4 and 5.0 kb species) were detected in both Oregon R and *ae*. The failure to detect any noticeable difference in *tsh* transcripts is not unexpected. The amount of transcript we suggest to be affected in the developing larvae is inconsequential in comparison to the total amount of *tsh* transcript that remains in the *ae* mutant.

Staining of third instar larvae with *tsh* antibodies also supports the idea that *ae* is a region specific null allele of the *tsh* gene. The amount of *tsh* protein is unaffected in all tissues of the *ae* mutant compared to the Oregon R control except for the ventral wing hinge where we see a reduction in the amount of *tsh* protein detected. As in the Northern

analysis, the loss of *tsh* protein expression from the ventral hinge is insignificant in comparison to the total amount of *tsh* protein detected throughout the larval body, fat and imaginal discs.

***tsh*[04319] Derivative Chromosomes**

The polarity of alterations with respect to the *ry* and *lacZ* markers in the *P* element mutagenesis data is consistent with the molecular data collected. Sixteen out of seventeen of the derivative lines tested had 5' *P* element sequences in a parental conformation, 8/17 (~47%) of the lines expressed *lacZ* in a pattern similar to the parental line, and (7/17) 41% have 3' *P* element sequences in a position that resembles the parental construct. At the level of Southern analysis, 7/17 (41%) of the derivative lines tested showed that the P{PZ} construct remained unaltered with respect to 5' and 3' *P* element sequences, internal construct sequences, and 3' and 5' flanking genomic sequences. This excludes the two lines that appear to be the result of events independent of the *tsh* enhancer trap line. From this analysis one can conclude that 16/17 (94%) of the lines tested have at least part of the P{PZ} construct remaining. Furthermore, the remaining P{PZ} construct sequences are in the same position in the derivatives as in the parental *tsh*{04319} construct. The line with no detectable P{PZ} sequences remaining is the result of a deletion of the construct sequence as well as some adjoining genomic sequence. This also causes a *tsh* null (*tsh*[04319]^{12.2}). There is a trend in the derivative chromosomes analyzed. The lines with the larger constructs remaining in the 5' UTL of *tsh* ranged in severity from "weak" to "moderate", whereas in the lines with a deleted construct the severity of the alleles ranged from "moderate" to "strong" with defects in wings and thoracic cuticle.

The results from the *P* element mutagenesis experiments also suggest that the *ae* mutation may represent an allele of the *tsh* gene. The frequency which *ae* alleles were generated from the enhancer trap *tsh*[04319] chromosome suggested that if *ae* is a different locus, the two loci are likely physically close to one another. This, in turn, suggested that the new *ae* alleles may arise via a proximal jump (Tower et al., 1993). However all the *ae* alleles generated by this method retained the lethality associated with the parental *P* element, even though the lethality associated with *tsh*[04319] can be

reverted with a frequency of about 23% (**Figure 5**). Additional evidence that the *tsh* insertion (lethality) and the generation of the new *ae* allele are inseparable comes from the screen that selected for *ae* insertions independent of the *tsh* insertion (**Figure 5D**). This screen, in agreement with the *ae* tagging experiment, failed to generate any *ae* alleles independent of the *tsh* insertion (lethality).

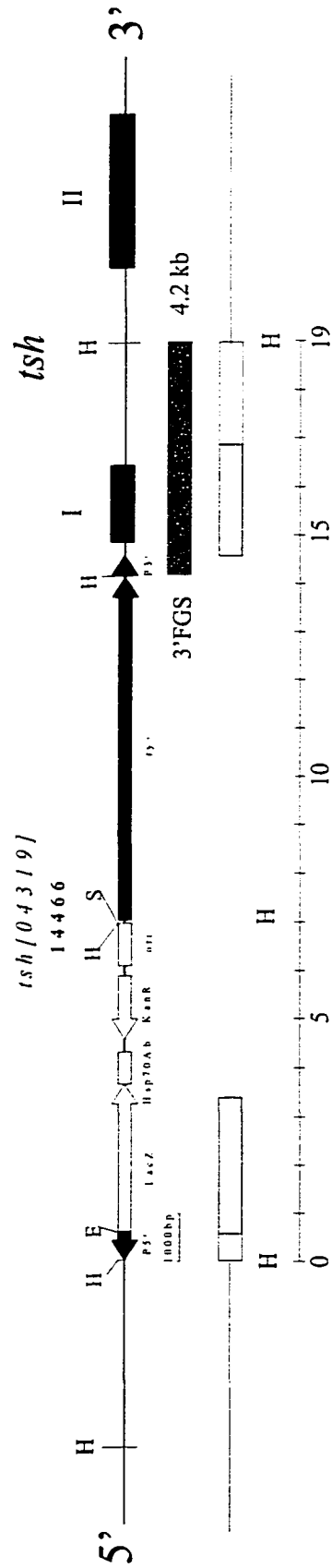
These experiments suggest that it is very difficult to generate a *P* element *ae* allele independent of the *tsh*[04319] insert. The reversion experiment, involving the two derivative lines *tsh*[04319]^{23.7} and *tsh*[04319]^{23.3}, also illustrates this point. These two derivative lines are both members of the group I category of derivatives and fail to complement *ae*, retain homozygous lethality for *tsh*, and at the resolution of a Southern analysis have an unaltered *P* element construct resembling the parental *tsh*[04319] line. However, excision of the *P* element in an attempt to separate the *ae* phenotype from the homozygous *tsh*[04319] lethality led to the simultaneous loss of both the *tsh* lethality and the *ae* phenotype. This suggests that both phenotypes in a *tsh*[04319] genetic background are dependent on the *P* element construct. Although both of these derivative lines from group Ia were considered weak alleles at the time of these reversion experiments, the expressivity of both lines was close to 50%. However, now *tsh*[04319]^{23.7} fails to exhibit any *ae* phenotype and the *tsh*[04319]^{23.2} allele is at approximately 20%. This is also reminiscent of the initial *ae b cn; ry* stock in which the expressivity would deteriorate after several generations, even within an isogenic stock.

The molecular and genetic data collected from the moderate and strong alleles of the group II derivative lines also indicate that the generation of the *ae* phenotype and *tsh* lethality are inseparable. Each of the derivative lines in group II a and b is associated with, or results from, from a 3' deleted P{PZ} construct, while the remaining construct sequences are still localized to the parental 5'UTL sequences and no other construct sequences are detected elsewhere in the genome. *HindIII* digests reveal that each of the 5' *P* element sequences of group II derivative lines are now linked to the 3' flanking genomic sequence (3'FGS), indicating that much of the construct sequence 3' to the 5' *P* element sequences have been deleted. The break occurs 5' to the internal *HindIII* restriction site within the construct (**Figure 6**). All of the group II derivative lines also fail to express the *lacZ* reporter gene, indicating that the break in the construct is

localized to within the first 3 kb of construct sequence, within the β -galactosidase gene. Each is also likely associated with a deletion in the 3' flanking genomic sequence that corresponds to the 5' UTL of *tsh*. The deletion leads to a *HindIII* fusion fragment, corresponding to the 3'FGS and the 5' end of the construct in the group II chromosomes. In derivative *tsh*[04319]^{7,9}, which contains the largest *HindIII* fusion fragment the total size of the fragment is now approximately 5.2 kb (**Figure 34**). The size of the 3'FGS from the parental chromosome is approximately 4.0 kb (approximately 4.2 kb if the 3' *P* element sequence are included). Without any duplication of flanking 3' genomic sequence in the 5.2 kb fused fragment, the most that could arise from the 3'FGS would be 4 kb. Therefore, the remaining 1.2 kb would consist of construct sequence. Approximately 600 bp (588 bp) corresponds to the 5' *P* element sequence (which is detected in Southern analysis) leaving approximately 600 bp to come from the β -galactosidase gene. However, it is also possible that as much as 3.0 kb of the *HindIII* fusion fragment could arise from construct sequences. Any more than 2.0 kb of sequence arising from the construct (1.6 kb of the β -galactosidase gene) would mean that the remaining 3.2 kb consists of the 3'FGS (**Figure 34**). Therefore, this would require a deletion of 800 bp of sequence from the 3'FGS (5' UTL of *tsh*). According to the published restriction map of the *tsh* gene (Fasano et al., 1991; McCormick et al., 1995), and the location of the P{PZ} insertion site (**Figure 6**), the approximately 4.0 kb *HindIII* fragment of genomic sequence would include the 5' UTL, the first exon and most of the intron. This 3'FGS contains approximately 800 bp of the *tsh* 5' UTL, therefore an 800 bp deletion of the 3' flanking genomic sequence would delete the translation start site. The other group IIa derivative chromosomes (*tsh*[04319]^{11,6}, *tsh*[04319]^{11,5}, *tsh*[04319]^{10,1}) have smaller *HindIII* fragments indicating a greater likelihood of a larger deletion of the β -galactosidase coding region and/or 3'FGS. This makes a deletion of the 5'UTL even more likely.

Although the Southern analyses performed were inconclusive in determining whether or not there is a deletion of the *tsh* transcribed region in group II chromosomes, a deletion is likely because of the following reasons. In the selection for chromosomes with *ae* phenotypes, approximately half of the derivative chromosomes tested are group II. These derivatives suggest that it is more than just the presence of the insert within the

Figure 34. A diagrammatic representation of the genomic organization of group IIa derivative chromosomes. The parental *tsh*[04319] chromosome is represented by a continuous line. The P{PZ} insert sequence is flanked by the 3' and 5' *P* element ends. I and II indicate the two *tsh* exons. The 3'FGS is (as defined by the *Hind*III fragment) represented by the blue box under the *tsh* coding region. The grey boxes represent the variable regions for the location of the break points of the respective derivative lines. The total of the two grey boxes must equal the respective size indicated at the far right of each derivative designations (eg 4.8 and 5.2 kb). The values in each of the brackets indicate the size range for the variable regions in order to account for the total size of each *Hind*III fusion fragment. 600 bp corresponds to the approximate size of the 5' *P* element sequence. The 4.8 kb and 5.2 kb values represent the total size of the respective *Hind*III fusion fragments. The open boxes below the *tsh*[04319] chromosome represent the derivative chromosome sequences detected by Southern analysis. The distance marker below the derivative chromosome is in kb. The abbreviations are as follows, H; *Hind*III, E; *Eco*RI, S; *Sal*I, 3'FGS; 3' flanking genomic sequence. The remaining abbreviations are as indicated in **Figure 6**.



11.6 and 11.5 600 bp + (200 - 3000 bp)

7.9 600 bp + (600 - 3000 bp)

+ (4000 - 1800 bp) = 4.8 kb

+ (4000 - 1600 bp) = 5.2 kb

5' UTL that is important for the generation of the *ae* phenotype, because the approximately 14 kb *tsh*[04319] P{PZ} construct located within the 5' UTL of *tsh* is able to complement the *ae* phenotype. If a simple insertion were responsible, then the 2-3 kb of sequence should not have any greater effect on the function of the *tsh* gene than the entire 14 kb. Because *ae* is a null allele and loss of function *tsh* alleles appear to be the only alleles that fail to complement the *ae* phenotype, this suggests that the *tsh*[04319] allele retains enough "function" to rescue the *ae* phenotype. Thus, the derivatives with only a 2-3 kb insert must lose this residual function. This suggests that the conversion of the *tsh*[04319] allele to a non-complementing *ae* chromosome requires more than just a simple deletion of the construct.

Complementation

The strong *tsh*[04319] allele is able to complement the *ae* phenotype, while the two *tsh* null alleles (the *Df(2L)TW161* and *tsh8* deficiencies), fail to complement the *ae* phenotype. This also suggests that *tsh*[04319] retains at least limited function. One can only speculate on how this *tsh*[04139] allele can provide enough function from the *tsh* gene in order to rescue the *ae* phenotype. One possibility is that the *tsh*[04139] allele is leaky and it provides only enough transcript to rescue the *ae* phenotype. If there was a lower threshold of activity required for rescuing the abnormal wing posture compared to the lethality, then a low level of *tsh* function or expression from the *tsh*[04319] allele could selectively rescue the *ae* phenotype and remain a homozygous embryonic lethal. If a weaker alternative promoter downstream of the P{PZ} insert site could be utilized to provide the low level of function required for normal wing posture, the loss of these sequences in group II derivative lines would also lead to a loss of the function required for normal wing posture. Interestingly, the identification of the two protein coding transcripts, the 5.4 and 5.0 kb RNA species (Fasano et al., 1991), (**Figure 6**) may represent the transcripts from the different promoters. The 5.0 kb RNA species therefore may be initiated from this hypothetical second alternative downstream promoter. If arising from an alternative promoter, the 400 bp difference would place the transcription initiation approximately 120 bp downstream of the insert site. This could be within the deletions of the group II derivative chromosomes.

A second less likely model to explain the complementation results would be if there was a read-through from the *P* element into the *tsh* coding region, resulting in a rescue of the loss of transcript due to the insert in the *ae* chromosome. All group I derivative alleles appear to contain an intact P{PZ} construct localized to the parental insert site, based on the *lac Z* reporter gene expression and Southern analysis. Perhaps some transcription directed from the *P* element of *tsh*[04319] is able to rescue *ae*, while a relatively minor change to this *P* element may eliminate this ability. However, due to the orientation of the construct, the open reading frame lying closest to the flanking *tsh* coding region is the transformation marker *rosy* (*ry*⁺). The direction of *ry*⁺ transcription is in the opposite orientation to *tsh* and therefore would be unable to transcribe the *tsh* gene. The *P* element promoter would also be a source for transcription initiation, but it is present at the 5' end of the construct distal to the *tsh* coding region. As a result of the data presented above, it is likely that the 3' flanking genomic sequence has also been deleted in the group II derivative lines.

The position of the derivative break points within the P{PZ} construct and in the *tsh* coding region also appears to be important. As indicated above in the group II derivatives, *Hind*III digests reveal that each of the 5' *P* element sequences is linked to the 3'FGS. This indicates that the breaks within the P{PZ} construct are localized to within the first 3 kb of the 5' end of the construct and the 3' breaks lie within the *tsh* gene in about the first 2 kb (**Figure 34**). If a simple null allele was important for generating the *ae* phenotype, then we might have expected to see at least some break points downstream of the sequences corresponding to the 3'FGS in addition to breaks within the *ry*⁺ coding region. Although it seems that the group IV derivative line is the result of a simple excision and deletion of flanking transcribed genomic sequences, one could expect to see many more of this class since this type of derivative doesn't appear to form a deleterious or weak stock in contrast to the group II lines. This would suggest that one has to seek another reason for these types of modifications to the P{PZ} construct, or that it's simply an artifact of the construct. It would be interesting to determine if any of the other *P* element constructs localized to this site in the *tsh* gene would behave the same way as the 14 kb P{PZ} construct in a screen for non-complementing chromosomes.

A third possibility is that the complementation between these two alleles is due to transvection (S. Kerridge, pers. comm.). Independent of a deletion in the derivative lines, if it was a simple transvection phenomenon the 14 kb P{PZ} insert in the *tsh*[04139] line would cause a greater disruption of somatic pairing and concomitant transactivation than the 2-3 kb derivative insert. One way to determine if transvection plays a role in complementation between the *ae cn b* chromosome and the *P* element *tsh*[04319] alleles was to determine whether we could disrupt somatic pairing by generating a rearrangement on the *tsh*[04319] chromosome and therefore presumably any transactivation via transvection. Out of approximately 5000 chromosomes from a cobalt 60 gamma radiation treatment, no *tsh*[04319] chromosomes failing to complement the *ae* phenotype were recovered. Similar experiments designed to disrupt transvection within the BX-C and the *dpp* loci revealed that rearrangements at both loci could be generated at a frequency of approximately 1% (De Jongh, 1975; Gelbart, 1992). If transvection fails to take part in complementation at the *tsh* locus, then these results are not unexpected. However, it is unexpected that the generation of a null allele of the *tsh* gene by a simple disruption of the coding region did not occur. These negative results were obtained even though lethals on the X chromosome were generated at a frequency of about 10%.

Similar to the P{PZ} derivative lines of *ae*, transposase mediated *P* element deletions of the upstream transposable element localized 5' to the coding region in *vg* reveals a phenotypic difference depending on the amount and type of *P* element sequence remaining behind. Like the derivative constructs herein, the more severe phenotypes are associated with a particular type of *P* element deletion. The stronger *vg* alleles were associated with an internal deletion of 3' *P* element sequences. The *P* element promoter and transcription start site remains in the deleted *P* element. The effect on *vg* function is believed to result from transcription initiation from the *P* element promoter (Staveley et al., 1995), which is an unlikely explanation for the *ae* derivative alleles.

A second example of the effect derivative *P* element sequences play on the function of a target gene can be seen from work on the RPII215 gene (Searles et al., 1986). The RPII215 gene encodes the largest subunit of RNA polymerase II in *Drosophila melanogaster*. Like the *ae* derivatives and the *tsh*[04319] parental enhancer trap, the *P* element associated with the RPII215 gene is inserted within the 5'

untranslated leader. Analysis of revertants of this gene revealed that the derivative *P* element sequences remaining determined the activity of the RPII215 gene. Similar to the results observed from the *ae* derivative lines, the ones with the larger remaining *P* element sequences in the RPII215 gene did not cause a greater reduction in RPII215 activity, as judged by genetic measurements (complementation index). These results suggested that the remaining *P* element sequences somehow affected the transcription initiation from the RPII215 gene. However, both of these lines of research deal with endogenous 2.9 kb *P* elements, unlike the greater than 14 kb of P{PZ} *P* element construct used in this thesis.

Genetic Interactions

Each of the abnormal wing posture mutants that are known to affect either musculature or neuronal defects failed to modify the *ae* phenotype (eg. *how* and *eag*). The failure to identify any interactions with the few wing posture mutants tested is not surprising, since most of these types of mutants are known to affect the muscle or neuronal structure or function; both of which are known to be unaffected in the *ae* mutant (**Figure 11 and 12**). Even mutants that exhibit cuticular alterations are often associated with the underlying primary etiology (eg *indented thorax* or *upheld*). The cuticular defects are often a secondary effect to the underlying muscle abnormalities. However, in the case of the *ae* mutant the defects in the hinge and pleural structures are not associated with any IFM or DFM defects or any of the neurons that innervate them.

Initially, a number of the “wings held out” mutants available through the Bloomington stock center and private collections were used in a screen to identify any possible dominant enhancers of the *ae* phenotype. Because *ae* is a null allele, it was possible that mutations in other genes in the same pathway would lead to a further reduction in the functioning of the pathway and be identified by an F1 screen. However, because of the initial variability of the *ae* phenotype these other wing posture mutants were not used in a screen to identify possible phenotypic suppressors. All double heterozygotes examined complemented the *ae* phenotype. A few of the wing posture mutants were combined with *ae* as double homozygotes and each combination gave a wings held out phenotype. However, since each of the wing posture mutants have a

similar phenotype it made it difficult to identify which, if any, of the phenotypes resembled a particular mutant in the cross.

There are problems with identifying apparent interactions with the *ae* mutant. As previously indicated, the original *ae* stock was not completely penetrant. Although the present stock used for most of the experiments within this thesis appears to be completely penetrant when crossed out to other chromosomes, the phenotype often exhibits the variability of the original stock. This suggests that the current stock may have picked up modifiers (enhancers) of the *ae* phenotype. Several alleles representing genes of putative transcription factors identified through the MatInspector database search were crossed into the *ae* background. The most convincing data for genetic interactions between *ae* and the homeotic alleles tested are the results from the *Scr[2]* and *Dfd[r]* alleles. The *Scr[2]* cross has an internal control for judging the phenotypic interaction. All of the *b cn ae; Scr[2]/TM3* females exhibit a suppression of the *ae* phenotype, while males of the same genotype exhibit the *ae* phenotype. The reduction in the number of *b cn ae; Dfd[r]/TM3* flies from the number expected suggests a possible genetic interaction. Also, the two regularly homozygous viable stocks (*ae* and *Dfd[r]*) could not be maintained as a doubly homozygous stock.

The cuticle defects associated with the abdomen of *ae; C(1)DX* flies were not completely penetrant. Females from these crosses of genotype *b cn ae/+; C(1)DX*, ranged in phenotype from the more extreme to wild type (as presented in **Figure 28**). Because this apparent interaction with the alleles found on the compound chromosome could not be repeated by using the individual mutants alleles on the attached X chromosome, the interaction may involve mutations induced on the chromosome independent of the C(1)DX chromosome. This apparent interaction was not pursued any further because of the failure to affect the thoracic cuticle.

Both the *30A-GAL4* and *b cn ae* chromosomes are homozygous viable. The *30A-GAL4; b cn ae* double homozygote exhibits a strong wing phenotype similar to the *tsh[04319]^{8.1}* phenotype. The wings are folded or crimped longitudinally and often are pinched at the distal regions of the wing margin. This aspect of the phenotype is infrequently seen for *ae* flies (<1%). However, in the *ae / tsh[04319]^{8.1}* transheterozygotes the penetrance is considerably higher with almost 95% of the flies

exhibiting this apparent interaction. The cause of this apparent phenotypic interaction in the wings is not likely due to ectopic expression of *tsh* in the wing pouch, because as described above the expression of *tsh* in the wing pouch leads to loss of wing tissue rather than abnormal folding of the wing. As discussed above, the defects in the wings of the *ae/tsh*[04319]^{8.1} transheterozygotes is more likely due to a complete loss of a domain of function from the *tsh* gene.

An analogy to the *nubbin* (*nub*) gene can be drawn to explain how a gene that is expressed and presumably plays a role in the development of the hinge can also affect more distal wing tissues. The *nub* gene appears to be involved in the establishment of a third organizing center required for the formation of the proximal-distal axis in the developing wing. Since its product has been implicated in the establishment of an organizing center for patterning and growth of the adult wing (Ng et al., 1995). This organizing center is thought to be localized within the wing hinge and is reminiscent of the D/V axis-organizing center with *nub* presumably acting as a mediator of the wing hinge organizer, analogous to *vg* and *sd* in the wing pouch. Clones lacking *nub* function in the wing hinge lead to defects in the distal tissues of the wing blade. These results imply that *tsh* may also have a role in the proper development of the distal regions in the wing blade. In the wing hinge *tsh* may play a similar role to that of *nub*.

A second possibility is that the wing defects are simply due to the wings dragging in the food and then sticking together. However, this also indicates a difference between the transheterozygotes (*ae/tsh*[04319]^{8.1}) and double mutants (*b cn ae 30A-GAL4*) compared to the *b cn ae* flies. There must be a difference in the wing hinge between these three groups to explain the difference in the wing posture to explain why the wings of the *ae* flies are less likely to be affected. Therefore, the transheterozygotes and the double mutants appear to exhibit a different, more severe (drooping) wing posture than the *ae* mutant alone (a more depressed wing posture).

The “Strong” *aeroplane* Phenotype.

The strong derivative *ae* alleles generated are likely complete loss of function mutations of the *tsh* gene, because they resemble the interaction observed between *ae* and the *Df*(2L) *tsh8* chromosome, which is a deletion of the *tsh* coding region and therefore a

true transcriptional null. Based on its phenotypic similarity to deletions of the *tsh* gene, presumably *tsh*[04319]^{8.1} represents a complete loss of function mutation. The thoracic defects associated with the *aeltsh8* or *aeltsh*(04319)^{8.1} transheterozygotes suggests *tsh* may play a role in cuticular pattern formation in the adult. The *ae* null mutation permits the removal of a sub-domain of *tsh* function during development, allowing for the observation of the role(s) of *tsh* within the adult. The *ae* allele in combination with either of the complete loss of function alleles leads to alterations of the pleural thoracic plates, sutures and wing hinge (**Figure 15**). In the transheterozygote it appears that the pre-alar apophysis (asterisk in panel C and D) is pushed anteriorly towards the vertical cleft (vc). It appears that the cuticle on the posterior side of the vc is forced into the vc or under the mp based on the reduced distance between the vc' and the ap' of the double heterozygote (double headed arrows in **Figure 15E** and **F**). This causes a buckling of the cuticle at the base of the wing (**Figure 15F** asterisk). There is also buckling of the cuticle in the suture between the notopleurite (np) and the mp, presumably this also causes the mp to be forced outwards in the region where the plate abuts the np (arrowhead **Figure 15F**). This loss of *tsh* function from the thorax reveals an, albeit slight, alteration to the pattern of the pleural plates and sutures within the region of the wing base indicating that it plays a role in patterning of these cuticle structures in the developing adult. In support of these findings, the *tsh* gene was also identified in a *tsh*-GAL4, *UAS*-y screen designed to look for genes involved in pattern formation in the adult cuticle (Calleja et al., 1996). The screen indirectly showed that *tsh* is expressed throughout the adult cuticle except within the distal appendages. Of particular relevance to this thesis, *tsh* is expressed within the pleural plates of the thorax (arrows **Figure 15A** versus **B**), the proximal wing hinge and base of the halteres (arrowheads **Figure 15A** versus **B**).

One possible reason for a more severe phenotype in the transheterozygotes compared to the *ae* mutant would be a requirement for transvection in the proper regulation of *tsh* expression. The domain of expression lost from the *ae* null allele is significantly smaller than the true *tsh* deficiency null alleles, *Df*(2L) *tsh8* and *tsh*(04319)^{8.1}. For simplicity, one can presume that *ae* has lost only the single cis-acting regulatory sequence. The deficiencies, however, have lost not only the *ae* enhancer sequence but also most other downstream regulatory sequences. If the phenotype were

simply a matter of losing a number of functional domains from each of the alleles, then the phenotype would result from common lost functional domains. Thus, the transheterozygote would only have the wing hinge *ae* phenotype as a result of the loss of the common *ae* functional domain from both alleles. However, this does not explain the thoracic defects associated with transheterozygote phenotype. A requirement of transactivation for proper regulation and expression of the *tsh* gene within the locus could explain the additional defects. Two copies of the *ae* allele are presumably identical in terms of their physical genomic organization with the loss of only the *ae* functional domain. The regulatory sequences for the remaining domains of expression would presumably be intact, and possibly require trans-activation via transvection for proper regulation. Within the *ae* mutant these transactivating sequences would be intact on each *ae* chromosome and as a result could provide the proper regulation for these functional domains of expression. The *ae* chromosome in combination with the deficiencies, however, would not be able to provide this domain of expression due to the loss of these sequences from the deficiency chromosomes. In particular, the other functional domains of expression in the transheterozygotes could correspond to the abnormalities associated with the pleural structures on the thorax at the base of the wing.

Enhancer Tested Fragments.

To determine if the I element insertion could be responsible for the disruption of any cis-acting *tsh* regulatory sequences which in turn result in the loss of *tsh* expression within the ventral wing hinge, the wild type E4.8 sequence was tested using the enhancer tester construct pCaSpeR hs 43 transformation vector. It is this E4.8 fragment in the 3' region of *tsh* that contains the insert in the *ae* genome. The results from the enhancer tester experiments indicate the existence of a 3' wing hinge and proximal haltere specific enhancer. Further subdivision of the 4.8 kb sequence revealed a 915 bp ventral hinge specific component (HB1.0). With reference to the fate map of the third instar imaginal wing discs, the results herein indicate that the expression of the reporter gene driven by the HB1.0 (915 bp) fragment is localized to the region fated to give rise to the pleural wing process, proximal ventral radius, and the yellow club structures. These are the structures that show abnormalities in the *ae* mutant. Identification of the cis-acting

regulatory sequences within the first 8 kb of 3' flanking genomic sequence supports the hypothesis originally proposed by Soanes and Bell, (1999). The identification of the 3' regulatory sequence (*ae* enhancer) downstream of the *tsh* coding region is not the first example of such a regulatory sequence downstream of the *tsh* coding region. Two such 3' regulatory elements have already been identified within the *tsh* gene (McCormick et al., 1995; Core et al., 1997). The 2 kb *Antp/Ubx* HOMRE is located about 13 kb downstream of the 5.5 kb *ae* insert. In addition, the *fushi tarazu* (*ftz*) protein binds to a 220 bp region 3' to the coding region, also downstream of the *ae* insert. *In vivo* evidence suggests that this region is capable of driving *tsh* expression in the even parasegments of the embryo (Core et al., 1997). The regulatory sequence proposed herein would be independent of the HOMRE and *ftz* enhancer because the deficiency *Df(2L)R6* removes both the HOMRE and *ftz* enhancer sequences (**Figure 10**) but is still capable of complementing the *ae* phenotype.

In addition, the HB1.0 fragment also exhibits larval brain (optic lobe) and midgut specific expression. Activation of reporter gene expression begins prior to the mid second instar larval stage at approximately the same time that *wg* is establishing the boundary that separates wing from notum tissue (Garcia-Bellido et al., 1976). To narrow the region within the HB1.0 sequence required for ventral hinge specific expression, the region was further subdivided. From the MatInspector results (**Table 8**), a number of putative transcription factor binding sites were identified within the 481 bp AT rich region, indicating that it may represent a candidate sequence for the enhancer element. The identification of putative transcription factor binding sites is not unexpected because of the overrepresentation of AT rich motifs in the region. The importance of the AT rich motifs in DNA binding sites has been well documented (Ekker et al., 1991; Florence et al., 1991; Beachy et al., 1988; Muller et al., 1989; Hoey and Levine, 1988; Desplan et al., 1985; Pick et al., 1990; Driever and Nusslein-Volhard, 1989). However, whether these binding sites are biologically significant has yet to be determined. *Dfd* is a good example of a DNA binding factor that can bind to a number of putative sites *in vivo*, but is unable to regulate gene expression from the majority of these sites (Li et al., 1999).

Larval Midgut Expression.

The 481 bp putative regulatory element was subcloned into the enhancer tester construct and was found to activate reporter gene expression only within the midgut and not within the ventral hinge, suggesting the region contains a gut-specific element and not the hinge enhancer. The 481 bp and a nested 209 bp fragment are both capable of only gut-specific expression within the third instar larval mid gut. Both of the 481 bp and 209 bp fragments overlap the H1.0 fragment by approximately 44 bp. The lack of any gut specific expression from the H1.0 fragment indicates that the minimal gut specific enhancer element can be localized to within a separate 165 bp genomic fragment within the 915 bp of the HB1.0 fragment (**Figure 20**).

The gut-specific expression observed from the independent inserts of the 481 bp, 209 bp, HB1.0, HB0.9 or the *DraI*- constructs indicate that the extensive gut-specific expression observed in the third instar midgut is not due to position effects within the genome but due to the constructs injected. Each of these constructs exhibit extensive staining throughout the midgut except for small patches of the gut tissue. A comparison between all the constructs listed above indicate that a common domain of expression within the gut is located approximately 50% of the way down the midgut. This suggests that all of the sequences tested contain the element that is capable of this expression pattern (posterior to the arrow in each panel, **Figure 23**). The more anterior cytoplasmic and nuclear expression associated with the HB1.0 (HB0.9 and *DraI*), 481 bp and 209 bp fragments, but not the larger E4.8 construct which exhibits only nuclear expression in the same anterior domains, suggests the presence of negative regulatory elements in the E4.8 sequence (assuming it isn't an artifact). The negative regulatory elements or silencers of the anterior expression would be located in the sequence not included in the HB1.0, 481 and 209 constructs.

The minimal heat shock promoter in the pCaSpeR hs 43-vector acts as an enhancer detector being activated when inserted into the genome near a functioning enhancer element. The hs 43 promoter consists only of a TATA box with no upstream sequences past base pair -43. Furthermore, all untranslated leader sequences from the heat shock gene have been deleted downstream of the promoter. This suggests that the expression pattern observed within the gut is likely not due to an endogenous regulatory

function of the construct but the result of the genomic fragment being tested. Generating a transgenic line with the pCaSpeRhs43 vector alone would answer the question, however, it is likely that the H1.0 transgenic line can act as a negative control for gut specific expression. The H1.0 line only exhibits a spreading of the expression within the domain of non-specific *lacZ* staining at 20 and 80% of midgut length (**Figure 23 D**). This indicates that the expression observed from all of the other lines is a result of the genomic sequence being tested rather than the construct. The lack of the central midgut specific expression from H1.0 indicates that there is no endogenous midgut specific regulatory function present in the pCaSpeR hs 43 capable of the central expression. The EB1.9 construct was lost so confirmation of the gut expression can't be verified. There are no obvious gut defects associated with the *ae* phenotype. Despite the slight reduction in the rate of development, it is unlikely that there are any gut defects because *ae* is a homozygous viable null mutant and any defects corresponding to the extensive expression pattern would likely be deleterious.

Eye Imaginal Disc Expression.

It has already been shown that *tsh* can function as a selector gene for eye development (Pan and Rubin, 1998). Ectopic expression of *tsh* is capable of inducing eye specific gene expression in tissues that regularly don't express the eye fate. *tsh* is expressed in the presumptive eye and antennal segments and has also been shown to be required for proper formation of the head structures including the eye (Bhojwani et al., 1995 and 1997). The analysis of the enhancer trap allele and the enhancer tester results herein suggest that a possible eye and antennal regulatory element is located within the 4.8 kb of sequence in the E4.8 transgenic line. Each of the lines; E4.8, HB1.0, H1.0 and 481 bp are all capable of activating reporter gene expression within the eye imaginal disc in a similar pattern to the enhancer trap allele. Although these lines all drive the reporter gene in the eye discs, the domains of expression do not appear to coincide with the presumptive ommatidia. The β -galactosidase expressing cells do not have the punctate appearance of the cells of presumptive eye tissue. The staining is localized to the larger cells on the surface of the peripodial membrane. This pattern of expression was not observed in *yw* or other P{PZ} enhancer trap lines tested, other than

the *tsh*[04319] line. This suggests that the staining is not an artifact specific to the eye discs either in the presence or absence of a *lacZ* transgene.

If a single regulatory module was responsible for the eye-specific expression, the ability of both the HB1.0 and H1.0 constructs to drive reporter gene expression in these tissues suggests that the expression may be an artifact of the pCaSpeR hs 43 construct. However, the location of each of these fragments with respect to one another makes it possible that they each possess a regulatory function required for peripodial membrane, eye specific expression. The 481 bp construct overlaps both of these tested fragments (H1.0 and HB1.0) and also expresses the reporter gene in an eye specific pattern. This could imply that the eye element is localized to this 481 bp fragment and could also be in the overlapping position of the H1.0 and HB1.0 fragments. As discussed above, part of this sequence also possesses the gut-specific regulatory function. A similar divisible or overlapping regulatory function has been seen within the autoregulatory element upstream of the *Dfd* coding region (Zeng et al., 1994). More than one of these separable modules has been implicated in mandibular and/or maxillary expression. If the staining is not an artifact, the data could indicate the presence of two regulatory modules capable of eye specific expression.

Antennal Disc Expression.

The antennal-specific expression within presumptive third antennal segments in the H1.0 constructs and *tsh*[04319] enhancer trap indicate that the antennal-specific element may be localized within the H1.0 fragment excluding the 45 bp of sequence that is common to both H1.0 and 481 bp. This pattern of *lacZ* expression has been observed in several of the P{PZ} enhancer trap lines other than the *tsh*[04319] insert, suggesting that it represents an artifact of the *lac Z* transgene. However, the possibility that a regulatory element located within the H1.0 fragment for the antennal specific expression has not been ruled out.

Reporter Gene Expression

pCaSpeRhs43 E4.8, EB2.9 and HB1.0 all exhibit strong activation of the *lac Z* reporter gene, at a level higher than the *tsh*[04319] enhancer trap. Comparing imaginal

disc staining of the presumptive hinge in each of the constructs to that driven by the reporter gene *tsh*[04319] suggests that each of the constructs contains strong activators of expression. In order to achieve the same or similar intensity of staining from each of the enhancer lines for the ventral specific enhancer expression, only 1-2 hours of incubation is required. However, for relatively the same intensity of staining from the *tsh*[04319] enhancer trap approximately 8-12hrs are required. The global expression of the enhancer trap line in third instar larvae (**Figure 7**) would be a good explanation for the different level of expression observed from the enhancer trap compared to the pCaSpeR lines in the wing and haltere imaginal discs. However, using the eye-antennal disc as an internal staining control reveals that this is not likely the entire explanation. A similar level or intensity of staining in the eye discs (compare **Figure 24 A, B and C**) of each of the lines is associated with a much stronger staining of the presumptive hinge in the derivative pCaSpeR lines than the *tsh*[04319] enhancer trap. This suggests that the regulatory elements driving expression in the presumptive hinge or the derivative lines may lack negative regulatory sequences required to down regulate the hinge expression to levels consistent with the enhancer trap line.

In discs from flies with the enhancer trap allele, as well as observations from *tsh* antibody staining, a slight but reproducible repression of *tsh* expression within the dorsal hinge at a region corresponding to the A/P boundary is observed (**Figure 21** arrowhead). However, in all the pCaSpeR transgenic lines this repression is lost and as a result there is a continuous band of expression in the dorsal hinge within this region (**Figure 21** arrowhead). Although this is a very subtle difference between the lines, it does represent a regulatory difference and indicates that there is likely a negative regulatory element missing from each of the pCaSpeR lines.

I element

The absence of any hinge specific expression from the ATTA rich fragment that appears to possess eye-antennal specific elements suggests that the hinge specific element is localized to within the remaining 478 bp of sequence of the 915 bp *HindIII/BamHI* fragment. This sequence is also known to contain the 5.4 kb I element insertion within a 34 bp *DraI* sequence (**Figure 19**). To test if the insert site sequences were responsible

for the ventral hinge specific expression, the 34 bp *DraI* sequence was removed from the HB1.0 fragment and the remainder was reintroduced into the enhancer tester. However deleting the 34 bp *DraI* fragment, and presumably the sequence containing the insert site within the *ae* mutation, failed to eliminate the ability of HB1.0 to drive reporter gene expression within the ventral hinge. These results suggest the ventral specific hinge enhancer element lies within the remaining 444 bp of sequence (**Figure 20**). Maintaining hinge-specific expression with the loss of the 34 bp *DraI* fragment and the insert site suggests that the insert is not directly disrupting any sequences that are causing the loss of expression of the *tsh* gene within the ventral hinge. Rather, it is likely the insertion is negatively regulating the cis-acting elements within the 444 bp sequence that is capable of driving reporter gene expression within the relevant tissues. The absence of any gut-specific defects associated with the *ae* mutant indicate that the I element insertion is not capable of negatively regulating the sequences responsible for driving the reporter gene expression in the midgut, which lies as close as 600 bp from the insert site. The insertion effect is not likely simply due to the displacement of the hinge-specific enhancer by 5.4 kb from its target. This is because the testing of each of the genomic fragments involved cloning the elements upstream of the *lacZ* reporter gene, which displaced the fragments a much greater distance from their 3' endogenous location than the 5.4 kb insert does.

Although this LINE-like retro-transposon is not directly disrupting any regulatory sequences required for wing and haltere specific expression, the actual mechanism by which this insert is able to perturb the wing hinge-specific enhancer remains unknown. However, there are several possible explanations for its effects on the regulatory elements within the region. One possibility is that the insertion separates two cooperative regulatory modules which are both required for proper regulation of *tsh* expression within the ventral hinge. The 5.4 kb insertion would, therefore, separate the two modules so they would fail to form the appropriate associations with one another for the proper activation of expression in the relevant tissues.

Another possible mechanism by which the I element can induce a negative regulatory affect on the *ae* enhancer is by the phenomenon first identified in plants referred to as co-suppression (Matzke and Matzke 1995). This phenomenon is seen in transgenic plant lines whereby an increase in the copy number of a particular transgene

leads to the silencing of all the transgenes, and the endogenous copy if it exists. A similar phenomenon has been observed in *Drosophila* whereby an increase in the copy number of a *white* promoter *Adh* fusion gene construct led to a reduction in expression from the construct and the endogenous *Adh* gene, rather than the increase in gene expression expected due to an increase in gene dosage (Pal-Bhadra et al., 1997). All copies of the *Adh* gene including both transgenes and the endogenous genes are affected by the co-suppression. The silencing of the genes appears to be a function of the alteration in chromatin structure similar to the effect observed for the silencing of the HOM-C genes along the anteroposterior axis of the developing embryo (Pirrotta, 1997). Mutations in the *Polycomb*-group genes (Pc-G) suppress the co-suppression phenomena seen. There is also direct evidence for the requirement of the Pc-G genes in co-suppression. The transgenic insertion sites at which the co-suppression occurs in the genome are also associated with the Pc-G proteins. The Pc-G proteins are proposed to regulate the homeotic genes and presumably the genes involved with co-suppression by altering the chromatin conformation such that the activator sites of the regulatory elements are inaccessible to transacting factors. It has been suggested that this mechanism in animals may have evolved to reduce viral gene products or maintain transposable elements in a repressed state (Ratcliff et al., 1997) so as to avoid the mutagenic effects.

Similarly, this phenomenon has been used to explain the regulation of I element transposition. The I element acts as a retrotransposon, transposing to new locations via a RNA intermediate which also acts as a bicistronic message encoding a putative nucleic acid binding protein and a reverse transcriptase essential for its transposition (Bouhidel et al., 1994). Regulation of the tissue-specific I element transposition and its repression within the Inducer strain (I) has been ascribed to the first 186 bp of the 5' untranslated region (5'UTR)(McLean et al., 1993). A sequence-specific DNA binding protein is known to bind within this first 186 bp and also may be involved in the two forms of I element regulation. There is a negative correlation between the level of transcription of the full length 5.4 kb RNA and the number of 5' untranslated leader sequences present in the genome. The fewer the number of I elements in the germline of a female the higher the level of transcription and transposition. An increase in copy number, in particular the

5' UTR, leads to a decrease in transcription of the I element and results in a reduction in the rate of transposition (Chaboissier et al., 1998). Once the copy number reaches what appears to be the limit of approximately 15 functioning I elements per haploid genome, transposition stops and the strain becomes an I strain.

Therefore the cause of the *ae* phenotype may be the result of two separate events. The first event would be the insertion of the I element into its current position into the 3' genomic sequences of the *tsh* locus. The second event would be the increase in the number of active or functional I elements within the stock to a point where the stock is no longer an R strain. This would require the presence of approximately 10-15 active copies per haploid genome. The repressive conformational change around the I element promoters would lead to a repression of I element transcription and transposition. This conformational alteration to the chromatin structure would then spread to flanking genomic sequence and in this case the *ae* enhancer. The location of the I element with respect to the *ae* enhancer element would require the conformational change over a short distance of no more than 350 bp. This distance would cover the remaining 481 bp of the minimal ventral hinge element. This would also explain why the *DraI*- deletion construct of the insert site failed to disrupt any of the hinge specific regulation of the *ae* enhancer.

The variable phenotype of the original *ae* stock could also be explained with this model. If the induction of the *ae* mutation was caused by the insertion of the I element, this suggests that the *b cn* parental stock was originally an R strain. Once the I element transposed into the *ae* enhancer region the variation in the number of functional I elements per fly would therefore lead to differences in R strain strength. Any I strain flies with a single I element would not exhibit the *ae* phenotype, whereas flies with a larger number of I elements approaching the 15 copies would be less active transcriptionally and transpositionally, presumably due to co-suppression-like phenomena. Selection for the *ae* phenotype would then select for I strain flies, repressed transposition, and presumably an altered conformation to the *ae* enhancer sequence surrounding the I element. This suggests the loss of *tsh* protein expression in the presumptive ventral hinge associated with the *ae* mutation could have resulted from an epigenetic conformational change within the region. This would also explain why from an isogenic stock one often observes the apparent spontaneous loss of the *ae* phenotype

after several generations of the full *ae* phenotype. A spontaneous mutation in genes required for the repression of the I element transcription within the *ae* I element insert or within I element promoter sequences required for repression would also lead to a loss of negative regulation.

Another possible model to explain this copy number effect localized to the 5'UTR of the I elements could be similar to that of the repeat-induced gene silencing of the white transgenes (Dorer and Henikoff, 1997; Martin-Moris et al., 1997). This phenomenon resembles position effect variegation (PEV). A tandem array of these transgenes acts to nucleate the condensation of the chromatin, resembling heterochromatinization. Single copy transgenes may be affected in a similar way. The homologue "dragging" of a reporter construct into a heterochromatic compartment within the nucleus could explain this effect. This transcriptionally repressive chromatin structure can spread to other flanking genes and is affected by suppressors of variegation (*Su(var)*) mutations. A binding protein recognizing the 5'UTR may act as a limiting activator for I element transcription (and therefore transposition). An increase in the copy number of the 5'UTR would titrate out this factor to a level which would fail to activate expression. The DNA binding factor that is known to bind the 5' UTR is not likely responsible for this function because disruption of its binding has little effect on the copy number phenomenon.

Etiology.

The apparent wing paralysis and drooping halteres of *ae* flies results from a subtle structural defect at the base of the haltere and in the hinge region of the wing. A fusion between the proximal ventral radius (PVR) of the wing hinge and the pleural wing process (PWP) of the thorax, as well as the loss of the yellow club (YC), is observed in the *ae* mutants, compared to wild type controls. In the halteres a similar cuticular fusion to the thorax is found on the ventral side, just below the ventral pedicellar sensilla (VPS).

Histochemical and antibody staining of third instar imaginal discs reveals that *tsh* is expressed throughout the wing disc except in the presumptive wing blade and dorsal hinge (Ng et al., 1996). *tsh* expression within the presumptive hinge, as observed by X-gal staining of pupal wings from the enhancer trap line *tsh*[04319] and antibody staining of third instar imaginal wing discs, reveals that *tsh* expression around the pouch extends

from the wing surface side of the disc around to the peripodial membrane side (**Figure 18A and B**). From optical sections through wing discs stained with *tsh* antibodies, a loss of *tsh* expression in the *ae* mutant is observed from the ventral hinge, but only in tissues found closest to the wing pouch. *tsh* localized to the peripodial membrane side of the disc in the region of the ventral hinge remains unaffected (**Figure 18A versus C**). In the *ae* mutant, the loss of *tsh* expression is localized to tissues derived from the region of the disc fated to become the PWP, PVR, YC and pleural plates of the ventral thorax and these structures are aberrant in the mutant.

A Role For *teashirt* in the Adult.

The spatially restricted loss of *tsh* expression within the *ae* mutant allows one to suggest a role for *tsh* in the developing adult. Firstly, the function of the *ae* regulatory domain of *tsh* appears to be limited to the adult cuticle because all underlying structures are unaffected, including the fine flight control direct flight muscles, the flight power-generating indirect flight muscles and the neurons that innervate the direct and indirect flight muscles. *tsh* has been shown to be required to set up the basal developmental fate for the trunk within the developing embryo (Roder et al.,1992). It is also possible that it is required to set up the basal developmental fate for the adult cuticle pertaining to the proximal structures of the appendages. As a result, removal of *tsh* function from this region would lead to the loss of proximal structure specification in the adult.

A second possibility could be that *tsh* plays a similar role in specifying the divisions between the pleural structures of the thorax and the proximal wing hinge. A functional parallel can be drawn between the role that *tsh* plays in the proximal wing hinge and the role *homothorax* (*hth*) is believed to play in development of the leg. Both *hth* and *tsh* are expressed within the proximal tissues in the wing, halteres and leg discs. *hth* function appears to be required for specifying the transition between the proximal leg segments and the notum. The loss of *hth* expression in the proximal tissues within the leg discs results in a fusion between the coxa and the notum. Presumably, this is due to the loss of a signal provided by *hth*, and as a result the division between the notum and the leg is no longer defined (Wu and Cohen, 1999). A similar explanation can be used to explain the fusion between the wing hinge and the thoracic structures in the *ae* mutant as

well as the homologous halteres. If *tsh* is required for defining the transition between thoracic tissue and wing hinge, then loss of this expression leaves no signal to define the transition, leading to the fusion of the wing and thoracic cuticle. However, X-gal staining of the pupae shows that the limits of *tsh* expression don't lie precisely at the boundary between the hinge and thorax. This suggests that there may be an additional factor involved in defining the break between the two structures, in a similar way that *tsh* cooperates with *Ubx*, *AbdA* and *Antp* in specifying the trunk fate in the embryo.

UAS-*tsh*; 30A-GAL4.

The results from the analysis of the *aeroplane* mutant and the UAS/GAL4 system provide a method for the identification of a role for *tsh* function in the development or specification of the proximal tissues of the developing appendages. By expressing *tsh* in different domains within the wing, we observe different effects in the adult. Mis-expression of *tsh* under the control of the 30A-GAL4 driver leads to a dramatic reduction in viability, presumably due to the ectopic expression of *tsh* within the central nervous system as a result of the 30A-GAL4 driver. Interestingly, the cuticular outgrowths observed from the hinge of UAS-*tsh*; 30A-GAL4 flies were much more dramatic in the dorsal than the ventral hinge, where the *ae* defects are observed. These dorsal defects are likely due to the ectopic expression of *tsh* in the dorsal hinge in a more distal domain than the endogenous *tsh* expression. Comparisons between the 30A-GAL4 line and the endogenous expression of *tsh* in the hinge reveal a difference in expression pattern between the two. Based on the reporter gene and the pCaSpeR hs 43 transgenic lines, the *tsh* gene is not normally expressed equally in the dorsal and ventral hinge of the wing or in the proximal haltere, as it is with the 30A-GAL4 driver (Brandt and Perrimon, 1993). A comparison between the *tsh* expression pattern from the *tsh*[04319] enhancer trap to the fate map presented by Bryant (1976), indicates that *tsh* is not expressed in the distal regions of the dorsal wing hinge or homologous structures in the halteres. Using that fate map, *tsh* is not expressed in the presumptive dorsal hinge tissues, UP, HP or the AS2. The most distal expression of *tsh* in presumptive dorsal tissues is in the mesonotum which is the dorsal thorax. The 30A-GAL4 line, however, drives GAL4 activator in the dorsal hinge within the UP, HP and AS2 presumptive tissues. The defects in the dorsal

hinge arise from hinge tissues as proximal as the tegula and as distal as the medial costa, with no observable cuticular defects visible in the mesonotum or pleura. See **Figure 1** for a list of the abbreviations and the corresponding locations of each of the tissues discussed.

The ventral defects are likely due to the overexpression of *tsh* in spatial domains similar to the endogenous pattern. The defects in the ventral hinge appear at the second knuckle of the PVR and more distally, which is at the same proximal-distal location as the defects associated with the dorsal hinge. The defects are more subtle and do not resemble those of the dorsal hinge. The ventral defects correspond to the location of the distal most *lacZ* reporter gene expression detected in pharate adults of the enhancer trap *tsh*[04319] (**Figure 17G**). Since *tsh* is regularly expressed in this domain, the defects may reflect the overexpression of *tsh* at the most distal edge of its normal domain. It could also represent a subtle difference between *tsh* and *30A-GAL4* in their proximal-distal domains of expression.

Based on the expression pattern in adult cuticle and wing discs, the loss of the dorsal specific enhancer element would likely lead to mesonotum defects, such as those defects identified in the strong *tsh*[04319]^{8.1} / *ae* transheterozygote. The expression of UAS-*tsh* under the control of the *30A-GAL4* driver (Brand and Perrimon, 1993) emphasizes the different domains of expression patterns of *tsh* and *30A-GAL4* in the presumptive proximal wing tissues. The outgrowths observed on the dorsal wing hinge exhibit characteristics of thoracic tissue. The color of the cuticular outgrowths (at least the anterior outgrowth), the presence of ectopic microchaetae of similar size to those on the mesonotum of the anterior wing hinge, and the pattern of the hairs resembling those identified on the pleural plates all suggest that these outgrowths likely represent thoracic tissues. The ectopic expression of *tsh* in this domain, leading to an apparent conversion of the dorsal wing hinge to thoracic fate, indicates that in the region of the dorsal hinge *tsh* appears to be able to specify thoracic fate. This apparent expansion of the mesonotum is at the expense of the dorsal wing hinge.

These results imply that *tsh* may be involved with the specification of the thoracic cuticle in the adult. The apparent differences in the requirement for *tsh* expression between the two surfaces of the hinge could be the result of different dorsal and ventral

specific gene expression of cofactors, which may affect the specificity of *tsh* action. Otherwise, you would expect notum or thoracic specific expression in the ventral hinge in the domain of *tsh* expression. The dorsal and ventral specific expression of gene products apparently leads to the establishment of a differential response to the affects of *tsh* expression. *extradenticle (exd)* is an example of a cofactor which is required for proper functional specificity of the HOM-C genes in regulating homeotic function. Although *exd* is required to enable the activation of *Dfd* function for proper regulation of target genes and cooperatively binds with *Ubx* and *Antp*, *exd* fails to interact with the *ae* mutant and has not been shown to function cooperatively or interact with the *tsh* protein or mutations. The differences in ventral and dorsal alterations in the presence of ectopic *tsh* expression could also reflect the differences in ventral and dorsal specific cofactors. *tsh* may function cooperatively with such cofactors, as it does with *Ubx* and *Antp* in the embryo to specify trunk segments. Plausible cofactor candidates are the Iroquois-complex genes described below.

The loss of *tsh* protein expression from the hinge of *ae* mutants, as observed in the wing discs, suggests a possible mechanism of action for the *tsh* gene. In order to determine if *tsh* could induce a thoracic fate on non-thoracic tissue more distal to the thorax or wing hinge, *tsh* was misexpressed under the control of a *vg*-GAL4 driver. The effect of *tsh* expression could be analyzed without the loss of viability due to the wing specific expression pattern of the *vg*-GAL4 driver. The misexpression of *tsh* under the control of the *vg*-GAL 4 line leads to a loss of wing blade tissues with only the wing hinge remaining. At a slightly lower temperature, and concomitant reduction in the expression of the GAL4 driver, the loss of wing blade tissue is reduced but still extensive. The tissues remaining possess some wing blade features, implying that the expression of *tsh* in these tissues failed to alter their fate. The loss of tissue and the triple row of bristles characteristic of the anterior wing margin also likely indicate a perturbation of wing development without an effect on wing fate. Interestingly, a double row of bristles can still be detected in the remaining wing tissue, implying that the distal most regions of the wing blade are still being specified in the presence of the ectopic *tsh*. It appears that in order for *tsh* to disrupt the distal most fate in the wing, it must be expressed at higher

levels to affect the factors required for distal wing specific fate in this region (dorso-ventral specific factors).

Although the misexpression of *tsh* under the control of the 30A-GAL4 driver failed to rescue all of the defects associated with the *ae* mutant, it did rescue the fusion observed between the PVR and the PWP of the lateral thorax. The failure to rescue the YC could reflect the differences in the domains of 30A-GAL4 expression and endogenous *tsh*. The more distal expression of 30A-GAL4 may fail to drive *tsh* in a domain that is proximal enough for YC-specific rescue. The failure to produce a structurally normal PVR is also not expected because of the more distal domain of expression of the 30A-GAL4 line in comparison to endogenous *tsh*, as seen from the results of the *yw*; UAS-*tsh*; 30A-GAL4 flies, which show a fusion between the two knuckles of the PVR (**Figure 29**).

***Rpw*, *vg*^U and E4.8.**

It was decided to determine if the expression pattern from the E4.8 construct or the enhancer trap *tsh*[04319] would be affected by mutations in genes involved with growth and pattern formation. To answer this question, the expression pattern of the E4.8 enhancer line in two dominant mutant backgrounds, *Rpw* and *vg*^U, was examined. These two mutations are in genes required for wing growth and patterning at different times during the formation of the wing. In the dominant *vg*^U mutant background there was a dramatic reduction in the size of the pouch, which is characteristically small for mutants defective in wing patterning and growth. However, the E4.8 expression pattern was unaffected in the double heterozygotes. The expression domain of the E4.8 reporter construct still respected the boundary of the reduced wing pouch (**Figure 27**). The reduction in normal *vg* function within the wing failed to lead to an ectopic expression of the *tsh*-specific E4.8 reporter gene in the substantially smaller wing pouch. The restriction of E4.8 enhancer expression from the pouch suggests that the expression or exclusion of *tsh* from the pouch is likely the function of a gene other than *vg*. However, the presence of a limited amount of functional *vg* protein is not ruled out as a possible negative regulatory factor for the exclusion of *tsh* from the pouch. Even though alterations to normal *vg* expression fail to provide the appropriate level of function for

proper wing development and growth, the threshold for the negative regulation of *tsh* may be substantially lower. The failure of vg^U to affect the expression of E4.8 is not unexpected, at least in the ventral hinge. The dramatic reduction in wing tissue in vg^U heterozygotes is associated with the loss of wing blade, but the ventral wing hinge is still present in these flies (Simmonds et al., 1997). Alterations to the dorsal expression pattern is also unexpected based on what is known about *tsh* function and the domain of expression within the dorsal hinge. A loss of dorsal hinge structures would not lead to a loss of *tsh* expression within the presumptive dorsal hinge because *tsh* is not normally expressed in the presumptive medial or distal hinge (and likely not the proximal hinge for that matter). Loss of *tsh* expression from the presumptive dorsal specific expression would likely have an affect on the mesonotum. In *vg* mutants, the flies often fail to lose all of the wing tissue and often are left with proximal hinge. This is because the formation of the hinge is not dependent on the D/V organizing function which *vg* modulates. Therefore, one might predict that the expression of *tsh* is also not dependent upon the formation of the rest of the wing.

The enhancer trap line *tsh*[04319] was also tested in conjunction with another dominant mutation in a gene required for proper patterning of the wing margin. The dominant *Serrate* allele, *Ripped wing* (*Rpw*), identified from one of the *P* element mutagenesis screens for wing posture mutants, was crossed into the enhancer trap *tsh*[04319] background. As with the dominant *vg* mutation, loss of tissue was observed in the presumptive wing tissue leading to a substantially smaller wing pouch. However, the enhancer trap line failed to spread into the pouch and, again as in the dominant *vg* mutant, the hinge and notum specific expression was unaffected in the double heterozygote. The similarity between the two is expected based on the requirement for *Ser* in the expression of *vg* (Diaz-Benjumea and Cohen, 1995; Kim et al., 1996). This reflects results by Ng et al. (1996) which also showed that loss of *vg* expression failed to lead to the spread of *tsh* into the normal *vg* domain, the wing blade. The phenotypic enhancement observed between the strong *tsh* allele, *tsh*[041319], and the dominant *Rpw* allele could simply be due to an increase in the length of time required for development in the double heterozygote as opposed to a genetic interaction between the two genes. This is likely for three reasons. The first is that *Rpw* and Bd^G both exhibit a dramatic

increase in the severity of the wing phenotype when grown at lower temperatures (18°C). The second reason is that there is no evidence as of yet for any interaction between the *tsh* and *Ser* genes during wing development. The third is that the effect that *Rpw* has on wing development is due to ectopic expression of *Ser* in the distal wing margin. This ectopic expression then leads to the disruption at the presumptive wing margin as observed by the loss of *wg* expression along the presumptive wing margin (*Ser^D* and *Rpw*, Thomas et al., 1995). The elimination of *wg* expression within the pouch would not likely have any effect on the hinge-specific *tsh* expression because the folds surrounding the wing pouch act as a physical barrier to the movement of the *wg* signal (Cadigan et al., 1998). If *wg* plays a role in *tsh* expression in the hinge, it is more likely that hinge-specific *wg* expression would provide a signal. As well, no alterations are seen for the *tsh*[04319] reporter gene expression in the *Rpw; tsh*[04319] double heterozygotes. However, as discussed above, *tsh* could affect the formation of the proximal-distal axis from the wing hinge organizing center as was suggested for the *nub* mutant (Ng et al., 1995).

It was also decided to determine if the zinc finger protein, *tsh*, played any role in localizing *vg* expression to the wing pouch, possibly as a negative regulator of *vg* expression. To do this, the loss of *tsh* expression from the ventral hinge in the *ae* mutant was tested to see if it would lead to the spread of *vg* expression into the ventral hinge domain. This idea arose as a result of mis-expression experiments driving *UAS-vg* with the *vg-GAL4* driver. The misexpression of *vg*, and presumably the over expression of *vg* that is associated with the use of the UAS/GAL4 system, led to an abnormal wing posture defect resembling the *ae* phenotype. The prediction was that the over expression of *vg* in a *vg*-specific pattern may produce the wing posture defect by spreading of *vg* into presumptive hinge, and thus negatively affecting *tsh* expression so as to resemble the altered protein expression pattern of *tsh* in the *ae* mutant. To test this, the expression of the *vg* quadrant-four enhancer was studied in an *ae* background. If the prediction was correct, one might expect to see a spread of *vg* expression into the presumptive ventral hinge in a position where loss of *tsh* expression was observed in the *ae* mutant. However, no alterations to the expression pattern of the quadrant four enhancer in an *ae* background were observed. This fits with the data collected from the SEM analysis of the wing

hinges from these flies. Although the *vg*-GAL4 / UAS-*vg* flies have an abnormal wing posture, the hinge region including the adult cuticle at the base of the wing is completely normal, indicating that the cause of the wing posture defect is different than in the *ae* mutant. This implies a functional or structural defect associated with the neurons or musculature of the flight muscles. This is consistent with the view that *vg* is required for the proper formation of the IFM. A possible negative regulation of *vg* in the hinge by *tsh*, however, is not ruled out based on the limited results herein, because the expression of *tsh* in the wing hinge of the *ae* mutant is normal on the peripodial membrane side of the wing disc. It has been suggested that the peripodial membrane side of the disc can also function in signaling to the wing proper side of the disc, suggesting that *tsh* could still be negatively regulating *vg* from the opposite side of the wing disc. However, it is more likely that *tsh* has no function in the restriction of *vg* expression to the wing pouch, indicating that factors other than *tsh* are involved. In addition to the data presented above, it is also likely that *vg* is not directly involved in limiting the expression of *tsh* to the hinge or at least in the presumptive dorsal hinge, because of the asymmetric expression of *tsh* in the presumptive hinge.

The development of the proximal/distal axis of the imaginal wing disc, like the leg disc, is believed to be the result of a series of increasingly larger concentric domains. The most distal (central within the wing disc) of these domains coincides with the presumptive wing blade or pouch corresponding to the *vg*/*sd* expression domain (Kim et al., 1996). The most proximal of these domains in the wing disc corresponds to the presumptive notum and is marked by the *Iroquois* homeodomain protein expression (Leyns et al., 1996; Gomez-Skarmeta et al., 1996). The three genes *araucan* (*ara*), *caupolican* (*caup*) and *mirror* (*mirr*) make up the *Iroquois* complex (Iro-C) which is believed to be functionally redundant and is required in the specification of the notum (Diez del Corral et al., 1999). Mutant clones for the Iro-C exhibit a transformation of notum to hinge-specific structures such as the axillary sclerite and the tegula (see **Figure 1** for the location of wing hinge and lateral thoracic structures). Within these mutant clones in third instar larval wing discs, there is a derepression of *tsh* expression. This is consistent with the findings herein, suggesting that *tsh* is required for the formation or specification of the wing hinge. In the domain specific null allele, *ae*, a fusion between

the thorax (lateral notum) and hinge structures is seen, which corresponds to a loss or reduction in *tsh* expression within the respective presumptive imaginal tissues.

The phenotypic interactions observed in the transheterozygotes (*ae/tsh δ* , *ae/Df(2L)TW161* or *ae/tsh[04319]*⁸⁻¹) and the results from the *UAS-y; tsh-GAL4* screen, which identified that *tsh* is expressed throughout the thoracic cuticle suggest that *tsh* may play a role in the formation or specification of the mesothoracic adult cuticle, particularly in the lateral regions of the notum (pleural plates) close to the base of the wing.

Over expression of *tsh* in the presumptive wing blade or proximal wing leads to a perturbation of wing development, however overexpression of *tsh* in the distal wing hinge leads to apparent outgrowths or alterations to the wing hinge fate. These results suggest that the overlapping expression of *tsh* with other factors determines the function of *tsh*. In terms of the concentric domains of the proximal distal axis, the most distal *tsh* protein expression is more distal than Iro-C expression but overlaps Iro-C expression in the presumptive lateral notum. The derepression of *tsh* in the more dorsal notal tissues suggests that it is down regulated under normal conditions, directly or indirectly via the Iro-C products. However the *tsh* protein levels are the highest in the presumptive lateral notum along with high levels of expression of the Iro-C genes. From the results where *tsh* function is removed from the lateral notum and the results from the *UAS-y; tsh-GAL4* screen, it appears that *tsh* is also required in some way for the development of these tissues. This implies a requirement for both *tsh* and the Iro-C genes in the development of these regions. A cooperation in the lateral notum between Iro-C and *tsh* function is proposed, analogous to the specification of trunk segments in the embryo, where *tsh* in conjunction with the homeodomain proteins *Ubx* and *Antp* is required for proper specification. In the thorax *tsh* may cooperate, in combination with regulatory factors such as the Iro-C genes, to specify the proper formation of the lateral thoracic pleural plates. Perhaps in the dorsal hinge, either these factors specify dorsal hinge fate or the absence of *tsh* determines these tissues as dorsal hinge. The ventral hinge up to and including the medial costa requires the expression of *tsh* in the absence of Iro-C function to produce the hinge structures. Likely the addition of the Iro-C expression would lead to a ventral hinge to lateral thorax transformation. However, it appears that *tsh* is also only able to lead to transformations in specific regions in the wing hinge and not the wing, just

as the *Iro-C* genes do. Mis-expression in more distal domains of the developing wing give differing results. Misexpression of *tsh* under the control of the *30A-GAL4* driver leads to outgrowths of what appear to be thoracic tissues, however activation of *tsh* expression in the presumptive wing blade under the control of the *vg-GAL4* line reveals that *tsh* can perturb wing growth while not affecting patterning. This is also suggestive of region specific factors cooperating with *tsh* in specifying pleural and hinge structures.

Orientation Dependent *lacZ* Expression.

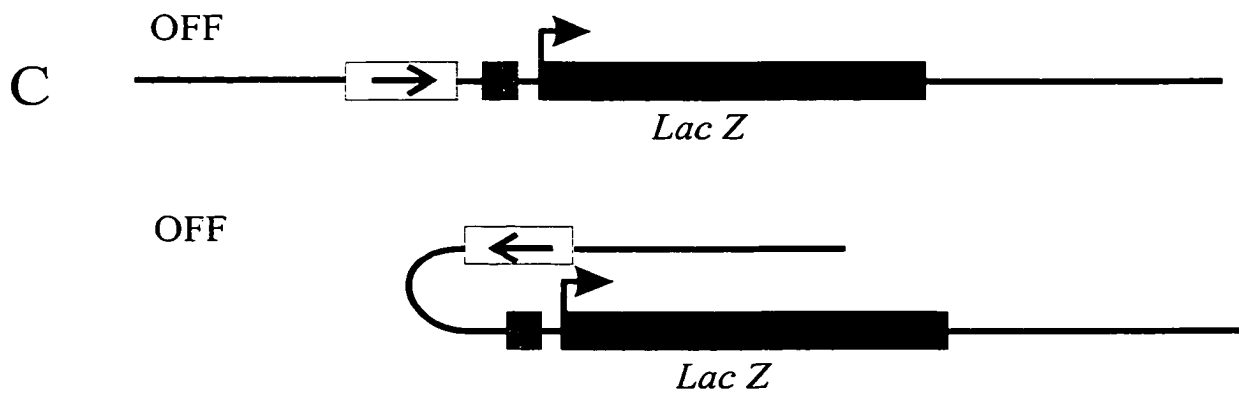
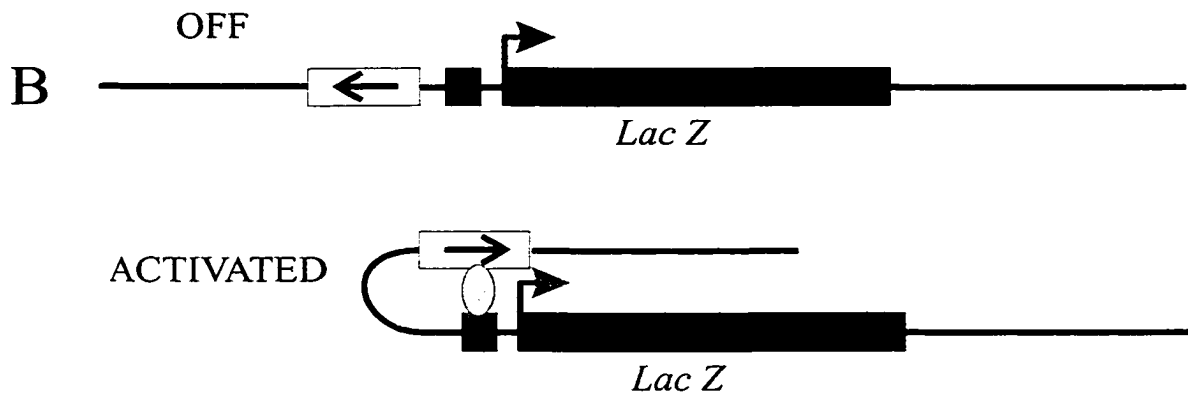
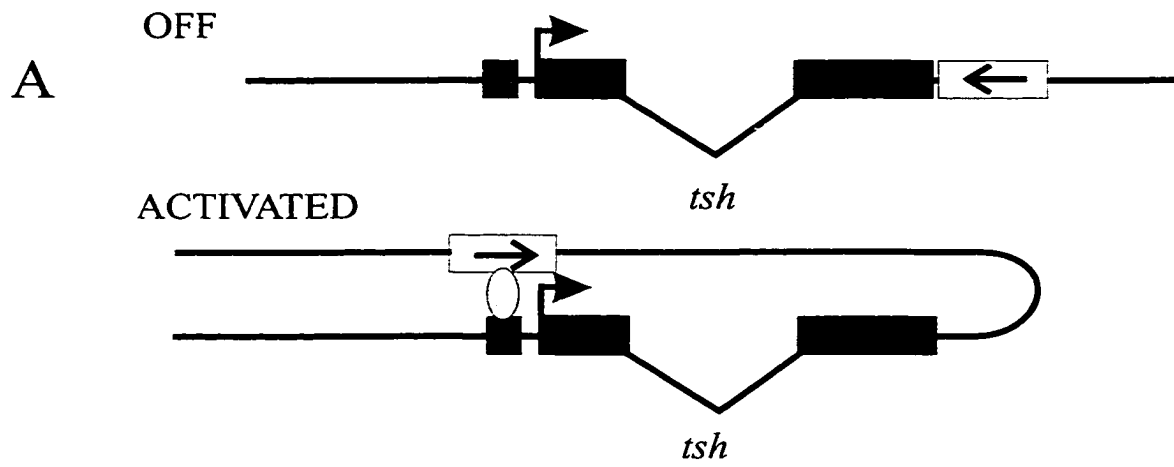
By identifying the underlying etiology of the *ae* mutant, an additional 3' cis-regulatory sequence of the *tsh* gene was discovered. This regulatory element is capable of driving the reporter gene within the presumptive wing hinge and proximal haltere structures. Each of the genomic fragments was inserted in the 5' orientation with respect to the reporter gene whereas each of the fragments originated from the 3' genomic sequences flanking the *tsh* coding region. Thus, the element acts like a true enhancer, capable of driving expression from both the 3' and 5' positions. The question of whether the enhancer elements can act in both orientations with respect to direction of transcription of the *tsh* gene is still unknown. However, some of the results herein suggest that the wing, haltere and gut specific expression is dependent on the orientation of these elements. Each of the fragments tested using the enhancer tester that was in the same orientation as the endogenous position exhibits reporter gene expression that differs from its *yw* control siblings. The E4.8, EB2.9 and HB1.0 constructs show wing and haltere specific expression and these as well as the 209 bp and 481 bp constructs show gut specific expression. The two remaining constructs H1.0 and HE1.0 are in the opposite orientation and show no obvious differences from their *yw* sibs. It was expected that at least one of these fragments, H1.0 or HE1.0, would show some wing hinge specific enhancer ability. The EB2.9 element is capable of both presumptive ventral and dorsal specific hinge expression. However the HB1.0 element is only capable of presumptive ventral specific expression. Presumably, the HE1.0 and H1.0 elements in the remaining 2.0 kb of sequence from the EB2.9 fragment encode the dorsal specific expression not observed from the HB1.0 element. The absence of expression from these constructs may not be due to the deficiency of such regulatory sequences, but the result of

the orientation of these sequences within the enhancer tester. Three of the pCaSpeR hs 43 constructs, H1.0, EB1.9 and HE1.0, are unable to activate *lacZ* expression from the minimal heat shock promoter. Coincidentally, the orientations of these constructs are opposite to HB1.0, DraI 1.0 and EB2.9, which are all capable of activating tissue specific expression.

Based on this information two questions come to mind. The first is whether these particular cis-acting regulatory elements conform to the definition of an enhancer. If the orientation of these regulatory sequences is important for regulation of the minimal hs 43 promoter, this suggests that they are not true enhancers. However, a regulatory element that is capable of activating expression from a distance, but is orientation dependent, is intriguing in itself. There doesn't appear to be a similar example to this in the literature yet. This seems counterintuitive, because presumably the 3' regulatory element will still be able to make contact with the promoter elements upstream or downstream by forming a loop and making contact between the promoter-transcription initiation complex and the enhancer-activator complex. If the orientation is important for the proper function of this regulatory element then the distance between the regulatory element and the promoter elements may cause a problem for regulatory-element-promoter interaction. The regulatory element at its endogenous locus may only require a simple single loop of the intervening sequence to make the appropriate contacts with the promoter (**Figure 35 A**). The same regulatory element upstream of the promoter in the pCaSpeRhs43 vector, about 120 bp away, would also only need to form a single loop to make similar contacts with the minimal promoter. However, the same regulatory sequences in the opposite orientation in the enhancer tester would need to form a 360° loop with the short stretch of sequence between itself and the promoter in order to make similar contacts to the endogenous regulatory element. If the regulatory element in the opposite orientation is too close to the promoter, this may provide a physical barrier to inhibit the activation of expression. Providing a greater distance between the promoter and the enhancer by inserting a fragment of DNA may allow the appropriate loop structure to form.

The second question that would have to be answered is whether the expression pattern missing from the HB1.0 reporter in the presumptive dorsal hinge, compared to

Figure 35. An enhancer model to explain the apparent orientation dependence on the expression from the tissue specific regulatory element in the *ae* enhancer. **A)** A schematic of the *ae* enhancer regulation of the *tsh* gene in the “off” and “activated” states. The black boxes in all panels correspond to coding regions of the respective genes. The arrows above each of the coding regions indicate the direction of transcription. A red arrow indicates the off state of the gene and a green arrow indicates the activated state of the gene. The open box in all panels corresponds to the *ae* enhancer element. The direction of the arrows in each of the enhancer boxes is arbitrary so the orientation of the enhancer element can be compared between panels. The thin lines indicate non-coding genomic sequence. The blue boxes upstream of the coding regions correspond to the promoter elements and the purple ovals represent activator proteins. **B)** and **C)** panels correspond to the two possible orientations of the *ae* enhancer element in the pCaSpeR hs 43 vector. The drawings are not to scale.



EB2.9, is present in one of the other two genomic fragments, thus representing a separable dorsal hinge regulatory module. If the H1.0 and HE1.0 fragments fail to drive reporter gene expression in either orientation, this would suggest that the composite of hinge expression observed from the EB2.9 construct requires the complete 2.9 kb sequence. This would suggest that the dorsal hinge regulatory element does not form a functionally divisible unit from the ventral hinge element in the HB1.0. This would imply a functional synergism or requirement for the independent HB1.0 enhancer module for the proper expression of the dorsal hinge module.

Future Directions.

It is reasonable to conclude from the evidence presented that the *ae* mutation identified and described herein is allelic of the original *ae* mutation. It is also reasonable to conclude that *ae* represents an allele of the homeotic gene *tsh* based on the information presented in this thesis. To conclude unequivocally that *ae* is an allele of the *tsh* gene would require rescuing the *ae* phenotype (abnormal wing posture and drooping halteres) with *tsh* expression. This can be accomplished by expressing *tsh* under the control of the ventral wing hinge and haltere specific regulatory element, the *ae* enhancer.

With the identification of a genomic fragment that possesses cis-acting regulatory function, the next step in the characterization would be to determine the specific sequences responsible for this regulatory function and to identify trans factors required for its proper regulation. This could be achieved by creating a screen designed to identify modifiers of the *ae* phenotype or alterations to the expression pattern of the enhancer construct lines. Although a preliminary analysis revealed that some of the abnormal wing posture mutants available through the Bloomington stock center failed to produce any phenotypic interactions with the *ae* mutation, a screen designed to look for modifiers of the *ae* phenotype or reporter gene expression could be attempted with genes already known to interact with the *tsh* gene. In recent publications (Gallet et al., 1998 and 1999), it was suggested that *tsh* plays a role in the modulation of the *wg* signal in establishing the denticle belts in the early embryo. Furthermore, *wg* also plays a role in the development of the hinge Neumann, and Cohen, 1996. In particular, *wg* is a good candidate for interactions with *ae* in the adult, because of the overlapping spatial and

temporal expression patterns observed in the adult and larvae (Calleja et al., 1996; Phillips and Whittle, 1993; and results presented herein).

Antp is another gene that would be a good candidate for a regulatory factor of the *ae* enhancer because it is already known to be required for development of the T2 and T3 segments where the *ae* phenotype is observed. *Antp* is able to activate *tsh* expression within tissues that don't regularly express *tsh*, and is already known to directly activate *tsh* expression by binding a 3' tissue specific enhancer of the *tsh* gene. *Antp* is also expressed within the presumptive hinge tissues in the wing discs.

The identification of cis-acting regulatory elements begs the question of what activators are responsible or required for proper regulation of the element. The methodology by which this type of analysis can be approached depends upon the identification of any interacting genes. Without the benefit of genetic interactions known to be capable of modifying the *ae* mutant or altering the expression pattern of any of the reporter constructs, a direct analysis of the sequences may be necessary and informative. Band shift assays can be carried out with imaginal disc preparations of soluble nuclear extracts to identify any factors capable of binding within the *ae* regulatory sequences. If genetic interactions between *ae* and other genes are ultimately identified, then the protein products can be tested to determine if the interaction observed is the result of a direct or indirect regulation of the enhancer sequences.

By using the GAL4/UAS system (Brandt and Perrimon, 1993), it should be possible to identify factors able to regulate the *ae* enhancer. The E4.8 enhancer construct line has been crossed into a *30A*-GAL4 driver and is maintained as an E4.8; *30A*-GAL4 stock. Crossing this to available UAS lines makes it is potentially possible to identify genes capable of modifying the expression of the reporter gene via the E4.8 regulatory element. This can be addressed simply by the analysis of the *lacZ* reporter gene expression from the F1 progeny.

In order to identify possible cis-acting sequences within the enhancer, a comparison with a related *Drosophila* species could also be used to look for relevant conserved non-coding sequences. A commonly used *Drosophila* species used for sequence conservation comparisons is *Drosophila virilis*. Even though the two species are separated by approximately 60 million years, the sequence conservation between

them has been invaluable in isolating proposed conserved sequence motifs. Examples of this type of analysis come from the genomic sequences flanking the *en* gene (Kassis et al., 1989), or the sequence conservation of the intron II boundary enhancer of *vg* (Williams et al., 1991). The identification of conserved sequences could then be used to identify any possible regulatory factors. Conserved sequences can be analyzed, regardless of knowing what these sites correspond to or what unidentified trans acting factors might recognize them. Site directed mutagenesis can be carried out on conserved sequences of the 2.9 kb regulatory element to determine what effect, if any, do sequence changes have on the regulatory function (i.e. *lacZ* reporter gene expression). Each of the H1.0, HB1.0 and HE1.0 fragments has been cloned into the *pAltered Site Directed* mutagenesis vector. Once conserved sequences have been found or binding sites have been identified via band shift assays (*Stratagene*), these conserved sequences can be altered and the effects analyzed.

Another question that can be addressed is whether the flanking 3' genomic sequences that failed to regulate gene expression from the minimal promoter are actually capable of activating reporter gene expression in the opposite orientation. This is currently being pursued. The three constructs which failed to activate the *lacZ* reporter gene expression when tested in the pCaSpeR hs 43 vector have had their orientations reversed when reintroduced into the vector. Injections of each of these constructs will go towards answering the two questions discussed above. Are the regulatory sequences within the EB2.9 fragment by definition enhancer elements and what fragment is required for proper expression within the presumptive dorsal wing hinge?

Initial characterization of the *ae* stock with respect to the presence of any 3' or 5' *P* element sequences revealed no such sequence in the stock. The subsequent identification of the 5' *P* element sequence upstream of the *tsh* coding region is particularly interesting (**Figure 32**). The 5' *P* element sequence is definitely present in the *ae* line used for characterization of the mutation because this isogenic line was used on three separate occasions for generating genomic DNA preparations. Each of the genomic isolations identify some 5' *P* element sequences localized to the 5' flanking genomic region of the *tsh* coding region. With the known complexity of the *tsh* regulatory sequences in flanking genomic sequences, it would be interesting to determine

if the 5' *P* element insertion also had some effect on the *ae* phenotype. Possibly the crippled *P* element insertion site could correspond to additional regulatory sequences responsible for the manifestation of the *ae* phenotype. However, the disruption of the 3' *ae* enhancer is likely the sole cause of the *ae* phenotype based on coincidental expression pattern of the enhancer and the tissues affected in the *ae* mutant. Analysis of this particular genomic sequence for any enhancer ability would be straightforward. Simply cloning the genomic fragment from the genomic lambda clone into the enhancer tester construct as discussed above would allow an assay of its affect on *tsh* expression.

Finally, the complementation of the *tsh* [04319] allele with the *ae* allele is intriguing. Although the gamma source failed to produce any non-complementing *ae* chromosomes, a larger screen could be carried out to ensure that alterations to somatic pairing would not affect the complementation observed between the *tsh*[04319] and *ae* alleles. There are two types of transvection, *zeste* dependent and independent. Examples of *zeste* regulated transvection can be seen in the *dpp*, *w* and *bx* pairing dependent gene expression. By introducing a *zeste* allele into the *ae* and *tsh*[04319] backgrounds it would be possible to ascertain whether *zeste* has an effect on the complementation phenomenon that was observed between these two alleles.

This initial characterization of the rediscovered *ae* mutation presented herein will help with the understanding of *tsh* regulation and its role in patterning in the developing adult, in particular the cuticle. Because all other null alleles of the *tsh* gene are embryonic lethals, *ae* will make an invaluable tool for the study of genetic interactions between *tsh* and other genes. As for many other genes, the characterization of *tsh* is still in its infancy, however the identification of the *ae* mutation has and will aid in the further characterization of this gene along several fronts.

Chapter VIII - Materials and Methods

Stocks and Crosses

All stocks and crosses were maintained at room temperature (23-25°C). Flies were grown on yeast agar media (Nash and Bell, 1968). The necessary genotypic and phenotypic information for some of the stocks used was obtained from Lindsley and Zimm (1992). The following stocks were obtained through the Bloomington Stock Center; *how*, *os^o*, *flw*, *tx*, *Df(2R)bw^{vDe2L} Cy^R / In (2LR)Gla*, *Bd^G*, *Df(2L)TW161/CyO*, *Df(2L)TW65/CyO*, *Dp(2:Y)H2*, *tsh[04319]/CyO: ry*, *l(2)[03832]/CyO: ry*, *l(2)[02074]/CyO: ry*, *tsh[4-3]*, *tsh[51]*, *w*; *tsh[B4-2-12]/CyO*, *A3-2-66/CyO*, *y^l w¹¹¹⁸*; *P{wtmW.hs=GawB} md621/CyO*; *P{wtmC=UAS-y.C}MCI/TM2*, *w*; *30A-GAL4*, *Dfd^l*. *Birmingham2*; *Sb/TM6 Ubx* and *w*; *Sp/CyO*; *Sb*, *Δ 2-3/TM6*. The origins of all stocks not obtained through the Bloomington stock center are listed in **Table 9**. *P* element mutagenesis was carried out by crossing all enhancer trap, ammunition chromosomes into the stable delta 2-3 transposase source (Robertson, et al., 1988) on the third chromosome (**Figure 5**).

Transmission Electron Microscopy (TEM).

Flies were fixed in 4% glutaraldehyde in phosphate-buffered saline (PBS) overnight at room temperature while rocking lightly. Whole flies were used as opposed to just the thorax, to ensure that the indirect flight muscles were not damaged in the processing. The flies were then washed three times in phosphate-buffered saline with 0.05% Triton-X (PBT) for 15 min, and fixed in osmium tetroxide (OsO₄) solution for ~1hr. The OsO₄ solution was then replaced with 20% ethanol and the samples dehydrated in a series of ethanol steps (30, 50, 70, 90 and then 98%). The ethanol series was followed by three changes of propylene oxide (PO) for 15 min each. The PO was then replaced with a 25% Epon: 75% PO mixture for at least 2hrs, followed by a 50:50 Epon/PO mixture overnight. Specimens were then placed in small embedding dishes to reduce the amount of trimming needed, covered with Epon and placed in a 60°C incubator for 48hrs. Each block was then trimmed in the shape of a trapezoid as close as possible to the specimen (Bazzola and Russell, 1992). The Epon is prepared and stored at -20°C. Epon preparation is as follows: 240 ml of solution A and 160 ml of solution B

were combined and mixed for half an hour before adding 6 ml of DMP30 accelerate (dimethyl aminomethyl pheno). To make solution A combine 100 ml of TAAB 812 (Epon) with 152 ml of DDSA (dodeceny succinic anhydride) and then mix for half an hour. To make Solution B combine 100 ml of TAAB 812 (Epon) with 82 ml of NMA (nadic methyl anhydride). The ratio of solution A to B is 6:4.

Thin sections were prepared by breaking fresh glass knives daily using the LKB knife maker. All sectioning was done on either a LKB III Ultramicrotome or the Reichert Ultracut E Ultramicrotome. Thin sections (1.0 - 0.5 μm thick) were used to analyze the gross morphology of the indirect flight muscles from *ae*, *Oregon R*, *IFM(2)-11* and *1113* mutants. Sections were fixed to the slide by drying the slides at 60°C, and stained with Richardson's stain (a solution of 1% toluene blue and 1% boric acid) at 60°C until the edge of the stain on the sections began to dry (approximately 5 min). The slides were then rinsed with dH₂O and allowed to dry on a hot plate until all H₂O has evaporated. The stained sections were then irreversibly fixed to the slide by applying permount and a coverslip. All thin sections were cut for analysis under bright field light microscopy.

Ultrathin sections of *ae* and *Oregon R* flies ranged between grey and gold interference colors which corresponds to between 60 and 100nm, respectively (Reid, 1975). Ultrathin sections were prepared by using either a diamond knife or freshly broken glass knives. All ultrathin sections were stained with lead citrate and examined using the Philips 210 transmission electron microscope (TEM). All photos were taken using a Zeiss Axiophot.

Table 9. Stocks and Origins.	
Stock	Origin
<i>Spread (D. simulans)</i>	Mel Green, unpublished
Quadrant 4 enhancer- <i>lacZ</i>	Kim et al., 1996
UAS- <i>vg</i> (III)	Sean Carroll laboratory
<i>vg</i> -GAL4 (II)	Sean Carroll laboratory
<i>Rpw</i> /TM6B	Soanes and Bell, unpublished
27 <i>YASH</i> (III)	Soanes and Bell, unpublished
32 <i>YASH</i> (III)	Soanes and Bell, unpublished
<i>exd</i> ^{em25} /FM7	Katzen and Bishop, 1996
C-92 <i>cn</i> /CyO ; <i>ry</i>	Brook, thesis (1994)
<i>YASH</i> 9 (I)	Hiromi, (1992)
<i>Df(2L)tsh8</i> /CyO	Fasano et al., (1991)
<i>Df(2L)R6</i> /CyO	McCormick et al., (1995)
<i>Df(2L)305</i> /CyO	Core et al., 1997
<i>w</i> ; UAS- <i>tsh</i> (III)	Steve Kerridge, unpublished

Table 9 indicates the origin of each of the stocks not obtained through the Bloomington stock center. The roman numerals in brackets indicate the chromosome to which the mutation is localized. The dominant *Spread* mutation was identified in *Drosophila simulans*.

Scanning Electron Microscopy (SEM)

All samples examined with the Scanning Electron Microscope were stored in 95% ethanol without fixation for at least two days prior to critical point drying. For examining whole flies, wing hinges, or halteres, the 95% ethanol from each sample was replaced and further dehydrated in fresh 95% ethanol, followed by absolute ethanol, overnight. Samples were then critical-point dried and gold labeled for examination. All samples were immobilized on posts with double-sided tape.

For direct flight muscle analysis, the dehydrated flies were split tangentially and the indirect flight muscles were teased from the thorax until the DFMs were observable. Samples were then further dehydrated in 95% ethanol, followed by absolute ethanol, overnight. Finally, the samples were critical-point dried, immobilized on posts with double-sided tape and gold-labeled for observation with the Scanning Electron Microscope. Each of the samples was sputter coated with gold twice to ensure samples were adequately covered to avoid charging. The SEM used for this analysis was a Jeol model JSM6301FXV.

Analysis of the wing posture mutants using the variable pressure SEM required very little preparation. Oregon R, *tx, os^o* and *b cn ae; ry* flies were selected and kept at -20°C for 10 min prior to observation with the variable pressure SEM. Flies were then mounted on double-sided tape and then examined with no further processing.

Histochemical Staining

All *LacZ* staining follows Bellen et al. (1989) with slight modifications. Wandering third instar larvae were washed and dissected in PBS, fixed in 0.75% glutaraldehyde for 15 minutes and then washed 3x in PBT (0.05% TritonX). Staining solution (10mM Na phosphate pH 7.2, 150mM NaCl, 1mM MgCl₂, 5mM K ferricyanide, 5mM K ferrocyanide and 0.1% X-gal in N,N-dimethylformamide) was prepared fresh daily and then added to the washed larvae and allowed to stain for a time of between one hour to overnight at 37°C, depending on the line. X-gal staining was periodically monitored and stopped when judged to be optimal. Staining was stopped by washing 3X with PBT (0.05%) for 5 minutes. Larvae were staged by timing the age after egg laying

and confirmed by analysis of the mouth parts according to Roberts (1986). Discs were mounted in 80% glycerol (PBS). Photographs were taken using a Zeiss Axiophot.

Antibody Staining.

All antibody staining follows the protocol of Simmonds et al. (1995) with slight modifications. Blocking in these experiments was performed in the absence of the normal goat serum. Rat anti-*tsh* antibodies were used at a concentration of 1:250 (pre-absorbed). The Goat anti-rat Cy3 conjugated secondary was used at a 1:250 dilution. Secondary antibodies were obtained from Jackson Immuno Research Laboratories (Bio/Can Scientific). All discs were dissected under low light conditions and examined within 12 hrs of mounting in 80% glycerol (PBS). Analysis was carried out using confocal microscopy (Molecular Dynamics CLSM Argon/Krypton laser). The *tsh* (Rat) antibodies were used at a working concentration of 1/250 (preabsorbed) with a secondary Anti-Rat (Goat) Cy3 conjugated antibody at a working concentration of 1/200.

Gamma Irradiation

Gamma irradiation was carried out according to Ashburner (1989). Adult *b cn ae*; *ry* males between 2 and 3 days old were irradiated with 40 grey using a cobalt 60 gamma source. Irradiated males (~25) were then crossed with at least 50 P1370 females (*tsh*[04319]/*CyO*). Every two days the flies were put on fresh food bottles. The F1 progeny were then screened for non-*Curly* flies with the *aeroplane* phenotype. Any phenotypically *ae* flies were crossed to the *w*; *Sp/CyO*; *Sbd2-3/TM6 Ubx* multiply balanced line. Single **/CyO*; **/TM6Ubx* flies were then back crossed to *w*; *Sp/CyO*; *Sbd2-3/TM6 Ubx*. **/CyO*; **/TM6Ubx* flies were then back crossed to **/CyO*; **/TM6Ubx* from the same cross. All lines generated were then back crossed to *tsh*[04319] to look for *b cn ae* chromosomes that failed to complement the *ae* phenotype. The asterisk indicates an irradiated chromosome.

Genomic DNA Extractions and Southern Blot Analysis

Genomic DNA extractions were performed as described by Sambrook et al. (1989) with slight modifications. 100-200 mg of adult flies from either frozen or fresh

stocks was ground in 3 mls of homogenizing solution # 1. Homogenizing solution #1 contains: 10 mM Tris-Cl (pH 7.5), 60mM EDTA, 0.15mM spermidine and spermine, and Proteinase K to a final concentration of 50 µg/ml (Gibco) which is added prior to use. The homogenate was poured into a 15 ml polypropylene Corning screw cap tube (or equivalent) and the tissue grinder was then rinsed out with 3 mls of homogenizing solution #2. This is then combined with the homogenate and incubated at 55-65°C in a Tyler Instruments rotating hybridization oven for 90 min. Homogenizing solution #2 consists of: 0.2M Tris-Cl (pH 9.0), 30mM EDTA, 2% SDS and Proteinase K to a final concentration of 50 µg/ml. The combined homogenate is extracted once with phenol, twice with a 50:50 phenol : chloroform isoamyl-alcohol mix and once with chloroform isoamyl alcohol. The genomic DNA is precipitated by adding 200mM NaCl and 2 volumes of 95% ethanol, spooled from the ethanol or recovered after centrifugation (>1600xg), and washed in 70% ethanol. Pellets were briefly dried under vacuum and then resuspended gently in 4 mls of TE to insure that shearing of the DNA was held to a minimum (often overnight on the bench top). DNase free RNase was added to a final concentration of 25 µg/ml and incubated at 37°C for 30min and removed by extracting the sample once with phenol/chloroform isoamyl alcohol and once with chloroform isoamyl alcohol. The DNA was then precipitated, washed and dried as above, and finally redissolved in 250-500 µl of sterile milli-Q H₂O. The OD 260/280 was determined later. DNA pellets were not completely dried making it easier to resuspend.

Genomic digests were performed in total reaction volumes of between 20 and 30 µl for ease of loading. Three micrograms of appropriate genomic DNA samples were digested and subject to electrophoresis on a 220-240 ml 1X TAE or 0.5X TBE 0.8% agarose gel in the large Tyler Instruments electrophoresis boxes. Genomic Southern blotting was performed according to Sambrook et al. (1989). DNA from the Southern blots was immobilized onto GeneScreen *Plus* hybridization transfer membranes (NEN Life Science Products) and then baked for 2hrs at 180°C, or left at room temperature overnight. For long term storage of the blots, they were sealed in a hybridization bag and kept at -70°C. Dried blots were prehybridized in 20-25 mls of 42°C prewarmed formaldehyde prehybridization solution for at least 2hrs prior to applying the denatured probe. The prehybridization solution consists of: 6X SSC, 5X Denhardt's, 0.5% SDS,

50% formamide DNA, and 100 µg/ml sonicated salmon sperm DNA. Sonicated salmon sperm DNA was made by drawing a 10 mg/ml solution up and down through a 21 gauge needle. The radiolabelled probe is diluted approximately 1 to 5 in prehybridization solution and then boiled for 10min in a screw capped tube to avoid boiling over and then added immediately to the prehybridizing blot. The blot was allowed to hybridize for at least 10hrs and then washed in 2X SSC twice at room temperature (R.T.) for 5min followed by 2X SSC / 1%SDS twice at 63°C for 30mins and finally 0.1%SSC twice for 15min at R.T. Exposure of the Kodak X-OMAT(AR) film was dependent upon intensity of bands.

Radioactive DNA probes were generated using the random oligonucleotide primer method. Pharmacia Biotech Lyophilized hexanucleotides were used as random oligonucleotides. DNA fragments used as probes were electrophoresed on agarose gels and extracted using the modified Gene clean protocol (as above). The appropriate DNA template was denatured by boiling for 10min in a screw capped microcentrifuge tube and then quick-frozen in liquid N₂. Ten microliters of a 5X Oligo-Labeling Buffer (OLB) was immediately added along with 2 µl of BSA (10 mg/ml). The 5X OLB mix is as reported in Sambrook et al. (1989). The OLB mix contained 1M HEPES (pH6.6) hexadeoxyribonucleotides at 27 OD260/ml; dATP, dGTP and dTTP each at 0.1mM; 50mM B-mercaptoethanol; 0.25M Tris-Cl, (pH8.0); and 25mM MgCl₂. The contents of the tube were allowed to melt on ice and then added to 3-5 µl of ³²P labeled dCTP (Amersham). Five units (1ul) of Klenow were added and mixed by pipetting and incubated at 37°C for at least two hours (or overnight). The ³²P labeled DNA fragments were separated from the unincorporated radiolabeled dCTPs by centrifuging the reaction mixture through a Sephadex G-50 column. All Sephadex G-50 columns were made fresh by centrifuging a Sephadex G-50 slurry through a 1 ml syringe with a glass wool stuffed tip, at ~1600xg for 4 min. This is repeated until only a 0.2 ml space remains at the top of the syringe and then the column is washed 3X with H₂O. The radiolabeled mixture is applied to the top of the column and spun for 4 min. The probe is collected at the bottom of the column and the unincorporated dCTPs are discarded along with the column.

Mini Plasmid Libraries

Thirty micrograms of genomic DNA were digested with the appropriate (BRL) enzymes and electrophoresed on a 0.8% 1X TAE agarose gel in an 8cm Tyler gel box using a single well comb. The genomic digests were fractionated by slicing the gel into 1-2mm sections and the DNA was extracted from each fraction using the modified Gene clean protocol with the following differences. To increase the recovery of genomic fragments, samples were incubated in 6M NaI on ice for up to 12hrs. To avoid shearing larger genomic fragments, glassmilk/DNA pellets were not resuspended during wash steps and were allowed to incubate for about 15min. The wash steps were performed using a NEET wash, prepared by making a 100mM NaCl, 1mM EDTA, 50% ethanol and 10mM Tris HCl pH 7.5 solution that is stored at -20°C. The 6M NaI (binding solution) was prepared as follows; 90.8 g of NaI with 1.5 g of Na₂SO₃ are dissolved in 100 ml of dH₂O and filtered using Whatman No.1 filter paper. It is then stored at 4°C in a foil-wrapped container and used while the solution remains colorless.

The fraction containing the fragment of interest was identified using either a *Taq* DNA polymerase, diagnostic PCR, or through Southern blot analysis. For the Southern blot analysis, 20-25% of each genomic fraction was electrophoresed on a 0.8% mini agarose gel. Southern blot analysis, genomic extractions, radiolabeling of DNA probes and autoradiography were performed as above.

The following description for the isolation of 3' flanking genomic sequence is for the *tsh*[04319]^{6.1} derivative line. However, the description for each of the mini-libraries created is identical. The ratio of the amount of the appropriate fraction to vector was determined to be between 1:3 and 1:4. In a total volume of 10ul, approximately 5-10 ng of a 5-6 kb insert was added to 10 ng of *Hind*III-digested pUC19 vector that was subjected to phosphatase activity. The reaction was allowed to ligate overnight or for 8 to 12hrs at 10°C. The ligation mix was then diluted one in ten with 90 µl of dH₂O. Ten microliters of each of the ligation reactions were used to transform 100 µl 18°C competent cells (see 18°C cells below), allowed to sit on ice for 45 min, and heat shocked for 30sec. Then, 890 µl of prewarmed LB were added to each of the mixtures and this was allowed to incubate for 1hr at 37°C. 100 µl of each transformation reaction were

spread on LBA (amp 50 µg/ml) plates impregnated with 20 µl of 8% X-Gal and 100 µl of 100 mM IPTG. Plates were allowed to incubate at 37°C for 16hrs or more.

Plates are then incubated at 4°C for at least one hour before colony lifts were performed. Precut Hybond-N nylon membrane discs were used for all colony and plaque lifts. Membranes were laid over cooled plates just long enough for the membrane to become wet (approximately 5 sec). The filters were allowed to dry at room temperature for 1.5-2 hrs before processing. The pre-drying appeared to help fix colonies to the membrane. Colonies were then lysed with 10% SDS for 3 min, followed by a denaturation step for 3min in 0.5M NaOH, 1.5M NaCl. Next the membranes were immediately transferred to a neutralizing solution for 3min in 0.5 M Tris-HCl (pH 7.5), 1.5M NaCl followed by a brief wash in 2XSSC for 5-10 sec. For the lysis, neutralization and denaturation steps a double thickness 3MM blotting paper was saturated with the appropriate solutions and the membranes were laid on top. The membranes were then baked at 80°C for 2hrs before being probed, as discussed under Southern analysis.

Ligations

All ligations were carried out using Gibco BRL T4 DNA ligase according to the manufacturer's specifications. All ligation reactions were carried out in a total volume of 10 µl at temperatures between 10 and 14°C in the Perkin Elmer GeneAmp PCR system 2400 from 8 to 12hr. Blunt end ligations were incubated at lower temperatures (between 7 and 10°C) for the same length of time.

Competent Cells

Competent cells were either prepared from DH5 α grown at 37°C using the calcium chloride method according to Sambrook et al. (1989) or from a DH5 α stock grown at 18°C according to Inoue et al. (1990). Standard SOB medium at 18°C was inoculated from fresh overnight DH5 α cultures. Two 250 ml cultures were set up and inoculated with 10 µl and 100 µl of the fresh overnights to ensure that at least one would be caught when it reaches the OD₆₆₀ of 0.6. If a culture went past the desired OD it could be diluted with sterile 18°C SOB.

RNA Extraction and Northern Analysis

All RNA was extracted from tissues using Trizol reagent (Gibco-BRL) according to the manufacturer's instructions. Embryos were collected on apple juice plates that had live yeast paste smeared on the surface. Apple juice plates were made as follows; 1 liter of milli-Q dH₂O was autoclaved with 40 gm of Bacto agar, 50gm of sucrose dissolved in IGA no name apple juice, then added to the molten agar and mixed on a heated stirrer. Six grams of p-hydroxy-benzoic acid methyl ester (Nipagen) dissolved in 100 mls of ethanol was then added and mixed thoroughly. Plates were poured and allowed to cool. Embryos and larvae were collected at 25°C, washed in PBS, and then flash frozen in liquid Nitrogen. Collecting larvae was done according to Roberts (1986).

The Northern analysis was carried out according to Paul Wong (pers. comm.). The RNA samples were then subjected to electrophoresis overnight on a 200 ml denaturing 1.0% Formamide / Formaldehyde gel in a fume hood at 34 volts with constant buffer mixing. The 1% agarose gel contains 36 mls of formaldehyde (~18%), 20 mls of 10X MOPS (3-[*N*-morpholino] propanesulfonic acid) (10%) and 144 mls of DEPC (diethyl pyrocarbonate) treated H₂O. The running buffer consists of 83 mls of formaldehyde (~8.3%) with 100 mls of 10X MOPS (10%) and 817 mls of deionized water, which doesn't have to be DEPC treated. Before loading, each sample consisting of 10 µg of total RNA in a total volume of 9 µl was mixed with 4 µl of 10X MOPS, 7 µl formaldehyde, 20 µl of formamide and 1 µl of EtBr (1 mg/ml). Samples were then heated to 55°C for 15min followed by incubation on ice for 5 min. Five microliters of a 10X RNase free loading dye is added to each cooled sample. Once the gel was finished running, a photograph was taken and the ribosomal RNA species can be used to quantitate the loading in each lane. The gel is rinsed in dH₂O for ~15min and then blotted onto GeneScreen Plus membrane (Du Pont) and baked for 2hrs before hybridization. The blotting protocol is identical to the Southern blotting method presented by Sambrook et al. (1989) and discussed above.

The hybridization is carried out in a rotating Tyler Instruments hybridization oven. First the blot was washed in 0.1X SSC, 0.1% SDS for an hour, followed with 30 mls of Hybrisol I (oncor) preheated to 65°C and prehybridized for approximately one hour. The ³²P radiolabeled DNA probe was created by the random oligo labeling

technique identical to the probes made for Southern blot analysis. Then 100 µl of probe were added to approximately 500 µl of Hybrisol I from the prehybridization bottle and boiled for 10min for denaturation. The entire probe was then added directly to the prehybridization bottle and hybridized at 65°C for at least 12 hrs. The radioactive hybridization solution was then discarded, the blot washed 2X in 2X SSC for 10min at room temperature, 1X in preheated 2X SSC, 1% SDS at 65°C for 30 min, and finally 1X in 0.1X SSC, 0.1% SDS for 10 min at room temperature. If the background was too high, the blot was washed further at 55-65°C for 10-15 min in 0.1X SSC, 0.1% SDS. The blot was then sealed in Labcor Ventes Techniques hybridization bags and exposed to Kodak Scientific Imaging Film (X-OMAT AR). The length of time required for exposure was empirically determined. MOPS and Hybrisol I were purchased from “oncor” and the 10X RNase free loading dye was purchased from the “3 prime 5 prime” company.

Polymerase Chain Reaction (PCR) and Sequence Analysis.

PCR optimization and reaction conditions were taken from the Perkin Elmer PCR technical information bulletin (Sardelli and Williams, The Perkin Elmer Corporation) and Bej et al. (1991). All reactions were carried out in a Perkin Elmer GeneAmp PCR system 2400.

***Taq* DNA Polymerase PCR.**

The 10X PCR master mix used contains 500mM Tris-HCl (pH 8.3), 15mM MgCl₂, 500mM KCl, 0.01% gelatin and 2mM of each dNTPs. The concentration of the 10X-primer stock was 5.0uM. The working concentration of primers was between 0.2 and 0.5uM. The standard *Taq* PCR reaction contained 100 ng of template genomic DNA, forward and reverse primers at a working concentration of between 0.2 and 0.5uM, 1U of *Taq* DNA polymerase (BRL), and a final 1X concentration of Master Mix (MM) to a total volume of 30 µl. PCR primers were selected using the PCR primer designer from Pedro’s BioMolecular Research Tools home page and manually (**Table 6**).

Elongase PCR Amplification of the *ae* Insert

A simple *Taq* amplification of the *ae* insertion site did not consistently generate significant amounts of product for sequencing. As a result, the ELONGASE amplification system from Gibco was utilized to amplify the *ae* insert and flanking sequence. Primers were designed to flank the 34 bp *Dra*I sequence, which was known to contain an approximately 5.4 kb insert. See **Figure 26** for the location of the primers with respect to the *Dra*I fragment. The primers used for amplifying the *ae* insert were as follows; KSO22: 5' CTGAAAGCGATCCTGTCTCTGCGAC 3' and KSO23: 5' TTGTT ACGTGCCCTGCTGACCACAC 3'. 150 µg of genomic target were used for each of the reactions. The PCR parameters for the amplification of the *ae* insert were as follows; [pre-amplification denaturation (94°C for 30 sec), thermal cycling denaturation (94°C for 30 sec), annealing (45 sec at 65°C), elongation (6 min at 68°C) 35 cycles]. The Elongase PCR product was then used as a template for a simple *Taq* PCR amplification to generate enough template for sequencing. For reasons unknown, amplification of the insert and flanking sequences using only the *Taq* DNA polymerase failed to work consistently from the genomic template, but worked well using the ELONGASE generated template. The product from this reaction was then purified by the modified "Gene Clean" protocol presented above and directly sequenced from the two PCR primers, KSO22 and KSO23. Sequencing was carried out on an automated sequencer.

PFU PCR

In order to maintain the sequence integrity for each of the fragments listed below, high fidelity PFU polymerase was used in place of *Taq* DNA polymerase. Cloned PFU DNA polymerase from Stratagene was employed for amplification of the 209 bp and the 481 bp fragments from the HB1.0 sequence and the HB1.0-hs43 fusion product from the pCaSpeRhs43 0.9 construct. Although dilutions of 1:15 PFU: *Taq* have been used for high fidelity PCR, all PFU reactions performed for this work were carried out in the absence of *Taq* DNA polymerase. All PFU PCR reactions were performed in a total volume of 30 µl with freshly prepared dNTPs and 2.5U of PFU polymerase were used for each reaction along with ~150 ng of genomic target DNA and 1 ng of vector template. The length of time recommended for the annealing step is 5min. However, I found that

for each reaction performed, that 1min was best. Each of these PCR reactions consisting of 35 cycles with annealing temperatures of 65°C and all extension temperatures were at 72°C for 60 sec / 30 base pairs. PFU also permitted the blunt end ligations of the PCR products directly into the pGEM7f+ *SmaI* digested vector. The amplification of the 481 bp and 209 bp fragments was performed directly from genomic Oregon R DNA to reduce any possible errors that may have been created during the cloning and subcloning of the genomic fragments.

Plasmid and Lambda Preparations

All reporter constructs, immobilized $\Delta 2-3$, and plasmid vectors were isolated by either equilibrium centrifugation in cesium chloride method according to the method of Sambrook et al. (1989) or using Quiagen Maxi preparation columns following the manufacturer's specifications.

All lambda particles were prepared by loading the bacteriophage suspension on a cesium chloride step gradient according to Sambrook et al. (1989), with slight modifications. Plating cells were prepared by inoculating 10 mls of LB with 0.2% maltose and incubating at 37°C overnight. The cells were pelleted for 5 min at 4K rev/min in a SS34 Sorval rotor and resuspended in 0.4 vol. of 10mM MgSO₄. Four mls of the plating cells are then inoculated with approximately 10⁸ plaque forming units (pfu) and allowed to absorb for about 15 min. This is then added to 400 ml of superbroth (10g NaCl, 10g Bacto Tryptone, 20g Bacto Yeast extract, pH 7.5 and 20 mls of sterile 1M MgCl₂ after autoclaving) at 37°C. One ml of chloroform is added after lysis is complete which is then put on a shaker for 10 min at 37°C. Forty grams of NaCl were then dissolved in the supernatant and allowed to stand on ice for 10 min, followed by centrifugation at 7K rpm for 10 min, and the addition of 40 g of PEG to the supernatant. Finally, the phage were allowed to precipitate overnight. The phage were then centrifuged at 5K rpm for 5 min and the pellet is redissolved in 4 mls of SM with 200 µg of RNase and DNase and allowed to stand for 15 min. The PEG was extracted from the phage particles with chloroform and centrifugation at 10K rpm for 10 min. The phage suspension was then applied to the top of a CsCl step gradient and centrifuged for 1.5 hrs at 35K at 20°C. A #22 gauge needle was used to extract the phage band from the

gradient at approximately 1.4 g/ml CsCl. The phage were then dialyzed 3X against 1000vol of 10mM NaCl, 50mM Tris-HCl (pH 8.0) and 10mM MgCl₂ to remove the CsCl. The DNA is extracted by adding EDTA, proteinase K and SDS to final concentrations of 20mM, 50 mg/ml and 0.5% respectively. The solution was next incubated for 60 min at 55°C, then extracted 1X with 1 volume of a 50:50 mix of phenol: chloroform isoamyl-alcohol followed by 1X with 1 volume of chloroform isoamyl alcohol. After the addition of each organic solution, the tubes were centrifuged at 1600 g for 5 min. The DNA was precipitated by adding NaCl to a final concentration of 200mM and 2 volumes of 95% ethanol. The pellet was then washed in 70% ethanol, dried and redissolved in dH₂O.

Enhancer Fragments and Enhancer Tester Constructs

The 4.8 kb *EcoRI* fragment (**Figure 26**) was subcloned into a pUC19 vector from the 10θ clone reported by Fasano et al. (1991). The 4.8 kb sequence is cloned into pUC19 in both orientations. *BamHI* digests and ligations of each of the two orientations produced a 2.9 kb (EB2.9) and a 1.9 kb (EB1.9) pUC19 cloned *EcoRI/BamHI* fragment. For the origins of each of the fragments with respect to the coding regions see **Figure 19** and **26**.

The 4.8 kb *EcoRI* fragment was cloned directly into the unique *EcoRI* site in the pCaSpeR hs 43-vector (E4.8). The 2.9 kb fragment was cloned directly as an *EcoRI/BamHI* fragment into pCaSpeR hs 43 (EB2.9) from the 10θ clone (Fasano et al., 1991). The *HindIII/BamHI* 915 bp fragment was removed from a pUC19 vector and subcloned as a *BamHI* fragment into the enhancer tester's unique *BamHI* site (HB1.0). The *DraI*-deleted HB1.0 fragment was first sub-cloned into the pGEM7f(+) vector and then removed by cutting with *EcoRI* and *BamHI*. This fragment was subjected to phosphatase activity and then digested with *DraI* and ligated into the *BamHI/EcoRI* digested pGEM7f(+) vector. The fragment was then sequenced to confirm the removal of the 34 bp *DraI* fragment, and then sub-cloned into the pCaSpeR hs 43 *EcoRI/BamHI* digested vector (DraI-). The ~1.0 kb *HindIII* and *HindIII/EcoRI* fragments were cloned into pGEM7F+ vector in order to generate the *EcoRI/BamHI* fragment used to clone into the enhancer tester transformation vector pCaSpeRhs43.

To test the 481 bp and 209 bp fragments for enhancer abilities, these fragments were amplified from Oregon R genomic DNA using the high fidelity PFU polymerase PCR protocol from Stratagene. All polymerase chain reactions were carried out in a Perkin Elmer GeneAmp PCR System 2400 PCR machine. The primer sets used for each of the fragments are as follows; the 481 bp: 5' (GG)AATTCGGCACGTTTCGCTGTG 3' and 220; 5' GGCACAGACATGAGTCTTAC 3'. Both used the same reverse primer 5' TGATTGGGCTGACGAAGTGAAAC 3'. Each blunt ended PCR product was then subcloned into a *Sma*I digested pGEM7f(+) (Promega) vector and removed by cutting with *Eco*RI and *Bam*HI and inserted into the *Bam*HI/*Eco*RI digested pCaSpeR hs 43 vector. All vectors and constructs were purified using the Qiagen protocol.

The wing hinge-specific GAL4 line was created by modifying the pGATB vector, by adding both the minimal heat shock promoter (hs 43) from the pCaSpeR hs 43 vector and the hinge specific enhancer sequences. Each pCaSpeR hs 43-enhancer construct that gave a positive result was amplified using the high fidelity PFU polymerase protocol. The primers were designed to amplify both the hs 43 promoter and the enhancer sequence capable of hinge specific activation of the reporter gene. The primers used were as follows; 5' hs primer; 5' GAAGATCTAAAGGGTTTTATTA ACTTACATA CATA C 3', 3' hs primer; 5' GAAGATCTGGGCCCTAGAGGATCAGCTTGG 3'. Both primers are written in 5' to 3' orientation and also have designed 5' *Bg*III sites.

In creating the pGAT-HB1.0 construct, the HB1.0 (pCaSpeR hs 43 HB1.0) was used as a template. The 5' and 3' hs primers were used to amplify the enhancer hs 43 promoter. The amplified fragment was subcloned into the *Sma*I digested pGEM7f+ vector and removed by cutting with *Bg*III. The *Bg*III fragment was ligated into the *Bam*HI digested pGATB vector (**Figure 36**). The HB1.0 hs 43 GAL4 fusion was then removed from pGATHB1.0 by cutting with *Not*I and subcloned into the transformation vector pCaSpeR 4. Both orientations were purified (**Figure 36**). The orientation that presents the mini *white* gene and the HB1.0-hs43-GAL4 fusion in the same orientation most closely resembles the pCaSpeR hs 43 H1.0 vector, which is known to give wing, hinge-specific expression. See microinjections for a description of the transformation protocol.

Restriction enzyme-digested pCaSpeR hs 43, pCaSpeR4 or pGATB vectors were phosphatased using United States Biochemical Shrimp alkaline phosphatase (SAP). For every 1.0 pmol of DNA 5' overhang ends 0.1U of SAP were incubated for one hour at 37°C. The SAP mixture was then heated at 75°C for 20 min to inactivate the phosphatase. The samples were used directly without any further processing.

Micro-Injections

Injections were carried out according to Rubin and Spradling (1983) with slight modifications. The 0-1hr yw embryos were collected from 2% agarose plates smeared with live yeast paste, washed thoroughly with water, and then dechorionated for 45-60 sec using 50% Javex Bleach. Embryos were then arranged posterior side out on blocks of agar cut to approximately the size of a cover slip. The agar blocks keep the embryos from drying out while arranging them on the slide. The embryos are then picked up from the agar blocks with slides prepared with adhesive strips. Adhesive slides were prepared by applying a small drop of glycerol to the slide followed by a cover slip, which keeps the cover slip from moving. Double sided 3M tape soaked in heptane is used as the adhesive for immobilizing the dechorionated embryos. The adhesive is applied along the edges of the cover slip and the heptane is allowed to evaporate, leaving the adhesive behind. The slides are then inverted and the adhesive is used to pick up the embryos from the agar blocks.

Desiccation times were empirically determined, but generally ranged between 8min 10 sec and 8 min 20 sec. Immediately following the desiccation step, embryos were covered with a one to one mix of series 56 and 700 weight halocarbon oil. Ten micrograms of each construct prepared for injection were combined with 2 µg of the delta 2-3 helper vector, then precipitated and dissolved in 10 µl of water. Needles were pulled with a Sutter instrument Co. Model P-87 Flaming / Brown Micropipette Puller and back filled with a pulled 50 µl disposable pipette. After the injections, the slide is examined under a compound microscope where all embryos past stage 3 (Pole cell formation) are removed. Once injections were complete, the embryos were covered with series 700 halocarbon oil and incubated for ~48 hrs in a humidified chamber at 18°C. Hatched first instar G0 larvae were picked from the oil and placed on formula 4-24

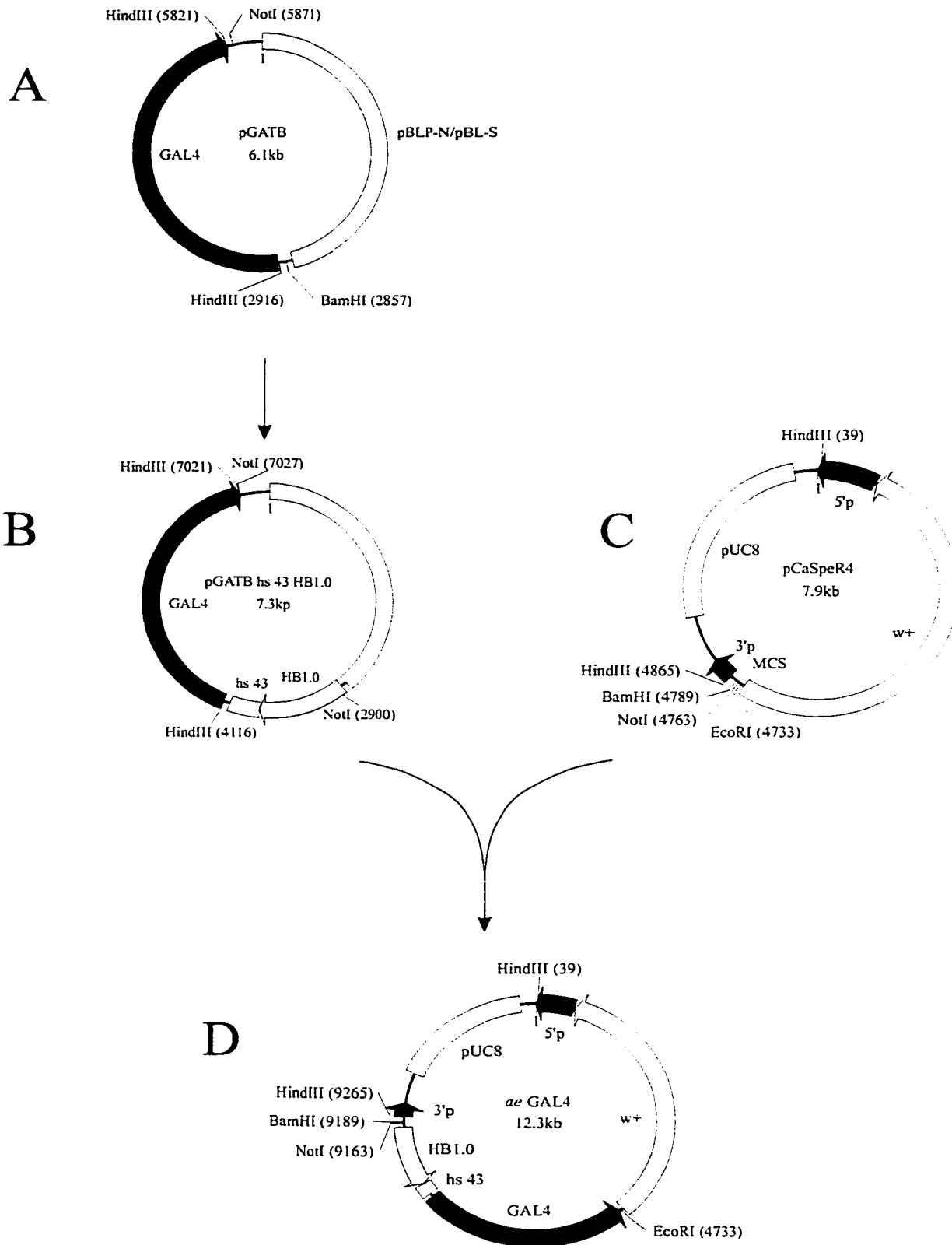
instant *Drosophila* media from Carolina Biological Supply Company. The instant food provides a soft surface for the first instar larvae to burrow into. However, in the absence of instant food scoring the surface also works well. Generally 25-33% of the embryos survived the injections and hatched. Of the first instar larvae that were picked, approximately 66% would survive to eclosion with approximately 80% of the adults were fertile. Adult G0s were crossed back to the *yw* strain used for the injections.

G1 transformants were then crossed back to balancer stocks and maintained as either homozygotes (when possible) or balanced over the TM6-SM1, double balanced translocation stock.

Table 6. Sequencing and PCR Primers.			
Primers	Sequence (5'-3')	Clone	T.M.(°C)
KSO7 (F)	AAAGCGATCCTGTCTCTGCG	HB1.0	62
KSO9 (F)	GGCACAGACATGAGTCTTAC	HB1.0	60
KSO10 (R)	CTGTGCCGTAAATCCGCATG	HB1.0	62
KSO11 (F)	(GG)AATTCGGCACGTTTCGCTGTG	HB1.0	70
KSO14(R)	TTGCCGCTTTCTGAATTACTTTC	HE1.0	60
KSO15(F)	AGCAATCCACGTCACACCC	H1.0	64
KSO16(R)	CACTAGGAGCTCCAGATATGG	EB1.9	64
KSO17(F)	TGCACGGGAAGCAGGCGCTG	EB1.9	68
KSO18(3')	TGGGCTGCAGATTGTTTAGC	pCaSpeR hs 43	60
KSO19(5')	GCATAGGCCACTAGTGGATC	pCaSpeR hs 43	62
KSO20(R)	GGAACTACCACAATCACAACC	HE1.0	62
KSO22(F)	CTGAAAGCGATCCTGTCTCTGCGAC	ae insert	78
KSO23(R)	TTGTTAC GTGCCCTGCTGA CCACAC	ae insert	78
KSO24	CTATCGACGGGACCACCTTATG	5' P element	68
B11R(R)	TGATTGGCTGACGAAGTGAAAC	H1.0	64
5'hs43	(GAAGATCT)AAAGGGTTTTATTAACCTACATACATAC	pCaSpeR hs 43	92
3'hs43	(GAAGATCT)GGGCCCTAGAGGATCAGCTTGG	pCaSpeR hs 43	94

(F) indicates forward primers and (R) indicates reverse primers relative to the sequence presented in **Figure 26**. The sequence from **Figure 26** is in the opposite direction of transcription from the *tsh* gene. KSO11 has a modified 5' end to give an *EcoRI* restriction site. 5' and 3' hs 43 primers were engineered with 5' *BglII* sites. All primers, were designed for sequencing and PCR analysis except for 5' and 3' hs 43 primers that were designed to amplify the minimal heat shock promoter and tested enhancer fragments within the pCaSpeR hs 43 vector. See **Figure 26** for the location of the primers with respect to the 4.8 kb sequence. KSO18 and 19 were designed to amplify the hs 43 minimal promoter and fragments inserted within the unique *BamHI* site in the pCaSpeR hs 43 vector. All primers are written in a 5' to 3' direction. The T_m of each primer is listed and the location of each primer within the 4.8 kb of sequence is also indicated under the column "clone".

Figure 36. Diagrammatic representation of the creation of the *ae* GAL4 vector. **A)** pGATB vector. **B)** is a modified pGATB vector by adding the PFU amplified hs 43 minimal promoter and HB1.0 enhancer upstream of the GAL4 coding region (details see materials and methods). **C)** is the pCaSpeR4 transformation vector. **D)** *ae* GAL4 (pCaSpeR HB1.0 hs 43 GAL4) was created by inserting the HB1.0-hs 43-GAL4 fusion construct into the unique *NotI* site of the transformation vector pCaSpeR4. The yellow fragment indicates the ventral hinge specific enhancer element (HB1.0) with the arrow indicating the orientation with respect to the direction of *tsh* transcription (see **Figure 25**). The arrows indicate the direction of transcription for each of the coding regions. For more details on the creation of **B)** and **D)** see materials and methods.



Bibliography

Aberle, H., Bauer, A., Stappert, J., Kispert, A. and Kemler, R. (1997). B-Catenin is a target for the ubiquitin-proteasome pathway. *EMBO J.* 16: 3797-3804.

Akam, M. (1989). HOX and HOM: homologous gene clusters in insects and vertebrates. *Cell* 57: 347-349.

Altschul, S. F., Gish, W., Miller, W., Myers, E. W. and Lipman D. J. (1990). Basic local alignment search tool. *J. Mol. Biol.* 215: 403-410.

Arnosti, D. N., Barolo, S., Levine, M. and Small, S. (1996). The eve stripe 2 enhancer employs multiple modes of transcriptional synergy. *Development* 122: 205-214.

Ashburner, M. and Wright, T. R. F. (1978). The genetics and biology of *Drosophila* vol.2c.

Ashburner, M. (1989). *Drosophila: a laboratory handbook*. Cold Spring Harbor Laboratory press.

Ayme-Southgate, A., Southgate, R., Saide, J., Benian, G. M. and Pardue, M. L. (1995). Both synchronous and asynchronous muscle isoforms of projectin (the *Drosophila* bent locus product) contain functional kinase domains. *J. Cell. Biol.* 128: 393-403.

Aza-Blanc, P., Ramirez-Weber, F. P., Laget, M. P., Schwartz, C., and Kornberg, T. B. (1997). Proteolysis that is inhibited by Hedgehog targets Cubitus Interruptus Protein to the nucleus and converts it a Repressor. *Cell* 89: 1043-1053.

Beachy, P. A., Helfand, S. L. and Hogness, D. S. (1985). Segmental distribution of bithorax complex proteins during *Drosophila* development. *Nature* 313: 545-551.

Beachy, P. A., Krasnow, M. A., Gavis, E. R., Hogness, D. S. (1988). An Ultrabithorax protein binds sequences near its own and Antennapedia P1 promoters. *Cell* 55: 1069-1081.

Beall, C. J. and Fyrberg. (1991). Muscle abnormalities in *Drosophila melanogaster* heldup mutants are caused by missing or aberrant troponin-I isoforms. *J. Cell Biol.* 114: 941-951.

Bej, A. K., Mahbubani, M. H. and Atlas, R. M. (1991). Amplification of nucleic acids by polymerase chain reaction (PCR) and other methods and their applications. *Critical Reviews in Biochemistry and Molecular Biology* 26: 301-334.

Bejsovec, A. and Martinez-Arias, A. (1991). Roles of wingless in patterning the larval epidermis of *Drosophila*. *Development* 113: 471-485.

- Bellen, H. J., O’Kane, C. J., Wilson, C., Grossniklaus, U., Pearson, R. K. and Gehring, W. J. (1989). P element-mediated enhancer detection: a versatile method to study development in *Drosophila*. *Genes and Dev.* 3: 1288-1300.
- Bender, W., Akam, M., Karch, F., Beachy, P. A., Peifer, M., Spierer, P., Lewis, E. B. and Hogness, D. S. (1983). Molecular Genetics of the Bithorax Complex in *Drosophila melanogaster*. *Science* 221: 23-29.
- Bhatnot, P., Brink, M., Samos, C. H., Hsieh, J. C., Wang, Y., Macke, J. P., Andrew, D., Nathans, J. and Nusse, R. (1996). A new member of the frizzled family from *Drosophila* functions as a wingless receptor. *Nature* 382: 225-230.
- Bhojwani, J., Shashidhara, L. S. and Sinha, P. (1997). Requirement of *teashirt* (*tsh*) function during cell fate specification in developing head structures in *Drosophila*. *Dev. Genes Evol.* 207: 137-146.
- Bhojwani, J., Singh, A., Misquitta, L., Mishra, A. and Sinha, P. (1995). Search for *Drosophila* genes based on patterned expression of mini-white reporter gene of a P lacW vector in adult eyes. *Roux Arch. dev. Biol.* 205: 114-121
- Bingham, P. M., Kidwell, M. G. and Rubin, G. M. (1982). The molecular basis of *P-M* hybrid dysgenesis: the role of the *P* element, a *P*-strain specific transposon family. *Cell* 29: 995-1004.
- Blackwood, E. M. and Kadonaga, J. T. (1998). Going the distance: A current view of enhancer action. *Science* 281: 60-63.
- Blair, S. S., Brower, D. L., Thomas, J. B. and Zavortink, M. (1994). The role of *apterous* in the control of dorsoventral compartmentalization and *PS* integrin gene expression in the developing wing of *Drosophila*. *Development* 120: 1805-1815.
- Bonicinelli, E., Somma, R., Acampora, D., Pannese, M., D’Esposito, M., Faiella, A., and Simeone, A. (1988). Organization of human homeobox genes. *Hum. Reprod.* 3: 880-886.
- Botas, J. (1993). Control of morphogenesis and differentiation by HOM/Hox genes. *Curr. Opin. Cell Biol.* 5: 1015-1022.
- Bouhidel, K., Terzian, C. and Pinon, H. (1994). The full-length transcript of the I factor, a LINE element of *Drosophila melanogaster*, is a potential bicistronic RNA messenger. *Nucl. Acid. Res* 22: 2370-2374.
- Bourbon, H. M., Martin-Blanco, E., Rosen, D. and Kornberg, T.B. (1995). Phosphorylation of the *Drosophila* engrailed protein at a site outside its homeodomain enhances DNA binding. *J. Biol. Chem.* 270: 11130-11139.

- Brandt, A. and Perrimon, N. (1993) Targeted gene expression as a means of altering cell fates and generating dominant phenotypes. *Development* 118: 401-415.
- Brook, W. J. (1994). Gene expression in regenerating imaginal discs of *Drosophila melanogaster*. Ph. D. thesis, University of Alberta, Canada. pp. 204.
- Brook, W. J., Diaz-Benjumea F. J. and Cohen S. M. (1996). Organizing spatial pattern in limb development. *Annu. Rev. Cell. Biol.* 12: 161-180.
- Brunner, E., Peter, O., Schweizer, L. and Basler, K. (1997). Pangolin encodes a Lef-1 homologue that acts downstream of Armadillo to transduce the Wingless signal in *Drosophila*. *Nature* 385: 829-833.
- Bryant, P. J. (1975). Pattern formation in the imaginal wing disc of *Drosophila melanogaster*: fate map, regeneration and duplication. *J. Exp. Zool.* 193: 49-78.
- Burke T. W. and Kadonaga, J. T. (1996). *Drosophila* TFIID binds to a conserved downstream basal promoter element that is present in many TATA-box-deficient promoters. *Genes and Dev.* 10: 711-724.
- Burke T. W. and Kadonaga, J. T. (1997). The downstream core promoter element, DPE, is conserved from *Drosophila* to humans and is recognized by TAF_{II}60 or *Drosophila*. *Genes and Dev.* 11: 3020-3031.
- Bussseau, I., Chaboissier, M. C., Pelisson, A. and Bucheton, A. (1994). *I* factors in *Drosophila melanogaster*: transposition under control. *Genetica* 93: 101-116.
- Busturia, A. and Bienz, M. (1993). Silencers in abdominal-B, a homeotic *Drosophila* gene. *EMBO J.* 12: 1415-1425.
- Cadigan, K. M., Fish, M. P., Rulifson, E. J and Nusse, R. (1998). Wingless repression of *Drosophila frizzled 2* expression shapes the wingless morphogen gradient in the wing. *Cell* 93: 767-777.
- Cadigan, K. M. and Nusse, R. (1997). Wnt signaling: a common theme in animal development. *Genes and Dev.* 11: 3286-3305
- Cañi, H. and Levine, M. (1995). Modulation of enhancer-promoter interactions by insulators in the *Drosophila* embryo. *Nature* 376: 533-536.
- Cañleja, M., Moreno, E., Pelaz, S. and Morata, G. (1996). Visualization of Gene Expression in Living Adult *Drosophila*. *Science* 274: 252-255.
- Cañniker, S. E., Sharma, S., Keelan, D. J. and Lewis, E. B. (1990). The molecular genetics of the bithorax complex of *Drosophila*: cis-regulation in the *Abdominal-B* domain. *EMBO J.* 9: 4277-4286.

- Chaboissier, M. C., Bucheton, A. and Finnegan, D. (1998). Copy number control of a transposable element, the *I* factor, a LINE-like element in *Drosophila*. *Proc. Natl. Acad. Sci. USA* 95: 11781-11785.
- Chan, S., Jaffe, L., Capovilla, M., Botas, J. and Mann, R. M. (1994). The DNA binding specificity of Ultrabithorax is modulated by cooperative interactions with Extradenticle, another homeoprotein. *Cell* 78: 603-615.
- Chang, C-P., Shen, W-F., Rozenfeld, S., Lawrence, J., Largman, C. and Cleary, M. L. (1995). Pbx proteins display hexapeptide-dependent cooperative DNA binding with a subset of Hox Proteins. *Genes and Dev.* 9: 663-674.
- Cheng, N. N., Sinclair, D. A. R., Campbell, R. B. and Brock, H. W. (1994). Interactions of polyhomeotic with Polycomb group genes of *Drosophila melanogaster*. *Genetics* 138: 1151-1162.
- Cohen, S. M. (1993). The development of *Drosophila melanogaster* vol. II. ed. Michael Bate and Alfonso Martinez Arias. 747-841.
- Cohen, B., Simcox, A. A. and Cohen, S. M. (1993). Allocation of the thoracic imaginal disc primordia in the *Drosophila* embryo. *Development* 117: 597-608
- Core, N., Charroux, B., McCormick, A., Vola, C., Fasano, L., Scott, M. P. and Kerridge, S. (1997). Transcriptional regulation of the *Drosophila* homeotic gene *teashirt* by the homeodomain protein *Fushi tarazu*. *Mech. Dev* 68: 157-172.
- Couso, J. P. Bishop, S. A., and Martinez-Arias, A. (1994). The wingless signaling pathway and the patterning of the wing margin in *Drosophila*. *Development* 120: 621-636.
- Couso, J. P., Bate, M. and Martinez-Arias, A. (1993). A wingless-dependent polar coordinate system in *Drosophila* imaginal discs. *Science* 259: 484-489.
- Deek, I. I. (1977). Mutations of *Drosophila melanogaster* that affect muscles. *J. Embryol. Exp. Morphol.* 40:35-63.
- De Jongh, L. F. (1975). "A study of chromosomal inversions and translocations induced by X-rays in premeiotic and postmeiotic germ cells of *Drosophila melanogaster* males." Ph.D. thesis, University of Wisconsin at Madison.
- DeSimone, S., Coelho, C., Roy, S., VijayRaghavan, K. and White, K. (1995). ERECT WING, the *Drosophila* member of a family of DNA binding proteins is required in imaginal myoblasts for flight muscle development. *Development* 121: 31-39.

- Desplan, C., Theis, J. and O'Farrell, P. H. (1985). The *Drosophila* developmental gene, engrailed encodes a sequences specific DNA binding activity. *Nature* 318: 630-635.
- Diaz-Benjumea, F. J and Cohen, S. M. (1993). Interaction between Dorsal and Ventral Cells in the imaginal Disc Directs wing development in *Drosophila*. *Cell* 75: 741-752.
- Diaz-Benjumea, F. J and Cohen, S. M. (1993). Serrate signals through Notch to establish a Wingless-dependent organizer at the dorsal/ventral compartment boundary of the *Drosophila* wing. *Development* 121: 4215-4225.
- Diez del Corral, R., Aroca, P., Gomez-Skarmeta, J. L., Cavodeassi, F. and Modolell, J. (1999). The Iroquois homeodomain proteins are required to specify body wall identity in *Drosophila*. *Genes and Dev.* 13: 1754-1761.
- Dimitri, P., Arca, B., Berghella, L. and Mei, E. (1997). High genetic instability of heterochromatin after transposition of LINE-like *I* factor in *Drosophila melanogaster*. *Proc. Natl. Acad. Sci. USA.* 94: 8052-8057.
- Dorer, D. R. and Henikoff, S. (1997). Transgene repeat arrays interact with distant heterochromatin and cause silencing in cis and trans. *Genet.* 147: 1181-1190.
- Driever, W., and Nusslein-Volhard, C. (1989). The bicoid protein is a positive regulator of hunchback transcription in the early *Drosophila* embryo. *Nature* 337: 138-143.
- Duboule, D., and Dolle, P.(1989). The structural and functional organization of the murine Hox gene family resembles that of *Drosophila* homeotic genes. *EMBO J.* 8: 1497-1505.
- Ekker, S., Jackson, D. G., Von Kessler, D., Sun, B. L., Young, K. E. and Beachy, P. A. (1994). The degree of variation in DNA sequence recognition among four *Drosophila* homeotic proteins. *EMBO J.* 13: 3551-3560.
- Ekker, S. C., von Kessler, D. P. and Beachy, P. A. (1992). Differential DNA sequence recognition is a determinant of specificity in homeotic gene action. *EMBO J.* 11: 4059-4072.
- Ekker, S. C., Young, K. E., von Kessler, D. P. and Beachy, P. A. (1991). Optimal DNA sequence recognition by Ultrabithorax homeodomain of *Drosophila*. *EMBO J.*10: 1179-1186.
- Emami, K. H., Jain, A. and Smale, S.T. (1997). Mechanism of synergy between TATA and initiator: synergistic binding of TFIID following a putative TFIIA-induced isomerization. *Genes Dev.* 11: 3007-3019.
- Ewing, A. W. 1979. The neuromuscular basis of courtship song in *Drosophila*: the role of direct and axillary wing muscles. *J. Comp. Physiol.* 130: 87-93.

- Fasano, L., Roder, L., Core, N., Alexandre, E., Vola, C., Jacq, B. and Kerridge, S. (1991). The *teashirt* gene is required for the development of *Drosophila* embryonic trunk segments and encodes a protein with widely spaced zinc finger motifs. *Cell* 64: 63-79.
- Fawcett, D. H., Lister, C. K., Kellett, E. and Finnegan, D. J. (1986). Transposable elements controlling I-R hybrid dysgenesis in *D. melanogaster* are similar to Mammalian Lines. *Cell* 47: 1007-1015.
- Featherstone, M. S., Baron, A., Gaunt, S. J., Mattei, M. and Duboule, D. (1988). *Hox5.1* defines a homeo-box-containing gene locus on mouse chromosome 2. *Proc. Natl. Acad. Sci. USA* 85: 4760-4764.
- Finnegan, D. J. (1989). Eukaryotic transposable elements and genome evolution. *Trends Genet.* 5: 103-107.
- Fleming, R. J., Zusman, S. B. and White, K. (1983). Developmental genetic analysis of lethal alleles at the *ewg* locus and their effects on muscle development in *Drosophila melanogaster*. *Dev. Genet.* 3: 347-363.
- Florence, B., Handrow, R. and Laughon, A. (1991). DNA-binding specificity of the fushi tarazu homeodomain. *Mol. Cell. Biol.* 11: 3613-3623.
- Fristrom, D. and Fristrom, J. W. (1993). The development of *Drosophila melanogaster* ed. Bate and Martinez-Arias vol. II. pg. 843-897.
- Fristrom, D. (1976). The mechanism of evagination of the imaginal discs of *Drosophila melanogaster*. III. Evidence for cell rearrangement. *Dev. Biol.* 54: 163-171.
- Fyrberg, C. C., Labeit, S., Bullard, B., Leonard, K. and Fyrberg, E. A. (1992). *Drosophila* projectin: relatedness to titin and twitchin and correlation with lethal(4) 102 CDa and bent-dominant mutants. *Proc. r. Soc. Biol. Sci.* 249: 33-40
- Gallet, A., Angelats, C., Erkner, A., Charroux, B., Fasano, L. and Kerridge, S. (1999). The C-terminal domain of Armadillo binds to hypophosphorylated Teashirt to modulate Wingless signaling in *Drosophila*. *EMBO J.* 18: 2208-2217.
- Gallet, A., Erkner, A., Charroux, B., Fasano, L. and Kerridge, S. (1998). Trunk-specific modulation of wingless signaling in *Drosophila* by teashirt binding to armadillo. *Curr. Biol.* 8: 893-902.
- Garcia-Bellido, A., Ripoll, P. and Morata, G. (1973). Developmental compartmentalization of the wing disc of *Drosophila*. *Nat. New Biol.* 245: 251-253.

Garcia-Bellido, A.(1975). Genetic control of wing disc development in *Drosophila*. In *Cell patterning*, Ciba Foundation Symposium (ed. S. Brenner), pp.161-182. Associated Scientific Publisher, New York, NY.

Garcia-Bellido, A., Ripoll, P. and Morata, G. (1976). Developmental compartmentalization in the dorsal meosothoracic disc of *Drosophila*. *Dev. Biol.* 48: 132-147.

Gelbart, W. M. (1982). Synapsis-dependent allelic complementation at the decapentaplegic gene complex in *Drosophila melanogaster*. *Proc. Natl. Acad. Sci.* 79: 2636-2640.

Geyer, P. K and Corces, B. G. (1992). DNA position-specific repression of transcription by a *Drosophila* zinc finger protein. *Genes and Dev.* 6: 1865-1873.

Goldborough A. S., and Kornberg, T. B. (1996). Reduction of transcription by homologue asynapsis in *Drosophila* imaginal discs. *Nature* 381: 807-810.

Gomez-Skarmeta, J. L., Diez del Corral, R., de la Calle-Mustienes, E., Ferrer-Marco, D., and Modolell, J. (1996). *araucan* and *caupolican*, two members of the novel Iroquois complex, encode homeoproteins that control proneural and vein formation genes. *Cell* 85: 95-105.

Gonzalez-Reyes, A. and Morata, G. (1990). The developmental effect of overexpressing a Ubx product in *Drosophila* embryos is dependent on its interactions with other homeotic products. *Cell* 61: 515-522.

Gorman, M. J. Kaufman, T. C. (1995). Genetic analysis of embryonic cis-acting regulatory elements of the *Drosophila* homeotic gene *Sex combs reduced*. *Genetics* 140: 557-572.

Graham, A., Papalopulu, N. and Krumlauf. R. (1989). The murine and *Drosophila* homeo box gene complexes have common features of organization and expression. *Cell* 57: 367-378.

Halder, G., Polaczyk, P., Kraus, M. E., Hudson, A., Kim, J., Laughon, A. and Carroll, S. (1998). The Vestigial and Scalloped proteins act together to directly regulate wing-specific gene expression in *Drosophila*. *Genes and Dev.* 12: 3900-3909.

Hayashi, S., and Scott, M. P. (1990). What determines the specificity of action of *Drosophila* homeodomain proteins? *Cell* 63: 883-894.

Haynie, J. L. (1975). Intercalary regeneration and pattern formation in imaginal discs of *Drosophila melanogaster*. Ph. D. thesis, University of California, Irvine.

- Heide, G. 1971. Die funktion der nicht fibrillaren flugmuskeln von *Calliphora*. Teil I: Lage, insectionsstellen und innervierungsmuster der Muskeln. *Zool. Jb. Physiol.* 76: 99-137.
- Henikoff, S. and Comai, L. (1998). Trans-sensing effects: The ups and downs of being together. *Cell* 93: 329-332.
- Higashijima, S., Shishido, E., Mausuzaki, M. and Saigo, K. (1996). Eagle, a member of the steroid-receptor gene superfamily, is expressed in a subset of neuroblasts and regulates the fate of their putative progeny in the *Drosophila* CNS. *Development* 122: 527-557.
- Hodgetts, R. 1980. A cytogenetic description of three duplications in which portions of proximal 2L have been inserted into the Y-chromosome. *D.I.S.* 55: 63.
- Hoey, T., and Levine, M. (1988). Divergent homeobox proteins recognize similar DNA sequences in *Drosophila*. *Nature* 332: 858-861.
- Inoue, H., Nojima, H. and Okayama, H. 1990. High efficiency transformation of *Escherichia coli* with plasmids. *Gene* 96: 23-28.
- Ip, Y. T., Kraut, R., Levine, M. and Rushlow, C. A. (1991). The dorsal morphogen is a sequence-specific DNA-binding protein that interacts with a long-range repression element in *Drosophila*. *Cell* 64: 439-446.
- Irish, V. F., Martinez-Arias, A. and Akam, M. E. (1989). Spatial regulation of the *Antennapedia* and *Ultrabithorax* genes during *Drosophila* early development. *EMBO J.* 8:1527-1537.
- Irvine, K. and Vogt, T. F. (1997). Dorsal-ventral signaling in limb development. *Curr. Opin. Cell Biol.* 9: 867-876.
- Jack, J., Dorsett, D., DeLotto, Y. and Liu, S. (1991). Expression of the cut locus in the *Drosophila* wing margin is required for cell type specification and is regulated by a distant enhancer. *Development* 113: 735-747.
- Jack, J., Regulski, M. and McGinnis, W. (1988). Pair rule segmentation genes regulate the expression of the homeotic selector gene *Deformed*. *Genes and Dev.* 2: 635-651.
- Jaffe, L., Ryoo, H. D. and Mann, R. S. (1997). A role for phosphorylation by casein kinase II in modulating *Antennapedia* activity in *Drosophila*. *Genes and Dev.* 11: 1327-1340.
- Jiang, J., Hoey, T. and Levine, M. (1991). Autoregulation of a segmentation gene in *Drosophila*: combinatorial interaction of the even-skipped homeo box protein with a distal enhancer element. *Genes and Dev.* 5: 265-277.

Jones, B. and McGinnis, W. (1993). The regulation of empty spiracles by Abdominal-B mediates an abdominal segment identity function. *Genes and Dev.* 7: 229-240.

Kadowaki, T., Wilder, E., Klingensmith, J., Zachary, K. and Perrimon, N. (1996). The segment polarity gene porcupine encodes a putative multitransmembrane protein involved in Wingless processing. *Genes and Dev.* 10: 3116-3128.

Karch, F., Bender, W. and Weiffenbach, B. (1990). *abdA* expression in *Drosophila* embryos. *Genes and Dev.* 4: 1573-1587.

Kassis, J. A., Desplan, C., Wright, D. K. and O'Farrell, P. H. (1989). Evolutionary conservation of homeodomain-binding sites and other sequences upstream and within the major transcription unit of the *Drosophila* segmentation gene engrailed. *Mol. Cell. Biol.* 9: 4304-4311.

Katzen, A. L. and Bishop, M. J. (1996). *myb* provides an essential function during *Drosophila* development. *Proc. Natl. Acad. Sci. USA* 93: 13955-13960.

Kazazian, H. H. Wong, C., Youssufian, H., Scott, A. F., Phillips, D. G., and Antonarakis, S. E. (1988). *Nature* 333: 164-166.

Kellum, R. and Schedl, P. (1992). A Group of scs elements function as domain boundaries in an enhancer-blocking assay. *Molec. Cell Biol.* 12: 2424-2431.

Kim, J., Sebring, A., Esch, J. J., Kraus, M. E., Vorwerk, K., Magee, J. and Carroll, S. B. (1996). Integration of positional signals and regulation of wing formation and identity by *Drosophila* vestigial gene. *Nature* 382: 133-138.

Kim, J., Irvine, K. D. and Carroll, S. B. (1995). Cell recognition, signal induction and symmetrical gene activation at the dorsal/ventral boundary of the developing *Drosophila* wing. *Cell* 82: 795-802.

King, D., and Tanouye, M. 1983. Anatomy of motor axons to direct flight muscles in *Drosophila*. *J. Exp. Biol.* 105: 231-239.

Kingston, R. E., Bunker, C. A. and Imbalzano, A. N. (1996). Repression and activation by multiprotein complexes that alter chromatin structure. *Genes and Dev.* 10: 905-920.

Kuziora, M. A. and McGinnis, W. (1989). A homeodomain substitution changes the regulatory specificity of the *Deformed* protein in *Drosophila* embryos. *Cell* 59: 563-571.

Lamond, A. I., and Earnshaw, W. C. (1998). Structure and function in the nucleus. *Science* 280: 547-553.

Lawrence, P., A. and Morata, G. (1994). Homeobox Genes: Their Function in *Drosophila* Segmentation and Pattern Formation. *Cell* 78: 181-189.

Lewis, E. B. (1954). The theory and application of a new method of detecting chromosomal rearrangements in *Drosophila melanogaster*. *Am. Nat.* 88: 225-239.

Lewis, E. B. (1978). A gene complex controlling segmentation in *Drosophila*. *Nature* 276: 565-570.

Lewis, E. B., Knafels, J. D., Mathog, D. R. and Celniker, S.E. (1995). Sequence analysis of the cis-regulatory regions of the bithorax complex of *Drosophila*. *Proc. Natl. Acad. Sci. USA* 92: 8403-8407.

Leyns, L., Gomez-Skarmeta, J. L. and Dambly-Chaudiere, C. (1996). *iroquois*: A prepattern gene that controls the formation of bristles on the thorax of *Drosophila*. *Mech. Dev.* 59: 63-72.

Li, X., Murre, C. and McGinnis, W. (1999). Activity regulation of a Hox protein and a role for the homeodomain in inhibiting transcriptional activation. *EMBO J.* 18: 198-211.

Lindsley, D. L. and Zimm, G. G. (1992). *The Genome of Drosophila melanogaster*. Academic Press, New York.

Lo, P. C. H. and Frasch, M. (1997). A novel KH-domain protein mediates cell adhesion processes in *Drosophila*. *Dev. Biol.* 190: 241-256.

Lundell, M. J. and Hirsh, J. (1998). *Eagle* is required for the specification of serotonin neurons and other neuroblast 7-3 progeny in the *Drosophila* CNS. *Development* 125: 463-472.

Macias, A., Casanova, J. and Morata, G. (1990). Expression and regulation of the *abdB* gene of *Drosophila*. *Development* 110: 1197-1207.

Mahaffey, J. W., Coutu, M. D., Fyrberg E. A., and Inwood. W. (1985). The flightless *Drosophila* mutant raised has two distinct genetic lesions affecting accumulation of myofibrillar proteins in flight muscles. *Cell* 40: 101-108.

Malicki, J., Schughart, K. and McGinnis, W. (1990). Mouse Hox 2.2 specifies thoracic segmental identity in *Drosophila* embryos and larvae. *Cell* 63: 961-967.

Mann, R. S., and Hogness, D. S. (1990). Functional dissection of *Ultrabithorax* proteins in *D. melanogaster*. *Cell* 60: 597-610.

Mann, R. S. and Chan, S. K. (1996). Extra specificity from *extra-denticle*: The partnership between HOX and *exd/pbx* homeodomain proteins. *Trends Genet.* 12: 258-262.

- Martin-Moris, L. E., Csink, A. K., Dorer, D. R., Talbert, P. B. and Henikoff, S. (1997). Heterochromatic trans-inactivation of *Drosophila* white transgenes. *Genetics* 147: 671-677.
- Martinez-Arias, A. and White, R. A. H. (1988). Ultrabithorax and engrailed expression in *Drosophila* embryos mutant for segmentation genes of the pair rule class. *Development* 102: 325-338.
- Mathies, L. D., Kerridge, S., and Scott, M. P. (1994). Role of the teashirt gene in *Drosophila* midgut morphogenesis: secreted proteins mediate the action of homeotic genes. *Development* 120: 2799-2809.
- Mathog, D. (1990). Transvection in the *Ultrabithorax* Domain of the Bithorax Complex of *Drosophila melanogaster*. *Genetics* 125: 371-382.
- Matzke, M. A. and Matzke, A. J. M. (1995). *Plant Physiol.* 107: 679-695.
- McCormick, A., Core, N., Kerridge, S., and Scott, M.P. (1995). Homeotic response elements are tightly linked to tissue-specific elements in a transcriptional enhancer of the *teashirt* gene. *Development* 121: 2799-2812.
- McGinnis, W., Garber, R. L., Wirz, J., Kuroiwa, A., and Gehring, W. J. (1984). A homologous protein-coding sequence in *Drosophila* homeotic genes and its conservation in other metazoans. *Cell* 37: 403-408.
- McGinnis, W., Levine, M. S., Hafen, E., Kuroiwa, A., and Gehring, W. J. (1984). A conserved DNA sequence in homeotic genes of the *Drosophila* Antennapedia and Bithorax complexes. *Nature* 308: 428-433.
- McGinnis, N., Kuziora, M., A., and McGinnis, W. (1990). Human *Hox 4.2* and *Drosophila Deformed* encode similar regulatory specificities in *Drosophila* embryos and larvae. *Cell* 63: 969-976.
- McLean, C., Bucheton, A. and Finnegan, D. J. (1993). The 5' untranslated region of the I factor, a Long Interspersed Nuclear Element-Like retrotransposon of *Drosophila melanogaster*, contains an internal promoter and sequences that regulate expression. *Mol. Cell. Biol.* 13: 1042-1050.
- Merli, C., Bergstrom, D. E., Cygan, J. A. and Blackman, R. K. (1996). Promoter specificity mediates the independent regulation of neighboring genes. *Genes and Dev.* 10: 1260.
- Merrill, V. K. L., Turner, F. R. and Kaufman, T. C. (1987). A genetic and developmental analysis of mutations in the *Deformed* locus in *Drosophila melanogaster*. *Dev. Biol.* 122: 379-395.

- Mihaly, J., Hogga, I., Gausz, J., Gyurkovics, H. and Karch, F. (1997). In situ dissection of the *Fab-7* region of the bithorax complex into a chromatin domain boundary and a *Polycomb*-response element. *Development* 124: 1809-1820.
- Miller, A. (1950). The internal anatomy and histology of the imago of *Drosophila melanogaster*. In *Biology of Drosophila* (ed. M. Demerec), New York. John Wiley and Sons Inc.
- Mlodzik, M. and Hiromi, Y. (1992). Enhancer trap method in *Drosophila* its application to neurobiology. *Conn. (Methods Neurosci.)* 1992: 397-414.
- Mogami, K. and Hotta, Y. (1981). Isolation of *Drosophila* flightless mutants which affect myofibrillar proteins of indirect flight muscle. *Mole. Gen. Genet.* 183: 409-417.
- Morcillo, P., Rosen, C. and Dorsett, D. (1996). Genes regulating the remote wing margin enhancer in the *Drosophila cut* locus. *Genetics* 144: 1143-1154.
- Morris, J. R., Chen, J-L., Geyer, P. A. and Wu, C-T. (1998). Two modes of transvection: Enhancer action in *trans* and bypass of a chromatin insulator in *cis*. *Proc. Natl. Acad. Sci. USA.* 95: 10740-10745.
- Morris, J. R., Geyer, P. K. and Wu C. (1999). Core promoter elements can regulate transcription on a separate chromosomes in *trans*. *Genes and Dev.* 13: 253-258.
- Morse, B., Rotherg, P. G., South, V. J., Spandorfer, J. M. and Astrin, S. M., (1988). *Nature* 333: 87-90.
- Muller, J., Thuringer, F., Biggin, M., Zust, B., and Bienz, M. (1989). Coordinate action of a proximal homeoprotein binding site and a distal sequence confers the Ultrabithorax expression pattern in the visceral mesoderm. *EMBO J.* 8: 4143-4151.
- Nachtigall, W., and Wilson, D. M. 1967. Neuro-muscular control of dipteran flight. *J. Exp. Biol.* 47: 77-97.
- Nash, D. J., and Bell, J. B. (1968). Larval age and the pattern of DNA synthesis in polytene chromosomes. *Canad. J. Genet. Cytol.* 10: 82-90.
- Nellen, D., Burke, R., Struhl, G. and Basler, K. (1996). Direct and long-range action of a Dpp morphogen gradient. *Cell* 85: 357-368.
- Neumann, C. J. and Cohen, S. M (1997). Long-range action of Wingless organizes the dorsal-ventral axis of the *Drosophila* wing. *Development* 124: 871-880.

- Neumann, C. J. and Cohen, S. M. (1996). A hierarchy of cross-regulation involving *Notch*, *wingless*, *vestigial* and *cut* organizes the dorsal/ventral axis of the *Drosophila* wing. *Development* 122: 3477-3485.
- Neuteboom, S. T. C., Peltenburg, L. T. C., van Dijk, M. A. and Murre, C. (1995). The hexapeptide LFPWMR in Hoxb-8 is required for cooperative DNA binding with Pbx1 and Pbx2 proteins. *Proc. Natl. Acad. Sci. USA* 92: 9166-9170.
- Ng, M., Diaz-Benjumea, F. J., Vincent, J.-P., Wu, J. and Cohen, S. M. (1996). Specification of the wing primordium in *Drosophila*. *Nature* 381: 316-318.
- Ng, M., Fernando, J., Diaz-Benjumea, F. J. and Cohen, S. M. (1995). *nubbin* encodes a POU-domain protein required for proximal-distal patterning in the *Drosophila* wing. *Development* 121: 589-599.
- Ohtsuki, S., Levine, M. and Cai, H. N. (1998). Different core promoters possess distinct regulatory activities in the *Drosophila* embryo. *Genes and Dev.* 12: 547-556.
- Orphanides, G., Lagrange, T. and Reinberg, D. (1996). The general transcription factors of RNA polymerase II. *Genes and Dev.* 10: 2657-2683.
- Orsulic, S. and Peifer, M. (1996). An *in vivo* structure-function study of Armadillo, the B-catenin homologue, reveals both separate and overlapping regions of the protein required for cell adhesion and for wingless signaling. *J. Cell Biol.* 134: 1283-1300.
- Otting, G., Qian, Y.Q., Billeter, M., Muller, M., Affolter, M., Gehring, W. J. and Wuthrich, K. (1990). Protein-DNA contacts in the structure of a homeodomain-DNA complex determined by nuclear magnetic resonance spectroscopy in solution. *EMBO J.* 9: 3085-3092.
- Pai, L. M., Orsulic, S., Bejsovec, A. and Peifer, M. (1997). Negative regulation of Armadillo, a Wingless effector in *Drosophila*. *Development* 124: 2255-2266.
- Pal-Bhadra, M., Bhadra, U. and Birchler, J. A. (1997). Cosuppression in *Drosophila*: gene silencing of *Alcohol dehydrogenase* by *white-Adh* transgenes in *Polycomb* dependent. *Cell* 90: 479-490.
- Pan, D., and Rubin, G. (1998). Targeted expression of *teashirt* induces ectopic eyes in *Drosophila*. *Proc. Natl. Acad. Sci. USA* 95: 15508-15512.
- Pelisson, A. (1981). The I-R system of hybrid dysgenesis in *Drosophila melanogaster*: Are I factor insertions responsible for the mutator effect of the I-R interaction? *Molec. gen. Genet.* 183: 123-129.

- Phillips, R.G. and Whittle, J. R. S. (1993). *wingless* expression mediates determination of peripheral nervous system elements in late stages of *Drosophila* wing disc development. *Development* 118: 427-438.
- Pick, L., Schier, A., Affolter, M., Schmidt-Glenewinkel, T., and Gehring, W. J. (1990). Analysis of the *ftz* upstream element: germ layer-specific enhancers are independently autoregulated. *Genes and Dev.* 4: 1224-1239.
- Pirrotta, V. (1997). Pc-G complexes and chromatin silencing. *Curr. Opin. Genet. Dev.* 7: 249-258.
- Protocols and Applications guide, Promega 2nd edition (1991).
- Ptashne, M. (1988). How do transcriptional activators work. *Nature* 335: 683-689.
- Ptashne, M. and Gann, A. (1997). Transcriptional activation by recruitment. *Nature* 386: 569-577.
- Quandt, K. Frech, K. Karas, H. Wingender, E. and Werner, T. (1995). MatInd and MatInspector - New fast and versatile tools for detection of consensus matches in nucleotide sequence data. *Nucl. Acids Res.* 23: 4878-4884.
- Quelprud, T. (1931). *aeroplane*, a second chromosome recessive wing mutant in *Drosophila melanogaster*. *Hereditas* 15: 97-119.
- Ratcliff, F., Harrison, B. D. and Baulcombe, D. C. (1997). A similarity between viral defense and gene silencing in plants. *Science* 276: 1558-1560.
- Reid, N., (1975). Ultramicrotomy. *Practical Methods in Electron Microscopy*. Ed. Glauert, A. M. Elsevier Biomedical Press. Elsevier/North-Holland Biomedical Press.
- Riley, G., Jorgensen, R., Baker, R. and Garber, R. (1991). Positive and negative control of the *Antenapedia* promoter P2. *Development* 1:177-185.
- Ritter, W. (1911). The flying apparatus of the blow-fly. *Smithsonian Misc. Collect.* 56: 1-77.
- Robbins D. J., Nybakken, K. E., Kobayashi, R., Sisson, J. C., Bishop, J. M. and Therond, P. P. (1997). Hedgehog elicits signal transduction by means of a large complex containing the kinesin-related protein Costal2. *Cell* 90: 225-234.
- Roberts, D. B. (1986). *Drosophila: a practical approach*. Oxford UK.
- Robertson, H. M., Preston, C. R., Phillis, R. W., Johnson-Schlitz, D., Benz, W. K., and Engels, W. R. (1988). A stable source of P-element transposase in *Drosophila melanogaster*. *Genetics* 118: 461-470.

- Roder, L., Vola, C. and Kerridge, S. (1992). The role of the *teashirt* gene in trunk segmental identity in *Drosophila*. *Development* 114: 1017-1033.
- Rubin, G. M. and Spradling, A. C. (1983). Vectors for P-element-mediated gene transfer in *Drosophila*. *Nucl. Acid Res.* 11: 6341-6351.
- Ruiz i Altaba, A. (1997). Catching a Gli-mpse of Hedgehog. *Cell* 90: 193-196.
- Sambrook, J., Fritsch, G.F., and Maniatis, T. (1989). *Molecular Cloning: a Laboratory Manual* 2nd ed. Cold Spring Harbor Laboratory, Cold Spring Harbor, N.Y.
- Sanchez-Herrero, E. (1991). Control of the expression of the bithorax complex genes *abdominal-A* and *abdominal-B* by *cis*-regulatory region in *Drosophila* embryos. *Development* 111: 437-449.
- Sanicola, M., Sekelshy, J. J., Elson, S. and Gelbart, W. M. (1995). Drawing a stripe in *Drosophila* imaginal discs: Negative regulation of decapentaplegic and patched expression by engrailed. *Genetics* 139: 745-756
- Scott, M. P., and Weiner, A. J. (1984). Structural relationships among genes that control development: sequence homology between the *Antennapedia*, *Ultrabithorax*, and *fushi tarazu* loci of *Drosophila*. *Proc. Natl. Acad. Sci. USA* 81: 4115-4119.
- Searles, L. L., Greenleaf, A. L., Kemp, W. E. and Voelker, R. A. (1986). Sites of P element insertion and structures of P element deletions in the 5' region of *Drosophila melanogaster* RPII125. *Mol. Cell Biol.* 6: 3312-3319.
- Simmonds, A. J., Hughes, S., Tse, J., Cocquyt, S. and Bell, J. (1997). The effect of dominant vestigial alleles upon vestigial-mediated wing patterning during development of *Drosophila melanogaster*. *Mech. Dev.* 67: 17-33.
- Simmonds, A. J., Brook, W. J., Cohen, S. M. and Bell J. B. (1995). Distinguishable functions for *engrailed* and *invected* in anterior-posterior patterning in the *Drosophila* wing. *Nature* 376: 424-427.
- Sisson, J. C., Ho, K. S., Suyama, K., Scott, M. P. (1997). Costal2, a novel kinesin-related protein in the hedgehog signalling pathway. *Cell* 90: 235-245.
- Skaer, H. (1993). *The Development of Drosophila melanogaster* vol II. Cold Springs harbor laboratory press. Pp 941-1012.
- Smale, S. T. (1997). Transcription initiation from TATA-less promoters within eukaryotic proteins-coding genes. *Biochim. Biophys. Acta.* 1351: 73-88.

- Small, S., Blair, A. and Levine, M. (1992). Regulation of even-skipped stripe 2 in *Drosophila* embryo. *EMBO J.* 11: 4047-4057.
- Soanes, K. and Bell, J. (1999). Rediscovery and further characterization of the aeroplane (ae) wing posture mutation in *Drosophila melanogaster*. *Genome* 42: 403-411.
- Speicher, S. A., Thomas, U., Hinz, U. and Knust, E. (1994). The Serrate locus of *Drosophila* and its role in morphogenesis of the wing imaginal discs: control of cell proliferation. *Development* 120: 535-544.
- Spradling, A. C. and Rubin, G. M. (1983). The effect of chromosomal position on the expression of *Drosophila* xanthine dehydrogenase gene. *Cell* 34: 47-57.
- St. Johnston, D., and Nusslein-Volhard, C. (1992). The origin of pattern and polarity in the *Drosophila* embryo. *Cell* 68: 201-219.
- Staveley, B. E., Heslip, T. R., Hodgetts, R. B. and Bell, J. B. (1995). Protected P-element termini suggest a role for inverted-repeat-binding protein in transposase-induced gap repair in *Drosophila melanogaster*. *Genetics* 139: 1321-1329.
- Struhl, G., Johnston, P. and Lawrence, P. A. (1992). Control of *Drosophila* body pattern by the hunchback morphogen gradient. *Cell* 69: 237-249.
- Tabata, T., Eaton, S. and Kornberg, T. B. (1992). The *Drosophila hedgehog* gene is expressed specifically in posterior compartment cells and is a target of *engrailed* regulation. *Genes and Dev.* 6: 2635-2645.
- Tan, P. B. and Kim, S. K. (1999). Signaling specificity: the RTK/RAS/MAP kinase pathway in metazoans. *Trends Genet.* 15: 145-149.
- Tanouye, M., and King, D. 1983. Giant fiber activation of direct flight muscles in *Drosophila*. *J. Exp. Biol.* 105: 241-251.
- Thummel, C. S., and Pirrotta, V. (1992). Technical Notes: New pCaSpeR P-element vectors. *D.I.S.* 71: 150.
- Thomas, U., Jonsson, F., Speicher, S. A. and Knust, E. (1995). Phenotypic and Molecular Characterization of *Ser^D*, a Dominant Allele of the *Drosophila* Gene *Serrate*. *Genetics* 139: 203-213.
- Tower, J., Karpen, G.H., Craig, N., and Spradling, A. 1993. Preferential transposition of *Drosophila* P elements to nearby chromosomal sites. *Genetics* 133: 347-359.
- Trimarchi, R., and Schneiderman, A. 1996. The motor neurons innervating the direct flight muscles of *Drosophila melanogaster* are morphologically specialized. *J. Comp. Neur.* 340: 427-443.

van Dijk, M. A. and Murre, C. (1994). extradenticle raises the DNA binding specificity of homeotic selector gene products. *Cell* 78: 617-624.

White, R. A. and Wilcox, M. (1984). Protein products of the bithorax complex in *Drosophila*. *Cell* 39: 163-171.

Willert, K., Brink, M. Wodarz, A., Varmus, H. and Nusse, R. (1997). Casein kinase 2 associates with and phosphorylates disheveled. *EMBO J.* 16: 3089-3096.

Williams, J. A., Bell, J. B. and Carroll, S. B. (1991). Control of *Drosophila* wing and haltere development by the nuclear vestigial gene product. *Genes and Dev.* 5: 2481-2495.

Williams, J. A., Paddock, S. W. and Carroll, S. B. (1993). Pattern formation in a secondary field: A hierarchy of regulatory genes subdivides the developing *Drosophila* wing disc into discrete subregions. *Development* 117: 571-584.

Williams, J. A., Paddock, S. W., Vorwerk, K. and Carroll, S. B. (1994). Organization of wing formation and induction of a wing-patterning gene at the dorsal/ventral compartment boundary. *Nature* 368: 299-305.

Williams, C. M., and Williams, M. V. 1943. The flight muscles of *Drosophila repleta*. *J. Morphol.* 72: 589-597.

Wu, J. and Cohen, S. M. (1999). Proximodistal axis formation the *Drosophila* leg: subdivision into proximal and distal domains by Homothorax and Distal-less. *Development* 126: 109-117.

Zaffran, S., Astier, M., Gratecos, D. and Semeriva, M. 1997. The held out wings (how) *Drosophila* gene encodes a putative RNA-binding protein involved in the control of muscular and cardiac activity. *Development* 124: 2087-2098.

Zalokar, M. 1947. Anatomie du thorax de *Drosophila melanogaster*. *Revue suisse Zool.* 54:17-53

Zeng, W., Andrew, D. J., Mathies, L. D., Horner, M. A., and Scott, M.P. (1993). Ectopic expression and function of the *Antp* and *Scr* homeotic genes: The N terminus of the homeodomain is critical to functional specificity. *Development* 118: 339-352.

Zeng, C., Pinsonneault, J., Gellon, G., McGinnis, N., McGinnis, W. (1994). Deformed protein binding sites and cofactor binding sites are required for the function of a small segment-specific regulatory element in *Drosophila* embryos. *EMBO J.* 13: 2362-2377.

Zhao, J. J., Lazzarini, R. A. and Pick, L. (1993). The mouse Hox-1.3 gene is functionally equivalent to the *Drosophila Sex combs reduces* gene. *Genes and Dev.* 7: 343-354.

de Zulueta, P., Alexandre, E., Jacq, B., and Kerridge, S. (1994). Homeotic complex and *teashirt* genes co-operate to establish trunk segmental identities in *Drosophila*. *Development* 120: 2278-2296.

Appendix

Table 3 presents each of the *P* element enhancer trap alleles identified as a dominant enhancer of the *Ser^{Rpw}* phenotype. The Stock # column indicates the Bloomington stock number for each of the respective *P* element stocks. The map position column indicates the cytological location of each of the *P* element inserts. At the time of the screen the *P* element alleles were not identified with any genes. However, any alleles that have been identified with particular genes are indicated as such under the synonym column heading while those yet to be identified have their lethal *P* element designations indicated.

Table 3. P element Enhancers of the Ripped wing (<i>Ser^{Rpw}</i>) Phenotype			
Stock #	Map position	Synonym	Strength
P935	050D05-07	l(2)00248 ⁰⁰²⁴⁸	Strong
P944	023C01-02	l(2)00632 ⁰⁰⁶³²	Strong
P962	057E03-04	l(2)00734 ⁰⁰⁷³⁴	Strong
P978	037F01-02	<i>spi</i> ⁰¹⁰⁶⁸	Strong
P1026	037B08-09	<i>plume</i> ⁰¹²⁶⁵	Strong
P1034	048C05-06	<i>Eflalpha48D</i> ⁰¹²⁷⁵	Weak
P1049	059B01-02	<i>ble</i> ⁰¹⁴¹⁰	Strong
P1062	029C03-05	l(2)01482 ⁰¹⁴⁸²	Strong
P1065	034A01-02	<i>Vha68-2</i> ⁰¹⁵¹⁰	Strong
P1076	033B08-12	l(2)01810 ⁰¹⁸¹⁰	Strong
P1106	059F02-03	<i>Dcp-1</i> ⁰¹⁸⁶²	Strong
P1190	026B01-02	<i>elf-4a</i> ⁰²⁴³⁹	Strong
P1209	030E01-02	l(2)02695 ⁰²⁶⁹⁵	Strong
P1278	030B05-06	l(2)03235 ⁰³²³⁵	Strong
P1294	027B04-C01	<i>Rcal</i> ⁰³³⁰⁰	Weak
P1336	049F07-08	l(2)03531 ⁰³⁵³¹	Strong
P1337	038B04-06	<i>neb</i> ⁰³⁵⁵²	Strong
P1338	051A01-02	l(2)03563 ⁰³⁵⁶³	Strong
P1352	039F01-02	l(2)03832 ⁰³⁸³²	Moderate
P1362	032E01-02	l(2)04008 ⁰⁴⁰⁰⁸	Strong
*P1370	040A01-04	<i>tsh</i> ⁰⁴³¹⁹	Strong
P1396	035D03-04	<i>CycE</i> ⁰⁵²⁰⁶	Strong
P1402	034C01-02	l(2)05337 ⁰⁵³³⁷	Strong
P1405	057E09-10	l(2)05351 ⁰⁵³⁵¹	Strong
P1463	024C08-D1	<i>slpl</i> ⁰⁵⁹⁶⁵	Strong
P1469	053C01-02	l(2)06214 ⁰⁶²¹⁴	Strong
P1482	030D03-04	l(2)06320 ⁰⁶³²⁰	Strong
P1478	028D03-04	l(2)06243 ⁰⁶²⁴³	Strong
P1481	023F05-06	l(2)06270 ⁰⁶²⁷⁰	Strong
P1495	088B01-03	<i>trx</i> ⁰⁰³⁴⁷	Strong
P1597	083A05-06	l(3)03644 ⁰³⁶⁴⁴	Strong
P1636	083C01-02	l(3)04696 ⁰⁴⁶⁹⁶	Moderate
P1651	092A01-02	<i>Di</i> ⁰⁵¹⁵¹	Moderate
P1684	089E10-11	l(3)06442 ⁰⁶⁴⁴²	Mild
P2320	024C07-09	l(2)06708 ⁰⁶⁷⁰⁸	Strong
P2333	021D02-03	<i>S</i> ⁰⁷⁰⁵⁶	Strong
P2339	051B07-10	l(2)07214 ⁰⁷²¹⁴	Strong
P2340	050E01-02	l(2)07659 ⁰⁷⁶⁵⁹	Strong
P2344	021B04-06	<i>kis</i> ⁰⁷⁸¹²	Strong
P2345	058A03-04	l(2)07837 ⁰⁷⁸³⁷	Strong
P2351	033A03-07	l(2)08307 ⁰⁸³⁰⁷	Strong
P2375	039B01-02	<i>bur</i> ¹⁰⁵²³	Strong
P2378	050A12-14	<i>drk</i> ¹⁰⁶²⁶	Strong